A Molecular Genetic Investigation into Stress Sensing in the Food-Borne Pathogen *Listeria monocytogenes*: Roles for RsbR and its Paralogues

Beth O' Donoghue

Thesis Presented for the Degree of Doctor of Philosophy (Microbiology) at the National University of Ireland, Galway

Supervisor of Research: Dr. Conor P. O'Byrne
Department of Microbiology,
School of Natural Sciences,
National University of Ireland, Galway.

November 2016

Table of contents

Acknowledgements

First and foremost, I would like to thank my supervisor, Dr Conor O' Byrne, for offering me the opportunity to pursue this project funded by Science Foundation Ireland and for the excellent guidance, support and expertise given to me from the first day to the last and during the many days between. I consider myself very privileged to have carried out a PhD in a place as welcoming and encouraging as the microbiology department at NUIG, and I'd like to thank all the staff and students for making it such an enjoyable experience, even when the research itself was occasionally less enjoyable. In particular, thanks to Dr Cyril Carroll and Dr Florence Abram for their guidance as members of my graduate research committee, and to Maurice, Ann and Mike for all their practical assistance. Outside NUIG, I would like to thank Prof Jorgen Johansson and Dr Teresa Tiensuu for sharing their insightful knowledge, Dr Kimon-Andreas Karatzas for help with experimental design and Claire Bennett and Alan Conneely from the NCLA at NUIG for help with light apparatus construction and physics-related queries. For the great scientific advice and even better memories over the years I'd like to thank Kate (with a solution for every science problem), Aileen, Paul (always sadly missed), Iain, Elizabeth, Maria, Justine and the 'Spice Girls' and so many others. I'd like to thank past and present members of the Bacterial Stress Response Group, particularly Amber, Marta, Conor, Yinka, Kerrie and Tara for their unending help and advice. Thanks especially to Kerrie and Tara for celebrating the highs and counselling me during the lows! Thanks to the Waterford and Cork girls for years of friendship. Thanks to Mum and Dad for your love and support over the years (financial, emotional and proof-reading) and to my granny for her prayers. Thanks Robert, Amy and Faye for the well wishes and holiday breaks. Finally thank you Ian for providing me with food and shelter and general emotional stability. You're a star.

Abstract

The alternative sigma factor σ^B is conserved across several Gram-positive bacteria species as the major general stress response (GSR) regulator. For the food-borne pathogen *Listeria monocytogenes*, σ^B enables the bacterium to persist in growth-limiting environments, thus posing a serious concern for food processing industries. Activation of σ^B is dependent on signalling from a multiprotein stress-sensing complex known as the stressosome. Here, we investigate the individual roles of the five identified stress sensor proteins: RsbR, the blue-light photoreceptor Lmo0799, Lmo0161, Lmo1642 and Lmo1842 which are thought to form a multi-protein stressosome complex. Mutant strains were constructed or obtained, each lacking RsbR or one of its-paralogues and were subjected to a number of phenotypic tests.

Blue (460-470 nm) light was found to have a clear inhibitory effect on growth. Removal of the Lmo0799 protein, whose light-sensing function was proven to be dependent on a conserved cysteine residue at position 56, did not affect σ^B-mediated survival in the presence of higher intensity blue light. Phenotypic test results suggested that there may be redundancy in stress sensing between several of the RsbR paralogues but the RsbR protein plays a core structural role in stressosome formation. Novel phenotypes initially observed for the *Δlmo1842* and *Δlmo1642* strains were found to be caused by the presence of an RsbV I23T amino acid replacement which prevented σ^B activation at 37 °C but not 30 °C. Additionally, we identified that at low levels of stress, the *ΔsigB* mutant displayed a growth advantage over the wild-type, highlighting the energy cost associated with activating the GSR. These findings provide new insight into the mechanisms by which *L. monocytogenes* senses and responds to its environment and may have potential implications for control of this pathogen in food environments.

List of figures

List of tables

.

List of abbreviations and symbols

A.....alanine

Amp.....ampicillin

(k)bp.....(kilo) base pairs

BHI.....brain heart infusion

C.....cysteine

C56A.....cysteine replaced by alanine at amino acid 56

Cml .....chloramphenicol

Erm.....erythromycin

Δ.....delta (deletion)

(k)Da.....(kilo) Daltons

dH_2O.....distilled water

DNA.....deoxyribonucleic acid

DM.....defined media

g.....standard acceleration due to gravity

GSR.....general stress response

I.....isoleucine

I23T.....isoleucine replaced by threonine at amino acid 23

LB .....Luria-Bertani

Lmo.....*Listeria monocytogenes*

LOV.....light, oxygen or voltage

OD.....optical density

NaCl.....sodium chloride

PCR.....polymerase chain reaction

ROS.....reactive oxygen species

Rsb.....regulator of sigmaB

S.....serine

σ.....sigma (sig)

T .....threonine

U.....enzyme unit (as specified by manufacturer)

v/v.....volume per volume

WT.....wild-type

w/v.....weight per volume

Chapter 1: Introduction

1.1 *Listeria monocytogenes* taxonomy

The foodborne pathogen *Listeria monocytogenes* is a Gram-positive, non-spore forming, facultative anaerobe commonly found in the environment (Farber & Peterkin, 1991; Mead *et al.*, 1999). First identified by E.G.D. Murray in 1926, the bacterium gained the name *Listeria monocytogenes* in 1940 and the first reported case of its associated disease, listeriosis, was recorded in 1979 (Murray *et al*., 1926; Farber & Peterkin, 1991). Although well adapted to and able to persist in a range of environments, *L. monocytogenes* is a highly effective pathogen, responsible for more human fatalities across the European Union than any other zoonotic agent under surveillance (Farber & Peterkin, 1991; EFSA & ECDC, 2015; EFSA, 2015).

The *Listeria* genus has been greatly expanded in the last decade and currently contains 17 species (Fig. 1.1), including the established species *L. innocua*, *L. monocytogenes*, *L. welshimeri*, *L. seeligeri*, *L. ivanovii*,, *L. grayii* and the newly identified species *L. marthii*, *L. roucourtiae L. fleischmannii*, *L. floridensis*, *L. aquatica*, *L. newyorkensis*, *L. cornellensis*, *L. rocourtiae*, *L.weihenstephanensis*, *L. grandensis*, *L. riparia*, and *L. booriae* (Orsi &Wiedmann, 2016; Bertsch *et al*., 2013; den Bakker *et al.* 2014; Lang Halter *et al*., 2013; Weller *et al*., 2015; Graves *et al.*, 2010; Leclercq *et al.*, 2010; Boerlin *et al.*, 1991). Of these species, *L. monocytogenes* and *L. ivanovii* are documented pathogenic strains, with only a handful of reported cases of *L. ivanovii* infections in humans (Snapir *et al.*, 2006). At present, *L. monocytogenes* strains are classified into 4 lineages: Lineages I, II, III and Lineage IV, which was formerly classified as a subset of Lineage III (Lomonaco *et al.*, 2015; Orsi *et al.*, 2011; Wiedmann *et al.*, 1997; Rasmussen *et al.*, 1995). Lineage I and II are predominantly associated with clinical and food isolates, whereas Lineage III and IV strains which are far less frequently isolated, appear to be

most associated with ruminants and non-primate animals. *L. monocytogenes* strains are also grouped by serotype: serotypes 1/2b, 3b, 4b, 4d and 4e have been assigned within Lineage I (Cheng *et al.*, 2008; Orsi *et al.*, 2011; Piffaretti *et al.*, 1989; Wiedmann *et al.*, 1997). Serotypes 1/2a, 1/2c, 3a, and 3c belong to Lineage II and Lineage III includes serotypes 4a and 4c and some strains belonging to serotype 4b (Cheng *et al.*, 2008). Serotypes 1/2a, 1/2b, and 1/2c are the types most frequently isolated from food or the food production environment while over 95% of human listeriosis cases are caused by serotypes 1/2a (Lineage II), 1/2b and 4b (both Lineage I) (Swaminathan & Gerner-Smidt, 2007). The commonly used lab strains EGD-e, EGD and 10403S are all serovar 1/2a. Strains of the 4b serotype were once the most frequently identified cause of human infections, however there appears to be a growing number of *L. monocytogenes* 1/2a and 1/2b serotype strains causing human infections (Swaminathan & Gerner-Smidt, 2007). Indeed, the strains responsible for the 2011 US multistate cantaloupe-associated listeriosis outbreak which resulted in 147 deaths, were typed as 1/2a and 1/2b (McCollum *et al.*, 2013). This change from 4b to 1/2a and 1/2b may be credited to improvements in detection and diagnosis methods as well as actual changes in strain serotypes causing infectious disease (Swaminathan & Gerner-Smidt, 2007).

Figure removed due to copyright issues

Figure 1 Relationship of *L. monocytogenes* species. Phylogeny based on concatenated amino acid sequences of 325 single copy core genes of members of the genus *Listeria*. The bar indicates the number of inferred nucleotide substitutions per site. Taken from Weller *et al.*, 2015.

1.2 Listeriosis

L. monocytogenes exists in two states, switching from a saprophytic lifestyle to a highly virulent form within the host. Typically, infection results from the ingestion of contaminated food and the crossing of the bacteria across the intestinal epithelium, although the bacterium is also fully capable of establishing infection in the blood when inoculated intravenously; and cutaneous listeriosis infection has also been recorded

(Lecuit *et al.*, 2001; Godshall *et al.*, 2013). Listeriosis outbreaks are associated with a wide range of food groups, however fish products (mainly smoked), followed by soft and semi-soft cheeses, ready-to-eat (RTE) meats and hard cheese are the most common foodstuffs contaminated with *L. monocytogenes* above acceptable threshold levels (EFSA & ECDC, 2015; EFSA 2015). Development of listeriosis is normally limited to immunocompromised individuals; however the associated mortality rates of up to 30% make it a serious concern for national health services and the food and clinical industries (Mead *et al.*, 1999; EFSA, 2015). Healthy individuals may develop gastrointestinal disorder-associated symptoms such as nausea, vomiting, diarrhoea and abdominal pain which resolve themselves within 24 hours (Swaminathan & Gerner-Smidt, 2007) but development of these gastrointestinal associated symptoms appears to be dependent on ingestion of very high numbers (10^9 CFU) of *L. monocytogenes* (Farber & Peterkin, 1991). If the disease is able to develop unchecked by the immune system it can cause bacteraemia, flu-like symptoms and abortion in pregnant women if allowed to cross the placenta, and meningitis or encephalitis if allowed to cross the blood-brain barrier (Mead *et al.*, 1999; Vazquez-Boland *et al.*, 2001).

1.3 *L. monocytogenes* invasion and infection

Once ingested, *L. monocytogenes* may reach the gastrointestinal (GI) tract, where the pathogen's InlA and InlB proteins bind to the epithelial surface proteins of cells of the villi, allowing the bacterium to translocate across the epithelial barrier of the GI tract (Lecuit *et al.*, 2001). Internalin surface proteins (Inl) carry N-terminal signal sequences and a LRR (leucine rich repeat) domain containing at least three repeats of 22 amino acids

(Bierne *et al.*, 2007). Few of the other 25 identified internalins have known functions although InlC, InlH and InJ have all been shown to contribute to virulence (Bierne *et al.*, 2007; Pizarro-Cerda *et al.*, 2012). InlA binds to E-cadherin, found on cells of the placenta, GI lining and blood- brain barrier. E-cadherin binds to other E–cadherin ligands on adjacent cells to form adherens junctions. InlB binds to Met, a receptor for HGH (hepatocyte growth hormone) (Mengaud *et al.*, 1996; Shen *et al.*, 2000). In order to establish a successful infection, *L. monocytogenes* must produce full length functional InlA (Jacquet *et al.*, 2004). Truncated InlA protein is associated with a reduction in virulence. Testing a panel of isolates from clinical and food samples, Jacquet *et al.* (2004), found that all 4b and 1/2b isolates produced full length internalin whereas the rarity of the 1/2c strains among clinical strains may be related to the finding that all 25 1/2c strains tested carry a truncated internalin gene.

InlA is required for entry into enterocytes and goblet cells (but does not target M-cells) of the intestinal lining (Lecuit *et al.*, 2001; Corr *et al.*, 2006; Nikitas *et al.*, 2011; Mengaud *et al.*, 1996; Tsai *et al.*, 2013). Goblet cells appear to be the preferred point of translocation for *L. monocytogenes*, leading to the lamina propria. E-cadherin is present on the basolateral surface of goblet and enterocytic cells of the intestine, but is also accessible along their lateral sides, and at villus epithelial folds (Yap *et al.*, 1997; Nikitas *et al.*, 2011). InlA-mediated entry into enterocytes is theorized to occur at the tips of the villi where the loss of apoptotic cells exposes E-cadherin in neighbouring cells (Lecuit *et al.*, 2007; Pentecost *et al.*, 2006). In goblet cells, mucous production alters cell folding to allow exposure of E-cadherin (Nikitas *et al.*, 2011). Despite contributions to invasion of other tissues (for example the fetoplacental infection; Lecuit *et al.*, 2004), InlB is not critical for crossing the intestinal epithelium, however its presence may increase the rate

at which endocytosis occurs (Pentecost *et al.*, 2010). InlB may also facilitate access into Peyer's patches of the intestine (Lecuit *et al.*, 2007)

In the traditional model, *L. monocytogenes* enters the cells of the GI endothelium in a phagosome. The pore-forming listeriolysin O and phospholipases C PlcA and PlcB are secreted from the cell to degrade the phagosome to release bacteria into the cytosol. ActA expression causes polymerisation of host cell actin into an actin 'comet' tail which enables the bacterium to move around the cell and 'push' into neighbouring cells. Entry from one cell into another results in the forming of a membrane-enclosed vacuole and the cells are released from the vacuole by the actions of LLO and phospholipase C. It has since been suggested that LLO and ActA, which polymerises host cell actin to form a comet tail for movement, are not usually required in crossing the GI tract membrane as *in vivo* studies now show that *L. monocytogenes* cells pass rapidly through the goblet cells into the lamina propria in pseudopod-like structures (Nikitas *et al.*, 2011; Disson & Lecuit, 2013). These proteins may be more important in later stages of infection and in macrophage escape (Disson & Lecuit, 2013; Veiga & Cossart 2005). Macrophages appear to be an important target for the bacteria and LLO and ActA play a prominent role in macrophage phagosome escape (Hamon *et al.*, 2012; Disson & Lecuit, 2013). When it does occur, movement directly between cells allows the bacterium to evade the humoral immune response system.

PrfA, the major virulence regulator, is a member of the Crp/Fnr transcription regulator family and directs transcription of genes involved in intestinal cell attachment, cell vacuole escape and cell-to-cell spread. Transcription of the 10 kb major virulence locus (LIPI-1) and other virulence genes have been found to be primarily PrfA-dependent, with *ΔprfA* strains shown to be avirulent (Vazquez-Boland *et al.*, 2001; Hain *et al.*, 2008, Mengaud *et al.*, 1991; Chakraborty *et al.*, 1992)

1.4 σ^B and the switch from saprophyte to pathogen

A key feature contributing to *L. monocytogenes*' success in different environments is its adaptability. In addition to the primary sigma factor SigA which guides transcription under normal cell conditions, *L. monocytogenes* possesses four alternative sigma factors which guide the transcriptional apparatus to specific promoter sites within the genome under different conditions: σ^L, σ^H, σ^C (the last of which is present in Class II lineages only) and SigB (σ^B), the general stress response (GSR) regulator (Glaser *et al.*, 2001; Chaturongakul *et al.*, 2008). The GSR regulon comprises hundreds of genes that are involved in stress protection, damage repair and the early stages of infection and invasion (Toledo-Arana *et al.*, 2009; Hecker *et al.*, 2007). PrfA may be the main virulence regulator but its expression and activation is tightly curtailed outside of the host and even in the early stages of infection (Toledo-Arana *et al.*, 2009). Thus σ^B plays a vital role in stress survival in the environment but also in enabling adaptation to the host from the external environment, particularly during the gastrointestinal stages of the infection.

Close to 300 genes have been identified as being directly or indirectly regulated by σ^B (Raengpradub *et al.,* 2008). These genes, identified by transcriptomic profiling, include transcriptional regulators, general stress proteins, genes required for glucose and amino acid metabolism, universal stress proteins (Hain *et al.*, 2008) cell wall associated proteins (Hain *et al.*, 2008), bile resistance genes, genes associated with motility repression (Raengpradub *et al.*, 2008; Toledo–Arana *et al.*, 2009) and genes associated with osmotic stress (Fraser *et al*., 2003; Abram *et al.*, 2008). The σ^B regulon comprises genes which are positively and negatively regulated by σ^B. Negative regulation is likely to occur via positive regulation of repressor genes. Current knowledge of the function of specific

components of the σ^B regulon is possibly restricted by the limited number of conditions under which transcriptome profiling has been carried out.

Not only is σ^B a core regulator, guiding transcription of multiple regulators but there is also considerable transcriptional cross-talk between this sigma factor and other regulators, highlighting its central role in adaptation (Hain *et al.*, 2008; Rangpaedub *et al.*, 2008). σ^B dependent transcription has been recorded for *prfA*, *clpC*, *hfq and* the chaperones *mcsA*, and *hrcA.* In addition, of 188 identified genes coregulated by a combination of σ^B, SigL, SigH, PrfA and the transcriptional repressor CtsR, the vast majority were coregulated by σ^B and one or more of these regulators. σ^B and SigH coregulated 92 genes, 31 genes were coregulated by σ^B and SigL, 37 genes by σ^B and CtsR and 10 genes by σ^B and PrfA (Chaturongakul *et al.*, 2011).

1.5 σ^B and virulence

Both σ^B and PrfA contribute to virulence, but are crucial to the pathogen's success in invasion and infection at different stages. σ^B regulates genes involved in the early stages of infection along with genes involved in energy and environmental stress protection (Ollinger *et al.*, 2008). Of 1206 genes whose expression is altered upon entry into the intestine, 232 displayed σ^B-dependent expression, indicating a central role for σ^B in the intestinal adaptation of the microorganism. Invasion of hepatocytes and enterocytes is significantly reduced for a Δ*sigB* strain and this appears to be directly related to the σ^B-dependent expression of InlA and InlB (Chaturongakul *et al.*, 2011; Kim *et al.*, 2005). The significant homology between *Bacillus subtilis*, *L. innocua and L. monocytogenes* σ^B pathways provides insight into the function of *L. monocytogenes* σ^B regulon genes. The

non-pathogenic *L. innocua* lacks approximately 15% of the genes in *L. monocytogenes*, most of which are linked to virulence (Cossart, 2011). At least 10 *L. monocytogenes* σ^B-regulated genes have no orthologues in *L. innocua*, including *inlH* and *bsh* (Hain *et al.*, 2008).

PrfA has a more narrowly defined focus, directing transcription of genes required for invasion, intracellular replication and cell-to-cell spread. This is reflected in its much smaller regulon comprising 73 genes (Ollinger *et al.*, 2008; Milohanic *et al.*, 2003). Conflicting data exist for the role of PrfA in invasion with the growth phase of cells apparently playing a critical role. Stationary phase *ΔprfA* show no invasion deficiency whereas contrasting results have been found for exponential phase cells (Kim *et al.*, 2005; Chaturongakul *et al.*, 2011). Transcription of the virulence locus has been found to be primarily PrfA-dependent and σ^B is not required for adaptation to the blood. While some σ^B-dependent genes are upregulated in the host cell, *ΔsigB* mutant strains show no defect in intracellular growth (Chatterjee *et al.*, 2006)

As discussed in Section 1.4., there is some overlap between these two regulons. Genes that carry both PrfA and σ^B recognition sequences upstream of start sites include internalin genes *inlA* and *inlB*, *prfA* itself and *bsh* (bile salt hydrolase): a gene which possesses a PrfA recognition site but does not appear to be affected by the presence of PrfA. (Dramsi *et al.*, 1993; Kazmierczak *et al.*, 2003; Dussurget *et al.*, 2002; Ollinger *et al.*, 2008; Nadon *et al.*, 2002). PrfA transcription can be directed from three different promoters: P_{prfAP1},P_{prfAP2} and P_{plcA}. P_{prfAP2} is a σ^B-dependent promoter, although transcription from this promoter appears to be primarily required for expression of PrfA in the transition to the host environment and does not contribute to intracellular PrfA expression (Schwab *et al*., 2005; Nadon *et al*., 2002; Kazmierczak *et al*., 2006; Freitag *et al*., 1993).

1.6 σ^B and environmental stress

As mentioned in Section 1.4, σ^B plays a role in the bacterium's adaptation to the host, but also in its environmental survival. *L. monocytogenes* encounters multiple stresses in the external environment and has shown an ability to suvive and persist in food and food-processing plants (Muhterem-Uyar *et al*., 2015). Hazard analysis and critical control points (HACCP) systems are employed to achieve food safety from biological, chemical, and physical hazards in production processes and food storage by designing measurements to reduce these risks to a safe level. These include the addition of preservatives such as osmotic or acidic agents to food and the use of multiple cleaning agents and regimes to prevent persistence of the bacterium in processing environments. The use of multiple, rather than one strong, hurdle or barrier to growth has proven to be more effective for pathogen containment in food processing areas (Leistner, 2000). Despite this, analyses of *Listeria* species distribution in food-processing factories have identified drains, floors, standing water and food contact sufaces as common resevoirs of *Listeria monocytogenes* (Leong *et al*., 2014; Cox *et al.,* 1989; Muhterem-Uyar *et al*., 2015). σ^B contributes to the bacterium's growth and survival in the presence of stress agents employed.

1.6.1 Osmotic stress

L. monocytogenes encounters osmotic stress in the natural environment, in food processing plants and on entry into the host. It has developed mechanisms to cope with this stress and can grow in media containing up to 2 M NaCl and survive in up to 3 M

NaCl (Cole *et al.*, 1990). Although not absolutely required, σ^B plays an important role in salt adaptation and at low salt concentrations can even hinder growth (Becker *et al.*, 1998; Abram *et al.*, 2008). One mechanism by which *L. monocytogenes* survives salt stress is through the uptake of osmolytes; small compatible solutes which act as osmoprotectants. *L. monocytogenes* preferentially accumulates glycine betaine and carnitine osmolytes through several different uptake systems. Removal of the σ^B-dependent gene *opuC* has been shown to result in lowered cell glycine betaine levels and an inability to utilize carnitine as an osmprotectant (Fraser *et al.*, 2003; Sleator *et al.*, 2001). Among many other σ^B-dependent genes that are known to be upregulated during salt adaption, the *ctc* gene has been shown to play a critical role in salt survival in the absence of osmoprotectants (Gardan *et al.*, 2003), although its function remains elusive.

Salt adaptation initiates cross protection against other stresses through the upregulation of stress protection genes, some of which are under σ^B regulation. Abram *et al.*, (2008) detected the upregulation of several σ^B-dependent genes, including acid resistance genes, and genes implicated in osmotic stress protection during salt stress At higher temperatures, salt adaptation can induce virulence gene transcription, such as the σ^B regulated *inlA* and *inlB* (Bergholz *et al*., 2012). Bergholz *et al.*, (2012) also observed an increase in the transcription of σ^B-dependent bile resistance genes, including *bilE*, *opuCA*, and *bsh* (Sleator *et al.*, 2005; Fraser *et al.*, 2003; Kazmierczak *et al.*, 2003). This cross protection phenotype is reflective of the typical stress protection requirements of *L. monocytogenes;* it is more likely that the cell would encounter multiple stresses such as during entry into the host or in the natural environment, rather than a single stress (Hecker *et al.*, 2007).

1.6.2 Acid stress

L. monocytogenes is subjected to acid stress in a range of environments including; on entry into the host stomach, in the host cell vacuole, in pickled and acid-preserved foods and in food processing environments. Strains have been shown to survive at pH conditions as low at pH 2.7 thanks to the presence of several acid tolerance systems including the glutamate decarboxylase (GAD) system, the arginine deiminase system, and the adaptive acid tolerance response system (ATR) (Davis *et al.*, 1996; Cole *et al.*, 1990; Smith *et al.*, 2013; Ryan *et al.*, 2009; Cotter *et al.*, 2001).

As is the case for osmotic stress, acid stress-mediated activation of σ^B results in upregulation of a number of stress response and virulence genes including *hrcA, bsh* and *inlA* (Ivy *et al*., 2012; Sue *et al.*, 2004, Wemekamp-Kamphuis *et al.*, 2004). σ^B contributes to acid survival via a number of mechanisms and loss of σ^B is associated with increased acid sensitivity in both exponential and stationary phase, although both wild-type (WT) and Δ*sigB* strains have been shown to develop increased resistance on entry into stationary phase (Ferreira *et al.*, 2003; Wiedmann *et al.*, 1998). The extent of the σ^B contribution varies between lineages. σ^B appears to be most important for acid survival in Lineage II strains while no significant difference has been recorded in survival between WT and Δ*sigB* strains from Lineage IIIA (Oliver *et al.*, 2010).

The GAD system decarboxylates glutamate to γ-aminobutyrate (GABA). This process consumes a proton and the intracellular pH of the cell is raised as a result. GABA is then typically, but not always, exported out of the cell via an antiporter in exchange for extracellular glutamate (Feehily *et al.*, 2014). Expression of several genes involved in the GAD system (GadD3, and GadD2 and GadT2 genes located on the same operon) has

been found to be under σ^B regulation, however there does seem to be variation in σ^B dependence between strains (Wemekamp-Kamphuis *et al.*, 2004, Abram *et al.*, 2008a; Kazmierczak *et al.*, 2003; Bowman *et al.*, 2012). In the arginine deiminase system the σ^B-dependent arginine deiminase Lmo0043 contributes to the processing of arginine into ornithine, which can be exchanged for more extracellular arginine molecules and carbon dioxide and ammonia, which interact with cytoplasmic ions to raise the intracellular pH and protect against acid damage (Ryan *et al.*, 2009; Cunin *et al.,* 1986; Hain *et al.*, 2008). Pre-exposure to a mild acid stress also increases acid tolerance of both exponential and stationary phase *L. monocytogenes* in a manner that is partially σ^B-dependent (Davis *et al*., 1996; Ferreira *et al.*, 2001; Ferreira *et al.*, 2003). However the molecular basis for this acid tolerance response (ATR) is still unclear.

1.6.3 Light stress

Concurrent with the rise in research examining bacterial photoreceptors, new attention has been focused on the use of visible light as a mechanism of bacterial inactivation (Maclean *et al*., 2014). Visible light has been shown to be generally less effective than ultraviolet (UV) light for bacterial inactivation purposes but it carries fewer associated health and safety risks for workers and is less damaging to surfaces (Maclean *et al.*, 2009; Kütting & Drexler, 2009; Andrady *et al.*, 1998). Studies have found that the inactivation levels produced by shorter wavelength blue light are greater than those achieved using longer light wavelengths (Nussbaum *et al*., 2002; Kumar *et al*., 2015). *L. monocytogenes* has been shown to be a suitable candidate for visible light inactivation, via photodynamic inactivation (PDI) with photosensitizers or by blue light alone (Lin *et*

al., 2012 Murdoch *et al.*, 2011; Endarko *et al*., 2012; Kumar *et al.*, 2015). Blue-violet light at a wavelength of 405 nm has been shown to be an effective inactivating agent for a range of bacteria, although it appears to be more deleterious for Gram-positive strains (Kumar *et al.*, 2015; McKenzie *et al.*, 2014; Maclean *et al.*, 2009; Murdoch *et al.*, 2011; Endarko *et al*., 2012).

Blue light has been shown to activate the *L. monocytogenes* GSR in a σ^B-dependent manner via the blue light receptor Lmo0799 (Tiensuu *et al.*, 2013; Ondrusch & Kreft, 2011). Red light has been shown to increase σ^B activity levels to a lesser degree, but the mechanism by which red light influences σ^B activation is not yet known (Ondrusch & Kreft, 2011). In *B. subtilis* red light (620-750 nm) is sensed through the RsbP/Q signalling pathway but this pathway does not exist in *L. monocytogenes* (Avila-Perez *et al.*, 2010). *L. monocytogenes* behaves similarly to blue and red light under some, but not all conditions (Ondrusch & Kreft, 2011). Both wavelengths can induce transcription of σ^B regulated internalins InlA and InlB, but only blue light inhibits swimming motility at 27 °C, in a σ^B-dependent manner (Ondrusch & Kreft, 2011; Tiensuu *et al.*, 2013). Red light (625 nm) induction of σ^B activity reporter genes was observed in a *Δlmo0799* strain and an additional stress was required to produce similar effects in the WT strains, suggesting that Lmo0799 is not responsible for red light sensing.

Research shows that the presence of light can stimulate the production of harmful reactive oxygen species (ROS) in some bacteria and while this has not been confirmed for *L. monocytogenes*, activation of the GSR may counteract any light-induced damage (Nitzan *et al*., 2004). The ability to sense light has multiple benefits for the bacterium. In the environment, light may also alert the cell to inhospitable environments, such as at the surface of the soil where predation, osmotic and other stresses are present. Alternatively,

light has also been suggested to act as a virulence priming agent, preparing the cell for entry into a new host following shedding from previous hosts (Hecker *et al*., 2007).

1.6.4 σ^B and biofilm

In the environment *L. monocytogenes* cells can move from a planktonic to a sessile biofilm lifestyle. Biofilms have been defined as cell aggregates adhered to each other and/or to surfaces or interfaces by extracellular polymeric substances (Costerton *et al.*, 1995). For biofilm formation to occur, planktonic cells must first adhere to a surface, and the bacteria then reproduce and produce extracellular polymeric substances which protect the cells. With time, a mature biofilm is formed with channels for nutrient influx and waste product efflux (Stoodley *et al.*, 2002). Biofilm offers many advantages to cells in suboptimal conditions, and *L. monocytogenes* biofilms are commonly formed in the environment. Host-associated biofilms have not been identified but the presence of bile has been shown to induce biofilm formation, suggesting that biofilm formation in the intestines could enable successful evasion of the host's defences (Begley *et al.*, 2009). Studies have concentrated on the problems posed by *L. monocytogenes* biofilm in food processing environments. These biofilms can be formed on a range of surfaces, including hydrophilic and hydrophobic materials and have proven more resistant than planktonic cells to disinfectants and sanitizers, acids, antimicrobials, and desiccation (Chavant *et al.*, 2002; van der Veen & Abee, 2010; da Silva *et al.*, 2013; Stewart & Costerton, 2001; Cabeça *et al.*, 2012; Elasri & Miller, 1999). The *L. monocytogenes* biofilm matrix is a complex structure consisting of carbohydrates, proteins and extracellular DNA. Carbohydrates identified include techoic acids and poly-β-(1,4)-N-acetylmannosamine

with terminal α-1,6-linked galactose (ManNAc-Gal) (Brauge *et al.*, 2016; Köseoğlu *et al.*, 2016). Several surface proteins have been identified in the extracellular matrix including InlA, PlcA, FlaA and ActA (Franciosa *et al.*, 2009; Lourenco *et al*, 2013). The extracellular DNA is thought to aid both structure and nutrition of cells in the biofilm (Guilbaud *et al.*, 2015; Zetzmann *et al.*, 2015). Extracellular DNA from lysed bacteria cells appears to promote bacterial adherence to surfaces in the early stages of biofilm formation (Harmsen *et al.*, 2010). Screening of a transposon mutagenesis library identified 38 genes involved in biofilm formation (Alonso *et al.*, 2014). Several of these genes are required for flagellar motility which is believed to be required for initial adherence (Lemon *et al.*, 2007; Alonso *et al.*, 2014). σ^B has been shown to contribute to biofilm formation at 30 °C and lower temperatures, under both continuous and static biofilm production conditions. (Lemon *et al.* 2010; van der Veen & Abee, 2010). The exact role of σ^B in promoting biofilm is unknown but it is interesting that σ^B plays a role in motility repression via control of flagella repressors MogR and a flagellum biosynthesis excludon (Toledo-Arana *et al.*, 2009; Kamp & Higgins, 2011).

1.7 Activation of σ^B

1.7.1 The pulsatile activation of σ^B

Fluorescent microscopy analysis of a *B. subtilis* strain carrying a *yfp* gene fused to a P_{sigB} promoter enabled Locke *et al.* (2011) to determine that energy stress activates *B. subtilis* σ^B protein in random (stochastic) pulses of activation. As the external stress increases in intensity or concentration, so too does the frequency of pulsing of σ^B activation (Locke *et*

al, 2011). However, environmental stress causes a single σ^B activation pulse homogenously across cells. The pulse amplitude, but not duration is increased by increases in the concentration of external stress (Young *et al.*, 2013). Additionally, the rate at which stress is added to the cells' environment affects the pulse amplitude, with rapidly occurring stresses increasing the pulse amplitude. A slow increase in stress addition has a diminishing effect, with a 400 min ramp in ethanol or sodium chloride addition resulting in almost no detectable σ^B activity. This rate-responsive activation of σ^B allows cross protective action between σ^B and other gene regulators (PrfA, SigA, etc) under fast stresses but at slower stresses, σ^B is reduced in activity, or prevented from action, and stress-specific responses are primarily responsible for cell repair and protection (Young *et al.*, 2013). It may be assumed that both energy and environmental stress activation of σ^B in *L. monocytogenes* follow this latter model as both energy and environmental stresses are integrated via a pathway similar to the *B. subtilis* environmental stress pathway (Chaturongakul & Boor, 2004).

1.7.2 The *sigB* operon

Activation of the expansive σ^B regulon is energetically costly and is therefore disadvantageous for the cell under normal growth conditions. For this reason its activity is tightly controlled via a pathway consisting of multiple protein-protein interactions. Most of this pathway's protein effectors are encoded by the *sigB* operon. The *L. monocytogenes sigB* gene is located on an 8 gene operon: *rsbR-rsbS-rsbT-rsbU-rsbV-rsbW-sigB-rsbX*, with a SigA–dependent promoter upstream of *rsbR* and an internal σ^B -dependent promoter upstream of *rsbV* (Glaser *et al.*, 2001; Ferreira *et al.*, 2004). This structure replicates that of the *B. subtilis sigB* operon and the σ^B activation pathway has

been best described in the *B. subtilis* model (Wise & Price, 1995; Kalman *et al.*, 1990; Hecker *et al.*, 2007).

1.7.3 The σ^B activation cascade

The *L. monocytogenes* σ^B activation cascade is thought to follow the better studied model in *B. subtilis* (Fig. 1.2). In the unstressed *B. subtilis* cell σ^B is present but sequestered by the antisigma factor protein RsbW, which prevents σ^B from interacting with RNA polymerase (Benson & Haldenwang, 1993). The RsbW kinase will dissociate from RsbW-σ^B complexes to bind the unphosphorylated form of the anti-antisigma factor RsbV for which it has a higher binding affinity (Dufour & Haldenwang, 1994). However, in the absence of stress RsbV is predominantly phosphorylated through the kinase activity of RsbW and in this form is unable to bind to RsbW (Dufour & Haldenwang, 1994).

Stress signals are detected by stressosome molecules, causing phosphorylation of stressosome RsbS and RsbR proteins and dissociation of RsbT (Kim *et al.*, 2004 Chen *et al.*, 2003; Yang *et al.*, 1996; Akbar *et al.*, 1997; Gaidenko *et al.*, 1999; Kim *et al.*, 2004a). RsbT then interacts with RsbU which, like RsbX, belongs to the PP2C subgroup of phosphatases (Yang *et al.*, 1996). RsbU shares similarities with RsbX at its C-terminal end which is the region of phosphatase activity (Yang *et al.*, 1996; Delumeau *et al.*, 2004). RsbT is thought to interact with the N-terminal region of RsbU phosphatase, and this interaction induces activity at the RsbU C-terminal end (Yang *et al.*, 1996; Delumeau *et al.*, 2004). Once activated, RsbU removes the phosphate group from RsbV-P, allowing RsbV to compete for RsbW (Dufour & Haldenwang, 1994; Yang *et al.*, 1996). RsbU appears to act on RsbV-P in an RsbU-RsbT complex; however it is still not known

whether RsbU activity is retained for some time after RsbT dissociation from RsbU-T (Delumeau *et al.*, 2004). As RsbW now interacts with dephosphorylated RsbV, σ^B is free to interact with RNA polymerase and direct it to stress response gene promoter sites (Benson & Haldenwang, 1993; Dufour & Haldenwang, 1994; Hecker *et al.*, 2007). RsbX acts to dephosphorylate the RsbS-P and RsbR-P components of the stressosome to allow RsbT to recomplex with the stressosome (Yang *et al*, 1996; Smirnova *et al.*, 1998; Chen *et al.*, 2004). This function of RsbX tempers over-activation of σ^B during prolonged stress conditions and resets the ground state in the absence of stress (Yang *et al.*, 1996; Smirnova *et al.*, 1998; Chen *et al.*, 2004).

As the stress signal recedes, the majority of RsbT proteins recomplex with the stressosome, the stock of RsbV becomes phosphorylated by RsbW and RsbW then preferentially interacts with σ^B. While the exact function of each of the homologues of these components in *L. monocytogenes* has not been tested, the requirement for RsbT, RsbV and RsbU for σ^B activation in response to energy and environmental stress has been confirmed suggesting the σ^B activation cascade is the same as, or at least highly similar to, the model proposed to operate in *B. subtilis* (Chaturongakul & Boor, 2004; 2006; Shin *et al.*, 2010).

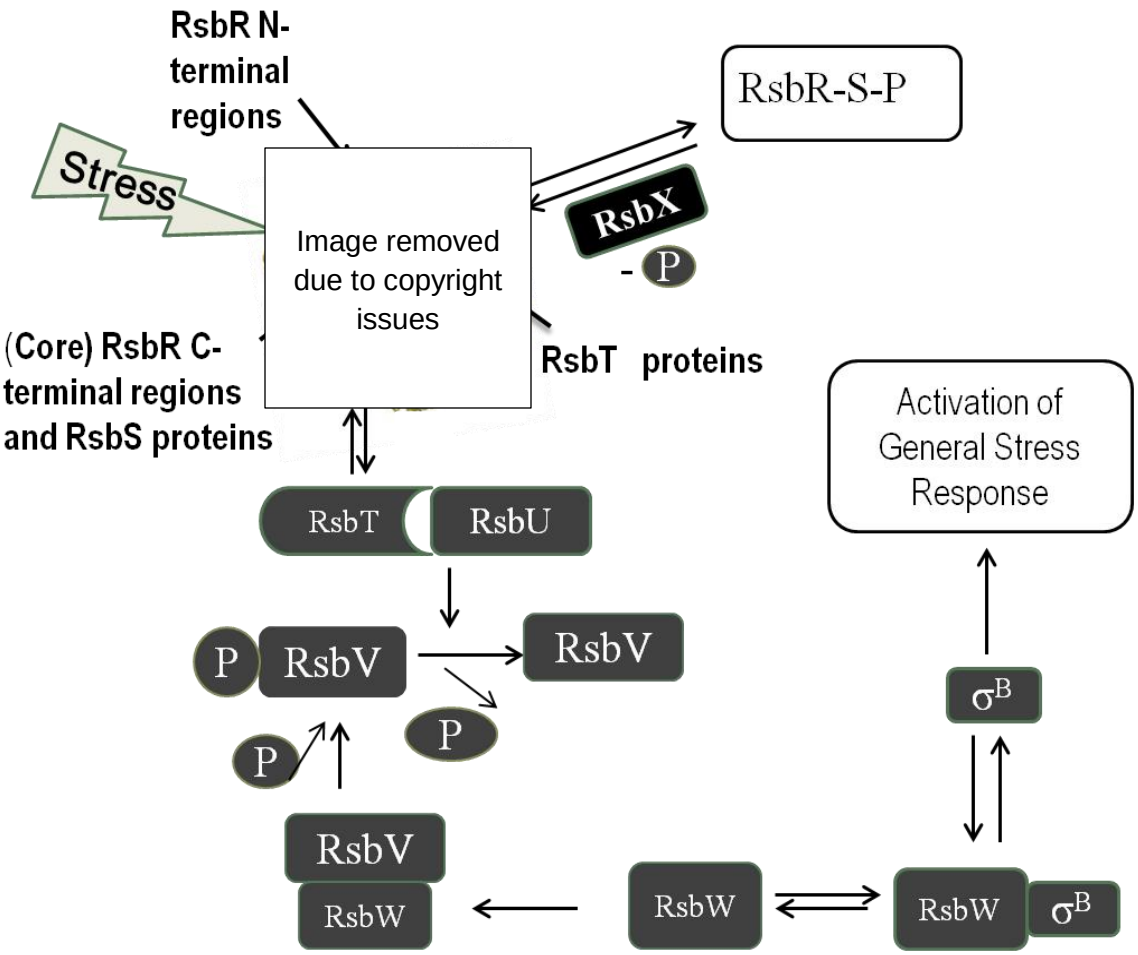

Figure 1.2 σ^B activation pathway. The stressosome complex which interprets stress signals consists of RsbR, RsbS and RsbT proteins. Stress signals are thought to be transduced to the stressosome core via the RsbR N-terminal regions. Phosphorylation events and other conformational changes within the stressosome lead to the release of RsbT. RsbT activates the phosphatase ability of RsbU. RsbU dephosphorylates the phosphorylated form of RsbV, allowing RsbW to release σ^B and bind to RsbV. σ^B can now activate the GSR. RsbX dephosphorylates RsbS (and RsbR). As stress signals are removed from the cell, RsbT recomplexes with the stressosome, RsbV supplies become phosphorylated and RsbW rebinds to σ^B. Stressosome image taken from Marles-Wright *et al.*, 2008.

1.8 The stressosome

Upstream of the σ^B activation pathway in *B. subtilis* lies a 1.5-1.8 kDa sensory complex known as the stressosome (Marles-Wright *et al.,* 2008; Marles-Wright & Lewis, 2010). The stressosome allows the integration of signals from a multitude of different stresses into a single output system, resulting in the activation of σ^B (Delumeau *et al.*, 2006; Marles-Wright *et al.*, 2008). All genes required for stressosome formation are conserved in *L. monocytogenes* and studies into the *L. monocytogenes* and *B. subtilis* σ^B activation pathways have accepted the well characterised *B. subtilis* stressosome- led pathway as a model. A recently presented oral paper by one of the leaders in research into *L. monocytogenes* behaviour has provided confirmation of the presence of the stressosome construct in *L. monocytogenes*, giving further validity for the approach taken by previous studies (Cossart, 2016).

B. subtilis has two main characterized pathways for σ^B activation. As well as the stressosome-led pathway that responds to environmental stress, the phosphatase RsbP is activated by RsbQ in response to energy depletion and this in turn modulates the phosphorylation state of RsbV independently of RsbT (Kang *et al.*, 1996; Yang *et al*,. 1996; Vijay *et al.*, 2000; Voelker *et al.*, 1995). Both pathways converge to activate σ^B (Fig. 1.3). Here, *L. monocytogenes* differs from *B. subtilis* as BLAST searches have failed to find RsbQ/P homologues in σ^B regulation pathways outside of the *B. subtilis* genome (Ferreira *et al.*, 2004) and the *L. monocytogenes* stressosome appears to have the ability to interpret both environmental and energy stresses (Chaturongakul & Boor, 2004; Chaturongakul & Boor, 2006). In addition, replacement of the *B. subtilis* sensory RsbR proteins with *L. monocytogenes* RsbR homologue also enabled energy stress stimulated

σ^B activation in *B. subtilis* via stressosome interactions (Martinez *et al.*, 2010). This is interpreted to mean that the *L. monocytogenes* stressosome sensory components differ from RsbRA in that these proteins can detect energy stress as well as environmental stress.

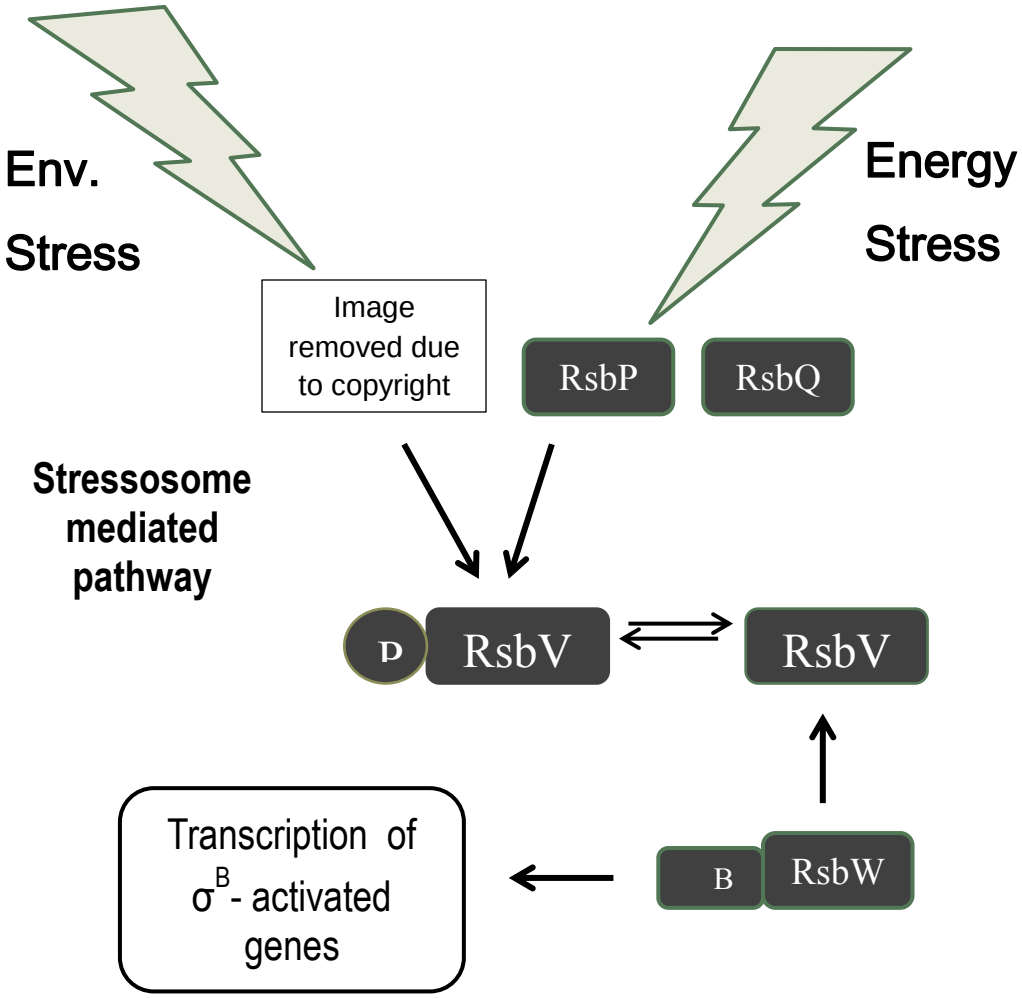

Figure 1.3 Energy stress and environmental stress σ^B activation in *B. subtilis.* Environmental stresses are signalled to the σ^B unit via a stressosome led pathway as outlined in Section 1.8.3. In *B. subtilis* energy stresses are intercepted by the PsbPQ phosphatase-hydrolase pathway in a manner which is not fully understood. Both RsbP, activated via the energy stress pathway, and RsbU, activated via the environmental stress pathway, act to dephosphorylate RsbV. In *L. monocytogenes* energy and environmental stresses are intercepted by the stressosome pathway. Stressosome image taken from Marles-Wright *et al.*, 2008.

1.8.1 Stressosome composition and interactions

In vitro analysis has found that the stressosome core is composed of 20 copies each of RsbS and RsbT and 40 RsbR proteins paralogues from which the N-terminal regions of the RsbR putative sensory proteins protrude (Marles-Wright *et al*., 2008). Five RsbR protein paralogues have been identified in *L. monocytogenes*: RsbR, Lmo0161, Lmo1642 and Lmo1842 and Lmo0799 (Heavin & O'Byrne, 2012; Ondrusch & Kreft, 2011). When stress signals are intercepted by the *B. subtilis* stressosome, conformational changes occur at the core which lead to its dissolution and the release of RsbT (Yang *et al.*, 1996; Chen *et al.*, 2003). RsbT, RsbRA and RsbS are coexpressed from the same promoter at similar levels; however RsbT appears to be the limiting factor in stressosome formation where it is present in the cell at 10% of the RsbRA protein level (Reeves *et al.*, 2010; Zhang *et al.*, 2005; Chen *et al.*, 2003). The proper functioning of RsbT seems to be strongly dependent on its coexpression with RsbR and RsbS (Chen *et al.*, 2004). Zhang *et al.* (2005) posit that RsbS exerts a stabilizing influence on the RsbT protein, preventing it from misfolding and that RsbT proteins that do not complex with RsbS or RsbU following synthesis are prone to misfolding and are then degraded. As supporting evidence, they show that when RsbT is expressed at a different locus, σ^B is not activated in response to stress unless RsbT is over-expressed.

The interactions that lead to expulsion of RsbT are only partially understood and much remains unknown as to how signals are transmitted to the stressosome and interpreted within the stressosome core. Outside of the stressosome RsbT acts to activate the RsbU phosphatase but within the stressosome complex it exercises its function as a serine threonine kinase on the RsbR and RsbS proteins (Yang *et al.*, 1996; Gaidenko *et al.*, 1999). The RsbS antagonist protein is a small protein comprising a sulphate transporters

and anti-sigma factor antagonist (STAS) domain with a conserved serine residue at position 56 in *L. monocytogenes* (position 59 in *B. subtilis*) which become phosphorylated upon stress signalling (Kim *et al.*, 2004; Kang *et al.*, 1996). Removal of the *rsbS* gene causes a massive upregulation in σ^B activity (Kang *et al.*, 1996). *In vitro* studies with *B. subtilis* have shown that phosphorylation at this residue creates a negative charge which decreases RsbS-RsbT binding (Kang *et al.*, 1996; Yang *et al.*, 1996). Prevention of phosphorylation at this residue restricts the cell's ability to activate σ^B, as observed for a *B. subtilis rsbS* S59A mutant which failed to activate σ^B in response to salt stress (Kang *et al.*, 1996). Thus phosphorylation of RsbS by RsbT has been credited with causing the release of RsbT from the stressosome. RsbS cannot capture RsbT alone and must complex with its co-antagonist RsbR (and its paralogues) to capture RsbT (Chen *et al.*, 2003; Akbar *et al.*, 2001; Akbar *et al.*, 1997; Kim *et al.*, 2004).

Questions remain over whether additional stress input signals occur following release of RsbT from the stressosome in *L. monocytogenes*. Utratna *et al.*, (2014) found significant RsbV-independent cold stress-induced σ^B activation during exponential growth, although whether this is due to signal inputs downstream of the stressosome, an inherent instability of RsbW or changes in the RsbW: σ^B ratio at colder temperatures is not known. Shin *et al.*, (2010) proposed that energy stress signals enter the σ^B activation cascade downstream of RsbT, although this conflicts somewhat with the findings that a *B. subtilis* strain carrying *L. monocytogenes* RsbR in place of its own RsbR paralogues developed stressosome-mediated activation of σ^B in response to energy stress (Martinez *et al.*, 2010).

It also appears that there may be additional means by which RsbT is induced to activate RsbU (Gaidenko *et al.*, 2014). When RsbS S59 in *B. subtilis* is altered to prevent phosphorylation (S59A), σ^B activity is reduced but not abolished upon exposure to

ethanol. A *B. subtilis rsbS* S59A strain retained 13% of the WT strain σ^B activity after exposure to 4% ethanol whereas a *ΔrsbU* strain was unable to stimulate a detectable increase. The authors suggest that this result is due to an additional input into the system, although it may simply be due to a residual ability of RsbR and RsbS S59A to allow some release of RsbT from the stressosome.

1.9 RsbR proteins

Within the stressosome the RsbR proteins are thought to have three main functions: to aid RsbS capture of RsbT, to promote the RsbS phosphorylation event and to act as stress sensor proteins. Stress sensing is thought to occur via the protruding N-terminal regions of the RsbR paralogues (Murray *et al*., 2005; Marles-Wright & Lewis, 2010). Of these proteins, only Lmo0799 has a confirmed function as a blue light photoreceptor (Ondrusch & Kreft, 2011). The N-terminal regions of these proteins are highly variable, differing in sequence from the *B. subtilis* homologues RsbRA,-RB, -RC, -RD (formerly RsbR, YkoB, YojH and YqhA) and YtvA (Murray *et al.*, 2005; Akbar *et al.*, 1997; Kim *et al.*, 2004a). The C-terminal regions are much more conserved, consisting of STAS domains which are called after sulphate transporters and antisigma-factor antagonists (Ondrusch & Kreft, 2011; Chen *et al.*, 2003; Aravind & Koonin, 2000). For example RsbR shares 22% identical amino acids in its N-terminal region but 77% identical amino acids at the C-terminus with RsbRA of *B. subtilis*. Each *rsbR* paralogue is located at a different transcriptional locus, with *rsbR* co-transcribed with *rsbS* and *rsbT* (Ondrusch & Kreft, 2011). None of these genes appear to be directly regulated by σ^B, however, *lmo0161*

transcripts are increased 2.2 fold in the WT strain compared to a σ^B deletion strain in stationary phase (Starr *et al.*, 2010).

1.9.1 RsbR phosphorylation and stressosome structure

RsbR has two phosphorylateable residues T175 and T209 (T171 and T205 in *B. subtilis*) (Gaidenko *et al.*, 1999; Ondrusch & Kreft, 2011). Phosphorylation of T171 and T205 appears to be RsbT-dependent but it seems the effects of phosphorylation have opposing results. It appears that RsbT-mediated phosphorylation of the RsbRA T171 promotes (but does not cause) RsbT phosphorylation of RsbS (Akbar *et al.*, 2001; Kim *et al.*, 2004; Eymann *et al.*, 2007). Phosphorylation of RsbRB, RC, and RD, as for RsbRA at T171 was found to occur during exponential growth. Phosphorylated RsbRC seems to be expressed at very low concentrations and no changes in response to any stress/starvation condition could be observed. Phosphorylation was found to occur at residues T186 and T181 for RsbB and RsbD, respectively (Eymann *et al.*, 2007). *In vivo* experiments have shown that RsbRA phosphorylated at T205 is not found in the unstressed cell in significant quantities and only develops upon exposure to strong stresses which negatively affect growth rate. Eymann *et al.*, (2011) found that a mutant carrying a non-phosphorylateable T205A substitution actually displayed increased σ^B activity under stress conditions compared to the WT strain. Based on these observations, they propose that the phosphorylation of T205 acts to mitigate overstimulation of the general stress response. Interestingly, while RsbRB also showed an increase in phosphorylation at T220 following strong stress, σ^B activity in a RsbRB T220A remained

similar to the WT (Eymann *et al.*, 2011). YtvA and Lmo0799 do not carry conserved threonines (Akbar *et al*., 2001; Ondrusch & Kreft, 2011).

1.9.2 Sensing functions of RsbR and RsbR paralogues

Little is known about how stress signals are detected by the stressosome. That the *L. monocytogenes* RsbR can function in *B. subtilis* to allow a successful σ^B-mediated response to physical stress, albeit with higher background levels of σ^B activity than in the WT *B. subtilis* strain, suggests that the stress signals remain similar between the two micro-organisms (Martinez *et al.*, 2011). Interestingly, the *L. monocytogenes* RsbR activated *B. subtilis* σ^B in response to energy stress as well as environmental stress. However this only occurred when all other native *B. subtilis* RsbR paralogues were absent (Martinez *et al.*, 2011). The majority of research into the function of the RsbR proteins has been carried out with the *B. subtilis* homologues. In *B. subtilis*, removal of all four RsbR (A,B,C,D) proteins results in constitutively active σ^B, however the presence of only one RsbR paralogue (but not YtvA) is enough to act as a co-antagonist with RsbS to block σ^B activation, although not to WT levels for RsbRC and RsbRD (Akbar *et al*., 2001; Kim *et al.*, 2004a; Reeves *et al.*, 2010). In the presence of other non-light-associated stresses, YtvA acts as a positive regulator that ameliorates the signalling of other RsbR proteins (Akbar *et al*., 2001). Unlike the other RsbR paralogues, the presence of YtvA alone, in the absence of other RsbR paralogues, does not prevent the activation of σ^B under normal cell conditions (Akbar *et al*., 2001). In several studies its contribution to stress sensing and stressosome formation has been considered irrelevant (Reeves *et al.*, 2010, Martinez *et al.*, 2011).

Even when RsbRD, found to be expressed at a low level just above detectable limits in unstressed cells, was placed under the control of the *sigB* operon promoter directly upstream of the *rsbRA* gene (which it replaced) to increase its abundance to RsbRA levels, it continued to allow higher background σ^B activity in the absence of all other RsbR proteins, despite an increase in stressosome abundance (Reeves *et al.*, 2010). RsbRD, and RsbRC, also enabled nutritionally induced σ^B activation when expressed as the sole RsbR protein, again, even when expressed from the *sigB* operon (Martinez *et al.*, 2011). This suggests that the nutritional stress sensing observed is a feature of the RsbRD N-terminal region rather than a side-effect caused by insufficient amounts of RsbR protein for stressosome construction. Surprisingly, in a strain that expresses both RsbRC and RsbRD, nutritional stress was only half as effective at activating σ^B as a strain expressing each of these genes singly (Martinez *et al*., 2010). It has been shown repeatedly that RsbRA and RsbRB are similar but not identical co-antagonists (Kim *et al*., 2004a; Eymann *et al.*, 2011; van der Steen *et al.*, 2012; Reeves *et al.*, 2010). Under certain conditions RsbRB may act as a negative regulator of σ^B activity, as seen in YtvA-mediated light induction of the GSR (Akbar *et al*., 2001; van der Steen *et al*., 2012). Increasing additions of RsbRB decreased the cells response to light stress. RsbRA and RsbRD have been shown to interact with all RsbR proteins, whereas RsbRB and RsbRD do not interact with YtvA and YtvA has been shown to localize away from the stressosome in strains expressing RsbRB, but not RsbRA,-C, or -D (Akbar *et al.*, 2001, van der Steen *et al*,. 2012). Given the low levels of RsbRD in the cell this may indicate that RsbRA plays a structural role in the cell. The implications of these findings for RsbR are unknown at present.

1.9.3 Sensing mechanisms of the RsbR proteins

Several possible theories have been put forward to explain how the RsbR co-antagonists function in sensing stress, none of which can yet be discounted. Firstly, it has been suggested that each of the sensors senses a different array of stresses, for example as Lmo0799 senses blue light. While some results with the *B. subtilis* RsbR homologues may suggest this is not the case, there is no data in *L. monocytogenes* to prove otherwise. Alternatively, it has been suggested that these proteins respond to the same stress signals, but at different sensitivities or thresholds. This would enable a sophisticated response, tailoring the response to the size of the stress. A third proposal, somewhat of a composite of the previous two suggests that one stress can generate multiple signals and that the RsbR proteins differ in their ability to detect these signals, perhaps caused by differences in binding affinity to signal molecules.

To date, no information is available about the function of the *L. monocytogenes* Lmo0161, Lmo1642 and Lmo1842 proteins and only one study has examined the function of RsbR (Martinez *et al.*, 2010). Close examination of the only RsbR paralogue with a defined function, Lmo0799, and elucidation of its mechanism of function, may provide some insights into the mechanism for stress sensing in *L. monocytogenes.*

1.10 The unique role of Lmo0799

As *L. monocytogenes* is widely found in the environment (Hecker *et al.*, 2007) it is not surprising that it possesses specific factors enabling it to sense and react appropriately to the presence of light. The blue light photoreceptor Lmo0799 has been shown to facilitate this sensory function (Ondrusch & Kreft, 2011). While Lmo0799 also possesses a C-terminal STAS domain, it differs from the other *L. monocytogenes* RsbR-like proteins in that it possesses a Light, Oxygen or Voltage (LOV) domain at its N-terminal region (Fig. 1.4A). Lmo0799 shares significant similarity with YtvA, its homologue in *B. subtilis*, and varying degrees of similarity with other LOV domain-containing photoreceptors found across a number of bacterial species (Losi *et al.*, 2002; Losi *et al.*, 2003).

1.10.1 Lmo0799 LOV structure

LOV domains belong to a subgroup of the Per-Arnt-Sim domain superfamily and function as flavin-binding blue-light photosensors (Taylor & Zhulin, 1999; Christie *et al.*, 1999; Herrou & Crosson, 2011; Salomon *et al.*, 2002). Initially identified in plants, the *B. subtilis* YtvA protein was the first confirmed bacterial LOV-carrying photoreceptor (Huala *et al.*, 1997; Losi *et al.*, 2002; Losi *et al.*, 2003; Gaidenko *et al.*, 2006). Since then, the number of identified LOV proteins has increased considerably. A recent bioinformatics study identified over 6,700 LOV-containing proteins among archaea, bacteria (1146), fungi, protists and land plants (Glantz *et al.*, 2016). In bacteria, LOV domains are coupled to a diverse variety of effector domains (Losi, 2004; Crosson *et al.*, 2003; Herrou & Crossson, 2011; Glantz *et al.*, 2016). LOV-STAS proteins, which include YtvA and Lmo0799,

account for 1.5% of the total LOV-domain proteins identified, but approximately 9% of bacterial LOV-domain containing proteins (Glantz *et al.*, 2016; Herrou & Crosson, 2011). The LOV domain structure consists of a 5-stranded anti-parallel β-sheet and helical connectors (Herrou & Crosson, 2011). A flavin cofactor is held in a pocket by hydrophobic interactions and hydrogen bonding (Crosson & Moffat, 2001). The cysteine residue of the core conserved sequence motif GXNCRFLQ (X being any amino acid) is located a short distance from the 4a carbon of the flavin molecule (Losi, 2004). Typically, upon illumination with blue light, a covalent adduct is thought to form between the flavin cofactor and this conserved cysteine residue (Fig. 1.4B) (Swartz *et al.*, 2001; Salomon *et al.*, 2000; Crosson *et al.*, 2003; Ondrusch & Kreft, 2011). The resulting conformational changes enable signalling from the effector domain and under dark conditions the protein returns to its original conformation (Crosson *et al.*, 2003; Möglich & Moffat, 2007; Salomon *et al.*, 2000).

Although flavin adenine dinucleotide (FAD) is available in the cell, Lmo0799 uses flavin mononucleotide (FMN) almost exclusively as its binding chromophore (Chan *et al.*, 2012). Lmo0799 shares significant similarity with YtvA (67%) and other bacterial photoreceptors (Heavin and O'Byrne 2012; Chan *et al.*, 2012), however, there are some distinct differences between these genes' sequences (Crosson *et al.*, 2003; Chan *et al.*, 2012; Ondrusch & Kreft 2011). Notably, the conserved arginine in the GXNCRFLQ motif is replaced by a smaller histidine residue in Lmo0799. Additionally at position X, Lmo0799 carries a serine rather than the positively charged lysine residue in YtvA (Crosson *et al.*, 2003; Chan *et al.*, 2012). These substitutions are thought to provide the covalent adduct formation with far less stability than that of the highly similar YtvA protein (Chan *et al.*, 2012). Lmo0799 adduct formation takes approximately 5.4 μs, a much longer process than for other LOV containing proteins and has a decay half life of 95

minutes at 20 °C (Chan *et al*., 2012). Additionally, at 26 °C and above it displays increasing spontaneous loss of the chromophore from its binding pocket into the media. By contrast, YtvA photoexcitation, adduct formation and recovery to dark state can occur in less than an hour and YtvA protein-flavin binding has been shown to be stable at 37 °C (Avila-Perez *et al*., 2009). The replacement of these residues may account for the reported discharge of significant amounts of FMN during storage, upon photoexcitation and at higher temperatures (Chan *et al.*, 2012; Losi *et al.*, 2003). The increased flexibility of the protein makes it a poor light sensor, and Chan *et al.*, (2012) posit that this indicates the protein has other functions in addition to light sensing, although no functions have yet been identified.

In some aspects, however, the proteins display significant similarity. YtvA exists as a dimer (Jurk *et al.*, 2010; Avila-Perez *et al.*, 2009) and Lmo0799 has been shown to form dimers *in vivo*, using a two-hybrid system (J. Johansson, personal communication). Instead of two conserved threonine residues, both proteins carry negatively charged glutamate residues: Glu168 and Glu202 for YtvA and Glu197 for Lmo0799. Lmo0799 also carries a histidine (His163) instead of the YtvA Glu168 beside a negatively charged aspartate (Ondrusch & Kreft, 2011). While YtvA cannot directly interact with RsbT, possibly due to the lack of the conserved threonines, it does stimulate RsbT-mediated phosphorylation of RsbS (Jurk *et al*., 2013) and a similar mechanism of activation is expected for Lmo0799. YtvA is permanently associated with the stressosome even in the absence of light stress (Jurk *et al*, 2013) but cannot do so in the absence of RsbRA or RsbRD. This explains why the presence of YtvA does not prevent constitutive σ^B activation in the absence of all other RsbR paralogues (Jurk *et al*., 2013, Akbar *et al*., 2001).

1.10.2 *Lmo0799*-associated phenotypes and regulation

Blue light signalling results in Lmo0799-mediated activation of the GSR, including virulence genes such as InlA and InlB and an antisense excludon of flagellar biosynthesis upstream of MogR in a σ^B-dependent manner (Ondrusch& Kreft, 2011; Tiensuu *et al*., 2013; Toledo-Arana *et al*., 2009). Cells which express *lmo0799* have an interesting phenotype in that they produce a ring phenotype of opaque and translucent rings when exposed to consecutive cycles of light and dark (Fig. 1.4C). Cells from the opaque rings have a thicker cell wall and excrete more extrapolymeric substances. Colonies taken from the opaque rings display increased survival when exposed to 60 mM hydrogen peroxide and increased survival over time, compared to colonies taken from the translucent rings and from *ΔsigB* and *Δlmo0799* strains. This indicates that prior exposure to light stresses (in cycles of light/dark) cross protects against hydrogen peroxide and other ROS- exposing conditions (Tiensuu *et al.*, 2013).

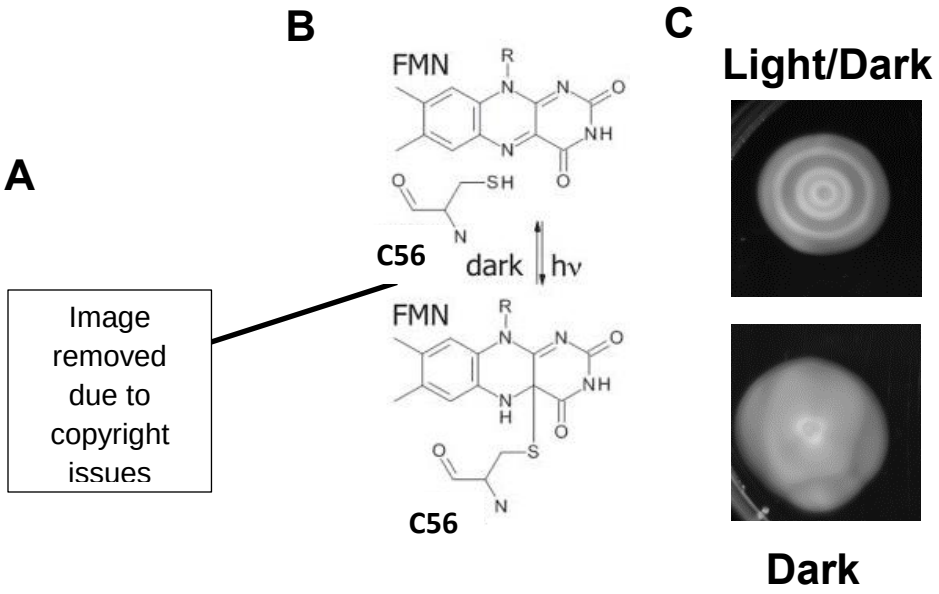

Figure 1.4 Lmo0799 light cycle (A) Lmo0799 LOV domain. Taken from Ondrusch & Kreft, 2011. **(B)** Light induced formation of covalent adduct between FMN and thiol residue of Lmo0799 C56. Modified from Crosson & Moffat, 2001. **(C)** Lmo0799-dependent light/dark ring formation (top) and dark-incubated colonies (bottom), prepared as described in Section 2.5.3.

1.11 Project aims

σ^B is a sigma factor that is crucial for stress survival. While inferences can be drawn from what is known about the *B. subtilis* stressosome components, very little information is available about the role of the *L. monocytogenes* proteins RsbR, Lmo0161, Lmo1642 and Lmo1842 in the general stress response. Genetic evidence for the proposed mechanism of function of the blue light sensor Lmo0799 has also not yet been provided.

The overarching aim of this project was to determine whether, and under what conditions, the RsbR paralogues contribute to activation of the GSR. To achieve this aim, several knockout mutants were constructed and subjected to phenotypic tests, as described in Chapters 4 and 5. σ^B activation levels were then analysed to examine whether novel phenotypes could be correlated with altered levels of σ^B activity. During the construction of these strains we also identified a mutant with a novel RsbV single nucleotide polymorphism mutation that caused an interesting temperature sensitive σ^B activation phenotype which is discussed in Chapter 5. As blue light is currently the only known stress signal that the stressosome can detect (Ondrusch & Kreft, 2011), a particular focus of this project was to examine the physiological effects of light stress on the cell and the contributions of the stress sensor proteins to the light-stress response. An Lmo0799 C56A 'blind' strain was designed and constructed in order to determine the mechanism of function of the Lmo0799 protein (Chapter 3).

With the information obtained from these assays, we hope to gain new insight into the function of RsbR and its paralogues and into the functioning of the σ^B activation cascade. Examination of the mechanisms by which blue light inactivates

L. monocytogenes may aid future research into the development of novel control methods for this important food-borne pathogen.

Chapter 2: Materials and Methods

2.1 Bacterial strains and plasmids preparation methods

The bacterial strains and plasmids used in this study are listed in Table 2.1. *Listeria monocytogenes* permanent stocks were prepared as follows: a single colony was inoculated into 5 ml Brain Heart Infusion (BHI) broth in a 50 ml Falcon tube (Greiner Bio-One) and incubated for 16-18 h at 37 °C with aeration (180 rpm) (Gio Gyrotory©) (New Brunswick Scientific Edison). The culture was centrifuged at 8,600 x*g* for 3 min and the pellet was resuspended in 2 ml BHI broth (LabM) supplemented with 7% (v/v) dimethyl sulfoxide (DMSO) (Sigma-Aldrich). One millilitre of the sample was aliquoted into a 2 ml cryovial and stored immediately at -80 °C. Strains were streaked from permanent stocks onto BHI agar plates. *Escherichia coli* strain permanent stocks and working stocks were prepared in the same manner, with Luria- Bertani (LB) broth (LabM) and agar (Sigma-Aldrich and LabM) used in place of BHI media. Agar plates were stored at 4 °C for up to one month before disposal. Before use, unless otherwise stated, broths (25 ml) were inoculated with a single colony from agar plate stocks and incubated overnight (16-18 h) in 250 ml Erlynmeyer flasks (Pyrex®) with aeration (180 rpm), at 37 °C. Where needed, chloramphenicol (Cml), erythromycin (Erm), and ampicillin (Amp) (all Sigma-Aldrich) antibiotics were used at a concentration of 10 µg ml^{-1} (Cml), 2 µg ml^{-1} (Erm) and 100 µg ml^{-1} (Amp) for *L. monocytogenes* and *E. coli*, respectively. The optical density of cultures was measured at OD_{600nm} using a spectrophotometer (Spectronic 20 Genesys) or at OD_{595nm} using a Sunrise™ absorbance platereader (Tecan).

2.1.1 Electrocompetent *L. monocytogenes* EGD-e cells

The method used to prepare electrocompetent *L. monocytogenes* cells was adapted from Monk *et al.,* 2008. Overnight cultures grown in BHI were diluted (1:100) into 500 ml BHI supplemented with 0.5 M sucrose (added before autoclaving) and incubated in a sterile 5 L conical flask, shaking (180 rpm) at 37 °C until an OD_{600nm} of 0.2 was reached. Ampicillin (10 µg ml^{-1}) was then added to the flask and the cells were incubated for approximately 2 h until an OD_{600nm} value of 0.4-0.6 was reached. The culture was decanted into 50 ml Falcon tubes and cooled on ice for 10 min in 50 ml volumes. From this point all cultures and media were kept on ice. Cells were harvested by centrifugation at 5,000 x*g* for 10 min at 4 °C (Hettich Universal R320 centrifuge) The cell pellets were washed with 500 ml total (autoclaved) ice cold Sucrose Glycerol Wash Buffer (SGWB) (0.5 M sucrose, 10% (v/v) glycerol, pH 7). Cells were then centrifuged and washed with 250 ml ice-cold SGWB (25 ml per tube). Following a third centrifugation, cells were resuspended in 50 ml ice cold total SGWB and combined into a sterile 250 ml conical flask. A 50 mg lysozyme per ml dH_2O stock solution was prepared and filter-sterilized. Lysozyme was added to the SGWB suspension at a concentration of 10 mg ml^{-1} and the contents were incubated for 20 min at 37 °C. Cells were then centrifuged in two Falcon tubes at 3000 x*g* for 10 min at 4 °C before resuspension in 12 ml SGWB. Cells were centrifuged and finally resuspended in 1.5 ml SGWB. Electroporation aliquots (100 µl) were stored immediately at -80 °C.

2.1.2 Electrocompetent *E. coli* cells

Overnight *E. coli* cultures grown in LB broth were diluted (1:100) into 500 ml fresh LB broth in a sterile 5 L capacity conical flask and incubated at 37 °C, shaking (180 rpm) until an OD_{600nm} value of 0.35-0.4 was reached. Cultures were cooled on ice and transferred to 50 ml Falcon tubes. All media, pipette tips and pipettes were chilled from this point. The cultures were centrifuged at 4 °C, 2,500 x*g* for 15 min. The supernatant was discarded and the pellets were resuspended in 50 ml total 10% (v/v) glycerol solution (100 ml glycerol, 900 ml dH_2O, autoclaved and chilled) in two tubes and centrifuged again. The pellets were washed a further three times in this manner (50 ml total 10% glycerol solution, centrifuged at 2,500 x*g*). The two pellets were then resuspended in 1 ml each of 10% (v/v) glycerol solution, combined in one tube and centrifuged. The pellet was finally resuspended in 1 ml 10% glycerol solution, and then pipetted into 100 µl aliquots and stored immediately at -80 °C.

2.2 Preparation of culture media

Culture media were prepared as outlined below. Glassware and media were sterilised in a Labo Autoclave (Sanyo) at 121 °C for 15 min. Solutions were filter-sterilised using a Millipore 0.2 µm pore single-use membrane filter (Merck), where specified.

2.2.1 Preparation of BHI and LB media

BHI and LB broth were prepared as directed by the LabM and Sigma-Aldrich media manufacturers. 37 g of LabM BHI broth powder or 20 g LB broth powder (Sigma-Aldrich) was added to 1 L distilled water (dH_2O) in Duran glass bottles (Sparks). For agar media, 15 g of Agarose No. 2 (LabM) was added per litre of broth solution. Solutions were immediately autoclaved (Sanyo). Antibiotics, when needed, were added to cooled agar media (40-50 °C) before being poured into Petri dishes. Antibiotics were added to broth media aliquots directly before use. Broth media was stored at room temperature for up to several months before use, agar plates at 4 °C for one month.

Table 2.1 Strains used in this study

Strains	Genotype	Acquired from
L. monocytogenes		
EGD-e	WT	K. Boor (Cornell University)
EGD-e *ΔsigB*	*ΔsigB* (*Δlmo0895*)	K. Boor (Cornell University)
EGD-e *ΔrsbR*	*ΔrsbR* (*Δlmo0889*)	This study
EGD-e Δlmo0799	*Δlmo0799*	Tiensuu *et al.,* 2013
EGD-e Δlmo0161	*Δlmo0161*	This study
EGD-e Δlmo1642	*Δlmo1642*	This study
EGD-e Δlmo1842	*Δlmo1842*	This study
EGD-e *lmo0799* C56A	Lmo0799 protein with change C56A	This study
EGD-e pMK4 *lmo0799*	pMK4 carrying full *lmo0799* gene	Tiensuu *et al*., 2013
EGD-e Δlmo0799 pMK4 *lmo0799*	*Δlmo0799 with* pMK4 carrying full *lmo0799* gene	Tiensuu *et al*., 2013
EGD-e WT pKSV7:: $P_{lmo2230}$-*egfp*	WT EGD-e carrying pKSV7:: $P_{lmo2230}$-*egfp* (transformant)	This study
EGD-e *ΔsigB* pKSV7:: $P_{lmo2230}$-*egfp*	EGD-e strain with *sigB* deletion carrying pKSV7:: $P_{lmo2230}$-*egfp* (transformant)	M. Utratna (NUI Galway)
EGD-e *ΔrsbR* pKSV7:: $P_{lmo2230}$-*egfp*	EGD-e strain with *rsbR* deletion carrying pKSV7:: $P_{lmo2230}$-*egfp* (transformant)	This study
EGD-e *Δlmo0799* pKSV7:: $P_{lmo2230}$-*egfp*	EGD-e strain with *lmo0799* deletion carrying pKSV7:: $P_{lmo2230}$-*egfp* (transformant)	This study
EGD-e *Δlmo0161* pKSV7:: $P_{lmo2230}$-*egfp*	EGD-e strain with *lmo0161* deletion carrying pKSV7:: $P_{lmo2230}$-*egfp* (transformant)	This study
EGD-e *Δlmo1642* pKSV7:: $P_{lmo2230}$-*egfp*	EGD-e strain with *lmo1642* carrying pKSV7:: $P_{lmo2230}$-*egfp* (transformant)	This study

EGD-e *Δlmo1842* pKSV7:: $P_{lmo2230}$-*egfp*	EGD-e strain with *lmo1842* deletion carrying pKSV7:: $P_{lmo2230}$-*egfp* (transformant)	This study
EGD-e pMAD::*Δ1642*	pMAD::*Δ1642* transformant	This study
EGD-e pMAD::***Δ****lmo1842*	pMAD::*Δ1842* transformant	This study
EGD-e RsbV I23T	EGD-e with a single base pair mutation in *rsbV* resulting in amino acid change $I_2$3T	This study
E. coli		
TOP10	F- mcrA Δ(mrr-hsdRMS- mcrBC) Φ80lacZΔM15 ΔlacX74 recA1 araD139 Δ(ara-leu)7697 galU galK rpsL (StrR) endA1 nupG	Invitrogen
TOP10 pMAD	TOP10 possessing plasmid pMAD	COB lab stock

Table 2.2 Plasmids used in this study

Plasmid	Characteristics	Acquired from
pMAD	*Amp^R, Erm^R, ori^{ts}*	Arnaud *et al.,* 2004
pMAD::Δlmo0161	pMAD carrying 300 bp upstream and 300 bp downstream of EGD-e *lmo0161*	This study
pMAD::Δlmo1642	pMAD carrying 300 bp upstream and 300 bp downstream of EGD-e *lmo1642*	This study
pMAD::Δlmo1842	pMAD carrying 300 bp upstream and 300 bp downstream of EGD-e *lmo1842*	This study
pMAD::*ΔrsbR*	pMAD carrying 300 bp upstream and 300 bp downstream of EGD-e *rsbR*	Tiensuu *et al.,* 2013
pKSV7::P$_{lmo2230}$-egfp	Amp^R, Cml^R, ori^{ts}, carrying 443 bp *egfp* gene fused to P$_{lmo2230}$	Utratna *et al.,* 2012
pCR2.1::*Δlmo0161*	F*mcr* A Δ(*mrr hsd* RMS *mc r*BC) Φ 80*lac* ZΔM15 Δ*lac* X74 *rec* A1 *ara* D139 Δ(*araleu*)7697 *gal* U *gal* K *rps* L (StrR) *end* A1 *nup* G	Eurofins Genomics
pEX-A:: *ΔrsbR*	FΦ80*lac* ZΔM15Δ(*lac* ZYA*arg* F)U169*deo* R *rec* A1 *end* A1 *hsd* R17(r**k**$^-$,m**k+**)*pho* A *sup* E44 *thi*- 1*gyr* A96 *rel* A1 λ$^-$	Eurofins Genomics
pEX-A: *Δ*:*lmo1642*	FΦ80*lac* ZΔM15Δ(*lac* ZYA-*arg* F)U169*deo* R *rec* A1 *end* A1 *hsd* R17(r**k**$^-$,m**k+**)*pho* A *sup* E44 *thi*- 1 *gyr* A96 *rel* A1 λ$^-$	Eurofins Genomics
pEX-A::Cys-Ala *lmo0799*	FΦ80*lac* ZΔM15Δ(*lac* ZYA-*arg* F)U169*deo* R *rec* A1 *end* A1 *hsd* R17 (r**k**$^-$,m**k+**) *pho* A *sup* E44 *thi*- 1 *gyr* A96 *rel* A1 λ$^-$	Eurofins Genomics
pEX-A:: *Δlmo1842*	FΦ80*lac* ZΔM15Δ(*lac* ZYA-*arg* F)U169*deo* R *rec* A1 *end* A1 *hsd* R17(r**k**$^-$,m**k+**)*pho* A *sup* E44 *thi*- 1 *gyr* A96 *rel* A1 λ$^-$	Eurofins Genomics

2.2.2 Preparation of defined media (DM)

The defined media for *L. monocytogenes* was adapted from Amezaga *et al.,* (1995). To make a working stock of DM, 810 ml of autoclaved dH_2O was mixed with 100 ml salt solution (10X), 10 ml magnesium sulphate solution (100X), 20 ml ferric citrate (50X), 10 ml amino acids solution (100X), 10 ml cysteine and tryptophan solution (100X), 20 ml glutamine solution (50X), 10 ml vitamin solution (100X) and 10 ml trace elements (100X). The solution was supplemented with glucose to a final concentration of 0.4% (v/v) for culture growth. Stock preparations are described below and all stocks were stored at 4 °C for a maximum time of 1 month. All chemical components were provided by Sigma-Aldrich.

2.2.2.1 Salt solution (10X)

The salt solution was made by adding 79.9 g of K_2HPO_4 (dipotassium hydrogen orthophosphate), 31 g of $NaH_2PO4.2H_2O$ (sodium dihydrogen orthophosphate) and 10 g of NH_4Cl (ammonium chloride) per 1000 ml dH_2O. This was then autoclaved and stored at room temperature.

2.2.2.2 Magnesium sulphate solution (100X)

The magnesium sulphate solution was made by adding 40 g $MgSO_4.7H_20$ (magnesium sulphate) per 1000 ml dH_2O and autoclaved and stored at room temperature.

2.2.2.3 Ferric citrate solution (50X)

Ferric citrate solution was made by adding 5 g $FeC_6H_5O_7$ (ferric citrate) per 1000 ml dH_2O. This was autoclaved and stored at room temperature.

2.2.2.4 Amino acids solution (100X)

An essential amino acid solution was made by adding 10 g each of L-leucine, L-isoleucine, L-valine and L-methionine and 20 g L-histidine monohydrochloride monohydrate and arginine monohydrochloride per 1000 ml dH_2O. This was filter-sterilised and stored at 4 °C.

2.2.2.5 Cysteine and tryptophan solution (100X)

The cysteine and tryptophan solution was made by adding 10 g each of L-cysteine hydrochloride and L-tryptophan per 1000 ml dH_2O. This was filter-sterilised and stored at 4 °C.

2.2.2.6 Glutamine solution (50X)

Glutamine solution was prepared by adding 30 g L-glutamine per 1000 ml dH_2O. This was filter-sterilised and stored at 4 °C.

2.2.2.7 Vitamin solution (100X)

To make the vitamin solution, 5 mg ± α-lipoic acid (DL- 6,8 thiotic acid) was added to 200 ml 70% ethanol. Four millilitres of this solution was mixed with 10 mg biotin, 100 mg thiamine, 100 mg riboflavin and 250 ml ethanol (95%). The solution was brought to a final volume of 1000 ml with dH_2O and filter-sterilised. The solution was stored at 4 °C in the dark.

2.2.2.8 Trace elements solution (100X)

A trace element solution was prepared by adding 6.75 g NaOH (sodium hydroxide) and 13.5 g $N(CH_2COOH)_3$ (nitriloacetic acid) per 800 ml dH_2O. This was then slowly added to a 160 ml solution containing 0.55 g of $CaCl_2.2H_2O$ (calcium chloride dihydrate), 0.17 g of $ZnCl_2$ (zinc chloride), 0.059 g of $CuCl_2.2H_2O$ (cupric chloride dihydrate), 0.06 g of $CoCl_2.6H_2O$ (cobaltous chloride 6-hydrate) and 0.060 g $Na_2MoO_4.2H_2O$ (sodium

molybdate dihydrate). Finally, the solution was brought to a final volume of 1000 ml with dH_2O and filter-sterilised. The solution was stored 4 °C.

2.2.3 Preparation of SOC media

Super Optimal broth with Catabolite repression (SOC) media was prepared through the addition of the following to 900 ml of dH_2O: 20 g Bacto tryptone (DIFCO), 5 g Bacto yeast extract (DIFCO), 2 ml of a 5 M NaCl solution, 2.5 ml of a 1 M KCl solution, 10 ml of a 1 M $MgCl_2$, solution, 10 ml of 1 M $MgSO_4$ solution and 20 ml of 1 M glucose solution. The SOC solution volume was adjusted to a litre and filter-sterilized before use or storage.

2.2.4 Preparation of phosphate buffered saline (PBS) solution

PBS solution was prepared by adding one PBS tablet (Sigma-Aldrich) to 200 ml dH_2O before autoclaving. This 10 mM phosphate buffer solution contains 2.7 mM potassium chloride and 137 mM sodium chloride of pH 7.4 at 25 °C.

2.3 Additions to culture media

2.3.1 Antibiotics

Chloramphenicol, erythromycin (both stored at room temperature) and ampicillin (stored at 4 °C) were supplied by Sigma-Aldrich. Stock concentrations of chloramphenicol and ampicillin were prepared by adding 50 mg ml^{-1} antibiotic to 5 ml ethanol (≥99.85%, Sigma-Aldrich) (Cml) and dH_2O (Amp), respectively. Stock concentrations of erythromycin were prepared by adding of 10 mg ml^{-1} erythromycin to 5 ml ethanol (≥99.85%, Sigma-Aldrich). Solutions were filter-sterilized and stored at -20 °C

2.3.2 Ethanol

Autoclaved agar was allowed to cool and ethanol (≥99.85%, Sigma-Aldrich) was added to the still-liquid agar at a concentration of 4% (v/v) directly before pouring into Petri dishes.

2.3.3 Acid

To determine defects in growth in the presence of acid, BHI agar and broth medium was acidified with hydrochloric acid. Acidified BHI was prepared by adjusting the pH of the media with hydrochloric acid before autoclaving the media. The pH was measured using a pH probe (Mettler Toledo) before autoclaving and acidified BHI was stored for one

week before disposal. For broth experiments, the pH probe was also used to verify the pH of a sample of the acidified broth before use in experiments.

2.3.4 Sodium chloride

Anhydrous sodium chloride (Sigma-Aldrich) was added to solid or liquid media at a 1 M concentration before autoclaving.

2.4 Growth assays

2.4.1 Growth experiments on solid agar

Strains were grown for 18-20 h in BHI with aeration at 37 °C before use. Culture optical densities were standardised to OD_{600nm} value of 1.0 in BHI broth and then serially diluted, tenfold in PBS to a 10^{-8} dilution. Four microlitres of each dilution from 10^{-1} to 10^{-8} was pipetted onto the surface of the BHI agar with a stress agent (sodium chloride, acid, and ethanol) and on agar without a stress (control). The agar plates were allowed to dry for approximately 30 min at room temperature. Plates were then sealed with parafilm (Parafilm M), wrapped in aluminium foil (where required) and incubated at 30 °C for 24 h, unless otherwise stated. Agar plates were placed with the inoculated surface facing downwards. Plates were imaged with a CCD camera (G:Box, Syngene) and the software package GeneSys (Syngene), using the bright white light filter

2.4.2 Growth experiments on agar in the presence of cold stress

Plates were wrapped in aluminium foil and incubated at 4 °C for 5 days. Growth was assessed visually and recorded as in Section 2.4.1

2.4.3 Growth experiments in liquid culture

Growth experiments were carried out either with 25 ml culture in 250 ml conical flasks using a Gio Gyrotory® shaker (180 rpm) or with 96-well plates in a Sunrise™ absorbance reader (Tecan) (Section 2.5.4). For growth curves in conical flasks overnight (16-18 h) cultures grown in BHI at 37 °C with aeration were diluted in fresh medium to an OD_{600nm} value of 0.05 in 25 ml fresh BHI broth and incubated with aeration at 30 °C or 37 °C. The optical density (as an indication of growth) was measured hourly for 10 h at OD_{600nm}, using a spectrophotometer (Spectronic 20 Genesys). A final measurement was taken at 24 hour's growth. The specific growth (μ) was calculated from the growth curves using the relationship $log_{10}N2-log_{10}N1 = \mu(t2-t1)/2.303$ where N refers to cell concentration and t to time. Figures were prepared using GraphPad Prism 5.

2.4.4 Acid survival assays

For acid survival assays, 1 ml aliquots of overnight cultures were centrifuged for 2 min at 13,000 x*g* in a microcentrifuge (Eppendorf). The supernatant was discarded and the pellets were resuspended in the same volume of BHI broth or BHI broth acidified to pH 2.5 through the addition of 5 M hydrochloric acid and incubated at room temperature on the bench. Aliquots were taken immediately from the resuspended BHI broth culture and from the acidified culture after 30 min, 1 h and 2 h. Samples were diluted 1:10 in PBS to a 10^{-6} dilution and 10 µl of the dilutions was plated in triplicate for each strain on BHI agar. Dunnett's test was used to identify significant differences in survival counts for deletion strains compared with survival counts for the WT strain. Figures were prepared using GraphPad Prism 5. *P*-values ≤0.05 were deemed to be significant.

2.4.5 Biofilm assay

This assay was adapted from Feehily, 2014. One millilitre of an overnight culture was centrifuged at 13,000 x*g* for 2 min. The pellet was washed once in 1 ml PBS, centrifuged and resuspended in 1 ml PBS. Five microlitres of the washed cells were added to 5 ml of either BHI broth or DM supplemented with glucose (1:100 dilutions). Two hundred microlitres of this resuspension was transferred to a flat bottomed 96-well tissue culture plate (Sarstedt) with six technical replicates for each strain/biological replicate. Sterile media was added to each plate as a control. The wells surrounding the samples were filled with sterile media or PBS to help prevent evaporation from sample wells. The plate was subsequently incubated statically for 48 h, unless otherwise specified, at the required

temperature. After incubation, the media was carefully removed from all wells using a pipette and each well was washed 3 times with 200 µl PBS. The plate was allowed to dry at 40-45 °C for 45 min and 150 µl of a 1% (w/v) crystal violet (Sigma-Aldrich) solution (10 g crystal violet in 1000 ml dH_2O) was then added to each well. The plate was incubated statically at 37 °C for 30 min and the crystal violet was removed. The plate was washed twice with 200 µl PBS and then gently rinsed with dH_2O to remove excess crystal violet. Finally, 160 µl 95% ethanol was added to each well. The plate was incubated for a further 30 min at room-temperature with gentle agitation, or until the crystal violet dissolved. The OD_{595nm} value for each well was recorded using a Tecan Sunrise plate reader and exported into a Microsoft Excel sheet. Dunnett's test was used to identify significant differences between biofilm formed by deletion strains and that produced by the WT strain. *P*-values ≤0.05 were deemed to be significant. Figures were prepared using GraphPad Prism 5.

2.4.6 Catalase assay

Overnight stationary phase aerobic cultures were prepared as described in Section 2.1. Aerobic cultures were also grown to exponential phase (OD_{600nm}= 0.5-0.6) following dilution of the overnight culture into fresh broth (starting OD_{600nm}= 0.05). Anaerobic stationary phase cultures were prepared by inoculating single colonies into 25 ml of broth in Sterilin Quickstart Universal polystyrene containers. These containers were incubated overnight in a sealed anaerobic chamber (Sarstedt) containing an Anaerogen sachet (Oxoid). Anaerobic and aerobic cultures were incubated at 30° or 37 °C.

Culture aliquots (5 ml) were transferred into Sterilin Quickstart Universal polystyrene containers and 100 µl of 30% hydrogen peroxide was added to each of the aerobic and anaerobic cultures. The cultures were gently swirled to allow mixing of the hydrogen peroxide throughout the cultures The oxygen released in the form of bubbles was visually monitored and photographed (Sony Xperia) after a 3 min period as a qualitative indication of catalase activity. Catalase assays were performed in triplicate under each condition.

2.5 Light exposure assay methods

2.5.1 Blue light apparatus

A high-power mounted 470 nm LED (ThorLabs, model M470L2) was the light source (designated LEDS1) used to investigate the effects of blue light across the surface of an agar plate (Fig. 2.1A&C). An aspheric condenser lens (Ø 75 mm) was used to create a uniform distribution of light across a circular area of 7 cm in diameter. An irradiance map was created using an optical power sensor (ThorLabs, model PM121D). This setup produced 1.5-2.0 mW cm^{-2}, which could be increased to an irradiance of 8.0 mW cm^{-2} by increasing the current using a T-cube LED driver (LEDD1B, ThorLabs). The lower irradiance setting was used for growth inhibition experiments while the higher setting was used for survival experiments.

An alternative setup (designated LEDS2), was used to test the effects of light across the area of a 96-well microtitre plate containing liquid medium (Fig. 2.1B&D) (O'Donoghue *et al*., 2016). This setup was composed of 80 blue (460 nm) 10 mm prewired LEDs

(Phenoptix) which were arranged in a 10 x 8 array, measuring 16 x 13.5 cm. A diffuser membrane (ThorLabs) was placed below the lights to help create a uniform distribution of light across the area of the plate. Again, an irradiance map was generated to confirm that a uniform irradiance was delivered across the area of the 96-well micro titre plate (it ranged from 1.5-2.0 mW cm^{-2} across all 96 wells). The lights were fixed in position approximately 16 cm above the 96-well plate.

2.5.2 Agar growth experiments

Cultures inoculated on BHI agar were exposed to 470 nm blue light (LEDS1; Fig. 2.1A&C) at 1.5-2.0 mW cm^{-2} or incubated in the dark (plates were wrapped in aluminium foil) at 30 °C for 24 h. The medium reduced the transmittance of light by approximately 50%. For experiments investigating the involvement of ROS in growth inhibition by light, catalase was added to medium by spreading 100 µl of 125 U ml^{-1} catalase (Sigma) on the surface of the agar. For comparison of the C56A 'blind' strain to the WT, *ΔsigB* and *Δlmo0799* strains, cells were diluted 1:10 from an OD_{600nm}= 1.0 to a 10^{-1} dilution and then 1:5 for all remaining dilutions to a final dilution of 1 in 781,250. Dilutions from 10^{-1} to a 1 in 761,240 dilution were inoculated on agar as described above in Section 2.4.1.

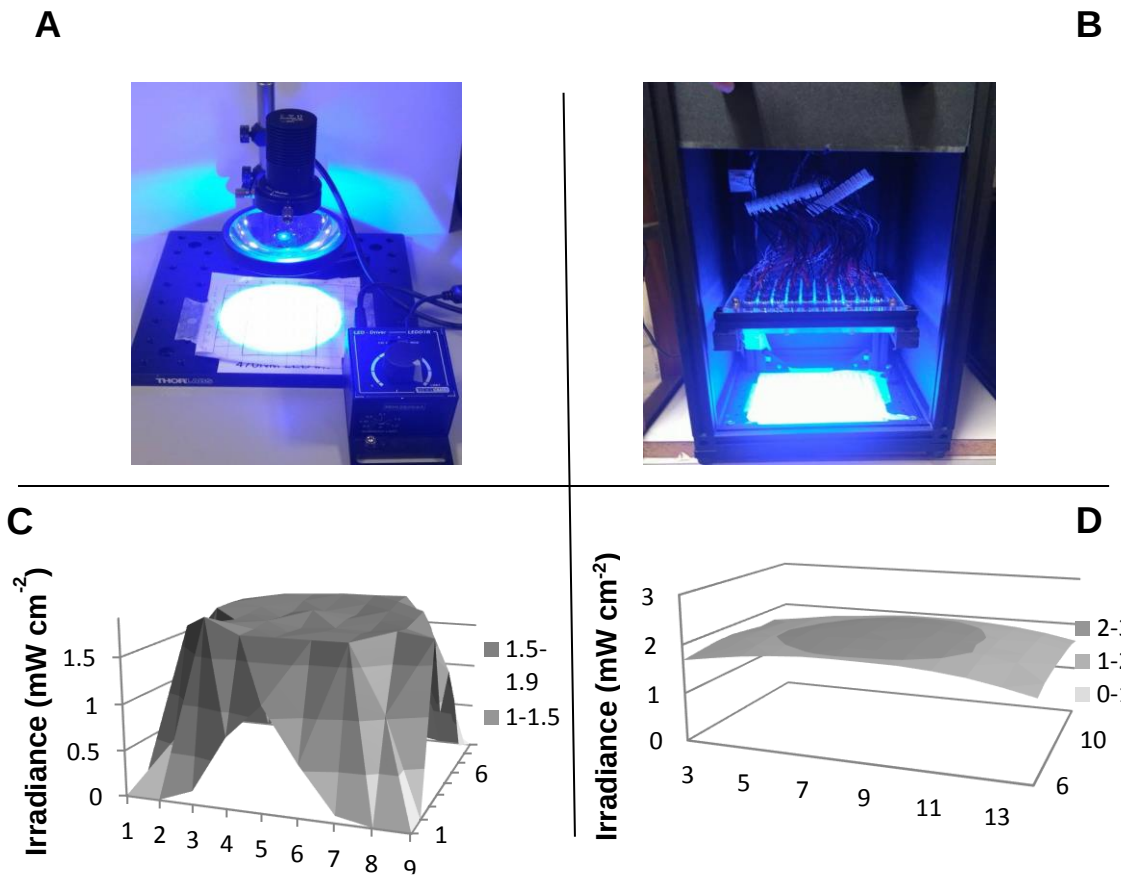

Figure 2.1 Blue light delivery apparatus. (**A**) The light exposure apparatus for use with solid media and light survival experiments consists of a blue light LED and an Ø75 mm aspheric condenser (both ThorLabs) which deliver an adjustable, uniform quantity of blue light at 470 nm to a surface 7 cm in diameter. (**B**) An alternative setup was composed of 80 blue (460 nm) 10 mm prewired LEDs (Phenoptix), designed to deliver blue light across a 96-well plate area. Light intensity values were mapped across an area measuring (**C**) 9 cm x 9 cm for LEDS1 and (**D**) 14 cm x 12 cm for LEDS2.

2.5.3 Ring phenotype and motility assays

For the colony ring phenotype assays, overnight cultures were standardised to an OD_{600nm} value of 2.0 and a 2 µl aliquot was inoculated onto the centre of a semi-solid BHI agar (0.3% w/v agar No. 2) (LabM). Plates were incubated with the inoculated surface facing upwards and exposed to five consecutive 12 h cycles of light (from white fluorescent bulbs producing a power density of approximately 0.1-0.2 mW cm^{-2}) and dark (wrapped in aluminium foil) at 30 °C. Colonies were then imaged with a CCD camera (G:box, Syngene) and the imaging software GeneSys (Syngene) using the bright white light filter. For motility assays, semi-solid BHI agar plates were inoculated in the same way and then incubated in the continuous light (from white fluorescent bulbs producing a power density of approximately 0.1-0.2 mW cm^{-2}) or dark (wrapped in aluminium foil) at 30 °C. Colony diameter (mm) was measured after a 60 h incubation period. Significant differences for colony diameters incubated in the light compared to those incubated in the dark were determined using the unpaired Student *t*- test. Figures were prepared using GraphPad Prism 5.

2.5.4 Light-exposed growth experiments in liquid culture

For light exposure experiments in liquid broth, overnight cultures incubated with aeration at 37 °C were inoculated into fresh BHI broth to provide a starting OD_{600nm} value of 0.05. The OD_{600nm} =0.05 culture was further serially diluted in BHI to a final dilution of 10^{-6}. 200 µl of each dilution was then added to two 96-well microtitre plates

One plate was wrapped in aluminium foil as a dark control, the other placed under the light apparatus (LEDS2) (Fig. 2.1B&D), which produced blue light at 460 nm with a power density of 1.5-2.0 mW cm^{-2} .These plates were incubated at 30 °C for 14 h and growth was monitored by recording the OD_{595nm} hourly on a Sunrise–Tecan plate reader. The light transmittance through the plates and medium was approximately 68% with this setup. To take these readings plates were removed from the light apparatus and incubator and were shaken for 10 s immediately prior to each reading. To avoid taking readings throughout the night a second set of plates was later set up using the same overnights. These were incubated as before in the presence of light or dark for 15 h overnight without taking readings. The OD_{595nm} was recorded at the 15 h time point, and subsequently every hour until 24 h was reached, allowing a full growth curve to be generated by combining the two sets of microtitre plate data. Light growth experiments were carried out with three biological replicates per condition. For experiments investigating the involvement of ROS in growth inhibition by light, catalase (Sigma-Aldrich) was added to the medium at a concentration of 125 U ml^{-1} prior to inoculation.

Lag phase was arbitrarily defined as the time taken to reach an OD_{595nm} value of 0.1 and this was derived directly from the growth curves. Unpaired Student *t*-tests were used to compare endpoint and lag times for strains under the various conditions tested at each dilution. Figures were prepared using Microsoft Excel. Differences were deemed statistically significant if the *p*-value ≤ 0.05. When comparing mutant strain endpoint and lag time values with those of the WT in light, a Bonferroni correction was employed to address the issue of multiple comparisons (*p*-value <0.0167).

2.5.5 Light survival assay

One millilitre of overnight culture (incubated at 30 °C or 37 °C) was centrifuged at 13,000 x*g* for 2 min, washed with PBS (Oxoid) and then resuspended in PBS. Resuspended cultures were incubated in 96-well round-bottomed (Thermo Scientific) plates at 30 °C in the presence of 8 mW cm^{-2} 470 nm blue light (ThorLabs) (Fig. 2.1A&C) or in the dark (wrapped in aluminium foil). Samples were removed from wells for viable counting at specified time points. The samples were serially diluted in PBS and 10 µl of each dilution was plated in triplicate on BHI agar plates, which were then incubated at 37 °C for 24 h before counting. Dunnett's test or the Student *t*-test were used to identify significant differences in survival counts for deletion strains compared with survival counts for the WT strain. Figures were prepared using GraphPad Prism 5. *P*-values ≤0.05 were deemed significant

2.6 DNA manipulation methods

2.6.1 Digestions

Fermentas restriction enzymes *Bam*HI and *Eco*RI and *Xma*I (Thermo–Scientific) were used to digest compatible vector and separate deletion inserts from the commercial vector. Digestion reactions with FastDigest™ enzymes *Bam*HI and *Eco*RI (Thermo Scientific™) were prepared in 20 µl aliquots as follows: 2 µl Fermentas FastDigest™ reaction buffer, 1 µl enzyme, 3 µl DNA, and 14 µl autoclaved dH_2O. For double digests,

the reaction was adjusted to include 1 µl of each enzyme and 13 µl of autoclaved dH_2O. Digestion reactions were incubated at 37 °C for 1 h before denaturation at 80 °C for 5 min. Denaturation was only performed when products were required for ligation. *Xma*I (*Crf*9I) was not available in the FastDigest™ range. Digestion reactions with *Xma*I were prepared as follows 2 µl *Xma*I (*Cfr*9I) (Thermo Scientific™) reaction buffer, 1 µl enzyme, 3 µl DNA, and 14 µl autoclaved dH_2O. *Xma*I digestion reactions were incubated at 37 °C for 2-3 h before denaturation at 65 °C for 20 min. For samples which required digestion with *Bam*HI or *Eco*RI and *Xma*I, plasmids were first digested with the FastDigest™ enzyme and the mixture was column purified (QIAquick PCR purification kit) and eluted with 20 µl dH2O to remove the FastDigest reaction buffer. Several samples were pooled and concentrated to increase the concentration of substrate before a second digestion with *Xma*I.

2.6.2 DNA purification

Digested plasmids were column purified using the QIAquick PCR purification kit and protocol (Qiagen). Inserts digested from commercial or other vector were run on 1% agarose gels and gel-extracted, using the GenElute™ gel extraction kit and protocol (Sigma-Aldrich). Samples were eluted into 30 µl volumes (QIAquick PCR purification kit) or 50 µl (GenElute™ gel extraction kit) autoclaved dH_2O. To improve insert and vector yields, multiple digests were pooled and concentrated into a smaller volume with the QIAquick PCR purification kit (Qiagen). Inserts and vector were quantified by running known quantities on a 1% agarose gel (Section 2.7.1) with a DNA quantification marker (HyperLadder 1, Bioline).

2.6.3 Ligations

Ligations were performed with T4 DNA ligase (Thermo Scientific). The ligation procedure was carried out overnight at 16 °C with 50 ng of digested, purified insert and digested column-purified vector quantities in a 1:1, 2:1 and 3:1 ratio. The amount of vector required was calculated as follows:

$$\frac{\text{Vector (ng)}}{} = \frac{\text{Insert (ng) x vector (kb)}}{\text{insert (kb)}} \text{ x ratio } \left[\frac{\text{vector}}{\text{insert}} \right]$$

Ligations were performed in 20 µl volumes with 2 µl 10X T4 DNA ligase buffer (Thermo Scientific), 1 µl T4 DNA ligase (5 Weiss U μl^{-1}(Thermo Scientific^{TM}), the required volume of vector and insert and made up to 20 µl with nuclease free water. The reaction was incubated at 16 °C overnight (16-18 h) and was either used in a transformation reaction or stored at -20 °C.

2.6.4 Plasmid transformation

Transformation was achieved via electroporation of competent cells with plasmid DNA. Two microlitres of plasmid were added to a 100 µl aliquot of freshly thawed competent *L. monocytogenes* EGD-e cells (plasmid DNA >500 ng) or to 40 µl *E. coli* TOP10 cells. A negative control reaction was prepared by adding sterilised dH_2O or cut plasmid in place of the circularised plasmid. Each reaction was transferred to a pre-chilled (on ice) 0.2 cm electroporation cuvette (BioRad) and placed in the Gene Pulser (BioRad) chamber. The following parameters were used for electroporation: resistance of 200 Ω,

capacitance of 25 µF and voltage of 1,500 V. Immediately after pulsing, the cuvette was removed from the chamber and 0.9 ml of BHI supplemented with 0.5 M sucrose was added to the *L. monocytogenes* cells. For the recovery of *E. coli* Top10 cells, SOC solution was used. The suspensions were incubated for 1-2 h at 37 °C with shaking (180 rpm). Aliquots of varying amounts (20-100 µl) were then spread on BHI (*L. monocytogenes*) or LB (*E. coli*) agar plates containing the appropriate selective agent (antibiotic) and incubated overnight at 30 °C or for 48 h.

2.6.5 Plasmid extraction

For plasmid extraction plasmid-containing *E. coli* strains were grown overnight in 5 ml volumes with ampicillin. Plasmids were extracted using the GenElute™ plasmid miniprep kit (Sigma-Aldrich) following the manufacturer's directions. Plasmids were eluted in 50 µl of autoclaved dH_2O and stored at -20 °C.

2.7 DNA analysis

2.7.1 Agarose gel electrophoresis

Agarose gels (1% w/v) were used to analyse PCR products and prepared with 1 X Tris-Acetate-EDTA (TAE) buffer. A 50 X stock solution of TAE buffer was prepared by adding 242 g of Tris base to 57 ml of glacial acetic acid and 100 ml of 0.5 M EDTA (pH 8; all

chemicals supplied by Sigma-Aldrich). The final volume of the solution was brought up to 1 L with autoclaved dH_2O and the resulting buffer was stored at room temperature. One percent (w/v) agarose gels were prepared by mixing the correct weight of agarose (low electroendosmosis agarose for molecular biology, Sigma-Aldrich) with 1 X TAE buffer. Mixes were heated to boiling (Panasonic microwave) (low power). Solutions were allowed to cool before adding the correct volume of Sybr Safe (Invitrogen) as required by the gel size (for a large 150 ml gel 15 µl of Sybr Safe was added). The gel was allowed to solidify. DNA samples were loaded with 5 µl loading dye. DNA samples were electrophoresed (PowerPack Consort E132) at 70 V or 100 V depending on gel size until the dye front had travelled halfway or two thirds along the gel. A DNA molecular weight marker (5 µl) was loaded on each gel for DNA product quantification or size evaluation (HyperLadder 1, Bioline). Gels were imaged with a CCD camera (G:Box, Syngene) and the software package GeneSys (Syngene), using the SybrGold (ultraviolet light) filter setting.

2.7.2 Gel loading dye

For gel loading dye, TE buffer (10 mM Tris-HCl and 1 mM EDTA prepared in dH_2O) was prepared and the solution pH was adjusted to pH 8.0. Sucrose was dissolved in the TE buffer to give a final concentration of 40% (w/v). Bromophenol Blue (Sigma-Aldrich) was then added at a concentration of 0.25% (w/v) so that the solution turned a dark blue colour. The dye was stored at room temperature and 5 µl was added to each 50 µl PCR sample before loading on a 1% agarose gel for DNA analysis.

2.7.3 Polymerase Chain Reaction (PCR)

Colony Polymerase Chain Reaction (PCR) was carried out with 1 µl of template using a sterile 0.5 ml tube. When PCR was performed on a single colony, the template was prepared by resuspending a small scraping from the colony into 500 µl of sterilised deionised dH_2O and an aliquot of 1 µl was used for PCR. For negative controls the template used was substituted with 1 µl of sterilised deionised dH_2O. PCR samples were prepared on ice and for the majority of reactions MyBio Taq DNA polymerase kits were used to amplify products (supplied by Bioline). For PCR amplification of products required for sequencing, Q5 DNA polymerase was used (New England Biolabs). To prepare multiple 50 µl PCR reactions mixes**,** a reaction master mix was first prepared, containing 35.5 µl of sterilised deionised dH_2O, 10 µl of 10 X PCR buffer (supplied with the polymerase kit), 1 µl of 10 mM dNTP mix (containing 10 mM of each dNTP (Invitrogen) and 0.5 µl of polymerase per PCR sample. The polymerase was added last and 47 µl aliquots of the master mix were pipetted into 0.5 ml tubes. One microlitre of template was then added, followed by the addition 1 µl of each of the appropriate forward and reverse primers (Eurofins Genomics) (Table 2.3) to opposite sides of the tube. The samples were centrifuged briefly (Bench top centrifuge 5418, Eppendorf) and loaded onto the PCR block (MastercyclerR gradient, Eppendorf). For the PCR using Bioline products an initial denaturation step for 2 min at 95 °C was followed by 30 repetitions of a three step cycle: first denaturation at 95 °C for 30 s, annealing (calculated as 5°C lower than primer melting temperature provided by Eurofins Genomics) for 30 s, and elongation at 72 °C for 1-2 min depending on the product size (2 min for products larger than 1 kbp in size). A final 5 min at 72 °C was then applied once. A similar programme was used for amplification of products for sequencing with Q5 polymerase with the exceptions that 35 and not 30

cycles were employed and the denaturation steps were set at 98°C. After the PCR cycles were completed, the resulting products were stored briefly at 4 °C before visualisation by agarose gel electrophoresis. For longer storage, products were stored at -20 °C

Table 2.3 Primers used in this study

Primer (COB).	Sequence (5'-3')	Description	Source
395	CAGGAAACAGCTATGAC	FOR M13 primer	Eurofins Genomics
396	GTAAAACGACGGCCAG	REV M13 primer	Eurofins Genomics
699	ACAAATGTAGCCGCCCTTC	FOR primer flanking *lmo0799* C56A	This study
700	CATCTCGCAACCTCTACCTC	REV primer flanking *lmo0799* C56A	This study
726	CTGGTTGCATCATTGTAAGTTC	FOR primer inside *Δlmo0161*	This study
727	AGTGAATCAAGCGTAGCC	REV primer inside *Δlmo0161*	This study
728	CCCTTTGCCAAATGGTTCTC	FOR primer inside *Δlmo1642*	This study
729	TCATCCACGTTTCCTCCTTC	REV primer inside *Δlmo1642*	This study
730	CCTGAAATCAAGCGTAGCC	FOR primer inside *Δlmo1842*	This study
731	GACAACGAATGAACGAATGAC	REV primer inside *Δlmo1842*	This study
736	CGCACATTTTTTACAAGGAGAC	FOR *lmo0799* Cys-Ala specific	This study
737	CCGGTGATGATAAGTTCTACG	REV *lmo0799* Cys-Ala	This study
754	AGTGCTGTGCGCTTCTTC	FOR primer flanking *Δlmo0161*	This study
755	AACGGTTGCTGATTTACTTCC	REV primer flanking *Δlmo0161*	This study
756	GCAGCAGAGGAAATCATCAAC	FOR primer flanking *Δlmo1642*	This study
757	GTCCTTAATTACTCGGCCATC	REV primer flanking *Δlmo1642*	This study
758	ATAAAGGAGGCCAAACATATGG	FOR primer flanking *Δlmo1842*	This study
759	GATGGGAAAGAAGCGAGAAC	REV primer flanking *Δlmo1842*	This study
780	GCAAACCGCACAATAAGAGAG	FOR primer inside *ΔrsbR*	This study
781	GCTCCGCTAAACGTAATTCC	REV primer inside *ΔrsbR*	This study
790	CATCATGCTCTCTTAACACTGCTAC	FOR primer for *bgaB* gene	K.NicAogáin, NUIG
791	GTGAGAATTGTGCTGTCG	REV primer for *bgaB* gene	K.NicAogáin, NUIG
792	CGCCTGACAGATAAAATTACGC	FOR primer flanking *ΔrsbR*	This study
793	GTTTTTCCAGACCACTTTCAAG	REV primer flanking *ΔrsbR*	This study
847	ATTCGACTGTGATTTCGCC	REV primer *rsbV*	This study
850	GAGTTGCATGATGACTTT	FOR primer flanking *rsbV*	This study

2.8 Construction of deletion mutants

2.8.1 Design of deletion mutant constructs

To delete regions of targeted genes, WT genes were replaced with deletion constructs by homologous recombination as described by Horton *et. al.* (1993). The DNA sequences for these genes and adjacent regions from the strain EGD-e were sourced at *http://genolist.pasteur.fr /ListiList/*. Each deletion cassette consisted of 300 bp directly upstream fused to 300 bp directly downstream of the WT gene, with the full deletion of the WT gene. Restriction enzyme recognition sites were added to each end to facilitate cloning into the pMAD suicide vector: *Bam*HI (ggatcc) and *Eco*RI (gaattc) for the *Δlmo0161, Δlmo1642* and *Δlmo1842* deletion cassettes and *Bam*HI and *Xma*I (cccggg) for the *ΔrsbR* gene. Additional base pairs were added before the recognition sites (cg or ggga for *Xma*I) to aid enzyme binding. These deletion cassettes were constructed and cloned into commercial vectors by Eurofins Genomics (Table 2.2). The presence of the deletion cassette was confirmed by PCR with primers 726-731, 780 and 781 (Table 2.3), depending on the specific gene.

2.8.2 Site specific mutagenesis of genomic target

A 762 bp *lmo0799* gene with a GCA (alanine) codon in place of the original codon TGT (cysteine) at amino acid position 56 was designed for synthesis by Eurofins Genomics. Silent mutations in three adjacent codons were also modified to facilitate detection by PCR during the strain construction (WT 5'-TCCAATTGTCAC to 5'-AGTAACGCACAT)

(primers 736). The reverse primer binds to both WT and mutated *lmo0799*. (primer 737) (Table 2.3). The altered gene was cloned into a commercial vector with additional *Eco*RI and *Xma*I restriction sites at each end in order to facilitate ligation with the pMAD suicide vector (Table 2.2). Additional base pairs were added before the recognition sites (cg for *Eco*RI ggga for *Xma*I) to aid enzyme binding.

2.8.3 Plasmid integration into genome

Integration was achieved via homologous recombination between the suicide vector carrying the deletion construct and the chromosome (Horton *et al*., 1993). Colonies containing pMAD vectors with deletion cassettes were streaked on BHI agar containing erythromycin and incubated at the non-permissive temperature of 42 °C to prevent plasmid replication, selecting for colonies in which the plasmid has integrated into the genome at the region homologous to the replacement gene (Fig. 2.1). Strains were restreaked after 48 h. PCR was used to identify colonies from the third streak plate where plasmid integration into the genome had occurred. For the *L. monocytogenes* pMAD::Δ*lmo0161* strain, the integration procedure was instead successfully carried out in BHI broth media at 41.5 °C with erythromycin as a selection agent. Strains were sub-cultured every 48 h or when the broth became turbid over an 8 day period. Colonies from the fourth sub-culture tested positive via PCR for the presence of integrated plasmid. The plasmid could integrate either upstream (Fig. 2.2A) or downstream (Fig. 2.2B) of the WT gene as both regions are present within the plasmid deletion cassette. Using sets of primers with one primer targeting the regions external to the integration sites (primers

754-759, 792,793, 736, 737) and one primer specific to the deletion cassette (primers 726-731, 780, 781, 699, 700) the location of integration was determined (Table 2.3).

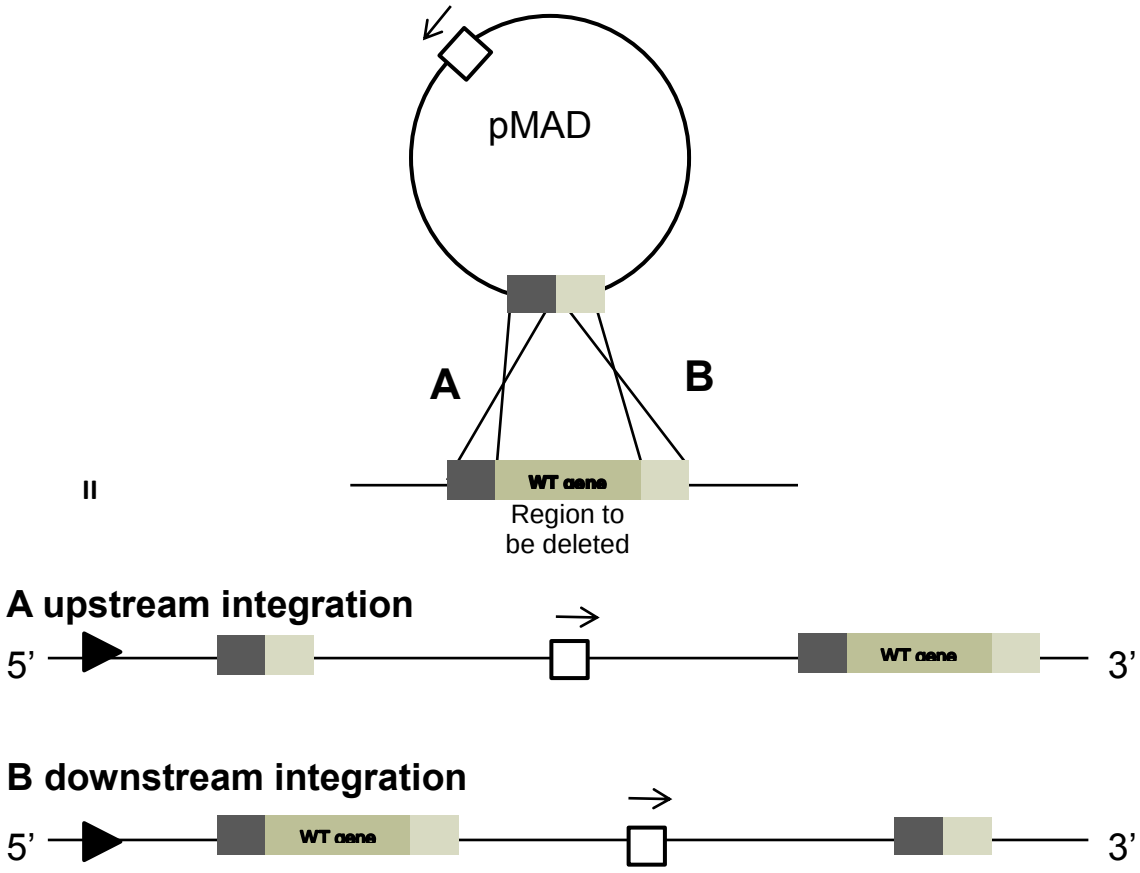

Figure 2.2 Integration of pMAD plasmid into cell genome. At non-permissive temperatures (~42 °C) in the presence of selective markers, the plasmid may integrate into the cell genome at regions cell DNA homologous to the plasmid insert (deletion cassette consisting of 300 bp upstream and 300 bp downstream of the region to be deleted). As the region of homology to the deletion cassette is separated by the WT gene on the genome, the plasmid was able to insert into the genome upstream (**A**) or downstream (**B**) of the WT gene, resulting in different chromosomal configurations as shown.

2.8.4 Passaging and screening for plasmid loss

To select for plasmid excision from the genome, BHI broth (25 ml) was inoculated with colonies from *L. monocytogenes* integrant strains and cultures were grown with aeration in conical flasks at a temperature permissive for plasmid replication (30 °C) in the absence of antibiotic selection. Cultures were sub-cultured every 12 h (1:100 dilution) over 6 days. At each 12 h point an aliquot was serially diluted in PBS to a 10^{-5} dilution. One hundred microlitres of the 10^{-5} dilution was plated on BHI agar and BHI agar with erythromycin (the selective marker on the pMAD plasmid). Colonies were taken from plates where antibiotic sensitivity was evident and were confirmed to be erythromycin sensitive by grid-plating. The plasmid could excise with the deletion cassette or the WT gene (Fig. 2.3). PCR was used to identify colonies in which the gene deletion remained but which displayed loss of the WT gene and the plasmid. Primers 790 and 791 specific to the pMAD *bgaB* gene were used to confirm loss of the plasmid (Table 2.3).

2.8.5 Gene and genome sequencing

Genome sequencing was carried out by MicrobesNG (Birmingham) and smaller DNA reads (≤ 1000 bp) were provided by Source Bioscience. Genomic DNA was extracted using the DNeasy Blood & Tissue Kit (Qiagen) following the manufacturer's directions for use. Gene products for sequencing were amplified via PCR and purified with the PCR purification kit (Qiagen), as outlined in Sections 2.7.3 and 2.6.2, respectively. Sequences were viewed with the programme DNA baser.

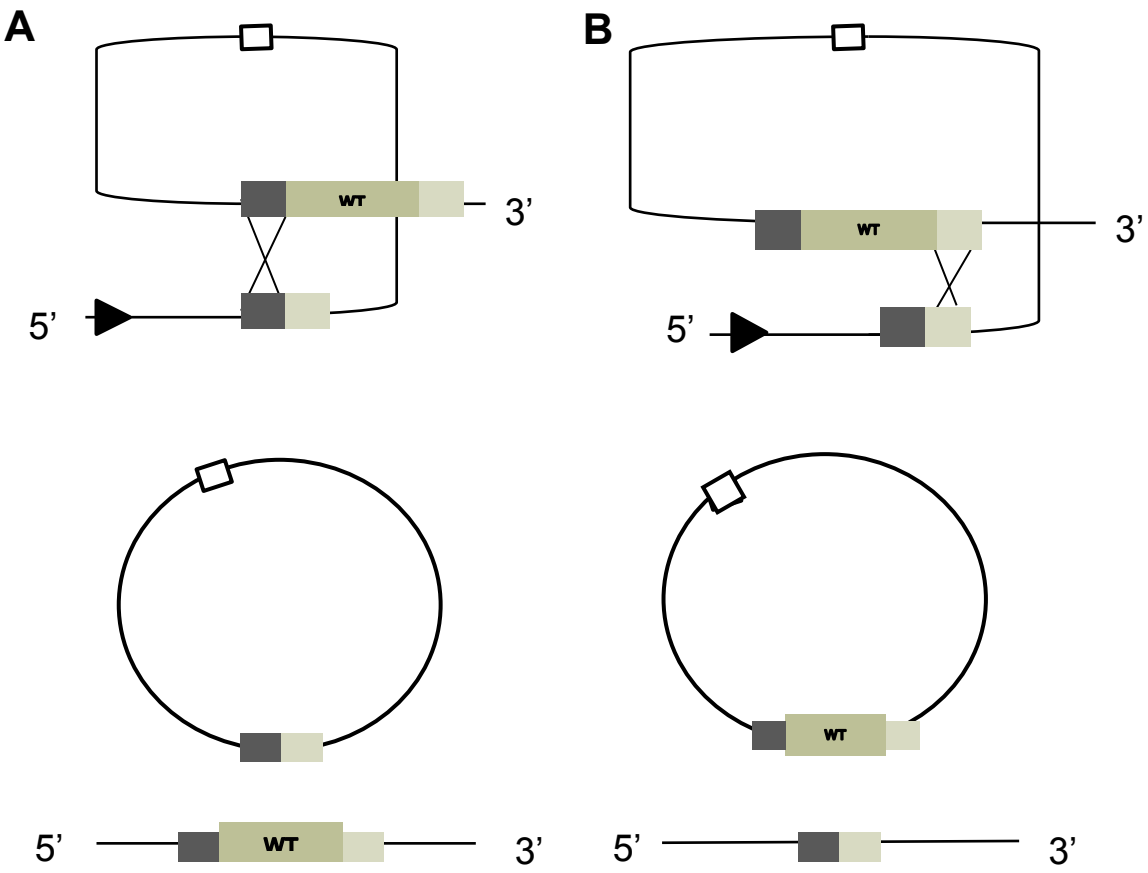

Figure 2.3 Excision of plasmid from genome Culturing cells at permissive temperatures in the absence of antibiotic selection allows the detection of excision of the plasmid from the genome. The plasmid can be excised with (**A**) the deletion cassette (leaving the WT gene on the genome) or with (**B**) the WT gene (allowing the deletion cassette to remain).

2.9 Western blotting method and preparation

σ^B activation was measured using an EGFP (enhanced green fluorescent protein) reporter system (Utratna *et al.,* 2012). EGFP has a single excitation peak at 488 nm and is suitable for fluorescence microscopy. The reporter system consists of a vector pKSV7 carrying an *egfp* gene fused to the promoter ($P_{lmo2230}$) of the highly σ^B-regulated gene *lmo2230* (Utratna *et al.,* 2012). This plasmid vector was transformed into strains to enable analysis of σ^B activation levels, using techniques outlined in 2.6.4.

2.9.1 Protein extraction

Bacteria were grown overnight at 30 °C or 37 °C in 25 ml BHI broth with chloramphenicol (10 µg ml^{-1}) selection where appropriate, shaking at 180 rpm. The stationary phase cultures were transferred to 50 ml Falcon tubes and stored on ice. Erythromycin (10 µg ml^{-1}) was then added to each culture to arrest protein synthesis. Cells were spun down for 15 min at 4 °C at 9,000 x*g* and resuspended in 2 ml sonication buffer (10 mM Tris-HCl, 0.1 mM EDTA and 5 mM $MgCl_2$, prepared in dH_2O and autoclaved) with 2 mg ml^{-1} lysozyme (Sigma-Aldrich) (added to sonication buffer immediately before use). Suspensions were incubated at 37 °C for 10 min before centrifugation at 9,000 x *g* for 15 min at 4 °C. Pellets were resuspended in 0.5 ml sonication buffer containing 1% (v/v) protease inhibitor cocktail (P2714, Sigma-Aldrich). To prepare this inhibitor solution, the contents of the Sigma-Aldrich bottle was resuspended in 100 ml autoclaved dH_2O and 50 µl aliquots were prepared and stored at -20 °C. Following resuspension, strains were

subjected to 10 min bead-beating in 2 ml sterile cryogenic vials (Greiner) containing 0.5 ml 0.1 mm glass beads and 0.25 ml 0.75 mm glass beads (Thistle Science). This method required 10 cycles of bead beating (using a vortex) with each cycle consisting of 30 s beating and 30 s resting cultures on ice. Strains were then centrifuged at 13,000 x *g* for 30 min to remove cell debris. The supernatant was removed and stored at -20 °C before protein quantification and analysis by Western blotting.

2.9.2 Protein concentration determination

Protein concentrations were determined using the BioRad Rc Dc Reagents Package assay. The BioRad protein assay is based on the Lowry assay (Lowry, 1951). For each assay, a set of protein standards ranging from 0 to 1.5 mg ml^{-1} was generated by dissolving bovine serum albumin (BSA) (Sigma-Aldrich) in sonication buffer (prepared as described in Section 2.9.1). Twenty-five microlitres of the protein standard samples were transferred to new 1.5 ml Eppendorf tubes. Twenty-five microlitres of 1:10 dilutions of the protein samples of unknown concentration in sonication buffer were also transferred to 1.5 ml Eppendorf tubes. One hundred and twenty-five microlitres of Reagent I was added to each of the samples and vortexed. Samples were incubated for 1 min at room temperature before the addition of 125 µl RC Reagent II. The tubes were again vortexed and then centrifuged at 15,000 x*g* for 5 min. The supernatant from each tube was discarded and residual liquid was removed by placing the opened inverted tubes on tissue paper on the bench for a number of minutes. During this time Dc Reagent A' was prepared by adding 5 µl of reagent S to 255 µl reagent A. When all liquid was drained from the tubes, 127 µl of Reagent A' was added to each tube and vortexed. Tubes were

incubated at room temperature for 5 min. One millilitre of Dc Reagent B was added to each tube and vortexed immediately. The samples were incubated at room temperature for 15 min. The absorbance readings of each sample were then recorded at 750 nm. A trend line was generated against the absorbance readings for the BSA protein standards and the concentration of the samples in buffer was determined from this trend line.

2.9.3 SDS-PAGE

Sodium dodecylsulphate polyacrylamide gel electrophoresis (SDS-PAGE) gels (7.5%) were prepared in a two-part process. Plates were assembled in a clamp (BioRad) and placed in the casting stand (BioRad). To make two gels, 4.85 ml dH_2O, 2.5 ml 1.5 M Tris-HCl separation buffer (1.5 M Tris-HCl in dH_2O, pH 8.8, stored at 4 °C), 2.5 ml 30% acrylamide/bisacrylamide (stored at 4 °C) (Fisher Scientific), and 100 µl 10% (w/v) SDS (Sigma-Aldrich) solution (10% w/v in dH_2O and filter-sterilized), were combined. Ten microlitres of ammonium persulfate solution (newly prepared for each gel run, 10% w/v in dH_2O) and 10 µl TEMED (*N*,*N*,*N*′,*N*′-Tetramethylethylenediaine, Sigma-Aldrich) (stored at 4 °C) were added to the solution, which was immediately mixed and applied to the gel plates, to reach a depth approximately 1.5-2.0 cm below the top of the front plate. One millilitre of N-butanol (Sigma-Aldrich) was applied to the top of the gels to generate a sharp line across the surface of the gel. The gels were allowed to polymerize for 40-45 min. The N-butanol was removed by rinsing the plate assemblies (in clamps) with distilled water until the alcohol odour was removed. The gels were returned to the casting stand and filter paper (BioRad) was used to remove excess water. The stacking gel mixture was prepared by adding 3.05 ml dH_2O to 1.25 ml Tris HCl stacking buffer (0.5 M Tris-

HCl, pH 6.8), 665 µl acrylamide/bisacrylamide and 50 µl 10% (w/v) SDS. Twenty five microlitres 10% w/v APS and 5 µl TEMED was added to the mixture which was quickly applied to the gel plates to reach the top of the front plate. Well combs (BioRad), with a 15 µl capacity per well were inserted. Filter paper (BioRad) was used to absorb any overflow from assembly. The stacking gel was allowed to polymerize for at least 20 min. Gels were then used in an SDS-PAGE or were sprayed with dH_2O and wrapped in tissue and clingfilm and stored at 4 °C.

Gels were clipped into the tank inset and placed in the SDS-PAGE tank (BioRad). The tank was filled with 1X running buffer to level indicated on the tank. Running buffer (10X) was prepared with 30.3 g Tris-base, 144 g glycine 10 g SDS, 1000 ml autoclaved dH_2O, stored at room temperature and diluted before use. Protein extracts were standardized to a 2 mg ml^{-1} concentration with 10 µl 5X protein sample buffer (0.25% bromophenol blue, 0.5 M dithiothreitol (Sigma-Aldrich), 50% glycerol (Sigma-Aldrich), 10% SDS, 0.25 M Tris-HCl (pH 6.8, stored at 4 °C) in 50 µl. Samples were incubated at 95-98 °C for 10 min (Eppendorf PCR block) and then centrifuged at 16,000 x*g* for 1 min to remove insoluble material. Fourteen microlitres of sample were then loaded into each gel well (total capacity 15 µl). For two SDS-PAGE gels, the settings were 150 V and 50 mA for 1 h (PowerPack Consort E835).

2.9.4 DNA transfer and Western blotting

SDS-PAGE gels were removed from the gel tank, the stacking gel was removed, and gels were washed in distilled water for 10 min, shaking at 70 oscillations min^{-1}. PVDF membrane (Immun-Blot® PVDF, BioRad) was cut to gel size and activated by placing the membrane in a methanol (≥99.8%, Sigma-Aldrich) solution for 30 s. Gels and PVDF were washed in transfer buffer for 10 min, shaking at 70 oscillations min^{-1}. Transfer buffer was prepared as follows: 2.8 g Tris-base, 11.3 g glycine in 700 ml autoclaved dH_2O. The solution volume was adjusted to 800 ml and 200 ml methanol was added before storage at 4 °C. Proteins were transferred from the SDS-PAGE gels to PVDF membranes using a transfer apparatus (Jencons SD20). Each transfer sandwich was stacked from bottom to top as follows: filter paper (BioRad Mini Trans-Blot® Filter Paper), PVDF membrane, SDS-PAGE gel and filter paper. The transfer sandwiches were wetted with transfer buffer and a pipette was rolled across the sandwich to remove air bubbles. The transfer apparatus was set to run at 100 mA and 5 V for 1 h (PowerPack Consort E835). Following this, PVDF membranes were removed and washed for 10 min (70 oscillations min^{-1}) in TBST (Tris buffered saline: 50 mM Tris-HCl, pH 7.5, 150 mM NaCl, autoclaved) containing 1% (v/v) Tween 20 (Sigma-Aldrich). Each membrane was then blocked in 15 ml skim milk solution (5 % w/v skim milk powder (Sigma-Aldrich) in TBST with 1% (v/v) Tween 20) for 1 h (30 oscillations min^{-1}) and then washed three times as previously described in TBST with 1% (v/v) Tween 20. Membranes were then incubated overnight (16 h) at 4 °C shaking (30 oscillations min^{-1}) using rabbit polyclonal anti-GFP antibody (Santa Cruz Biotechnology) diluted 1:3,750 in 15 ml 5% (w/v) skim milk solution. The membrane was again washed three times in TBST with 1% (v/v) Tween 20 before incubation with the secondary antibody (HRP (horseradish peroxidise) conjugated to

goat Anti-rabbit IgY, Santa Cruz Biotechnology) diluted 1:3,750 in 5% (w/v) skim milk. Blots were washed a final three times in TBST with 1% (v/v) Tween 20. Blots were viewed by adding a chemiluminescent substrate (SuperSignal® West Pico Chemiluminescent Kit, Pierce) and captured in a dark room using a light sensitive film (Kodak Hyperfilm ECL, GE Healthcare) and an AGFA CP1000 processor. Developed films were scanned using a CanoScan 9000F Mark II scanner and saved as .TIF files.

2.10 Fluorescence microscopy

Fluorescence microscopy was used to examine σ^B activation in strains carrying pKSV7 $P_{lmo2230}$-*egfp* (Utratna *et al.,* 2012) by visualising EGFP.

2.10.1 Sample preparation

Aliquots (1 ml) were removed from stationary phase cultures grown with chloramphenicol (10 mg ml^{-1}), and standardised to OD_{600nm}= 0.6 in BHI in 15 ml Falcon tubes. Standardised samples were fixed with an ice-cold ethanol-methanol solution (1:1 ethanol: methanol, both >99.8%, Sigma-Aldrich) in a 1:1 ratio and placed at -20 °C for 20 min. Samples were then centrifuged at 9000 x*g* for 10 min at 4 °C. The supernatant was discarded and pellets were each suspended in 1 ml PBS. Samples were then used immediately in fluorescence microscopy or were stored at -20 °C for up to 1 month. Tubes were wrapped in aluminium foil and lights were dimmed during sample preparation to minimise the amount of light-induced EGFP bleaching.

2.10.2 Microscopy specifications

Five microlitres of fixed cell suspensions were placed directly onto glass slides (Thermo Scientific) with cover slips (Thermo Scientific) and viewed immediately at 40X magnification under a Leica DMI 3000B inverted microscope. Cells were focused in brightfield before viewing images with a florescence filter of 470 nm. Images were captured using the Leica Application Suite programme. For fluorescence images, the settings were fixed at the following: exposure times 4 s, saturation 0.85, gamma of 0.65, gain 1. For bright field images the settings were as follows: exposure 2 s, saturation 0.85, gamma 0, gain 5. Images were saved as .TIF files.

Chapter 3: Blue Light Inhibition of *Listeria monocytogenes* Growth is Mediated by Reactive Oxygen Species and is Influenced by σ^B and the Blue Light Sensor Lmo0799

Declaration of author contribution

The majority of data presented in this chapter (including the introduction and discussion) has been published in the joint author paper *Blue-light inhibition of Listeria monocytogenes growth is mediated by reactive oxygen species and is influenced by σ^B and the blue-light sensor Lmo0799* (O'Donoghue, B., NicAogáin, K., Bennett, C., Conneely, A., Tiensuu, T., Johansson, J. and Conor O'Byrne) (2016). Data provided by K. NicAogáin including the effect of DMTU on cell growth is referred to in the text and Fig. 3.2 was prepared by K. NicAogáin.

.

3.1 Introduction

Listeria monocytogenes is a Gram-positive bacterium commonly found in the environment. It is a foodborne pathogen, capable of causing a severe systemic infection in humans and is associated with mortality rates of up to 30% (Farber & Peterkin,1991; Mead *et al.,* 1999; EFSA & ECDC, 2015). Although incidence levels remain far lower than those for outbreaks involving pathogens such as norovirus and salmonella, cases of listeriosis have risen annually in Europe between 2009 and 2013 and are linked primarily with the consumption of ready-to-eat foods (EFSA & ECDC, 2015). *L. monocytogenes* displays a number of stress adaptations that aid its survival in a wide range of habitats including foods, food-processing environments and the mammalian gastrointestinal tract. In particular it displays a notable tolerance to osmotic stress, low temperature and bile and acid stress (Ferreira *et al.,* 2001; Moorhead & Dykes, 2004; Sue *et al.,* 2004; Hardy *et al.,* 2004). Many of the stress resistant properties of *L. monocytogenes* are under the control of the stress-inducible sigma factor, σ^B, which drives the transcription of the general stress regulon (O'Byrne and Karatzas, 2008; Hecker *et al.,* 2007; Kazmierczak *et al.,* 2003; Toledo-Arana *et al.,* 2009). The regulation of σ^B is not fully understood in *L. monocytogenes* but it is believed to involve a signal transduction cascade that ultimately modulates the availability of σ^B to associate with RNA polymerase. Environmental signals are thought to be sensed and integrated into the regulatory pathway by a high molecular weight multi-subunit complex called a stressosome (O'Byrne & Karatzas, 2008; O'Byrne & Heavin, 2012). Although the structure of this complex has not been determined in *L. monocytogenes* it is likely to be similar to the stressosome from *B. subtilis,* whose structure has been partly solved (Marles-Wright *et al.,* 2008), since all of the genes involved are conserved between these

species (Ferreria *et al.,* 2004). In *B. subtilis* the current model proposes that stress signals are sensed by protrusions on the surface of the stressosome that are formed by the N-terminal domains of RsbRA and its paralogues, RsbRB, RsbRC and RsbRD (Marles-Wright *et al.,* 2008; Marles-Wright & Lewis, 2010). These sensory signals are then transduced to the core of the stressosome resulting in phosphorylation events that lead to the release of RsbT from the stressosome. RsbT then interacts with RsbU to bring about the activation of σ^B. It is thought that RsbRA and its paralogues (in *L. monocytogenes* they are RsbR, Lmo0799, Lmo0161, Lmo1642 and Lmo1842) can integrate different environmental stress signals, allowing σ^B activation under a variety of stress conditions, but thus far only blue light has been shown to be sensed by the stressosome (Ondrusch & Kreft, 2011; Tiensuu *et al.,* 2013; Avila-Perez *et al.,* 2006; Möglich & Moffat, 2007).

Blue light sensing in *L. monocytogenes* requires Lmo0799, a widely- conserved protein predicted to be associated with the stressosome that has a light oxygen voltage (LOV) domain at its N terminal and a sulphate transporter, anti-sigma factor (STAS) domain at its C-terminal (Ondrusch & Kreft, 2011). Mutants lacking *lmo0799* have increased motility in the presence of light compared to the WT, fail to show enhanced invasion into mammalian cells in response to light (Ondrusch & Kreft, 2011), and are unable to form opaque/translucent rings on semi-solid agar in response to repeated cycles of light and dark (Fig. 1.4C) (Tiensuu *et al.,* 2013). The mechanism of light-sensing by Lmo0799 has not yet been fully elucidated, although it is clear that it exhibits photochemical activity similar to the related light sensor from *B. subtilis*, YtvA, and the formation of a flavin-cysteinyl adduct in response to light was postulated (Chan *et al.,* 2012). In YtvA this adduct forms between C4 of the FMN ring and the cysteine residue at position 62 (Möglich & Moffat, 2007), which is conserved in the *L. monocytogenes* protein but located

at position 56. In the present study we sought to elucidate the mechanism of sensing by mutating Cys 56 to determine the impact on light sensing and also to clarify the contribution of Lmo0799 to the growth and survival of *L. monocytogenes*.

The use of visible light as a suitable containment treatment has drawn increasing notice and several studies have been published that examine the effects of violet-blue (405 nm) light on bacterial cells (Murdoch *et al.,* 2012; Endarko *et al.,* 2012; McKenzie *et al.,* 2014; McKenzie *et al*., 2013; Maclean *et al.,* 2009). Although blue light is known to activate σ^B in *L. monocytogenes* the impact of visible light on growth and survival in this pathogen has not been studied in detail (Ondrusch & Kreft, 2011).

In this study, we investigate the influence of visible light on the physiology of *L. monocytogenes*. We use blue light with a wavelength of 460-470 nm as this is the wavelength that has been shown to activate the general stress response via the light sensor Lmo0799 and σ^B. We show that quite low doses of light at this wavelength inhibit the growth of this pathogen in both liquid and solid growth media. We show that the inhibitory mode-of-action is dependent on the production of reactive oxygen species. The role of σ^B and Lmo0799 in the response of *L. monocytogenes* to blue light is further clarified and the conserved cysteine residue in Lmo0799 is shown to be essential for light sensing.

3.2. Blue light affects *L. monocytogenes* behaviour

3.2.1 Construction of blue light delivery systems

In order to examine the effects of blue light on *L. monocytogenes* a suitable blue light exposure apparatus was required, that was capable of delivering a known quantity of blue light to the cells in liquid and solid (agar) media. Initial experiments were carried out using single blue light LEDs (Phenoptix) within plastic drain piping tubes, however it was quickly realised that a more sophisticated blue light delivery system was required.

Two types of light exposure apparatus were constructed (Fig. 2.1) and are described in Section 2.5.1. The first apparatus (LEDS1) provided 470 nm light at adjustable intensity across a circular area approximately 7 cm in diameter. The second apparatus (LEDS2) provided 460 nm light at a fixed intensity of 1.5-2.0 mW cm^{-2} across an area equal in size to a 96-well plate.

3.2.2 Blue light inhibits *L. monocytogenes* growth

Examining the effect of light on WT *L. monocytogenes* cells, it is clear that blue light at an intensity of 1.5-2.0 mW cm^{-2} has an inhibitory effect on cell growth. After a 24 h incubation for WT cells (standardized to an OD_{600nm} of 1.0 and then diluted serially to a 10-5 dilution) spotted on BHI agar, growth was apparent on plates incubated in the dark, however no growth was observed for cells exposed to the light (Fig. 3.1). This displays the clear inhibitory effects of blue light at 470 nm on *L. monocytogenes* growth under the conditions tested. When plates exposed to light were then incubated in the dark, growth

was restored (data not shown), indicating that at this intensity light has an inhibitory but not killing effect on *L. monocytogenes* under these conditions. In liquid BHI medium, the same light irradiance significantly inhibited both the culture yield (final optical density at 24 h) and the lag time (time to reach OD_{600nm} of 0.1), although growth was not completely inhibited (Fig. 3.2B). The inhibitory effects of blue light (470 nm) were found to be dependent on the cell density, since only more-dilute cultures (those containing $<10^7$ CFU ml^{-1}) were found to be inhibited on agar plates (Fig. 3.2A). This was also the case in liquid BHI medium, in which the effects of blue light on the 24 h culture OD_{600nm} and the lag time were more pronounced as the cell concentration decreased (Fig. 3.2B). At high cell densities ($>10^7$ CFU ml^{-1}) essentially no inhibition of growth was observed at this dose of light (Fig. 3.2).

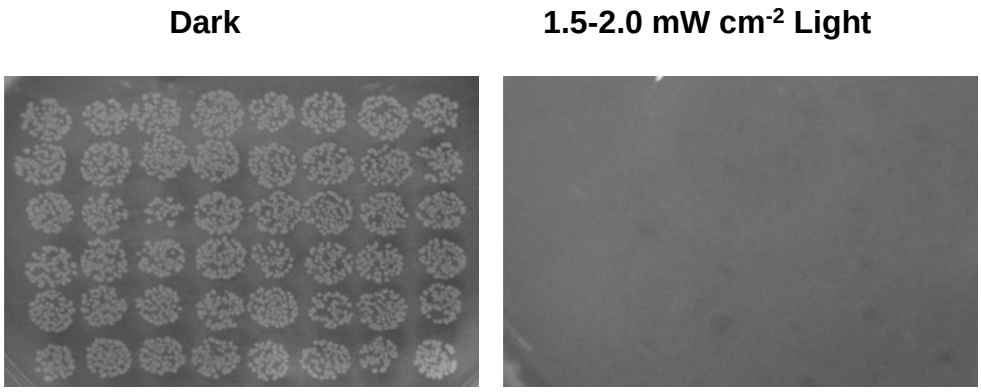

Figure 3.1 Blue light has an inhibitory effect on cell growth. Overnight cultures were standardized to an OD_{600nm}= 1.0, diluted 1: 10 to 10^{-5} dilution (approximately equal to 10^4 cells) and inoculated in 4 µl aliquots across an agar plate. Plates were incubated for 24 h at 30 °C in the dark or in the presence of 1.5- 2.0 mW cm^{-2} 470 nm blue light.

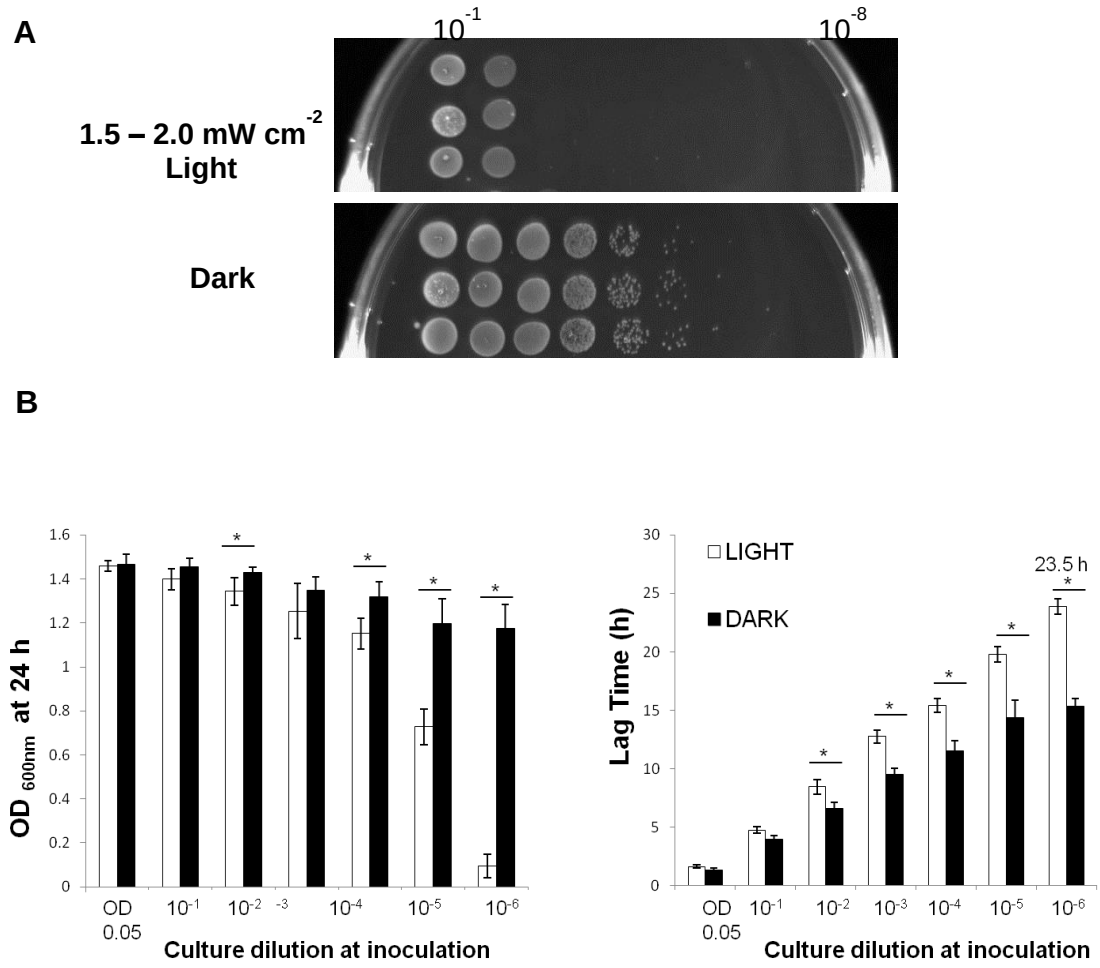

Figure 3.2 Cell density influences the extent of growth inhibition of EGD-e by blue light. Dilutions of EGD-e stationary phase cultures were illuminated with blue light (460 to 470 nm, 1.5-2.0 mW cm^{-2}) either on BHI agar (**A**) or in BHI liquid culture (**B**). (**A**) Overnight cultures were standardized to an OD_{600nm} of 1.0 and serially diluted 1:10 to 10^{-8}. Four microlitres of each dilution was spotted in triplicate onto BHI agar and grown at 30 °C for 24 h. (**B**) White bars represent growth in the presence of light, and the black bars represent the dark control. The graphs show final OD_{600nm} measurements (left) and lag times (right). Starting cells were equalized to an OD_{600nm} of 0.05 and diluted to 10^{-6}. Cultures were grown in 96-well plates at 30 °C for 24 h. The values represent the means of the results from three individual replicates. The error bars represent the standard deviations from the mean. Student's *t*-test was carried out to determine the statistical difference ($p \leq 0.05$), indicated with an asterisk) between culture dilutions grown in light and dark.

3.2.3 The inhibitory effects of blue light are caused by the generation of ROS

Light-induced generation of ROS species was posited as a possible cause for the light-dependent growth inhibition. Assays found that the ROS scavenger dimethylthiourea (DMTU) conferred a significant protective effect against blue light both on solid medium and in liquid medium. It was observed that the addition of catalase to WT cultures grown either in BHI broth or on BHI agar, enabled growth in the presence of 1.5-2.0 mW cm^{-2} 470 nm blue light, at levels similar to those seen for the cells incubated in the dark (Fig. 3.3A&B). WT strains inoculated on BHI agar spread with a control solution containing BSA protein and exposed to light were unable to overcome the inhibitory effects of light, indicating that the hydrogen peroxide-degrading ability of catalase was responsible for the light protective effects observed (data not shown). Examining the growth of strains in BHI broth, the time taken to reach an OD_{600nm} of 0.1 was significantly shorter for cells to which catalase was added. The OD_{600nm} reading at 24 h for strains also differed significantly between cells grown in the light with or without catalase at varying cell dilutions.

The findings provide evidence supporting the theory that the presence of light induces the generation of ROS, including hydrogen peroxide, and this is likely to be the principal reason for growth inhibition. The addition of catalase also moderately enhanced the growth of strains cultured in the dark when compared with those grown in the absence of catalase. This was visible on BHI agar after 24 h and in the lag time calculated between cells grown in the dark with or without catalase (Fig. 3.4A&B). This may be attributed to the protection offered by the catalase against ROS species produced during normal metabolic processes.

WT EGD-e cells have previously been shown to grow in a series of concentric opaque and translucent rings when exposed to consecutive cycles of light and dark at 30 °C or lower temperatures (Tiensuu *et al.,* 2013). This phenotype is dependent on the presence of σ^B and is not observed when WT cells are grown continuously under light or dark conditions (Tiensuu *et al*, 2013). WT cells spotted onto low-agar spread with catalase solution retained the ability to form light/dark 'rings' in a manner similar to WT cultures grown in the absence of catalase (Fig. 3.3C). Ambient white light was used for this experiment and all other motility experiments as the light intensity provided by the blue light exposure apparatus was too high and inhibited the development of the 'ring' phenotype (data not shown).

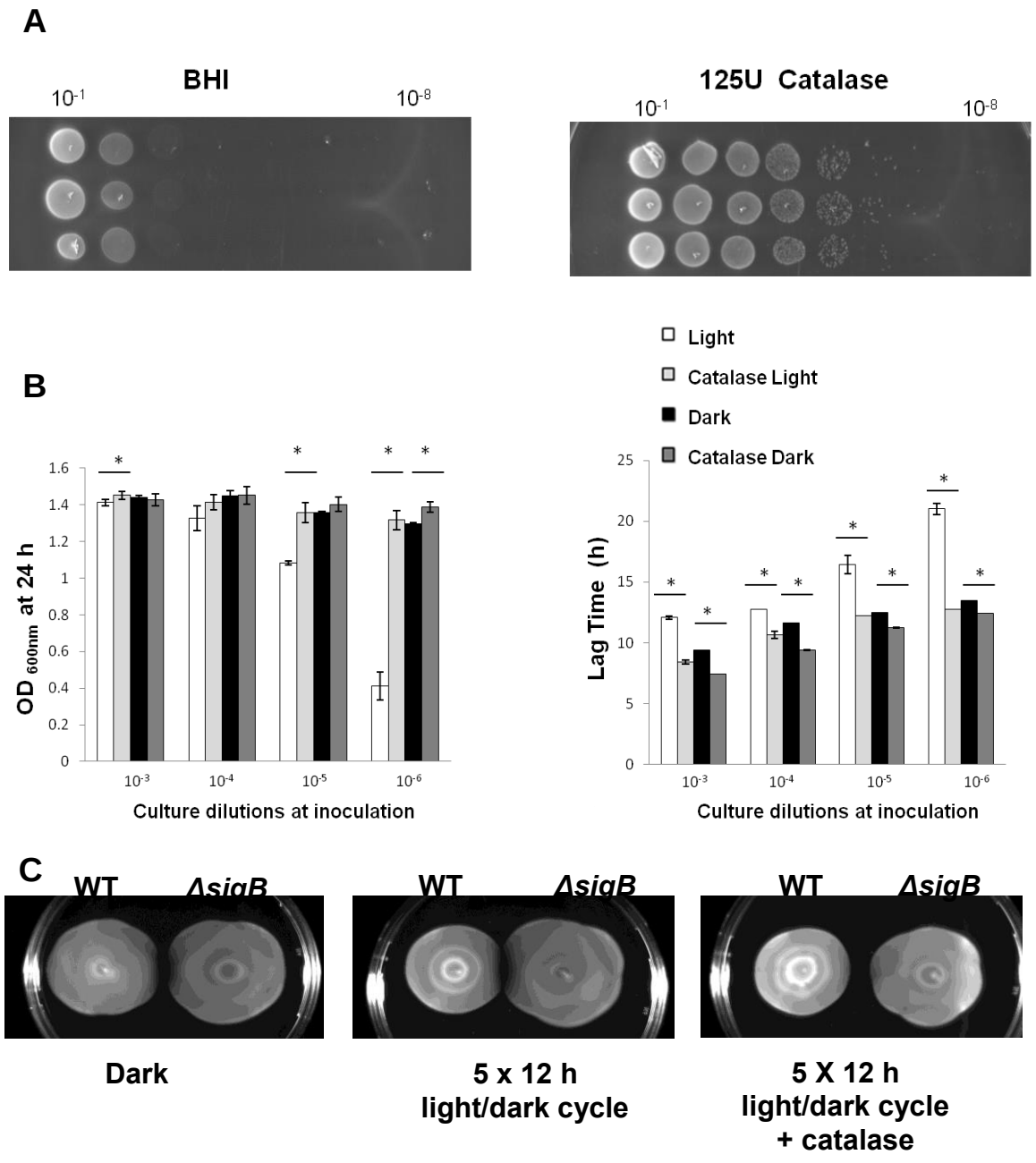

Figure 3.3 Contributions of catalase to cell protection. (**A**) WT overnight cultures were standardized, diluted serially, and spotted on BHI agar spread with catalase or on agar plates without catalase. The plates were incubated in the presence of light or absence for 24 h. (**B**) WT overnight cultures were diluted to an OD_{600nm} of 0.05 and serially diluted 10-fold to a 10^{-6} dilution. The dilutions were grown for 24 h in the presence or absence of light, with or without catalase at a concentration of 125 U ml^{-1}. The 24 h

endpoint and the time taken to reach an OD_{600nm} of 0.1 were calculated for each strain condition at each dilution. The error bars represent standard deviations .between samples. Unpaired *t*-tests were used to determine the significance of differences ($p \leq 0.05$, indicated by asterisks) between endpoint and lag-phase values between cultures with and without catalase. (**C**) Overnight cultures of WT and *ΔsigB* strains were standardized to OD_{600nm}= 1.0 and spotted on to low motility agar catalase spread with 200 µl of catalase at a concentration of 2000-5000 U ml^{-1}. Plates were incubated for 5 consecutive 12 h periods in ambient light and dark for 24 h in the presence or absence of catalase.

3.2.4 Catalase activity is affected by oxygen exposure during growth

In order to examine the effects of growth conditions on catalase production within the cells, cultures were grown anaerobically or aerobically at 30 °C or 37 °C to stationary phase and the level of 'bubbling' activity following the addition of hydrogen peroxide, indicating catalase presence, was measured by photography (Fig. 3.4A). A distinct difference in catalase activity between anaerobically and aerobically grown stationary phase cultures was recorded at both 30 °C and 37 °C. For aerobically grown stationary phase EGD-e WT and *ΔsigB* strain cultures, the addition of 10 µl 30% hydrogen peroxide solution produced a mild bubbling reaction and vigorous bubbling was observed upon the addition of 100 µl 30% hydrogen peroxide solution. However, the addition of 100 µl of this solution did not have a visible effect on anaerobically grown stationary phase cultures (Boura *et al.,* 2016). Additionally, at exponential phase for aerobically grown cultures, the addition of 10 µl hydrogen peroxide was not sufficient for observation of bubbling activity, indicating that there may be an increase in cell catalase production sometime between exponential phase and entry into stationary phase (Fig 3.4B). A small difference was seen in the amount of bubbling observed for the aerobically grown WT

and *ΔsigB* strains, with the *ΔsigB* strain producing slightly more bubbles than the WT at 30 °C and 37 °C (Fig. 3.4A). This phenotype was more pronounced for the 10403S WT and *ΔsigB* strains (Boura *et al.,* 2016). Experiments carried out testing the survival of *L. monocytogenes* following exposure to hydrogen peroxide produced highly variable results (data not shown) and it may be that differing levels of oxygen tension in cultures during growth contributed to this variability. Clearly, these results highlight oxygen exposure during growth as a key factor in determining cell's ability to respond to hydrogen peroxide, and presumably, other ROS.

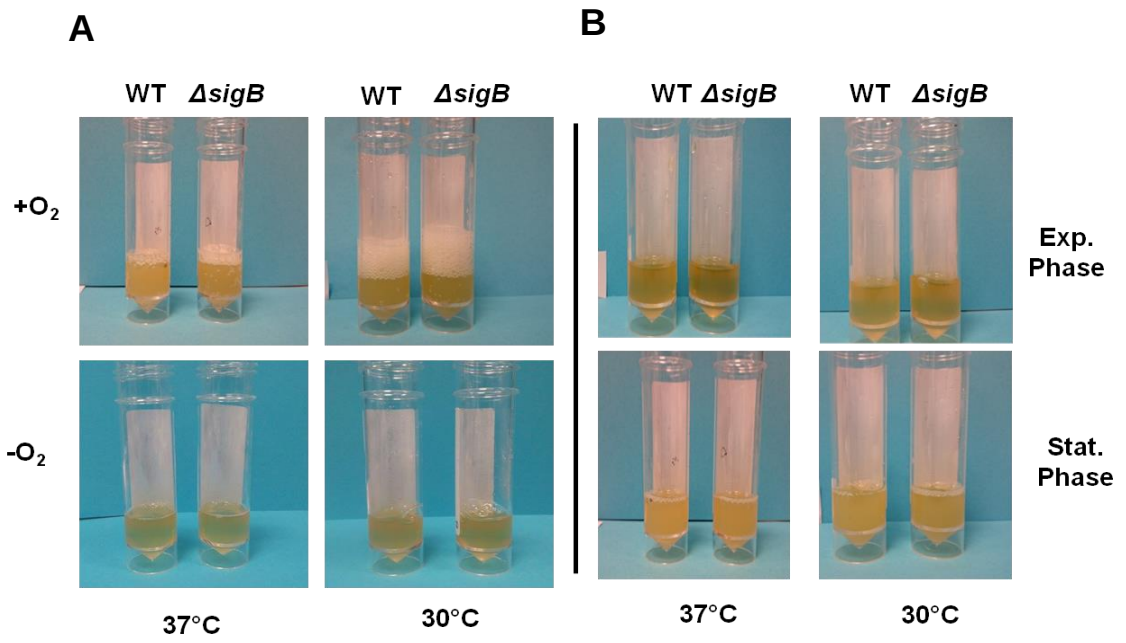

Figure 3.4 Oxygen exposure during growth affects catalase activity. (**A**) *L. monocytogenes* WT and *ΔsigB* cultures were incubated at 37 °C or 30 °C in flasks, shaking (+O_2) or in a sealed gas chamber with an AnaeroGen sachet (Oxoid) (-O_2) overnight to stationary phase. 100 µl of 30% H_2O_2 was added to each 5 ml aliquot and images were taken of the bubbling reaction which occurred (Section 2.4.6). (**B**) WT and *ΔsigB* cultures were incubated aerobically at 37 °C or 30 °C to exponential (above) or stationary phase (below). 10 µl of 30% H_2O_2 was added to each 5 ml culture sample and images were taken of the bubbling reaction which occurred (Section 2.4.6).

3.3 Construction of a light insensitive mutant

3.3.1 Design of a putative light insensitive or 'blind' *lmo0799* C56A strain

Lmo0799 was established as a blue light sensor by Ondrusch and Kreft, (2011) and its mechanism of function was proposed to involve the light-induced formation of a covalent bond between a conserved cysteine residue on Lmo0799 and an associated flavin cofactor. To investigate the contribution of this protein to the light-stress response further, a light insensitive or 'blind' mutant was constructed and a *Δlmo0799* strain was acquired from Prof J. Johansson at Umeå University for further studies (Tiensuu *et al.,* 2013). In order to construct a 'blind' strain, a replacement gene in which the conserved cysteine was replaced by an alanine, *lmo0799* C56A, was designed (Section 2.8.2). Alanine is a non-phosphorylateable residue which cannot form covalent adducts but whose presence does not affect protein folding within the LOV domain (Harper *et al.,* 2003; Gaidenko *et al*., 2006). The sequence of the *L. monocytogenes* EGD-e *lmo0799* gene was sourced at *http://genolist.pasteur.fr/ListiList/*. At codon 56, the TGT (Cys) codon was changed to GCA (Ala). Silent mutations in three adjacent codons were also included in the sequence to facilitate detection by PCR during the strain construction (WT, 5'-TCCAATTGTCAC to 5'-AGTAACGCACAT). The altered gene, which was 762 bp in length, was synthesized by Eurofins Genomics with additional *Eco*RI and *Xma*I restriction sites at each end in order to facilitate cloning into the pMAD suicide vector.

This replacement gene was transformed on the pMAD plasmid vector into electrocompetent EGD-e cells, prepared as described in Section 2.1.1. The transformation procedure was followed by two homologous recombination events. Above 42 °C, the pMAD plasmid cannot replicate independently and only plasmids that integrate

into the *L. monocytogenes* genome at the regions homologous to the replacement gene cassette are retained. A second homologous recombination event was achieved by passaging the cells at 30 °C to cause excision of the plasmid from the genome with the replacement cassette or with the wild-type (WT) gene and surrounding regions.

3.3.2 Construction of a pMAD::*lmo0799* C56A cassette

The replacement allele encoding the “blind” variant C56A was provided on vector pEX-A by Eurofins Genomics and was transformed into *E. coli* TOP10 electrocompetent cells to provide a stock strain. The plasmid was then extracted and digested with *Xma*I and *Eco*RI to separate the insert from the vector (Fig. 3.6B). pMAD, which carries a thermosensitive origin of replication that prevents independent replication at 42 °C, was chosen as a suitable vector for allele replacement and was also digested with these enzymes. The digested pMAD vector and *lmo0799* C56A insert products were purified and quantified as directed in Sections before ligation (Section 2.6.3). Ligation procedures were carried out with 50 ng of insert and vector quantities in a 1:1, 2:1 and 3:1 insert: vector ratio.

3.3.3 Cloning of the deletion cassettes into *E. coli* TOP10

Ligation reactions were transformed into electrocompetent *E. coli* Top10 cells and plated on LB agar with ampicillin (10 µg ml^{-1}) to select for pMAD::*lmo0799* C56A containing cells. Colonies were obtained for the 2:1 insert:vector ligation reaction. Individual colonies were screened for presence of the insert using primers COB 736 and COB 737, of which COB 736 was designed to specifically bind to the altered base pairs of the C56A

gene (primer table 2.3). COB 737 binds to DNA within the *lmo0799* gene present in both the WT and mutant allele. M13 primer binding sites, which are commonly encoded on plasmid vectors to aid screening processes, are not present in the pMAD vector.

3.3.4 Transformation and integration of pMAD::*lmo0799* C56A

Following the identification *E. coli* TOP10 pMAD::*lmo0799* C56A transformant strains, the deletion cassette plasmids were extracted from the *E. coli* strain, concentrated, and transformed into *L. monocytogenes* EGD-e (as described in Sections 2.1.1 & 2.6.4). Transformed cells were plated on BHI agar with erythromycin (2 μg ml^{-1}) to select for successful transformants. The presence of a β-galactosidase gene on pMAD was hoped to aid the screening process for successful transformants as these colonies should be blue in colour when grown on plates spread with X-Gal (40 mg ml^{-1} in dimethylformamide) (both products supplied by Sigma-Aldrich). This process was quickly abandoned as all colonies, including those that tested positively for the presence of the plasmid via PCR and erythromycin resistance, grew as creamy white colonies. Successful transformants were identified by PCR, using the primers COB 736 and COB 737 which had been previously used to identify the presence of the deletion cassette in *E. coli.* Primers COB 736 and COB 737 were used in PCR to screen colonies for the presence of the C56A 'blind' gene (Fig. 3.5B).A PCR product was not observed for the WT strain with these primers as COB 736 does not bind to the WT *lmo0799* gene.

3.3.5 Chromosomal integration of pMAD::*lmo0799* C56A

The first homologous recombination event involved the integration of the deletion cassette plasmid into the genome at regions homologous to the cassette. The pMAD plasmid carries a thermosensitive origin of replication which prevents it replicating independently at 42 °C (Arnaud *et al.*, 2004). Six colonies of the EGD-e transformants carrying pMAD::*lmo0799* C56A cassettes were plated on BHI agar containing erythromycin (2 µg ml^{-1}) and incubated at the non-permissive temperature of 42 °C to select for colonies in which the plasmid integrated into the genome (Section 2.8.3). Strains were restreaked several times until growth without fail (non-'patchy' growth) occurred.

Colonies from the third and fourth restreak plate were tested for integration of the plasmid into the genome with two sets of primers. In each primer set one primer bound to the replacement gene DNA sequence and one to the chromosomal DNA (Fig. 3.5). Successful integrants were chosen from the third restreak. The replacement cassette could integrate upstream or downstream of the region of homology on the chromosome, however only plasmids which integrated downstream of the *lmo0799* could be identified here, as only the forward primer COB 736 possessed binding specificity for the *lmo0799* mutant allele and not the WT gene (Fig. 3.5 (i)). The second set of primers COB 699 and COB 737 provided a PCR product of equal length for both the WT strain and strains that displayed plasmid integration downstream of the WT gene (Fig 3.5).

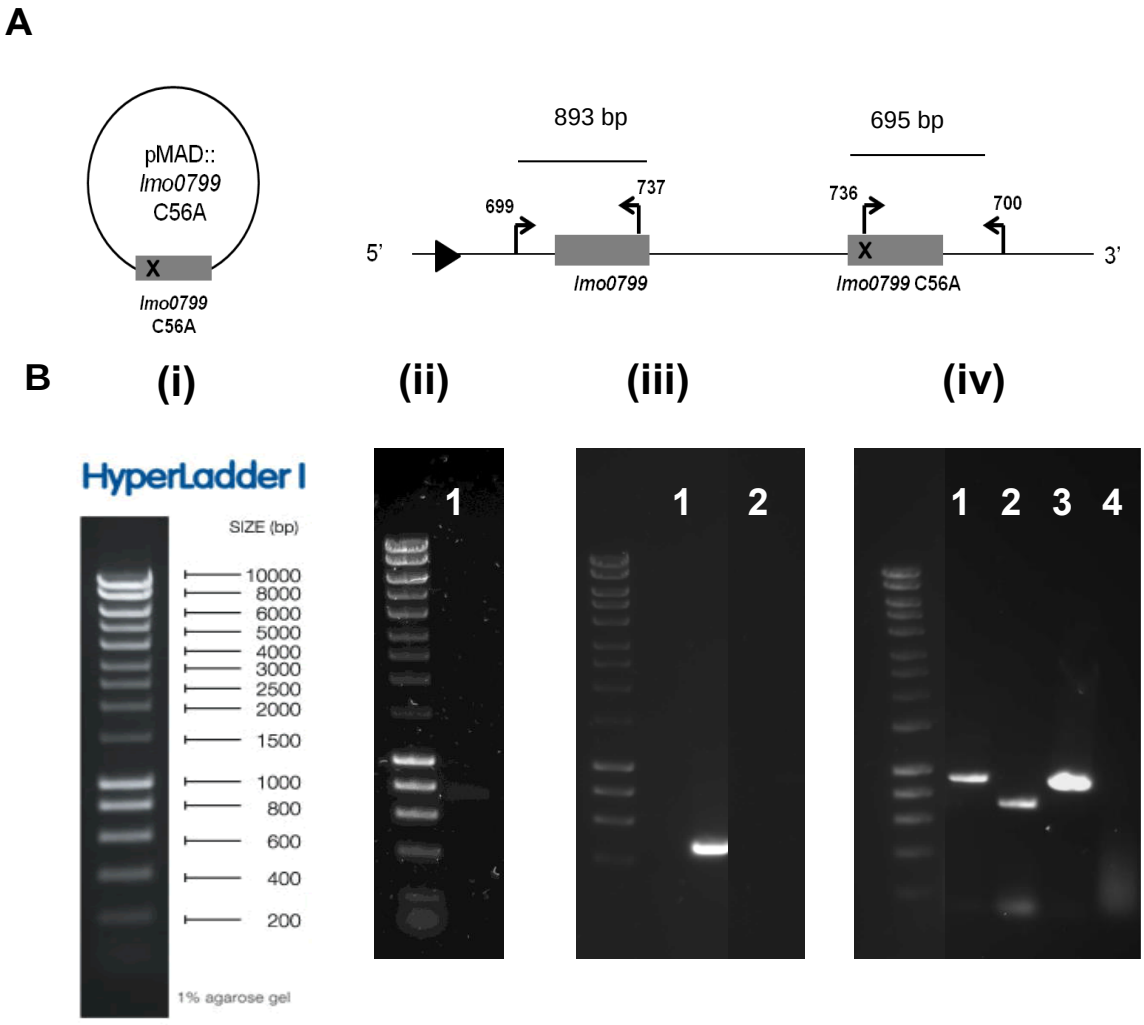

Figure 3.5 Transformation and integration of pMAD-*lmo0799* C56A. (A) The pMAD::*lmo0799* C56A cassette can exist within the cell in a circular form or can integrate into the cell genome. Primers COB 736 and COB 700 allow detection of downstream integration. **(B)** PCR detection of transformants and integrant**s.** (**i**) HyperLadder 1 (Bioline). (**ii**) *lmo0799*-C56A (5 µl) digested from pEX-A::*lmo0799* C56A with *Xma*I and *Eco*RI (**iii**) Identification of EGD-e pMAD*::lmo0799* C56A transformant (lane 1- 498 bp) with COB 736 and 737 primers. WT EGD-e was used as a negative control (lane 2) (**iv**) Identification of EGD-e pMAD-*lmo0799* C56A integrant strain via PCR. Primers 699 and 799 provide an 893 bp product for integrant strains (lane 1) and the WT (lane 3). PCR with COB 736 primer specific to the altered region in the mutant allele and COB 700 primer provide 695 bp product for EGD-e pMAD::*lmo0799* C56A integrant (downstream integration) (lane 2). Lane 4 shows no DNA product (WT negative control).

3.3.6 Selection of *lmo0799* C56A strain

In the final stages of mutant construction a second homologous recombination event causes the excision of the plasmid from the genome. Following PCR confirmation of an EGD-e pMAD::*lmo0799* C56A integrant strain, the integrant was passaged at 30 °C in liquid media in the absence of a selective agent to promote excision of the plasmid from the genome and subsequently, its loss from the cell (described in Section 2.8.4). Cultures were subcultured into new media every 12 s and samples were taken from each passage, starting with the third subculture. These cells were plated on BHI agar and incubated overnight, before colonies were screened for erythromycin sensitivity. Colonies displaying erythromycin sensitivity were tested via PCR with COB 736 and 737 for the presence of the mutant *lmo0799* allele (Fig. 3.7). Over 150 colonies were tested via PCR. Colonies which tested positive for presence of the C56A-encoding allele were also screened with primers COB 790 and 791 against the *bgaB* gene (1,530 bp product) to ensure loss of the plasmid had occurred. PCR with COB 736 and 737 produced a faint positive result band product when testing the WT control strain (Fig. 3.7). This was likely due to non specific primer binding, allowing binding despite the presence of several different residues. Long-term freezer stocks were made of this new strain. The mutant's altered sequence was confirmed by Sanger sequencing (Source Bioscience) with primers COB 699 and COB 737, using a PCR product amplified from the mutant strain with primers COB 699 and COB 700.

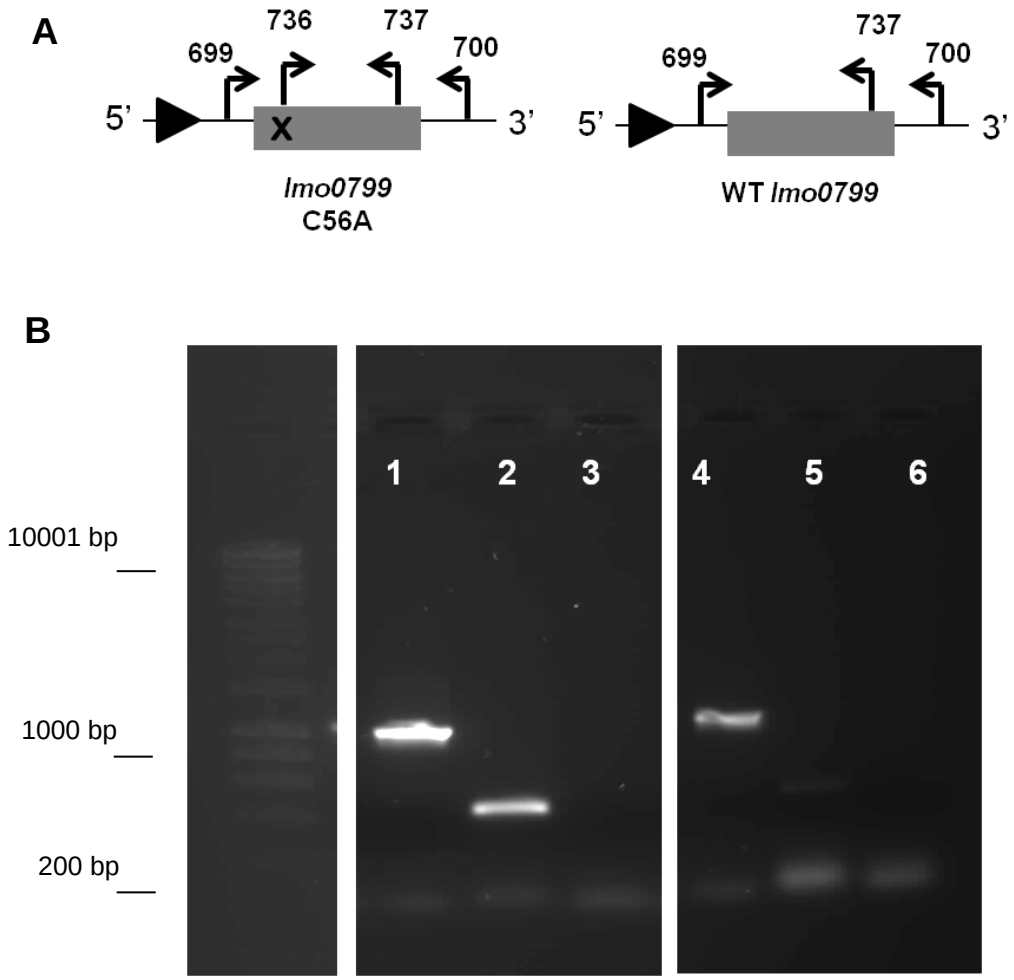

Figure 3.6 PCR to identify EGD-e *lmo0799* C56A mutants (**A**).PCR primer map for (left) *lmo0799* C56A mutant strain or WT *lmo0799* strain.(**B**) PCR to identify *lmo0799* C56A mutant strain. PCR with primers COB 699 and 700 for the EGD-e l*mo0799* C56A (lane 1- 1085 bp) and WT (lane 4-1085 bp) strains. PCR with COB 736 and 737 testing for the presence of the mutant allele EGD-e *lmo0799* C56A (lane 2-495 bp) and with a WT negative control (lane 5) strain. A faint band was identified with these primers and the WT strain, possibly due to some non-specific primer binding. PCR with primers COB 790 and COB 791 testing for the presence of the *bgaB* (on the pMAD plasmid) show absence of plasmid in EGD-e *lmo0799* C56A (lane 3) and WT negative control (lane 6).

3.4 Light-stress phenotypes for *lmo0799* and *sigB* mutant strains

3.4.1 Motility is restored for the C56A mutant in light

At and below 30 °C, the presence of light is known to inhibit EGD-e WT motility. This loss of motility is derepressed in the strains lacking *sigB* or *lmo0799* (Ondrusch & Kreft, 2011). Comparing EGD-e strain behaviour under conditions of ambient light, motility inhibition was also found to be derepressed for the C56A blind mutant, indicating that C56 is required for this Lmo0799–dependent phenotype (Fig. 3.7).

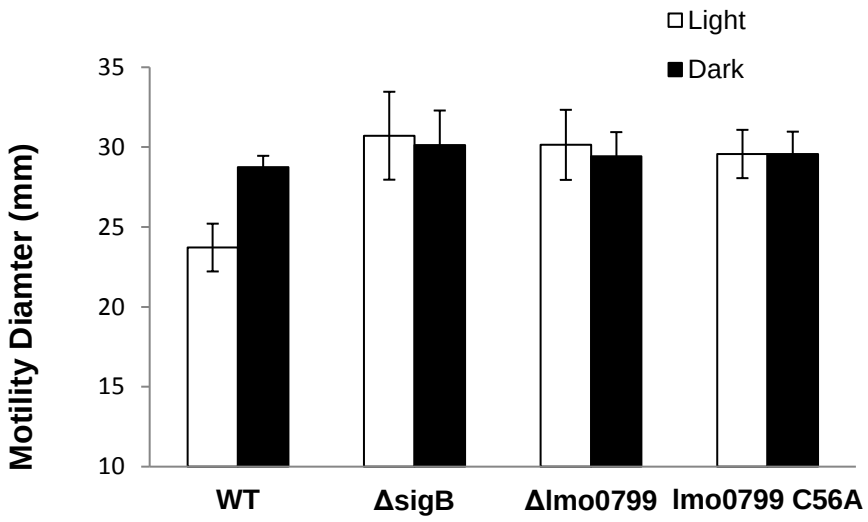

Figure 3.7 The *lmo0799* C56A blind mutant displays derepressed motility in light. Strains were inoculated on semi-solid (0.3% w/v agar) BHI plates and colony diameter was measured 60 h after exposure to ambient white light/incubation in dark at 30 °C as described in Section 2.5.3. The values represent the means of the results from eight replicates (two technical replicates for each of four biological replicates). The error bars represent the standard deviations from the mean. The Student *t*-test was used to identify significant differences between light- or dark-incubated colony diameters for each strain. An asterisk indicates a *p*-value of ≤0.05.

3.4.2 Light /dark ring phenotypes are abolished for the blind mutant

The ring formation phenotype observed for WT EGD-e cells in response to consecutive cycles of light and dark is abolished in the *Δlmo0799* mutant as in the *ΔsigB* mutant (Tiensuu *et al*, 2013). The presence of C56 was crucial for this phenotype as this phenotype was abolished for the C56A blind mutant (Fig. 3.8). This phenotype and the phenotype displaying derepressed motility for the C56A blind mutant highlight the importance of C56 in Lmo0799 blue light sensing and provide genetic evidence towards its suggested mechanism of light sensing.

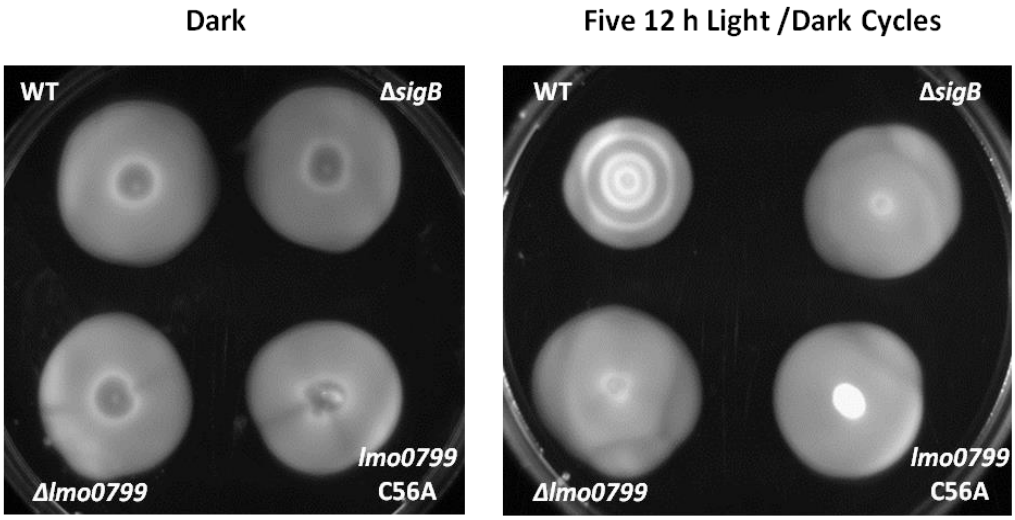

Figure 3.8 Light-dark ring formation is abolished for the blind *lmo0799* C56A mutant. Overnight cultures were standardized and spotted onto 0.3% BHI agar as described in Section 2.5.3. The plates were incubated in the dark for 60 h or exposed to five consecutive 12-h periods of ambient light and dark.

3.4.3 Lmo0799 does not contribute to biofilm production in light or dark.

To examine the effects of light on biofilm production strains were incubated at 37 °C or 30 °C in defined media for 24 h in the presence or absence of ambient light. A negligible reduction in biofilm formation was observed for strains exposed to light at 30 °C, compared to dark-incubated strains (Fig. 3.9A). Ambient light appeared to have a greater inhibitory effect on biofilm formation at 37 °C however biofilm production in both light and dark was reduced at this temperature compared to at 30 °C (Fig. 3.9A&B). A general trend was observed in which the *ΔsigB* produced less biofilm than the WT at 30 °C, as is expected (van der Veen & Abe*e,* 2010; Tiensuu *et al.,* 2013), however no statistical significance was found due to variability between assays. Neither the loss of Lmo0799 nor the presence of the blind C56A Lmo0799 variant had a significant effect on biofilm production in the light or dark compared to WT biofilm production at 30 °C, or 37 °C. These findings correlated with results presented by Tiensuu *et al.* (2013), for biofilm production in light at 23 °C.

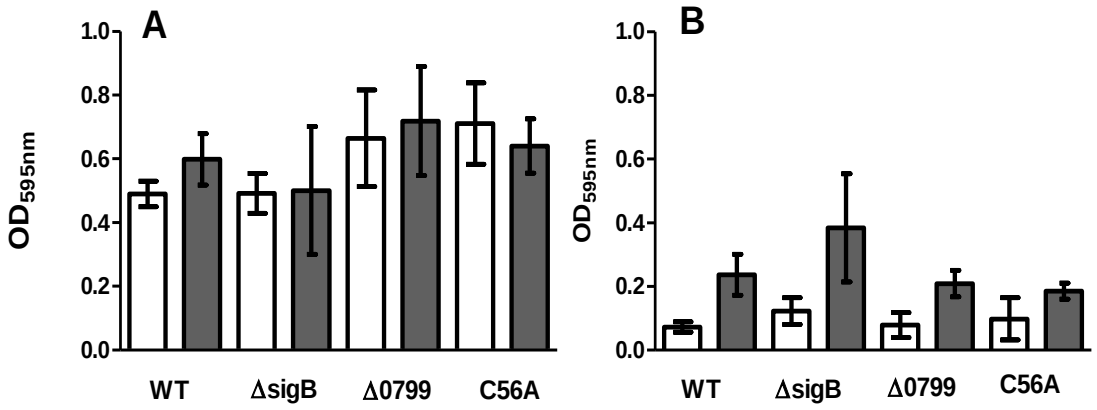

Figure 3.9 Lmo0799 does not contribute to biofilm production in the dark or light. Overnight stationary phase cultures were washed with PBS and resuspended in DM. Two hundred µl of each suspension was placed in a 96-well plate and incubated for 24 h in the presence or absence of light at 30 °C (**A**) or 37 °C (**B**). Each value represents an average of four biological replicates (6 technical replicates per biological replicate). Dunnett's test found no significant differences between biofilm production of mutant strains compared to the WT.

3.4.4 A mutant lacking σ^B or *lmo0799* has decreased sensitivity to blue light.

In the presence of an inhibitory dose of blue light, the *ΔsigB* and *Δlmo0799* mutants were found to display enhanced growth compared to the WT strain. This effect was apparent on BHI agar plates and at lower dilutions in liquid medium (Fig. 3.10A&B). In liquid broth at lower dilutions both strains displayed reduced times to reach an OD_{600nm} =0.1, compared to the WT (Fig. 3.10B). The *lmo0799* C56A mutant repeatedly displayed an intermediate phenotype between that of the WT and the *Δlmo0799* mutant on BHI agar (this was not apparent in liquid, possibly due to limitations of the experimental set-up). These data may indicate that the C56A version of Lmo0799 is still able to transmit light-related signals that lead to σ^B activation and a corresponding decrease in growth.

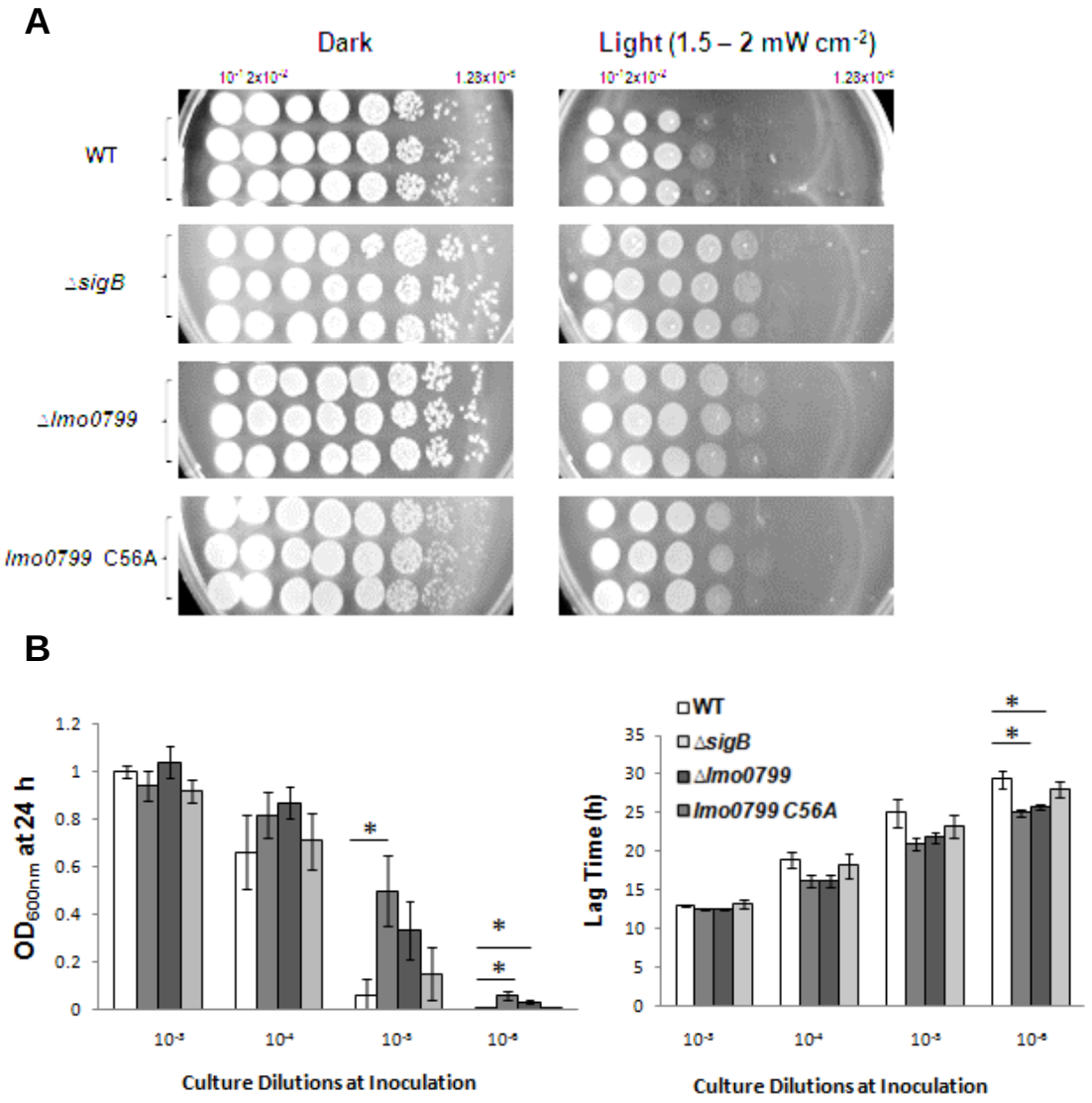

Figure 3.10 Removal of σ^B or Lmo0799 decreases the inhibitory effect of blue light on cell growth. (**A**) Cultures were standardized to an OD_{600nm} of 1 and diluted, first 10-fold, followed by 1:5 dilutions in PBS. The dilutions were spotted on BHI agar and incubated in the presence or absence of 470 nm blue light (**B**) Overnight cultures were diluted to an OD_{600nm} of 0.05 and serially diluted 10-fold to a 10^{-6} dilution. The dilutions were grown for 24 h in the presence or absence of 460 nm blue light. The 24-h endpoint and the time taken to reach an OD_{600nm} of 0.1 were calculated for each strain at each dilution. Dunnett's test was used to identify endpoint and lag-phase values that differed significantly from those of the WT strain ($p \leq 0.05$). The values represent the means of the results from three individual replicates. The error bars represent the standard deviations from the mean.

3.4.5 Reintroduction of Lmo0799 restores growth to WT levels

The reintroduction of *lmo0799* on plasmid pMK4 removed the growth advantage observed for the Δ*lmo0799* mutant in the presence of 1.5-2.0 mW cm^{-2} blue light and restored levels similar to those seen for the WT (Fig. 3.11). Furthermore, the introduction of additional Lmo0799 (via pMK4 *lmo0799*) to the WT negatively affected growth (Fig. 3.11).

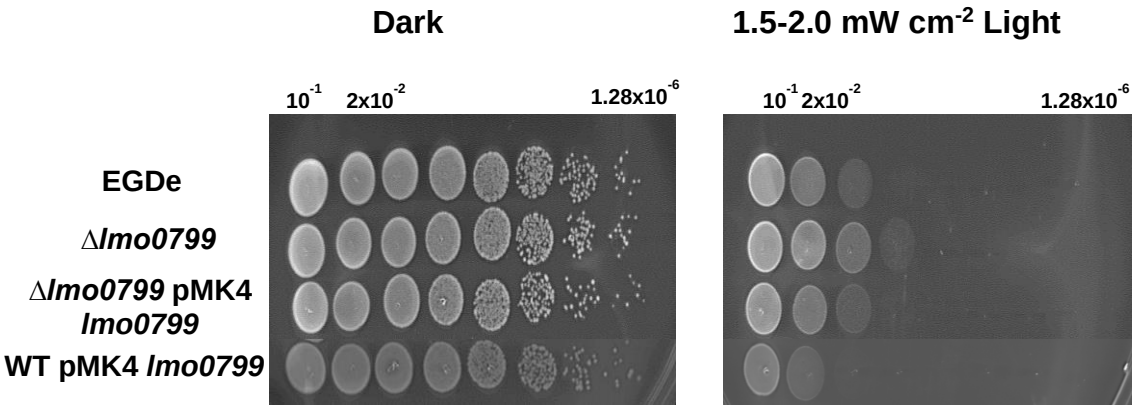

Figure 3.11 The presence of Lmo0799 negatively affects growth in low intensity blue light. Overnight cultures were standardised to an OD_{600nm}= 1 and diluted, first tenfold followed by 1 in 5 dilutions in PBS. Dilutions were spotted on BHI agar and incubated for 24 h at 30 °C in the presence or absence of light (470 nm, 1.5-2.0 mW cm^2).

3.4.6 σ^B, but not Lmo0799, contributes to survival in high intensity blue light.

By increasing the light intensity, killing of cells was achieved. A 12 h exposure to 7.5-8.0 mW cm^{-2} blue light was determined sufficient to enable detection of survival differences between strains (Fig. 3.13) Comparing strain viability after 12 h exposure to 7.5-8.0 mW cm^{-2} blue light, there was an approximate 10,000-fold reduction in cell counts for the *ΔsigB* strain, while no significant loss was observed for the WT (Fig. 3.14). This reflects the central role for the σ^B -regulated GSR in cell protection. Interestingly, we found no significant reduction in numbers for the Δ*lmo0799* or C56A 'blind' mutant strain. This suggests that σ^B is activated in the presence of this high intensity stress via an Lmo0799-independent sensory pathway, perhaps as a result of sensors responding to signals relating to oxidative stress or cell damage caused by oxidative stress.

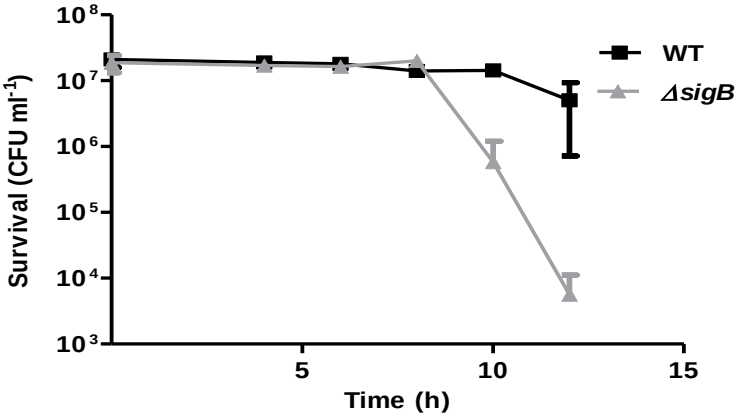

Figure 3.12 Determination of optimum 470 nm light exposure time for survival assays. Overnight cultures of WT and *ΔsigB* cells were washed, resuspended in PBS and exposed to 7.5-8.0 mW cm^{-2} 470 nm light. Samples were removed at each time point as described in Section 2.5.5. The values plotted represent the means of three independent replicates. A Student *t*-test identified a significant ($p \leq 0.05$) reduction in *ΔsigB* cell survival counts compared to starting counts after 12 h exposure. The error bars represent the standard deviations from the means.

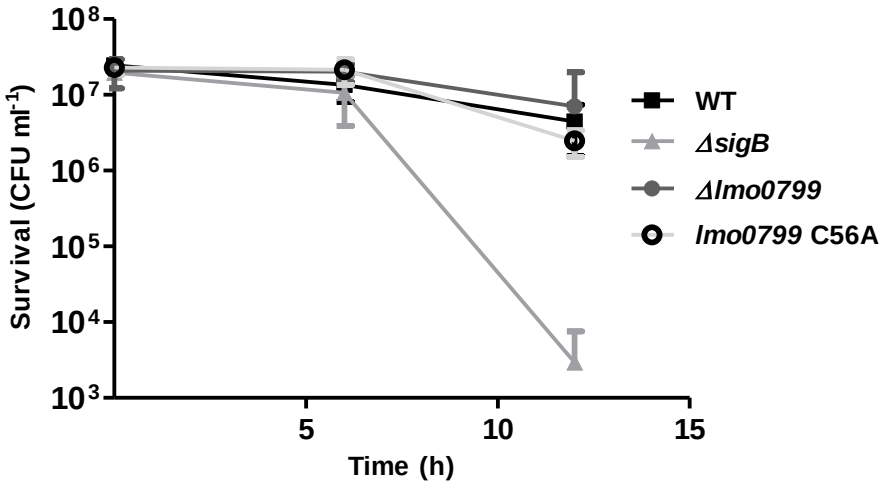

Figure 3.13. The *ΔsigB* mutant displays a survival defect in higher intensity blue light. Overnight cultures were washed and resuspended in PBS and exposed to 8 mW cm^{-2} 470 nm blue light as described in Section 2.5.5. Dunnett's test identified a significant difference ($p \leq 0.05$) between WT and *ΔsigB* strains' survival counts after 12 h light exposure. The values represent the means of the results from six individual replicates. The error bars represent the standard deviations from the mean.

3.5 Discussion

Here we provide evidence that blue light at 470 nm has a clear inhibitory effect on *L. monocytogenes* growth, without the requirement for an exogenous photosensitiser (Fig. 3.3 & Fig. 3.11). Increasing the dose results in apparent lethality suggesting the possibility of using blue light alone as a decontamination method for surfaces. It seems from experiments conducted with catalase and DMTU that growth inhibition is due to light-induced generation of ROS (Fig. 3.3) (O'Donoghue *et al*., 2016). Previous studies have described a number of pathways by which light may induce the production of ROS (Maclean *et al.,* 2008; Endarko *et al.,* 2012). One such pathway involves the excitation of porphyrin molecules (Gábor *et al.,* 2001; Hamblin and Hasan, 2004; Nitzan & Ashkenazi, 2001). As the genes for heme biosynthesis are present in *L. monocytogenes* (Panek & Brian, 2002) it seems likely that photosensitising porphyrin intermediates could contribute to the light sensitivity observed.

While the presence of light causes the generation of damaging ROS, lack of exposure to oxygen during growth negatively affects the ability to degrade hydrogen peroxide, and presumably other ROS not measured (Fig. 3.4A). In addition the reduced catalase activity in anaerobically grown stationary phase cultures (Fig. 3.4A) correlates with decreased survival upon addition of hydrogen peroxide (Boura *et al.,* 2016). It could be inferred from this that pre-exposure to low levels of light (and thus some amount of ROS) may encourage some levels of tolerance to higher inhibitory or killing intensities of light. Light / dark 'ring' formation was not prevented by the addition of catalase, which suggests that light (via Lmo0799 signalling) stimulates the development of these rings independently of ROS accumulation.

The protective response to oxidative stress is known to be partially under σ^B control (Ferreira *et al.,* 2001) and so it was somewhat unexpected to discover that the *ΔsigB* (and *Δlmo0799*) mutant displayed an enhanced capacity to withstand the inhibitory effects of light at 1.5-2.0 mW cm^{-2} (Fig. 3.10). Enhanced growth of *sigB* mutants has been reported by others both in *L. monocytogenes* and *B. subtilis*. Abram *et al.* (2008a) observed that a 10403S *ΔsigB* mutant had a faster growth rate than the wild-type parent in a chemically defined medium with 0.5 M added NaCl. Mutations in *rsbT* and *rsbV* that are predicted to negatively affect σ^B activity also produce a fast-growth phenotype under some conditions (Chaturongakul & Boor, 2004). Although these results have not been explained to date it has been suggested that these effects could arise from sigma factor competition for core RNA polymerase (O'Byrne & Karatzas, 2008). In this model the increase in growth rate of the mutant lacking *sigB* arises because the housekeeping sigma factor σ^A has greater access to the core polymerase and can therefore transcribe genes with growth-related functions more efficiently. The finding that *E. coli* cells develop loss of function mutations in the stress-inducible sigma factor *rpoS* gene when subjected to continuous culture under growth limiting environments in the absence of other stresses provides some further support for this theory. It has been hypothesised that these mutations result in increased permeability and increased transcription of genes involved in transport in order to facilitate nutrient scavenging Notley-McRobb *et al.,* 2002 and it is perhaps of interest that the cell wall of an *L. monocytogenes ΔsigB* mutant display weaker integrity (Abram *et al.,* 2008; Begley *et al*., 2006)

Despite contributing to the reduction in growth of the WT in low intensity blue light, possession of σ^B is clearly advantageous for the cells exposed to lethal intensities of light (Fig. 3.12 & Fig. 3.13). Intriguingly, the *Δlmo0799* mutants and *lmo0799* C56A mutant survived killing intensities of light at a rate similar to the WT indicating that σ^B is being

activated via a pathway that is not dependent on Lmo0799 activity at these higher intensities of light (Fig. 3.13). It is possible that indirect stress signals (e.g., oxidative damage caused by ROS) are generated at this higher dose of light. These signals can be sensed independently of Lmo0799, perhaps via RsbR or one of its paralogues (the putative sensory subunits of the stressosome), thereby ensuring an effective stress response independently of light sensing.

A similar model has been proposed to account for the accumulation of *rpoS* (encoding σ^S, the general stress response sigma factor) mutations in *E. coli* when grown under limiting conditions (Schweder *et al.,* 1999; King *et al.,* 2006). The energetic cost of deploying the general stress response (with associated homeostatic and repair energy requirements) may also contribute to the negative effect on growth rate. As both the Δ*sigB* and Δ*lmo0799* mutants behave in a similar manner at inhibitory low doses of blue light (Fig. 3.10A) it suggests that the activation of the general stress response by σ^B at this dose of light, which occurs following light sensing and signal transduction by Lmo0799 (Ondrusch & Kreft, 2011), produces a negative effect on cell growth. Indeed it was recently observed that a nonsense mutation in *rsbU*, predicted to affect σ^B activity negatively, also produces reduced light sensitivity to low intensity light (NicAogáin & O'Byrne, unpublished data).

When comparing the response of strains to blue light, we found genetic evidence for the role of the conserved C56 in underpinning the mechanism of light sensing of Lmo0799. A phenotype similar to that observed for the removal of the intact Lmo0799 protein was achieved by preventing formation of the predicted light-induced cysteinyl- C4A adduct via a C56A replacement (Fig. 3.7 & Fig. 3.8) (Tiensuu *et al.,* 2013; Ondrusch & Kreft, 2011). Previous modelling studies have found the Lmo0799 protein structure to be nearly identical to that of YtvA in *B. amyloliquefaciens* (Ondrusch & Kreft, 2011; Ogata *et al.,*

2009) with both having the conserved cysteine in the FMN-binding pocket. Gaidenko *et al.*(2006) have shown that the YtvA conserved residue C62 is critical for light-induced σ^B activation of the stress-response in *B. subtilis*. The photocycle of the Lmo0799 protein has been elucidated by Chan *et al.* (2012) and the authors predicted an important role for C56. Replacement of this residue with an alanine produced phenotypes (loss of ring formation during light-dark cycles and increased motility in the presence of blue light) similar to those observed for the removal of the full Lmo0799 protein and suggests that the predicted light-induced cysteinyl-flavin mononucleotide adduct is crucial for light sensing (Fig. 3.7 & Fig. 3.8) (Ondrusch & Kreft, 2011; Tiensuu *et al.,* 2013). This single amino acid change likely results in the uncoupling of the Lmo0799 LOV domain from its FMN chromophore, resulting in the loss of blue-light sensing capacity. The enhanced growth phenotype of the *lmo0799* C56A mutant was not as pronounced as the Δ*lmo0799* or Δ*sigB* mutants on BHI agar plates in the presence of a sub-lethal blue light dose (Fig. 3.10A) suggesting that σ^B might be partially activated by light in this strain, but this difference was not found to be significant in liquid BHI medium (Fig. 3.10B). It is worth noting that the impact of Lmo0799 on the overall structure and assembly of the stressosome has not been investigated in *L. monocytogenes* and it is possible that the deletion mutation might have indirect effects on the sensing capacity of the stressosome independent of the loss of the Lmo0799 protein itself. This could have contributed to the subtle differences in the behaviour of the *lmo0799* C56A and Δ*lmo0799* mutants on BHI agar plates in the presence of light. Alternatively the Lmo0799 protein might have a secondary sensing function, as has been postulated by Chan *et al.* (2012), which remains unaffected in the *lmo0799* C56A mutant.

These findings add to the growing area of research into the use of visible light to prevent bacterial contamination of surfaces (Maclean *et al.* 2008; Murdoch *et al.,* 2012;

Lin *et al.,* 2012; Maclean *et al.,* 2009). Overall the study raises the interesting possibility that blue light-emitting diode lights, which are comparatively cheap, energy efficient and widely available, might be used to control the growth and survival of this pathogen in food processing environments. Additionally, as Lmo0799 does not appear to contribute significantly to σ^B-mediated light stress survival, questions were raised as to whether other stressosome sensors (RsbR, Lmo0161, Lmo1642 and Lmo1842) also play a role in light stress (or ROS-related stress) sensing. This will be explored further in Chapter 4.

Chapter 4: Contributions of the Stressosome Sensor Proteins to the *Listeria monocytogenes* Light Stress Response

4.1 Introduction

In a 2011 study, the *L. monocytogenes* protein Lmo0799 was established as a functional blue light receptor which stimulated σ^B-dependent transcription of genes in response to blue light (Ondrusch & Kreft, 2011). In the previous chapter we further examined the physiological effects of blue light on *L. monocytogenes* and the contribution of the stressosome protein Lmo0799 and alternative sigma factor σ^B to light-associated phenotypes. Several interesting observations relating to Lmo0799 activity and the effects of light on gene transcription were recorded in the study by Ondrusch & Kreft (2011). It was demonstrated that blue light-induced transcription of the σ^B regulon was reduced for the *Δlmo0799* strain but abolished only in the *ΔsigB* strain. Additionally, it was observed that red light affected σ^B-dependent gene transcription in a *Δlmo0799* strain.

Research into the mechanisms of function of the Lmo0799 homologue YtvA in *B. subtilis* suggests that Lmo0799 mediates light-dependent σ^B activation through its interactions as a component of the stressosome: a multiprotein sensory complex (Ondrusch & Kreft, 2011; Gaidenko *et al.*, 2006; Akbar *et al.*, 2001; Jurk *et al.*, 2013; Marles-Wright *et al.*, 2008). In *L. monocytogenes* energy and environmental stress signals are incorporated into the σ^B activation cascade via this stressosome structure (Chaturongakul & Boor, 2004; Chaturongakul & Boor, 2006). This pathway is outlined in detail in Sections 1.8.3 and 1.9 In contrast, the σ^B activation model in *B.subtilis* carries separate pathways for energy stress and environmental stress induced activation of σ^B (Yang *et al.*, 1996; Vijay *et al.*, 2000; Hecker *et al.*, 2007). In *B. subtilis* blue light induces σ^B activation via the environmental stress pathway whereas red light appears to be introduced to the σ^B activation cascade via the RsbP/Q energy stress pathway which is absent in *L. monocytogenes* (as described in Section 1.9).

The existence of the *L. monocytogenes* stressosome structure has been confirmed in a recently presented oral paper and the following proteins had been identified as putative sensor proteins: RsbR, Lmo0161, Lmo1642 and Lmo1842 (and Lmo0799) (Cossart, 2016; Ondrusch & Kreft, 2011). These proteins have conserved C-terminal regions, but highly variable N-terminal domains, similar to other stressosome-associated sensor proteins (Heavin & O' Byrne 2012; Ondrusch & Kreft, 2011; Murray *et al.*, 2005; Marles-Wright *et al.*, 2008). Very little is known about the function of the *L. monocytogenes* stressosome sensor proteins. Based on the *B. subtilis* stressosome model it is expected that they complex with RsbS and RsbT proteins, with the RsbR-like proteins' N-terminal regions extruding from the core as the point of stress signal sensing (Marles Wright *et al.*, 2008, Marles-Wright & Lewis, 2010). Heavin and O'Byrne (2012) found significant similarity between RsbRA in *B. subtilis* and RsbR (Lmo0899) in *L. monocytogenes*. Lmo0161, Lmo1642 and Lmo1842 all showed similarities to RsbRD of *B. subtilis* (but also RsbRC and RsbRB). As in *B. subtilis*, each *L. monocytogenes rsbR* homologue is encoded on a separate operon suggesting that differential transcriptional regulation may play an important role in sensor contributions (Ondrusch & Kreft, 2011; van der Steen *et al.*, 2012).

Due to the high variability of these protein N-terminal regions it is difficult to draw any inferences about sensing function, however based on the findings of Ondrusch and Kreft (2011) it is possible that more than one sensor contributes to light stimulated activation of the GSR. Removal of Lmo0799 does not fully prevent σ^B activation in the presence of blue light, and red light also stimulates the σ^B activity. This suggests that other sensors of the GSR may contribute to some aspect(s) of light signalling sensing. As there is only one major pathway for σ^B activation that incorporates both energy and stress signals it is possible that this Lmo0799 independent light-induced σ^B activation relies on light signal

interpretation by the stressosome complex (Chaturongakul & Boor, 2004; Utratna *et al*., 2014).

In order to determine whether any of the four alternative proteins (in addition to Lmo0799) were involved in detecting signals produced by blue light stress, we constructed a number of gene deletion mutants lacking the individual RsbR paralogues and exposed them to various light stress assays. This chapter describes the construction of these deletion mutants and investigates their capacity for light-induced motility inhibition, their ability to produce rings in response to light/dark cycles, and their growth and survival in the presence of light.

4.2 Construction of stress sensor mutants

In order to determine the contribution, if any, of the putative stressosome sensor proteins, strains lacking one of each of the sensor genes were constructed: *L. monocytogenes* EGD-e *ΔrsbR*, *Δlmo0161*, *Δlmo1642*, and Δ*lmo1842*. A *Δlmo0799* strain had previously been acquired (Tiensuu *et al.*, 2012). To construct each mutant, a plasmid carrying a deletion cassette was transformed into EGD-e electrocompetent cells. The deletion cassette consisted of DNA homologous to the regions on either side of the gene to be deleted. The transformation procedure was followed by two homologous recombination events. Above 42 °C, the pMAD plasmid cannot replicate independently and only plasmids that integrate into the *L. monocytogenes* genome at the regions homologous to the deletion cassette are retained. A second homologous recombination event is achieved by passaging the cells at 30 °C to cause excision of the plasmid from the genome with the original deletion cassette or with the WT gene and surrounding regions.

4.2.1 Design of mutant replacement genes

Deletion mutants were constructed using techniques which induced homologous recombination events (Horton *et al.*, 1993). Replacement genes or deletion cassettes were designed to replace the selected WT gene in each strain. The WT gene sequences from EGD-e were sourced at *http://genolist.pasteur.fr/ListiList/.* Each deletion construct consisted of 600 bp; 300 bp directly upstream and 300 bp directly downstream of the WT gene (Table 4.1). Care was taken not to include promoter or start sites of genes downstream of the target gene. Deletion cassettes on plasmids pCR2.1*::Δlmo0161*, pEX-A::*Δlmo1642* and pEX-A::*Δlmo1842* were designed with *Bam*HI and *Eco*RI recognition sites. As an EcoRI recognition site is present within the *ΔrsbR* gene sequence, plasmid pEX-A::*ΔrsbR* was constructed with *Bam*HI and *Xma*I recognition sites. To increase enzyme recognition of restriction sites at the ends of sequences, two (with *Bam*HI and *Eco*RI) or four (with *Xma*I) additional base pairs were added to each end of the deletion gene constructs. The constructs were synthesized by Eurofins Genomics and received on commercial plasmids.

Table 4.1 Deleted genes and deletion cassettes

Gene Deleted	Deletion cassette size (bp)	Deleted region (bp)	Additional restriction sites
rsbR	618	837	*Bam*HI, *Xma*I
lmo0161	616	831	*Bam*HI, *Eco*RI
lmo1642	616	804	*Bam*HI, *Eco*RI
lmo1842	616	825	*Bam*HI, *Eco*RI

4.2.2 Construction of pMAD-deletion cassette plasmids

The commercial plasmids were transformed (Section 2.6.4) into *E. coli* TOP10 electrocompetent cells (prepared as described in Section 2.1.2) to provide a stock strain. The plasmids were then extracted and digested with *Bam*HI and *Eco*RI (or *Bam*HI and *Xma*I for pEX-A::*ΔrsbR*) to separate the deletion cassette from the commercial vector (Fig. 4.1). The pMAD plasmid was digested with the same enzymes to provide compatible ends for binding. Digested vectors and deletion inserts were purified and quantified before ligation (Sections 2.6.5 & 2.7.1). Ligation procedures were carried out with 50 ng of insert and vector quantities in a 1:1, 2:1 and 3:1 ratio (Section 2.6.3).

4.2.3 Cloning of the deletion cassettes in *E. coli* TOP10

The ligation reaction was then transformed into *E. coli* TOP10 competent cells and these cells were plated onto LB plates with ampicillin (10 µg ml^{-1}) to promote selection for transformant strains. As pMAD does not possess M13 primer binding sites, which are commonly encoded on plasmid vectors to aid screening processes, PCR primers were designed that were specific to the deletion cassette. A successful clone for each of the constructs was found in strains transformed with a 3:1 ligation ratio mixture. These transformant strains were named *E. coli* pMAD::*ΔrsbR*, pMAD::*Δlmo0161*, pMAD::*Δlmo1642* and pMAD::*Δlmo1842*.

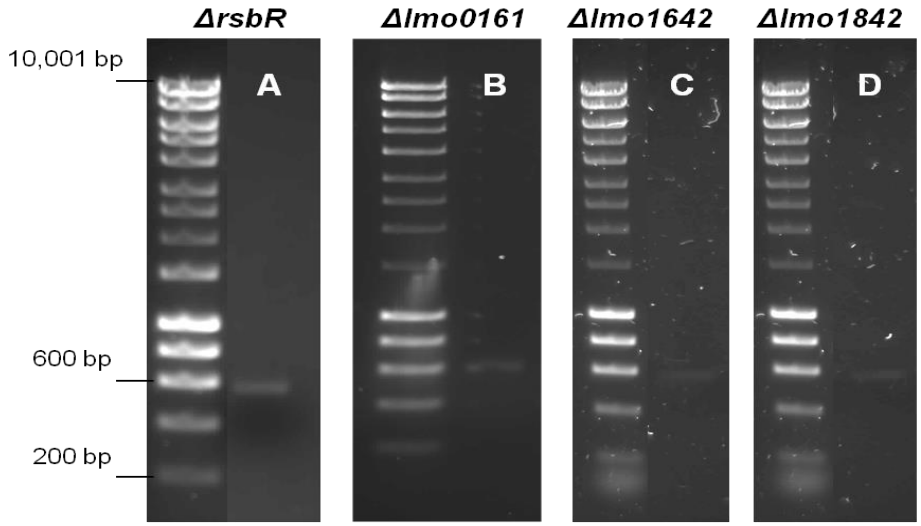

Figure 4.1 Purified deletion gene inserts. Inserts (610 bp) were extracted from commercial vectors with complementary digestion enzymes (Fermentas) and purified (Qiagen), as described in Sections 2.6.1-.2. One microlitre aliquots were run on a 1% agarose gel with DNA marker HyperLadder 1 (Bioline) (**A**) Purified *ΔrsbR* extracted from pEX-A::*ΔrsbR* with *Bam*HI and *Xma*I. (**B**) Purified *Δlmo0161* extracted from with pCR2.1::*Δlmo0161* with *Bam*HI and *Eco*RI. (**C**) Purified *Δlmo1642* extracted from pEX-A::*Δlmo1642* with *Bam*HI and *Eco*RI. (**D**) Purified *Δlmo1842* extracted from pEX-A::*Δlmo1842* with *Bam*HI and *Eco*RI.

4.2.4 Transformation of *L. monocytogenes* with deletion cassette plasmids

Following the identification *E. coli* TOP10 transformant strains, the deletion cassette plasmids were introduced into *L. monocytogenes* EGD-e (as described in Sections 2.1.1 & 2.6.4). Plasmids were extracted from the *E. coli* strains, concentrated and transformed into EGD-e electrocompetent cells. A sample of each deletion cassette plasmid was first digested and visualized on an agarose gel to confirm the presence of the correct deletion cassette on the plasmid. pMAD::Δ*lmo0161*, pMAD::Δ*lmo1642*, pMAD::*Δlmo1842* and pMAD::*ΔrsbR* were then transformed into *L*. *monocytogenes* EGD-e electrocompetent cells. Transformed EGD-e cells were plated on BHI plates with erythromycin (2 µg ml^{-1}) to isolate successful transformants.

Successful transformants were identified by PCR, using the primers that had been previously used to identify the presence of the deletion cassette in *E. coli.* As the deletion cassette is comprised of 300 bp DNA sequence upstream and downstream of the *L. monocytogenes* gene to be deleted, these primers also bound to these regions on the WT genomic DNA in EGD-e. The deletion cassette PCR product was distinguished from the product produced from WT DNA by its size (Fig. 4.2). Primers binding to the genome produced a larger PCR product, due to the regions being separated by the gene to be deleted. Despite the presence of two sites for primer recognition in transformants strains (on the deletion cassette and on the genomic DNA), single band products were viewed on agarose gels following PCR. The primers appeared to preferentially amplify the smaller region corresponding to the deletion cassette.

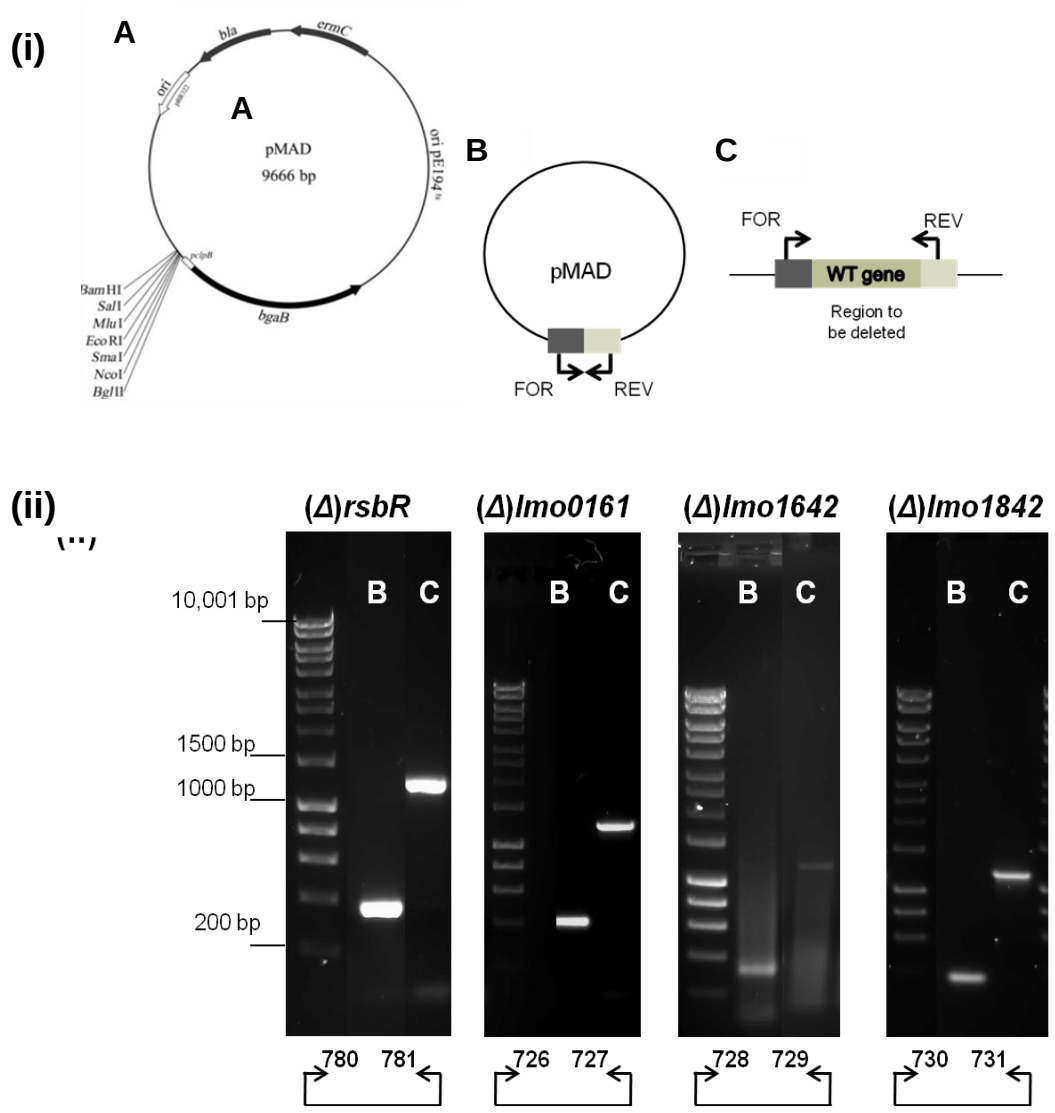

Figure 4.2 PCR to identify EGD-e transformants. (**i**) (**A**) pMAD vector with multiple cloning site, *ermC*, *bgaB* and *bla* genes illustrated (Arnaud *et al.*, 2004). Primers designed to (**B**) bind to the deletion cassette on pMAD also (**C**) bind to the identical regions on the genome surrounding the gene to be deleted in the WT strain. (**ii**) ***(Δ)rsbR***: EGD-e pMAD::*ΔrsbR* (**B**) (361 bp) and WT (**C**) (1198 bp) with primers COB 780 and COB 781.***(Δ)lmo0161****:* (**B**) EGD-e pMAD::*Δlmo0161* (414 bp) and (**C**) WT (1245 bp) with primers COB 726 and COB 727. (***Δ*)*lmo1642*** :(**B**) EGD-e pMAD::*Δlmo1642* (320 bp) and (**C**) WT (1124 bp) with primers COB 728 and COB 729. ***(Δ)lmo1842***: (**B**) EGD-e pMAD::*Δlmo1842* (366 bp) and (**C**) WT (1191 bp) with primers COB 730 and COB 731.

4.2.5 Chromosomal integration of deletion cassette plasmids

The first homologous recombination event involved the integration of the deletion cassette plasmid into the genome at regions homologous to the cassette. The pMAD plasmid was chosen as a suitable vector as it carries a thermosensitive origin of replication which prevents it replicating independently at 42 °C (Arnaud *et al.*, 2004). Five or ten colonies of each of the pMAD-deletion cassette containing EGD-e transformants were plated on BHI agar containing erythromycin (2 µg ml^{-1}) and incubated at the non-permissive temperature of 42 °C to select for colonies in which the plasmid integrated into the genome (Section 2.8.3). Strains were restreaked several times until growth without fail (non-'patchy' growth) occurred. Successful integrants were isolated from the third restreak for the pMAD::Δ*rsbR,* pMAD::Δ*lmo1642* and pMAD::Δ*lmo1842* containing strains. Attempts to encourage integration of pMAD::Δ*lmo0161* using this method failed. For this plasmid, the integration procedure was instead successfully carried out in BHI broth media at 41.5 °C with erythromycin (2 µg ml^{-1}) as a selection agent. An integrant strain was isolated from the fourth subculture. In all strains, the plasmid could integrate either upstream or downstream of the WT gene as the plasmid deletion cassette consisted of DNA homologous to regions upstream and downstream of the gene (Fig. 4.3). Using a combination of primers sets in which one primer targets a region on the chromosome flanking the integration site and the second primer binds to the deletion cassette DNA sequence, the location of integration was determined (Fig. 4.3). For the EGD-e pMAD::*ΔrsbR*, pMAD::*Δlmo0161*, and pMAD::*Δlmo1642* strains, colonies were selected in which integration occurred downstream of the WT gene. For the pMAD::*Δlmo1842* strain, integration occurred upstream of the WT gene (Fig. 4.3).

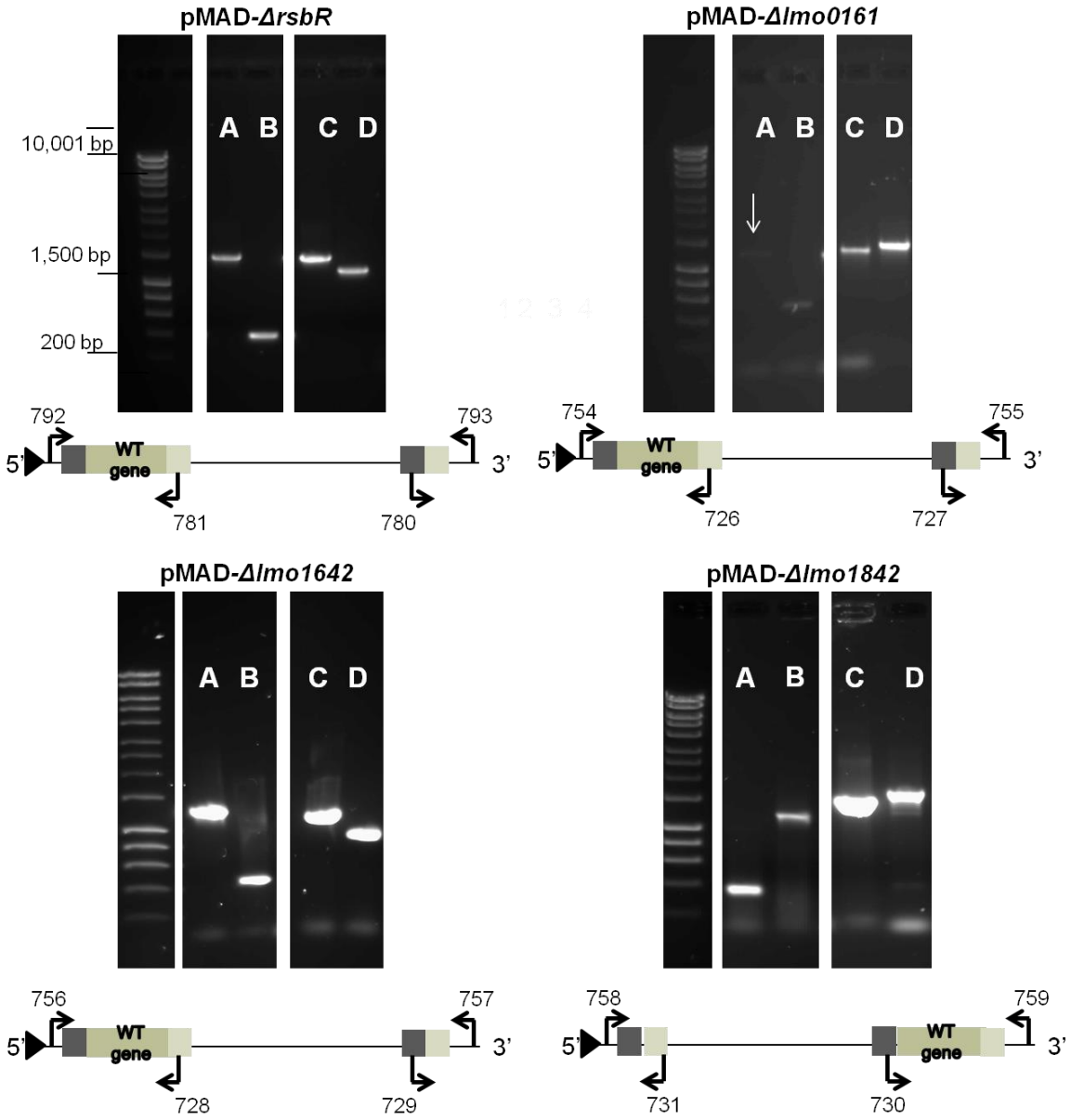

Figure 4.3 PCR identification of integrants with WT controls. Using several combinations of primers in which one primer bound to a flanking region on the genomic DNA and one primer bound to the deletion cassette, the orientation of integration was determined for the integrant strains EGD-e pMAD::*ΔrsbR,* EGD-e pMAD::*Δlmo0161,* EGD-e pMAD::*Δlmo1642* (downstream integration) and EGD-e pMAD::*Δlmo1842 (*upstream integration). **pMAD::*ΔrsbR*:** (**A**) EGD-e pMAD::*ΔrsbR* integrant and (**C**) WT- with primers COB 792 and COB 781 (1481 bp). (**B**) EGD-e pMAD::*ΔrsbR* integrant (400 bp) and (**D**) WT (1237 bp) with primers COB 780 and COB 793. **pMAD::*Δlmo0161*:** (**A**) EGD-e pMAD::*Δlmo0161* integrant and (**C**) WT with primers COB 754 and COB 727

(1306 bp). (**B**) EGD-e pMAD::*Δlmo0161* integrant (580 bp) and (**D**) WT (1411 bp) with primers COB 726 and COB 755. **pMAD::*Δlmo1642:*** (**A**) EGD-e pMAD::*Δlmo1642* integrant and (**C**) WT with primers COB 756 and COB 729(1370 bp). (**B**) EGD-e pMAD::*Δlmo1642* integrant (496 bp) and (**D**) WT (1300 bp) with primers COB 728 and COB 757. **pMAD::*Δlmo1842:*** (**A)** EGD-e pMAD::*Δlmo1842* integrant (443 bp) and (**C**) WT (1268 bp) with primers COB 758 and COB 731. (**B**) EGD-e pMAD::*Δlmo1842* integrant and (**D**) WT with primers COB 730 and COB 759 (1408 bp).

4.2.6 Passaging and selection of EGD-e sensor deletion strains

Integrants corresponding to each of the four deletion cassettes were subsequently passaged at 30 °C in the absence of antibiotic selection to promote excision and loss of the plasmid from the cell. At the end of the third and subsequent passages samples were serially diluted and plated onto BHI agar with or without antibiotic selection marker. Erythromycin-sensitive colonies for all four strains were isolated after the fourth passage. Between 150 and 200 colonies for each strain from the fourth and fifth passages displaying erythromycin sensitivity were tested via PCR to determine the presence of the gene deletion with the deletion cassette specific primers. The possibility existed that the plasmid would be excised from the genome leaving the wild-type allele rather than the deletion allele behind. Colonies which tested positively for the presence of the WT gene were discarded. For putative deletion mutants in which the WT gene had been lost, loss of the plasmid was confirmed by PCR with primers against the β-galactosidase gene (*bgaB*) on the plasmid (Fig. 4.4). Permanent stocks were made of the confirmed deletion mutants EGD-e *ΔrsbR*, *Δlmo0161*, *Δlmo1642*, and Δ*lmo1842* (Section 2.1).

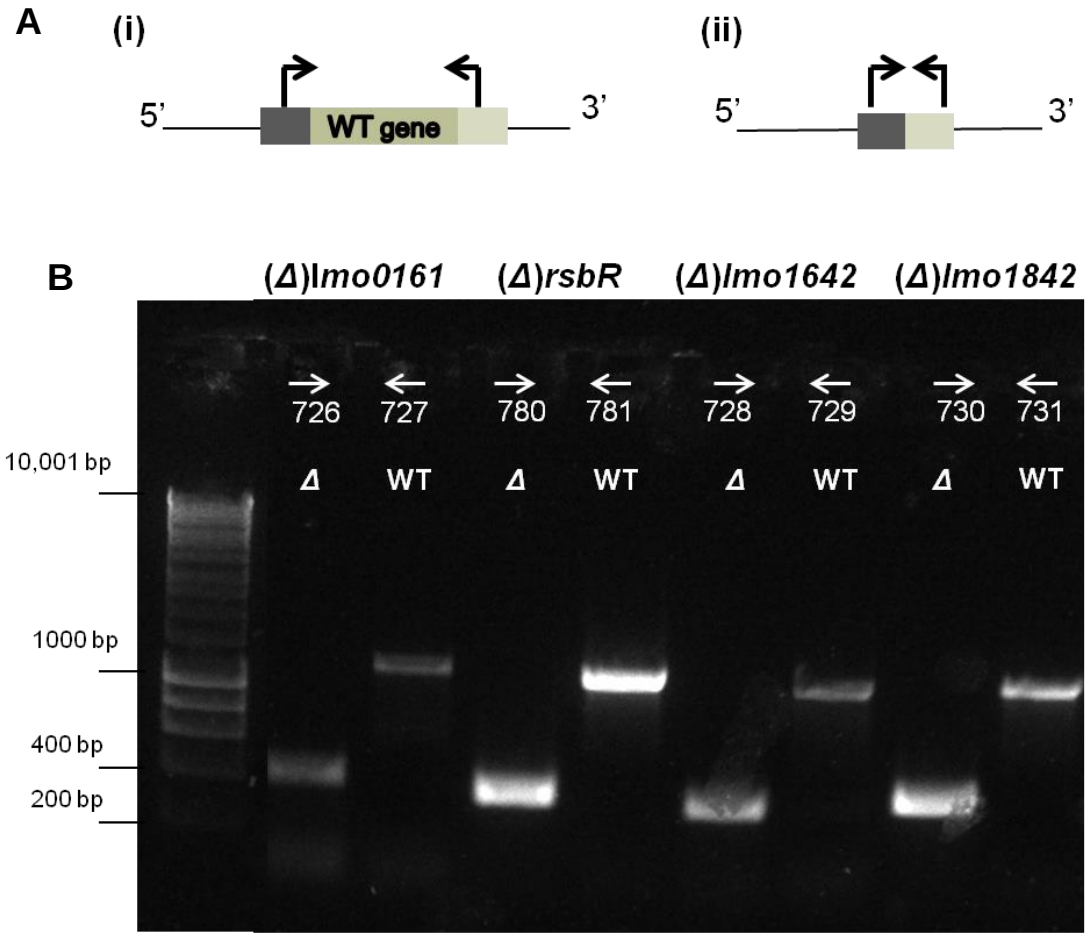

Figure 4.4 Confirmation of deletion sensor strains. Successful deletion gene strains were screened with primers which bind to the deletion cassette or to genomic DNA outside the region to be deleted (WT gene) (**A**) PCR product size differed between strains in which (**i)** the WT gene remained or (**ii**) was replaced by a deletion cassette. (**ii**) (left-right) HyperLadder 1 (5 µl) with (***Δ***) *Δlmo0161* (414 bp) and **WT** (1245 bp) both with primers COB 726 and 727. (***Δ***) *ΔrsbR* (361 bp) and **WT** (1198 bp) both with primers COB 780 and 781. (***Δ***) *Δlmo1642* (320 bp) and **WT** (1124 bp), both with primers COB 728 and 729. (***Δ***) *Δlmo1842* (366 bp) and **WT** (1191 bp), both with primers COB 730 and 731.

4.3 Characterisation of RsbR paralogue deletion mutants

4.3.1 Sensor deletion strains do not display growth defects in BHI

A series of growth curves were carried out in BHI in order to reveal any growth defects in the mutant strains. When the WT and mutant strains were grown aerobically at 37 °C or 30 °C there were no significant differences observed in the lag times, final OD readings (at 24 h) or growth rates between strains (Fig. 4.5). Strains appeared to grow equally well at both temperatures. The average generation time was calculated as 41.6 min (with a standard deviation of ±2.0 min between strains) for strains incubated at 37 °C and 40 min (±1.8 min) for strains incubated at 30 °C (Fig. 4.5).

4.3.2 The *ΔrsbR* strain displays depressed motility in ambient light

Motility inhibition at 30 °C or lower has been characterized as a light-associated phenotype which is abolished in the *ΔsigB* and *Δlmo0799* strains (Ondrusch & Kreft, 2011). Testing the remaining strains, it appears that the *Δlmo0161*, *Δlmo1642* and *Δlmo1842* strains display reduced motility on low-agar agar when exposed to ambient light, compared to colonies of the same strains grown in the dark (Fig. 4.6). The *ΔrsbR* colonies however, show no difference in motility between dark- and light-incubated conditions.

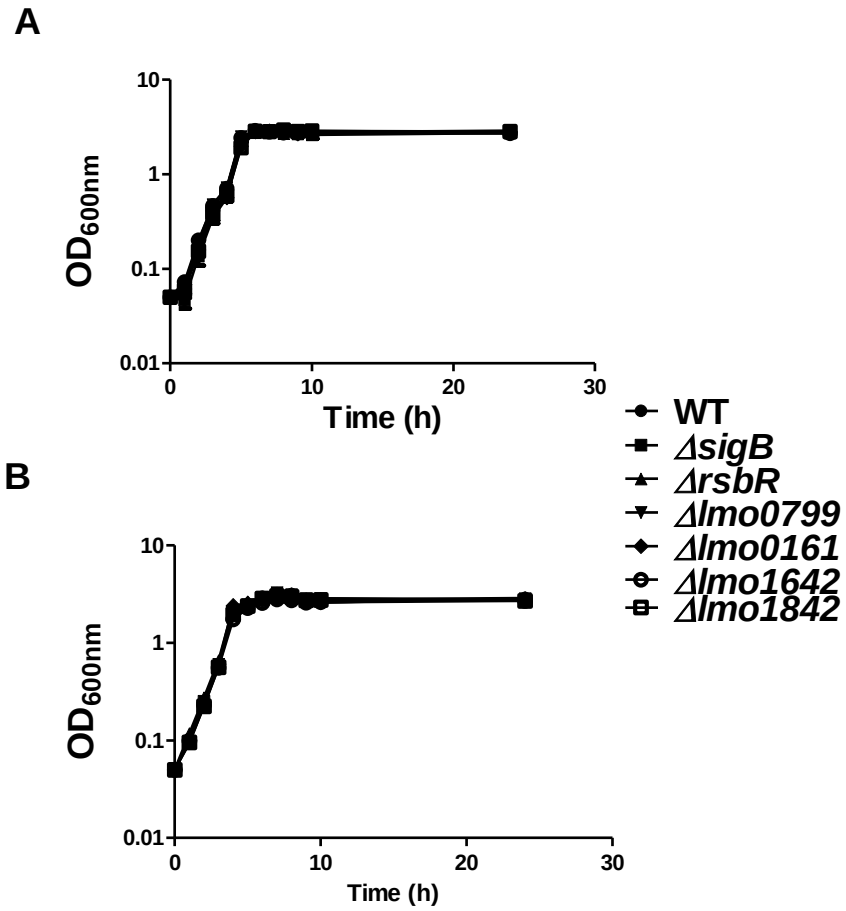

Figure 4.5 Growth curve of WT and sensor deletion strains. Cells were grown at (**A**) 30 °C or (**B**) 37 °C from a starting inoculum of OD_{600nm}= 0.05. Each time point on the graph represents the mean of 4 biological replicates. Errors bars represent the standard deviation from the mean.

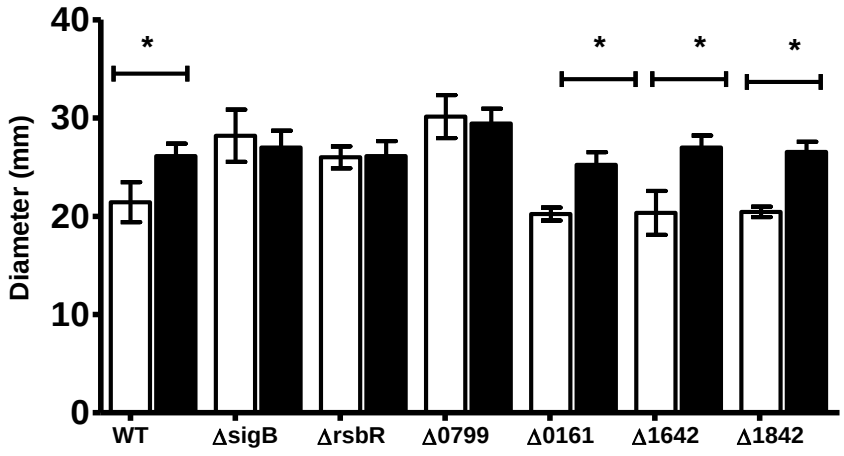

Figure 4.6 Comparison of motility of light- and dark-incubated strains Overnight cultures were standardised to OD_{600nm}= 1.0 and spotted onto BHI plates with 0.3% agar. Strains were incubated at 30 °C for 60 h in ambient white light (white) or wrapped in aluminium foil (black). Diameters for each colony were measured. Each strain is represented by a mean of at least 6 biological replicates. Significant differences between the mean colony diameter of strains grown in the dark compared to light-exposed strains' colony diameter were determined using a student *t*-test. An asterisk (*) indicates a *p*-value ≤0.05

4.3.3 Light/dark ring formation phenotype is abolished for the *ΔrsbR* strain

When exposed to consecutive cycles of light and dark at 30 °C or lower temperatures, WT EGD-e cells grow in a series of concentric opaque and translucent rings. This phenotype is not observed when cells are exposed to light or incubated in the dark alone and is abolished for *Δlmo0799* and *ΔsigB* strains (Tiensuu *et al.*, 2013). Comparing phenotypes of the sensor deletion strains exposed to five consecutive 12 h light and dark periods, it was observed that this ability was abolished in the Δ*rsbR*, *Δlmo0799* and Δ*sigB*

deletion mutants (Fig. 3.8). Ring formation capacity was retained by Δ*lmo0161*, Δ*lmo1642* and *Δlmo1842* strains (Fig. 4.7).

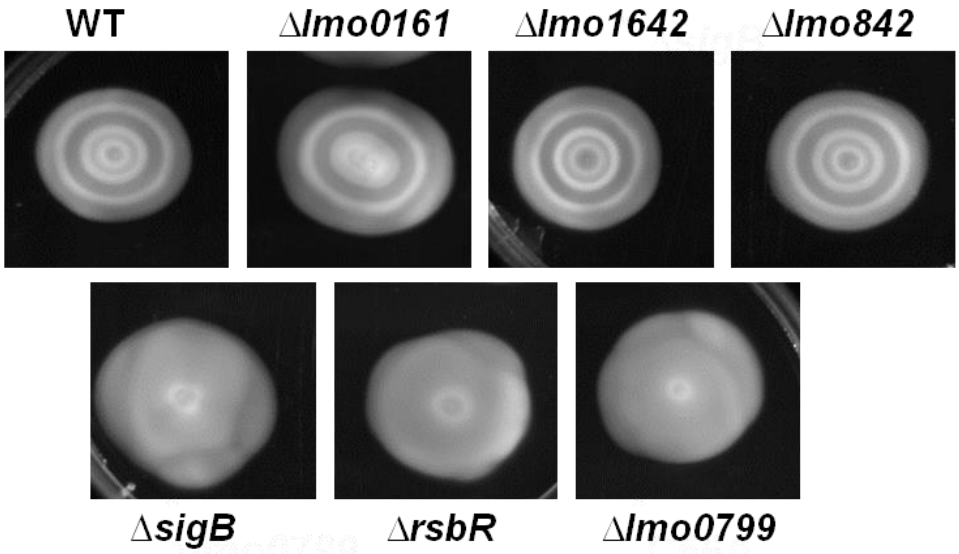

Figure 4.7 Light/dark ring phenotypes for WT and deletion mutant strains. Overnight cultures were standardised to OD_{600nm}= 1.0 and spotted onto low agar (0.3%) BHI plates. Plates were incubated at 30 °C for 5 consecutive 12 h periods of ambient white light and dark. Images were captured using a CCD camera (Section 2.5.3).

4.3.4 The *ΔrsbR* strain showed enhanced growth in 1.5-2.0 mW cm^{-2} blue light.

Blue light has previously been shown to have an inhibitory effect on EGD-e growth (Section 3.2.2). The inhibitory effects of 1.5-2.0 mW cm^{-2} blue light were clearly seen for all strains diluted using a 10-fold serial dilution in PBS and inoculated on BHI agar (Fig. 4.8). However, while the *Δlmo0161*, *Δlmo1642* and *Δlmo1842* strains' growth was inhibited at a level similar to that seen for the WT, the *ΔrsbR* mutant displayed enhanced

growth compared to the WT, at levels similar to these seen and described for the *Δlmo0799* and *ΔsigB* mutants (O'Donoghue *et al.*, 2016).

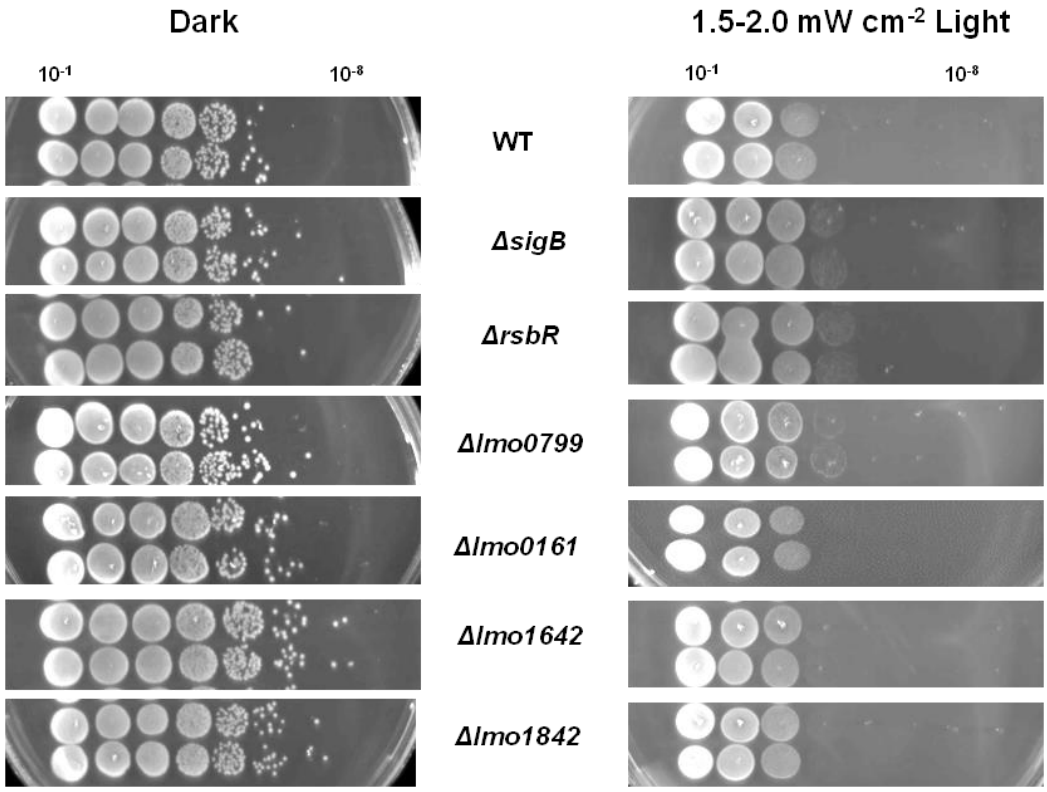

Figure 4.8 Effects of 1.5-2.0 mW cm^{-2} 470 nm blue light on cell growth. Cultures were standardised to an OD_{600nm}= 1.0 and diluted 1 in 10 in PBS. Four microlitre aliquots of each dilution was spotted on BHI agar and incubated at 30 °C in the dark (left) or presence of 1.5-2.0 mW cm^{-2} 470 nm light (right). Plates were incubated for 24 h before images were captured using a CCD camera.

When comparing growth of strains in liquid culture, again a clear inhibitory effect on growth is seen in the presence of light (Fig. 3.2 & Fig. 3.10B). For growth curves with a starting inoculum of OD_{600nm}= 0.05, no difference is seen between strains' ability to grow in the presence of light (data not shown). This may be due to the protective effect afforded by increasing cell density (O'Donoghue *et al.*, 2016). However, when starting inocula were diluted further (1:10 serially to a 10^{-6} dilution) a difference in growth is seen between the WT and *ΔsigB*, *ΔrsbR* and *Δlmo0799* strains (4.9A&B) (differences between the WT and *ΔsigB* or *Δlmo0799* strains are shown in Fig. 3.10). Analysing these differences between strains with a starting inoculum of OD_{600nm}= 0.00005 or lower, changes in lag phase times (defined here as the time required to reach an OD_{600nm}= 0.1) were observed. The shorter lag phase for these strains accounts for the higher OD_{600nm} readings at the final 24 h time point at more dilute cell concentrations. The size of the light deliverance system limited the number of strains tested to four strains per experiment. Although the *ΔsigB* strain consistently displayed faster growth than the WT for liquid media growth experiments in the presence of light, the collation of WT and *ΔsigB* strain data removed any significant difference seen between strains. This can be attributed to the variability in results between experiments. For this reason, the sensor deletion strains are compared only to the specific WT and *ΔsigB* strain controls for that experiment.

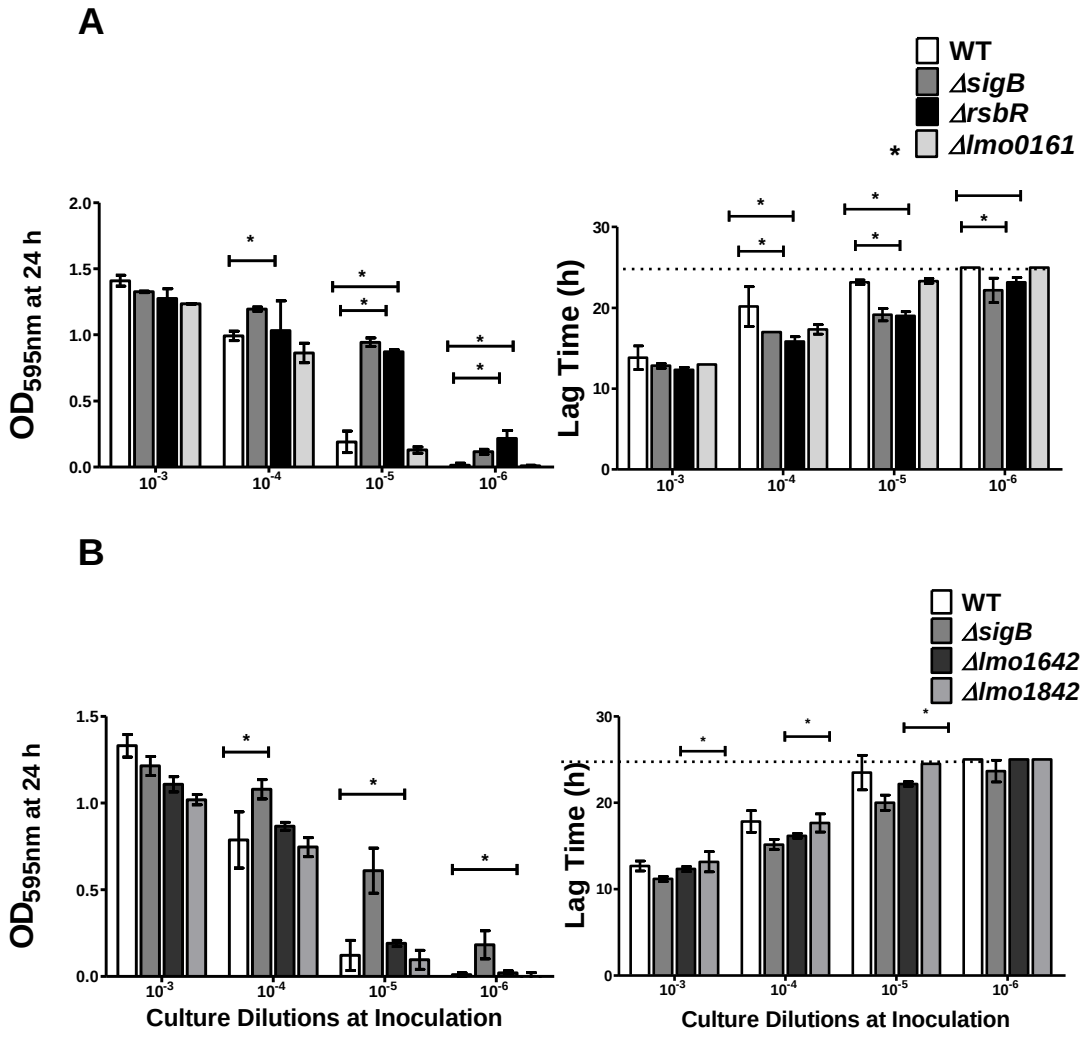

Figure 4.9 Comparison of (A) endpoint readings and (B) lag phase duration of strains grown in liquid media in 1.5-2.0 mW cm^{-2} blue (460 nm) light. Overnight cultures were diluted to an OD_{600nm}= 0.05 and diluted tenfold serially to a 10^{-6} dilution. Dilutions were grown for 24 h at 30 °C in the presence or absence of light. (A) The 24 h endpoint and (B) the time taken to reach OD_{600nm} = 0.1 were calculated for each strain at each dilution. Results for the 10^{-3} to 10^{-6} dilutions are presented. Dunnett's test was used to identify endpoint and lag-phase values which differed significantly from that of the WT strain (* indicates *p*-value ≤0.05). Values for the *Δlmo0799* strain are presented in Fig. 3.10B

4.3.5 Loss of σ^B, RsbR and Lmo1642 reduces survival in 7.5-8.0 mW cm^{-2} blue light

Previously (Fig. 3.12 & Fig. 3.13) the *ΔsigB* mutant was found to be significantly more sensitive to lethal doses of light than the WT. Comparing WT and deletion strains' survival after 12 h exposure to 7.5-8.0 mW cm^{-2} blue light showed that two sensor mutant strains displayed reduced survival (Fig. 4.10). Cell counts for the *ΔrsbR* mutant were similar to those recorded for the Δ*sigB* mutant. While survival counts measured for the *Δlmo1642* were higher than those obtained for the *ΔsigB* mutant strain, it showed a 2 common log reduction in survival compared to the WT.

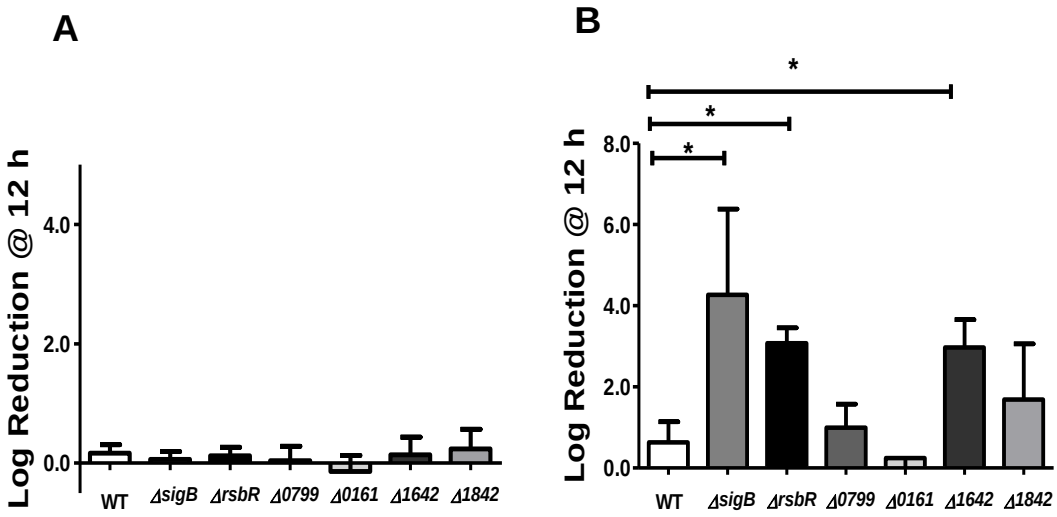

Figure 4.10 Strain survival in high intensity blue (470 nm) light. Overnight cultures were washed and resuspended in PBS and (**A**) incubated in the dark or (**B**) exposed to 8 mW cm^{-2} blue light at 30 °C. Viable cell counts were performed at the 0 and 12-h time points. The values represent the means of the results from five or more individual replicates. Dunnett's test was used to identify strains with significantly different survival counts compared to the WT (* indicates a p-value of ≤0.05). The error bars represent the standard deviations from the mean.

4.4 Discussion

Four stressosome sensor deletion strains were successfully constructed: EGD-e Δ*rsbR*, Δ*lmo0161*, Δ*lmo1642*, Δ*lmo1842*, and a Δ*lmo0799* strain was obtained. These strains showed no defects in growth in BHI at 30 °C or 37 °C (Fig. 4.5), and strains' growth rates under both temperature conditions were similar. In Chapter 3 blue (470 nm) light was shown to have a clear inhibitory effect on *L. monocytogenes* growth (Fig. 3.1), and this is also apparent for each of the sensor deletion strains. Phenotypic assays were carried out to identify any differences in the mutant strains' capacity to respond to light stress and the *ΔrsbR* and *Δlmo1642* strains were revealed to behave differently from the WT under certain conditions (Fig. 4.8-Fig. 4.10).

The Δ*lmo0161* and Δ*lmo1842* strains behave similarly to the WT under all light stress conditions tested (Fig. 4.6-Fig. 4.10). Both display motility inhibition at 30 °C in ambient light, and opaque–translucent rings when exposed to consecutive cycles of ambient white light and dark. Ambient light was used for these assays as the irradiance levels provided by the blue light delivery apparatuses were too high and slowed growth considerably. A previous study had found a significant 2.2-fold difference in transcription levels for *lmo0161* in the WT compared to *ΔsigB* stationary phase cultures (Starr, 2010), however, the loss of Lmo0161 (unlike the loss of σ^B) did not impede the survival of stationary phase cultures in high intensity blue light (Fig. 4.10).

Loss of RsbR had a marked effect on the bacterium's light exposure phenotype, with Δ*rsbR* strain assay results comparable to those reported for the Δ*sigB* strain. This is similar to observations in *B. subtilis*, where the absence of RsbRA (the *B. subtilis* homologue with which RsbR shares most similarity) removes activation of the blue light

sensor mediated stress response (Heavin & O'Byrne, 2012; van der Steen *et al.*, 2012). This has led us to suggest that either RsbR is the sensor paralogue that contributes most to signal transduction in the *Listeria* stressosome or that it plays an integral structural role in stressosome formation. When cells were exposed to inhibitory levels of blue light (1.5-2.0 mW cm^{-2}), a similar difference in cell growth was observed for the *ΔrsbR* compared to the WT strain as was observed for the *Δlmo0799* and *ΔsigB* strains (Chapter 3, Section 3.4.4). While there is a clear inhibitory effect on growth observed, the strain is able to grow comparatively better than the WT. As suggested in Chapter 3 (Section 3.5) this may be due to the high energy cost associated with activating σ^B under conditions of mild stress. σ^B mediates the transcription of approximately 200 genes, and an inability to activate this pathway will clearly allow more energy and other resources (such as transcriptional capacity) to be diverted to the processes involved in cell growth (Guldiman *et al.*, 2016).

In Chapter 3 it was observed that σ^B appears to be required for survival in the presence of 7.5-8.0 mW cm^{-2} light but the blue light sensor Lmo0799 did not appear to contribute significantly to this survival (Chapter 3, Section 3.4.6). It was observed that the *Δlmo1642* and *ΔrsbR* strains displayed survival defects when compared to the WT under these conditions. This initial observation led to the suggestion that Lmo1642 plays a role in light stress survival. The strain does not show enhanced growth in the presence of lower intensity light, and its ability to form opaque and translucent rings in response to consecutive light–dark cycles is not impaired, suggesting the strain is not responding to the presence of light itself, but some other (possibly ROS-related) signal. However, further studies with this strain revealed the presence of a secondary mutation in the strain which prompted a reassessment of the Lmo1642 protein's contributions to light survival.

Both the discovery and effects of this secondary mutation will be outlined in detail in Chapter 5.

Red light has also been shown to stimulate σ^B-dependent transcription of genes in an unknown manner (Ondrusch & Kreft, 2011). In *B. subtilis*, red light has been shown to affect GSR gene transcripts via an alternative activation pathway (Avila-Perez *et al.*, 2010). This pathway consists of the PP2C phosphatase RsbP and an associated α/β hydrolase RsbQ (Vijay *et al.*, 2000; Brody *et al.*, 2001; Kaneko *et al.*, 2005). Bioinformatics searches have not identified red light sensors or RsbP/Q homologues in *L. monocytogenes* (Ondrusch & Kreft, 2011; van der Horst *et al*., 2007; Losi & Gartner, 2008; Karniol *et al*., 2005). However, sensors may respond to an intermediate signal created by the presence of light. The stressosome-led pathway appears to be responsible for sensing both environmental and energy depletion stresses in *L. monocytogenes* (Chaturongakul & Boor, 2004; Chaturongakul & Boor, 2006). Indeed, replacement of the stressosome sensors in *B. subtilis* with the *L. monocytogenes* putative sensor RsbR sensitized the *B. subtilis* stressosome-mediated σ^B activation cascade to nutritional stress (Martinez *et al.*, 2010). It is possible, therefore, that the activities of the remaining stressosome sensor proteins RsbR, Lmo0161, Lmo1642 and Lmo1842 to light sensing in *L. monocytogenes* may have contributed to the observed Lmo0799-independent activation of stress response gene transcription. The alternative possibility that the sensors also play a role in directly sensing red light appears less likely, although as the effect of red light on cells was not tested in this study, it cannot be dismissed.

Once light stress associated phenotypes have been established for the sensor deletion strains, measurement of σ^B activity is necessary to correlate the sensor gene- associated phenotypes with alterations to σ^B-dependent gene transcription. This will be investigated in Chapter 5. Additionally, while Lmo0161, Lmo1842 and Lmo0799 appear here not to

play a role in light stress survival, it is possible that there may be some redundancy among sensors in the light stress sensing system. The construction and testing of triple or quadruple mutants under light (and other) stress conditions would provide further insight into the contributions of each of these proteins to light survival.

Chapter 5: Investigation into the Sensor Components of the σ^B Activation Cascade and Identification of an RsbV I23T Variant with Novel Temperature-Dependent Activity

5.1 Introduction

L. monocytogenes is particularly adept at surviving stress conditions such as those encountered in food processing plants and on entry to the human host. Of the several different mechanisms the bacterium employs to respond appropriately to stress conditions, the σ^B-activated GSR has garnered the most attention from researchers due to its central role in stress survival and virulence and its presence in other Gram-positive bacteria. Although the regulon under the control of σ^B has been characterised under several conditions (Hain *et al.,* 2008; Chaturongakul *et al.,* 2011; Raengpradub *et al.,* 2008), little information is available regarding the function of the sensing components of this system.

σ^B activation is energetically costly and so its regulation is tightly controlled via a number of protein–protein interactions, as outlined in Section 1.6.2 (Fig. 1.2). In brief, σ^B is present in the unstressed cell but it is prevented from interacting with RNA polymerase, as the protein is bound by RsbW kinase (Benson & Haldenwang, 1993). Stresses are signalled to the multiprotein sensory complex known as the stressosome, which consists of RsbR, RsbS and RsbT proteins (Chen *et al.,* 2003; Delumeau *et al*, 2006; Marles-Wright *et al.,* 2008). This triggers the σ^B activation cascade through the release of RsbT which then interacts with an RsbU phosphatase. The RsbW kinase preferentially binds to RsbV, but only to the unphosphorylated form of RsbV (Dufour & Haldenwang, 1994). The active RsbU dephosphorylates RsbV, RsbW then binds to RsbV and σ^B associates with the RNA polymerase machinery to guide transcription from σ^B recognition promoter sites (Benson & Haldenwang, 1993; Dufour & Haldenwang, 1994; Yang *et al.,* 1996). RsbX acts to dephosphorylate RsbS-RsbR complexes, allowing RsbT to recomplex with

the stressosome and the process to continue (Chen *et al*., 2004; Smirnova *et al.,* 1998; Yang *et al.,* 1996).

Within the stressosome sensory complex, the RsbR protein and its paralogues, Lmo0799, Lmo0161, Lmo1642 and Lmo1842, have been identified as the sensory components (Heavin & O'Byrne, 2012; Ondrusch & Kreft, 2011). This has been confirmed for the Lmo0799 protein, which carries a LOV domain (as described in Section 1.11) at its N-terminus (Ondrusch & Kreft, 2011). Few papers have been published on the contributions of the RsbR paralogues to stress sensing in *B. subtilis* and even fewer on *L. monocytogenes* stress sensors. In the previous chapter we investigated the contributions of each of the stress sensors to the light stress response by recording the response of single stress sensor deletion strains to varying conditions of light stress. From these assays we determined that RsbR contributed significantly to the light stress response. Additionally, we found that the blue light photoreceptor Lmo0799 negatively affects growth under mild blue light stress conditions, but its presence is not required for blue light stress survival at lethal doses of light.

In this Chapter the contributions of RsbR and its paralogues to sensing and responding to other stress conditions were investigated To achieve this, sensor deletion strains were subjected to a number of phenotypic tests and σ^B activity was measured using a highly σ^B-dependent promoter fusion to the *egfp* gene. This study provides some of the first insights into the protein functions and structure of the *L*. *monocytogenes* stressosome, with evidence indicating that RsbR plays a structural role in the stressosome unit. Analysis of the contributions of the stressosome proteins to σ^B activity also enabled further understanding of aspects of the σ^B activation cascade and σ^B activity. A temperature-dependent difference in σ^B activity and σ^B-mediated contributions to the acid stress response between 30 °C and 37 °C was highlighted by these assays. In addition,

the generation of an unwanted secondary mutation occurred during the construction of the *Δlmo1642* and *Δlmo1842* strains producing a strain with a novel phenotype in which σ^B activation was abolished at 37 °C but not 30 °C. The identification of this RsbV I23T variant provides insight into the mechanism of activity of the RsbV protein in *L. monocytogenes* operon but also highlights the importance of sequencing the *L. monocytogenes sigB* operon following the construction of new strains.

5.2 Characterisation of sensor deletion strains

5.2.1 *ΔrsbR* and *ΔsigB* exhibit reduced growth inhibition under osmotic stress

Having ascertained that each of the Δ*rsbR* deletion strains grow equally well in BHI (Fig. 4.5), the growth of these strains in the presence of mild stress was compared with that of the WT and Δ*sigB* deletion strains. When inoculated on BHI agar, the addition of ethanol (4% total concentration) or hydrochloric acid (pH 5.0) or incubation at 4 °C the growth of each strain was impeded to a similar extent, comparable to WT (Fig. 5.1). The presence of salt stress also reduced cell growth, observed at 24 h, to varying degrees between strains (Fig. 5.2). Though displaying reduced growth compared to cells incubated in the absence of sodium chloride, colonies of the *ΔsigB* and *ΔrsbR* strains were detected in a 10-fold more dilute sample than the WT control, suggesting less growth inhibition. The addition of salt to BHI had been previously shown to affect Δ*sigB* and WT strains equally (Ferreira *et al.,* 2001). The differences in salt tolerance recorded here were only observed at lower cell dilutions suggesting a role for cell density-dependent protective effects similar to those observed for deletion strains grown in the

presence of 1.5-2.0 mW cm^{-2} blue light (Fig. 4.8). Thus while none of the sensor mutants displayed sensitivity to ethanol, refrigeration temperature, salt or reduced pH, both the Δ*sigB* and Δ*rsbR* mutants displayed a reproducible growth advantage when salt was present in the medium.

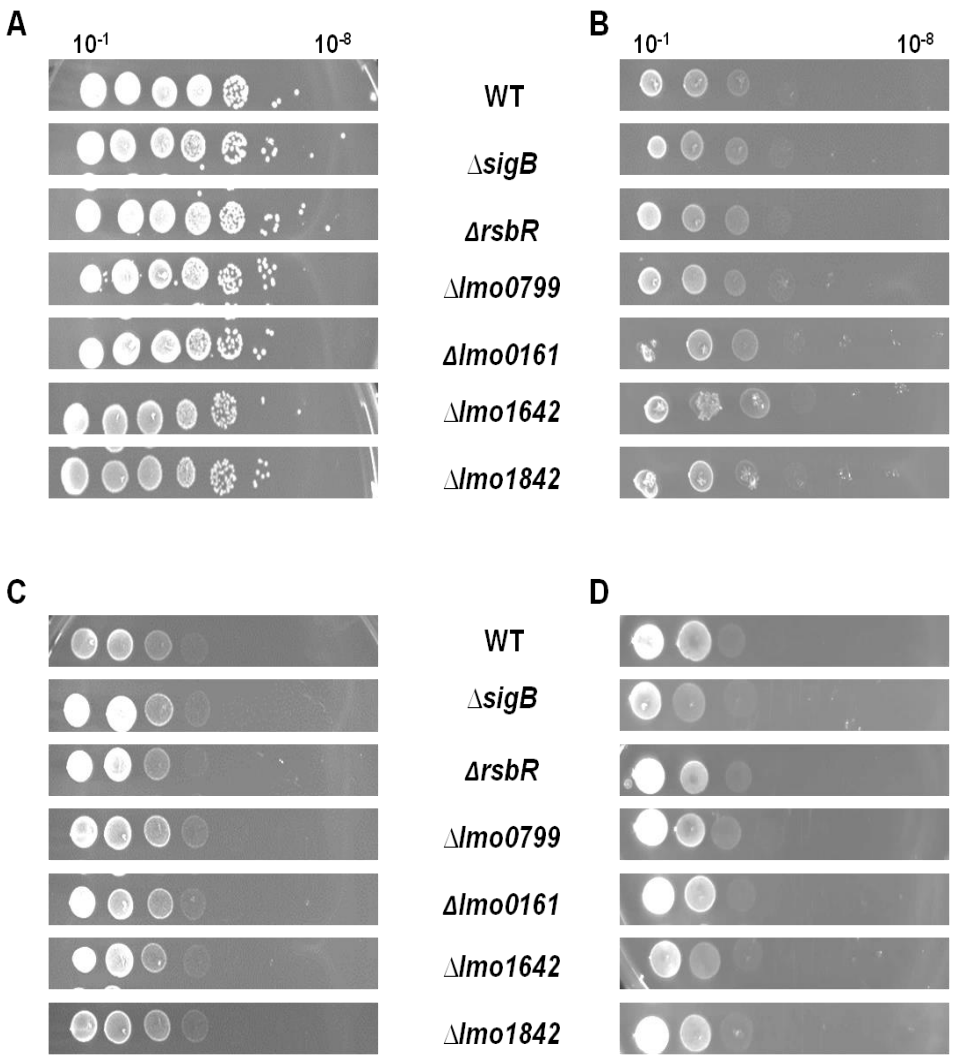

Figure 5.1 Effects of mild ethanol, acid and cold stress on strain growth. Stationary phase cultures (grown at 37 °C) were standardised to and OD_{600nm} = 1.0 and diluted tenfold in PBS to a 10^{-8} dilution. Dilutions (4 µl) were spotted on (**A**) BHI agar and BHI agar containing (**B**) HCl (pH 5.0) or (**C**) ethanol (4% v/v) as described in Section 2.4.1. Plates were incubated wrapped in aluminium foil for 24 h at 30 °C or at (**D**) 4 °C for 10 days. Plates were imaged using a CCD camera.

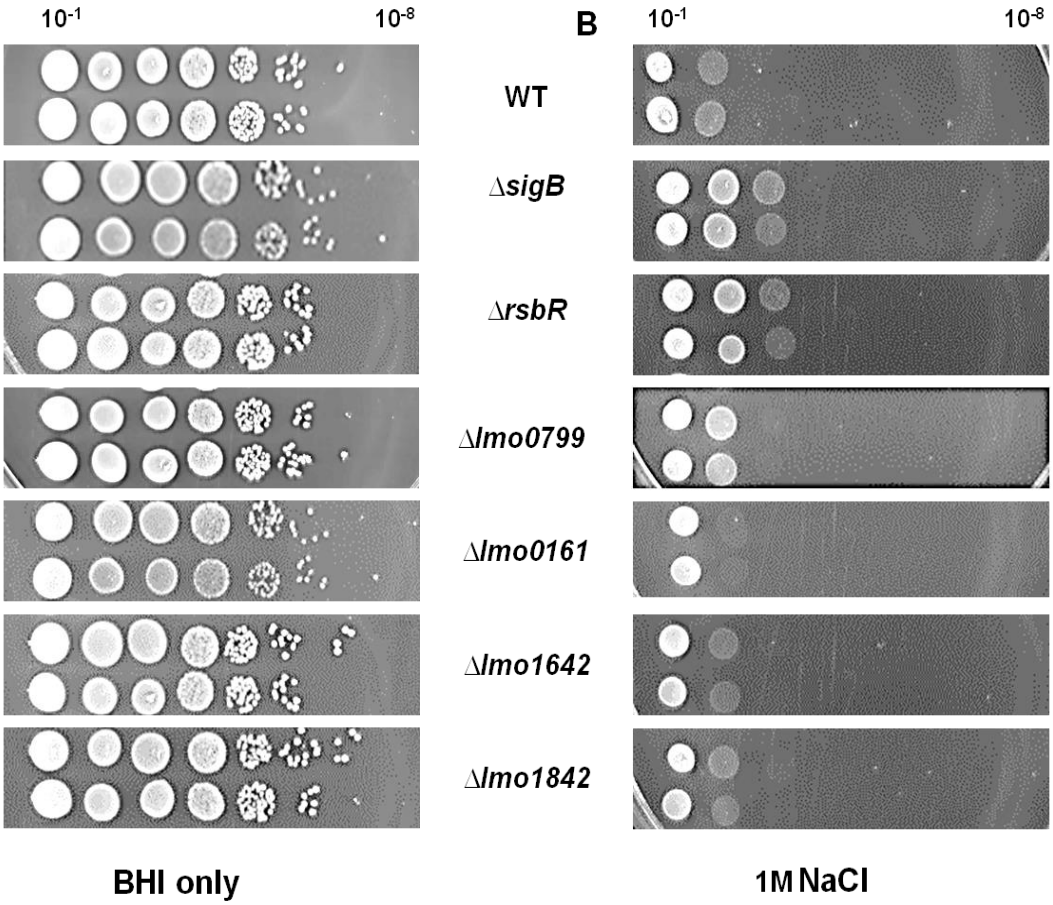

Figure 5.2 Effect of 1 M NaCl on cell growth. The *ΔsigB* and *ΔrsbR* strains, but not the WT strain, show growth at the 10^{-3} dilution on BHI plates containing 1 M sodium chloride. Stationary phase cultures (grown at 37 °C) were standardised to an OD_{600nm} = 1.0 and diluted tenfold in PBS to a 10^{-8} dilution. Dilutions (4 µl) were spotted on BHI agar and BHI agar containing 1 M NaCl and incubated for 24 h wrapped in aluminium foil at 30 °C. Plates were imaged using a CCD camera.

5.2.2 The *ΔrsbR*, *Δlmo1642* and *Δlmo1842* strains display decreased acid survival

While there was no significant difference in the growth of the sensor deletion and WT strains at pH 5.0, several strains behaved differently upon exposure to pH 2.5. The loss of σ^B has previously been shown to be detrimental to acid survival (Ferreira *et al*., 2001) and exposure of *ΔrsbR* stationary phase cultures to pH 2.5 also resulted in significantly lower survival counts than those recorded for WT cultures (Fig. 5.3). Cell counts for the *ΔrsbR* strain fell below the detection limit (10^3 CFU ml^{-1}) within 2 h. In contrast, the WT strain showed a one decimal log difference in survival after a 2 h exposure to pH 2.5. When tested under these conditions, the *Δlmo1642* and *Δlmo1842* strains displayed an intermediate phenotype between that of the WT and *ΔsigB* deletion strains, with statistically significant differences ($p \leq 0.05$) between the WT and *ΔsigB*, *ΔrsbR*, *Δlmo1642* or *Δlmo1842* strains recorded after one hour acid exposure (Fig. 5.3).

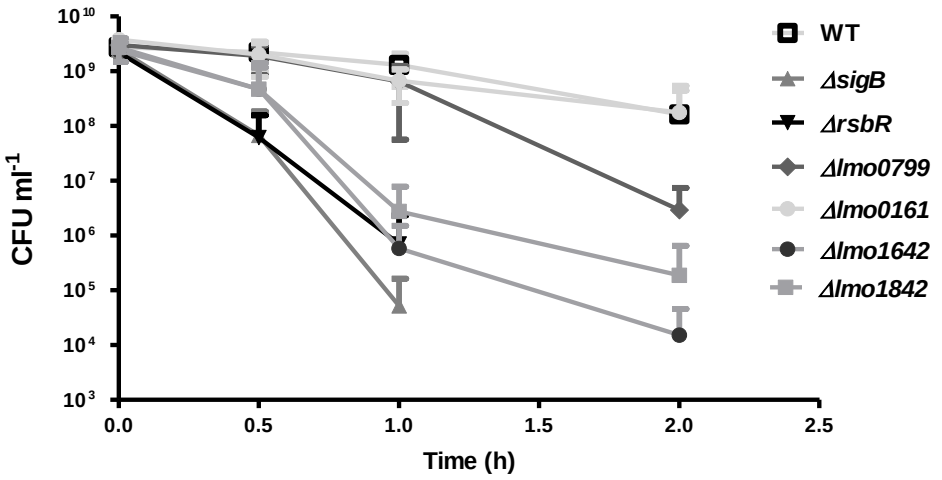

Figure 5.3 WT and deletion strain survival at pH 2.5. Stationary phase cultures (grown at 37 °C) were centrifuged and pellets were resuspended in BHI or BHI acidified to pH 2.5. Samples were removed from the acidified culture at specific time points and survival counts were determined using the method described in Section 2.4.4. Significant differences in cell survival between the WT and *ΔsigB*, *ΔrsbR*, *Δlmo1642* or *Δlmo1842* were observed after a 1 h ($p \leq 0.05$) incubation in acidified BHI. The mean of a minimum of 5 (maximum 6) biological replicates were used to represent strain counts at each time point. Statistically significant differences between WT and deletion strain survival counts were determined using Dunnett's multiple comparison test.

5.2.3 Several strains display enhanced biofilm production phenotypes at 37 °C

Previously the *ΔsigB* deletion strain has been reported to produce less biofilm than the WT at 30 °C and lower temperatures, although PrfA has been shown to be a more significant contributor to biofilm formation at higher temperatures (Lemon *et al.,* 2010; Zhou *et al.,* 2011). When incubated statically at 30 °C in BHI and a chemically defined media (DM) optimised for *L. monocytogenes* growth (Amezaga *et al*., 1995) the *ΔsigB* and the *ΔrsbR* deletion strains followed this previously described trend (Fig. 5.4A&C). At

the increased temperature of 37 °C no differences were observed between the biofilm production of the WT and the *ΔsigB* deletion strain incubated in BHI, similar to the findings described by Lemon *et al*. (2010). Unexpectedly however, in DM the *ΔsigB*, *ΔrsbR* and *Δlmo1642* and *Δlmo1842* deletion strains produced significantly ($p \leq 0.05$) more biofilm production compared to the WT (Fig. 5.4D)

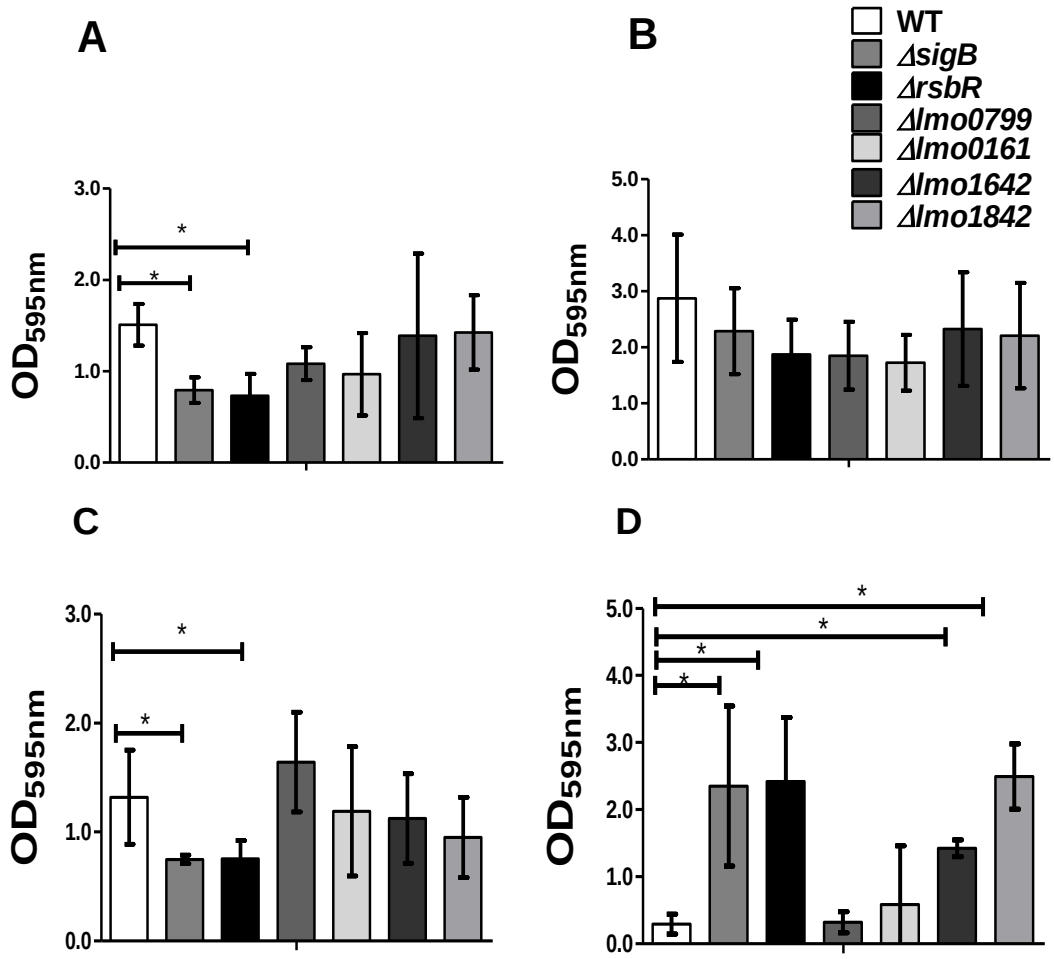

Figure 5.4 Biofilm production varies with temperature and culture media. Biofilm was quantified via crystal violet staining after cultures were incubated statically for 48 h at (**A**) 30 °C in BHI, (**B**) 37 °C in BHI, (**C**) 30 °C in DM or (**D**) 37 °C in DM. Crystal violet stained biofilm was quantified as described in Section 2.4.5. Significant differences (* indicates a *p*-value ≤0.05) in biofilm production for the deletion strains compared to the WT were determined using Dunnett's test.

5.3 Analysis of σ^B activity

5.3.1 Transformation of pKSV7 $P_{lmo2230}$-*egfp* σ^B activity reporter system

Having identified significantly different phenotypes (reduced acid survival, enhanced or reduced biofilm production, enhanced osmotic resistance and reduced light survival) for several of the stressosome sensor deletion strains, a reporter gene system was used to investigate σ^B activity levels in these strains compared with activity in the WT and *ΔsigB* strains. This system, described by Utratna *et al*. (2012) consists of an *egfp* (enhanced green fluorescent protein) gene fused to a 443 bp region containing the highly σ^B-dependent promoter $P_{lmo2230}$ to provide a 1.2 kb insert on a pKSV7 plasmid vector backbone. This plasmid was transformed into WT EGD-e cells and each of the deletion sensor strains and transformants were plated on BHI agar with antibiotic selection (10 µg ml^{-1} chloramphenicol). A *ΔsigB* pKSV7::Pl_{mo2230}-*egfp* strain had previously been constructed (Utratna *et al*., 2012). Uptake of the plasmid was confirmed by PCR using M13 primers.

5.3.2 σ^B activity is abolished in *ΔsigB* and *ΔrsbR* strains and for *Δlmo1642* and *Δlmo1842* strains incubated at 37 °C

Visualisation of fluorescent EGFP via microscopy enabled a qualitative assessment of σ^B activity. Stationary phase pKSV7::$P_{lmo2230}$-*egfp* plasmid-containing cultures grown at 30 °C and 37 °C were tested via fluorescence microscopy as σ^B activity is known to be at maximal levels in stationary phase in otherwise unstressed cells (Utratna *et al*., 2014).

Additionally, EGFP produced in stationary phase cultures was detected by Western blotting, using antibodies specific for GFP or EGFP (Section 2.9). Several interesting results were revealed via fluorescence microscopy and Western blotting. It was discovered that σ^B activity appears to be greater in WT (and *Δlmo0799*) cultures incubated at 30 °C than at 37 °C. This phenotype was more clearly visible on Western blots and was also true for the *Δlmo0799* strain (Fig. 5.5). As expected, EGFP fluorescence was absent in the *ΔsigB* strain (Utratna *et al.,* 2012) (Fig. 5.6). The *ΔrsbR* strain behaved similarly to the *ΔsigB* strain under all phenotypic tests and this strain's σ^B activity levels resembled those of the non- fluorescent *ΔsigB* strain, although small amounts of fluorescence were visible for the *ΔrsbR* strain via microscopy (Fig. 5.5) This level of fluorescence observed with fluorescence microscopy was too low in quantity to be detected by Western blotting and the absence of fluorescence in the ∆*rsbR* mutant is thus attributed to an inability to sufficiently activate σ^B. While σ^B activity was recorded for the *Δlmo1642* and *Δlmo1842* strains at 30 °C, a dramatic reduction in σ^B activity was observed for these strains at 37 °C compared with WT σ^B activity (Fig. 5.5 & Fig. 5.6). This lack of σ^B activity could not be ameliorated through the addition of sodium chloride, which has been shown previously to increase EGFP fluorescence in exponential phase cells with low σ^B activity (Utratna *et al*., 2012). σ^B activity was also investigated in acid-exposed cells (pH 2.5), however the addition of acid caused smearing and loss of fluorescence within 15 min of acid exposure, presumably due to denaturation of the EGFP protein (data not shown).

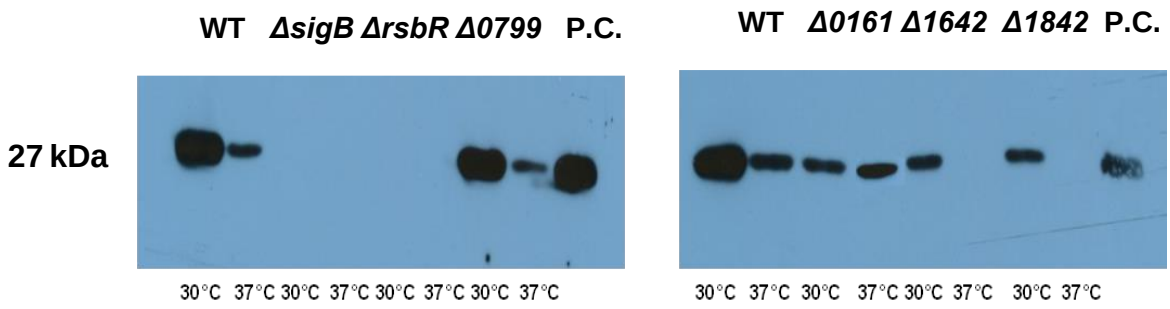

Figure 5.5 Analysis of σ^B activity with anti-GFP antibodies Protein extracts from stationary phase cultures containing the pKSV7::$P_{lmo2230}$-*egfp* reporter plasmid grown at 30 °C or 37 °C were standardised to 2 mg ml^{-1} and separated via SDS-PAGE as outlined in Section 2.9. σ^B activity in cultures was determined by Western blot with polyclonal anti-GFP antibodies against the EGFP produced upon activation of σ^B. Constitutively expressed GFP from a P_{gadX}-*gfp* fusion gene in *E. coli* BW25113::P_{gadX}- *gfp* was used as a positive control (P.C.)

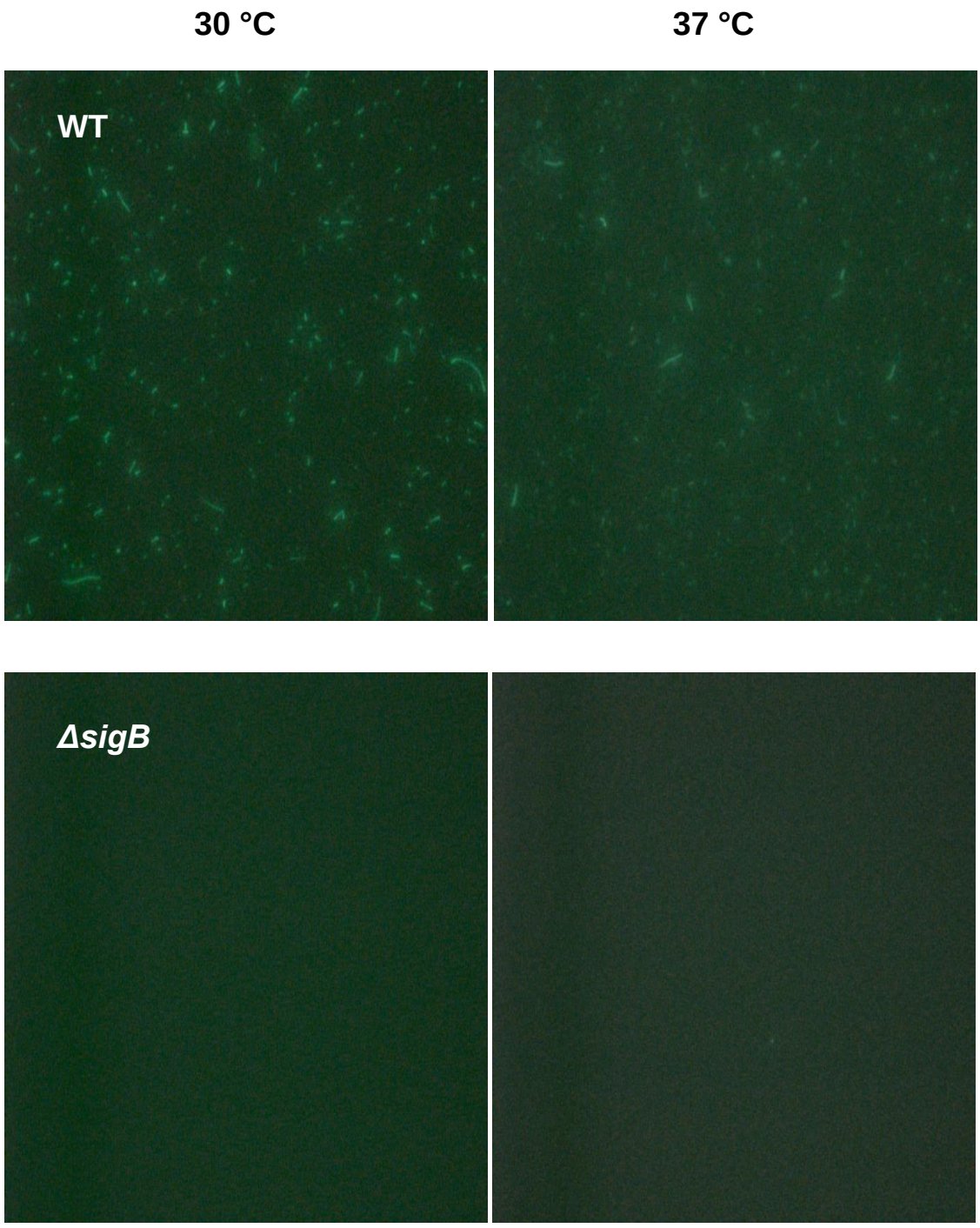
30 °C
37 °C
WT
ΔsigB

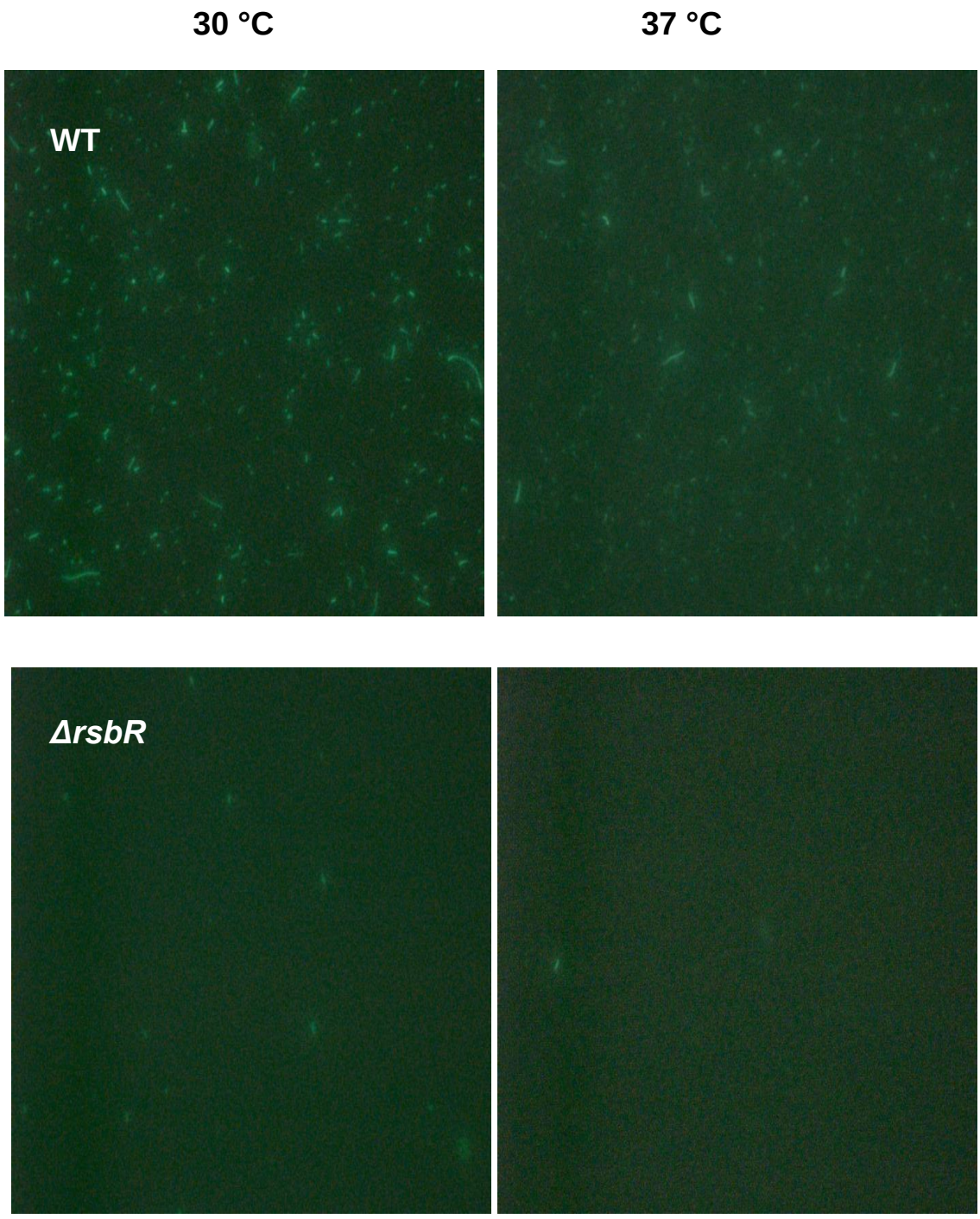
30 °C
37 °C
WT
ΔrsbR

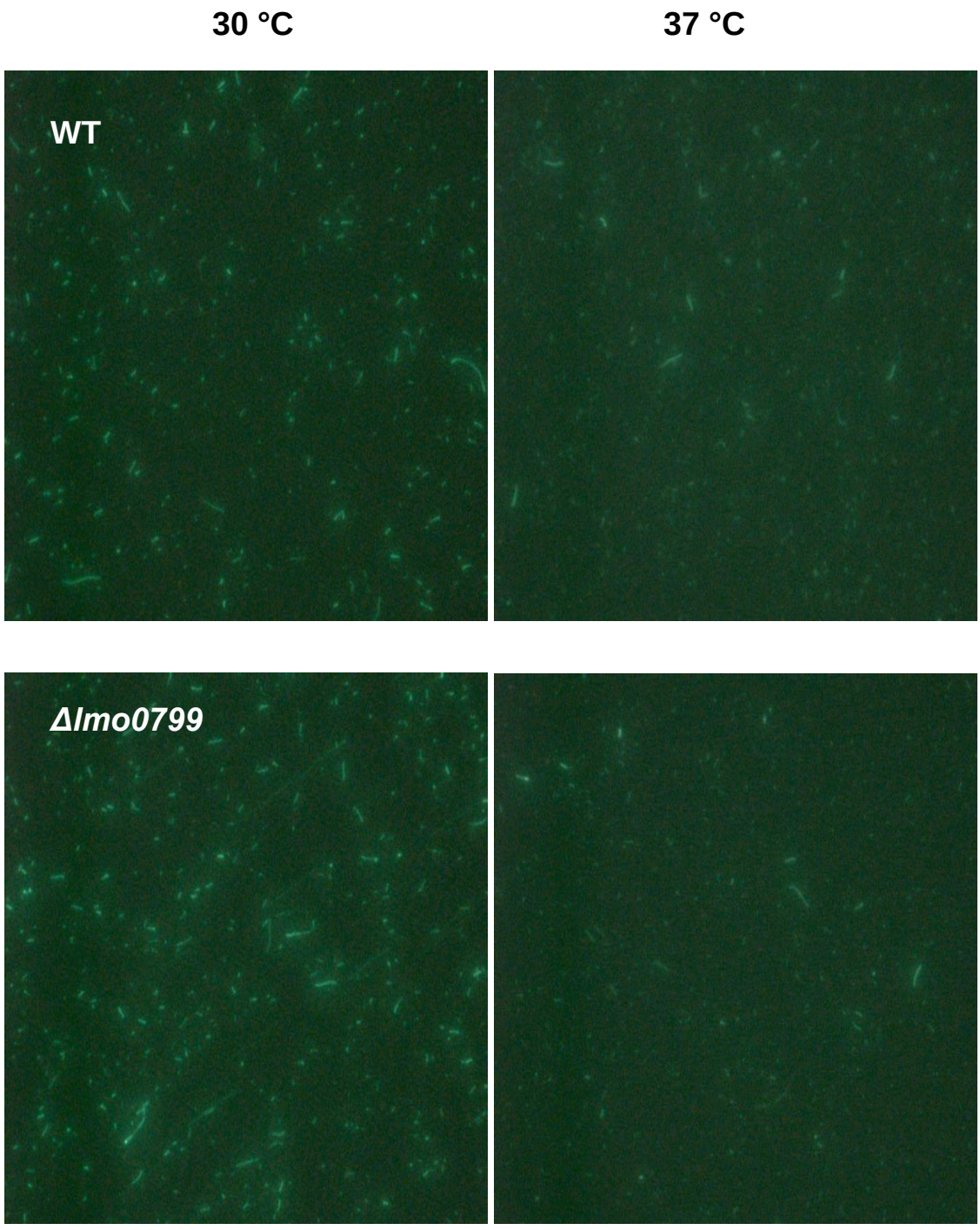
30 °C
37 °C
WT
ΔImo0799

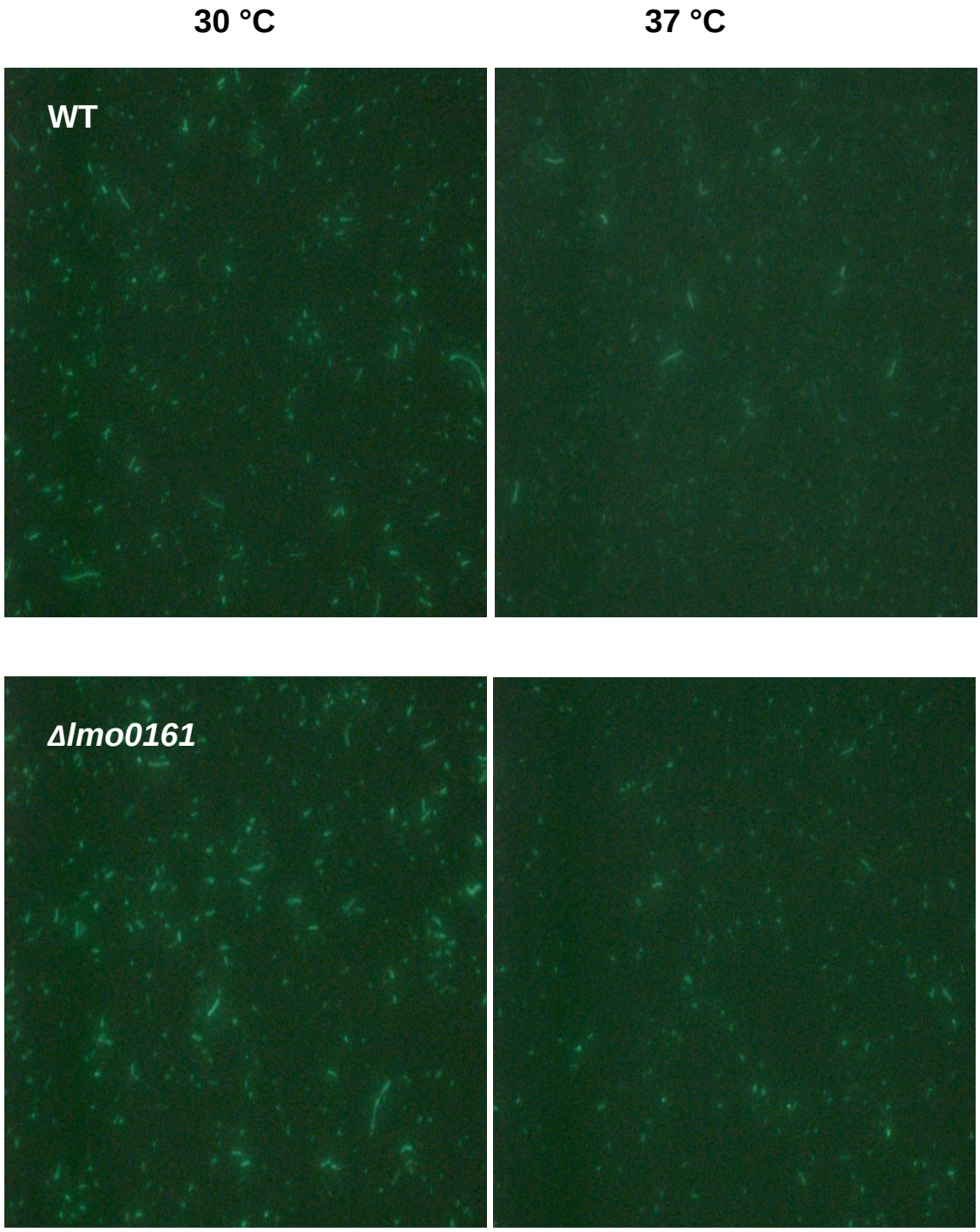
30 °C
37 °C
WT
Δlmo0161

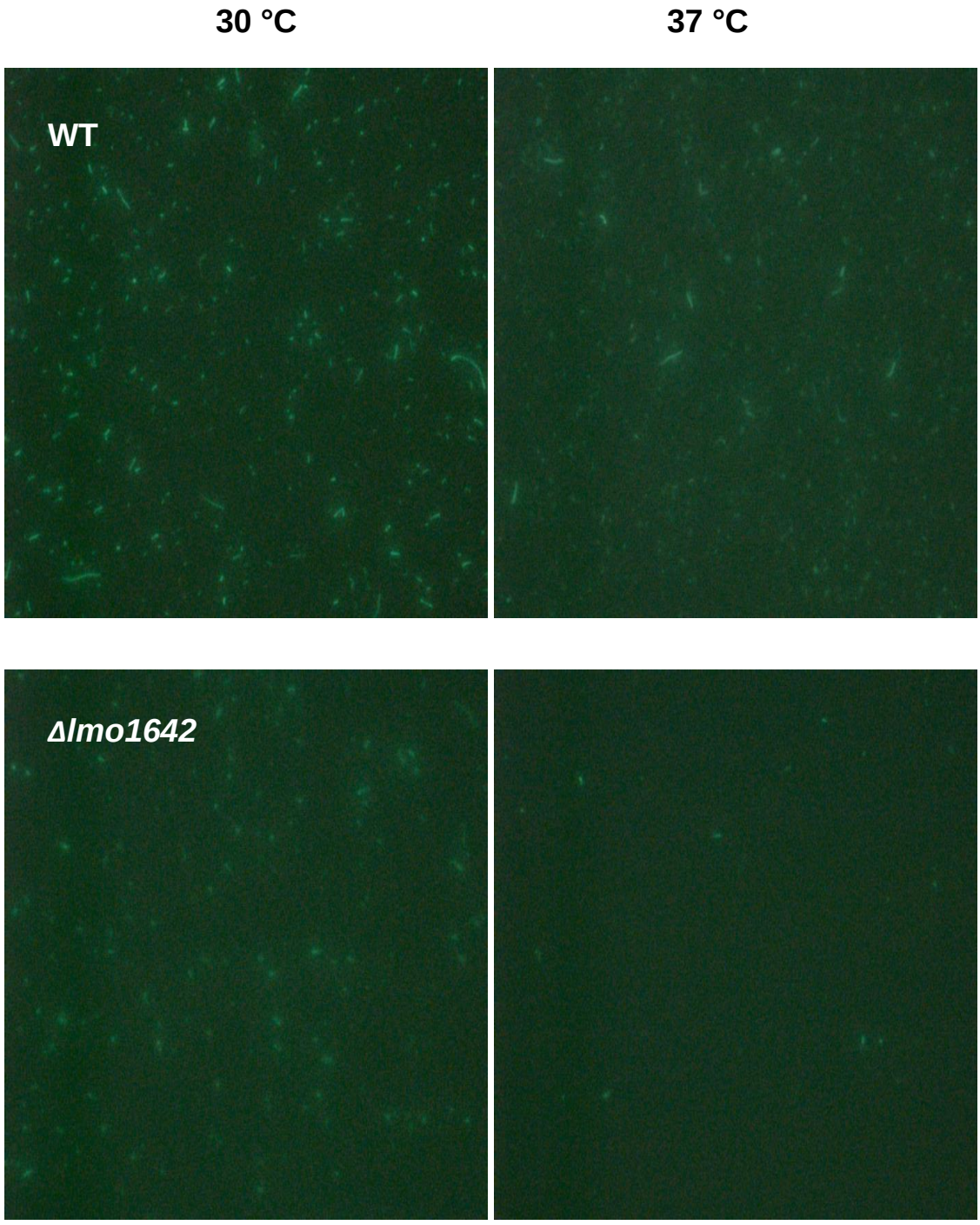
30 °C
37 °C
WT
Δlmo1642

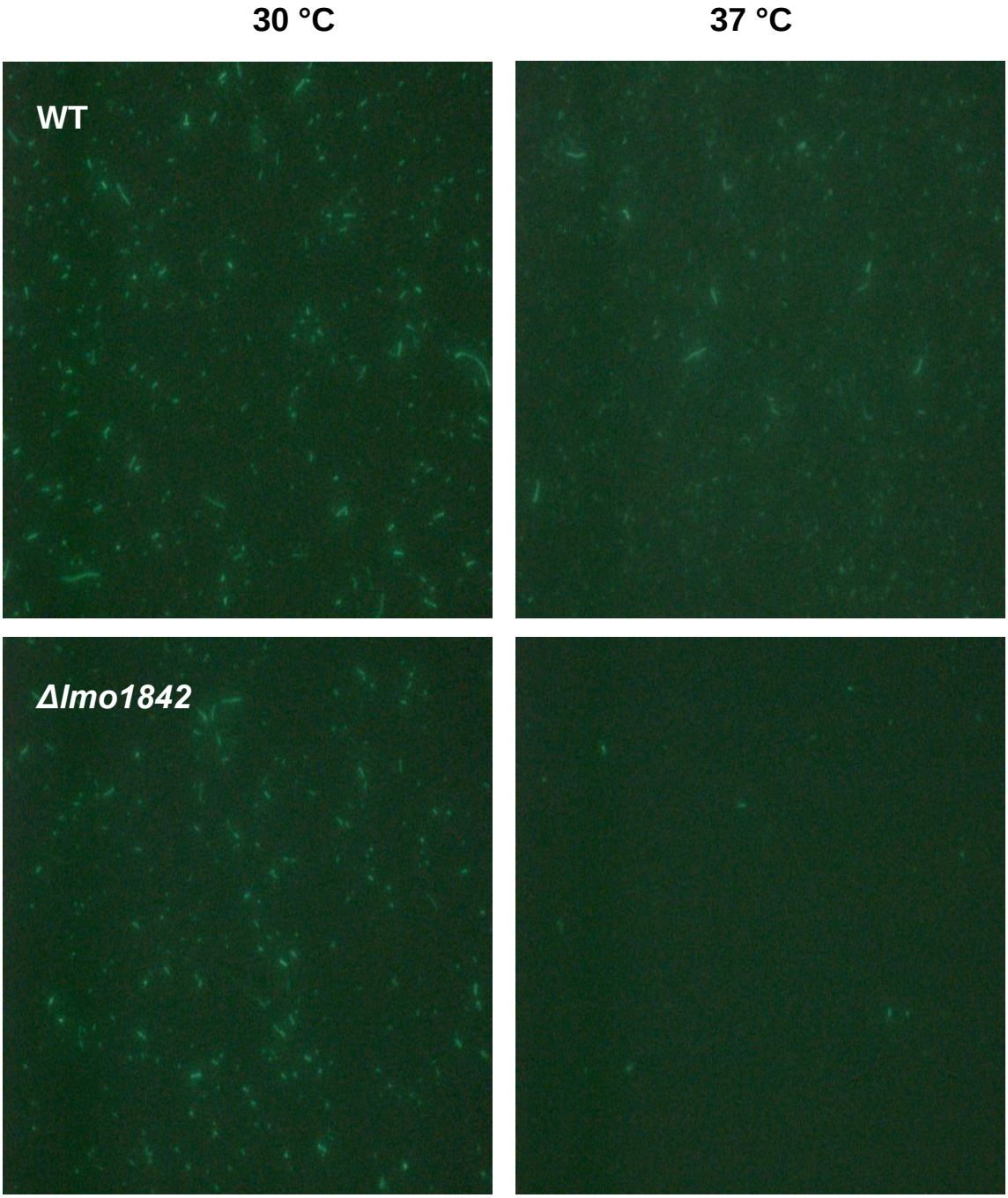

Figure 5.6 Analysis of σ^B activity in stationary phase cultures. Aliquots (5 µl) of standardized (OD_{600nm}= 0.6) fixed stationary phase cultures grown at 30 °C or 37 °C were resuspended in PBS and viewed via fluorescence microscopy (Section 2.10). Samples were prepared from the stationary phase cultures incubated at 30 °C or 37 °C for the following strains: **WT** pKSV7::$P_{lmo2230}$- *egfp,* ***ΔsigB*** pKSV7::$P_{lmo2230}$- *egfp*, ***ΔrsbR*** pKSV7::$P_{lmo2230}$- *egfp*, ***Δlmo0799*** pKSV7::$P_{lmo2230}$- *egfp*, ***Δlmo0161*** pKSV7::$P_{lmo2230}$- *egfp*, ***Δlmo1642*** pKSV7::$P_{lmo2230}$- *egfp*, ***Δlmo1842*** pKSV7::$P_{lmo2230}$- *egfp*.

5.3.3 Reduced acid resistance of *Δlmo1642 and Δlmo1842* is due to σ^B inactivity

The finding that σ^B activity was significantly impaired in the *Δlmo1642* and *Δlmo1842* strains at 37 °C (Fig. 5.5 & Fig. 5.6), suggested that this temperature–dependent loss of σ^B activity was responsible for the acid sensitivity, increased biofilm production at 37 °C and light sensitivity phenotypes recorded for these two strains. Comparing survival of strains incubated to stationary phase at 30 °C or 37 °C before exposure to pH 2.5, it was observed that the *Δlmo1642* and *Δlmo1842* strains did not display increased acid sensitivity at 30 °C, and produced survival counts similar to the WT (Fig. 5.7). Significant differences in survival between the WT and *Δlmo1642* or *Δlmo1842* strains were only observed when cultures were incubated to stationary phase at 37 °C prior to acidification. The differences in acid sensitivity observed must therefore result from the differences in the levels of σ^B activity present in the overnight cultures prior to acidification.

σ^B contributed significantly ($p \leq 0.05$) to the acid survival of WT cells incubated at both 30 °C and 37 °C (Fig. 5.7) However, from these data it appears that σ^B plays a smaller role in acid survival at 30 °C than at 37 °C. Acid-exposed WT cultures provided similar survival counts regardless of prior incubation temperature. The *ΔsigB* strain however displayed a much smaller reduction in survival when cells are incubated at 30 °C instead of 37 °C prior to acid exposure. This finding was unexpected as fluorescence microscopy and Western blotting had indicated that σ^B activity is lower in stationary phase WT cultures incubated at 37 °C than at 30 °C (Fig. 5.5 & Fig. 5.6).

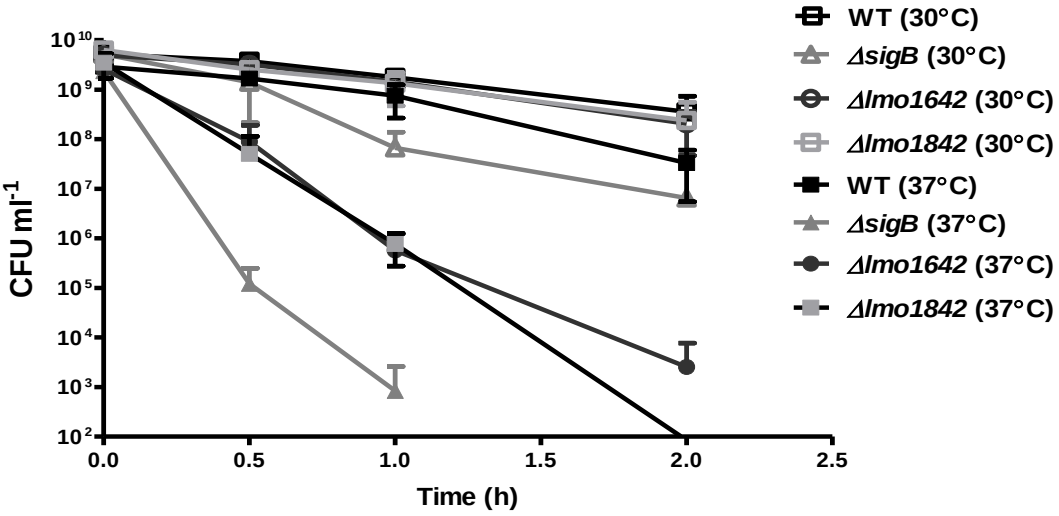

Figure 5.7 Analysis of prior incubation temperature on acid survival. Stationary phase cultures incubated at 30 °C or 37 °C were pelleted and resuspended in BHI or acidified BHI and incubated at room temperature. Survival counts were determined at specific time points as outlined in Section 2.4.4. Statistically significant differences ($p \leq 0.05$) were recorded between survival counts for the WT (30 °C) and survival counts for the Δ*sigB* (30 °C) strains after 1 h or 2 h incubation in acidified BHI (pH 2.5). Statistically significant differences ($p \leq 0.05$) were also recorded between the survival counts for the WT (37 °C) and the *ΔsigB* (37 °C) or *Δlmo1642* (37 °C) or *Δlmo1842* (37 °C) strains after 1 h or 2 h exposure to acidified BHI. The values displayed at each time point represent the mean of six biological replicates. Dunnett's test was used to determine significant differences in survival counts between each WT control and deletion strains incubated to stationary phase at the same temperature.

5.4 Identification and characterisation of an RsbV I23T strain

5.4.1 The *Δlmo1642* and *Δlmo1842* strains carried a secondary *rsbV* mutation

Upon the identification of several novel phenotypes for the *Δlmo1642* and *Δlmo1842* strains, genomic DNA was prepared for sequencing as described in Section 2.8.5. Sequence comparison of the *sigB* operons revealed a single base pair mutation in *rsbV* in both deletion strains compared to the EGD-e WT sequence. This mutation was a T to C transition at base number 68 (atc-acc) which resulted in the replacement of an isoleucine with a threonine, I23T (Fig. 5.8). This mutation is present within one of three conserved regions that are found also in SpoIIAA homologues, identified by Lee *et al.* (2004).The conserved sequence GE/DI_{23}DAY, in which the I23T change is located (Fig. 5.8) has been suggested to form part of the region which interacts with the RsbW kinase or RsbU phosphatase (Lee *et al.,* 2004). This finding suggests the possibility that increasing temperature induces alterations to the conformation of this region in the RsbV I23T variant, which prevents interaction with RsbW or RbU or both proteins. If RsbW is unable to phosphorylate RsbV, either through an inability to bind to the RsbV protein, or due to an inability of RsbU to dephosphorylate RsbV for RsbW interactions, this would abolish the RsbW-mediated release of σ^B.

5.4.2 Rescue of an RsbV I23T strain

Amplification by PCR (with oligonucleotide primers COB 847 and COB 850) and sequencing (Section 2.8.5) of the *rsbV* gene in the *Δlmo0799, ΔrsbR* and *Δlmo0161* mutants confirmed that these strains retained the WT *rsbV* sequence. Sequencing of the *rsbV* gene in EGD-e carrying pMAD::*Δlmo1642* or pMAD::*Δlmo1842* transformant strains, used in the preparation of the sensor deletion strains, also revealed the presence of an *rsbV* C to T transition mutation at position 68 of the open reading frame (Fig. 5.8). This indicates that the secondary mutation had entered the genomic DNA during or before the transformation process, perhaps during the preparation of competent EGD-e cells. In order to study the phenotypic properties associated with the RsbV I23T protein variant separately from the *lmo1642* or *lmo1842* deletions, these transformant strains were cured of their pMAD*::Δlmo1642* and pMAD::*Δlmo1842* plasmids by passaging strains at 30 °C in the absence of antibiotic selection to obtain an RsbV I23T mutant strain. PCR using plasmid-specific oligonucleotide primers was used to confirm the loss of the plasmids from these transformant strains (Fig. 5.9). The presence of wild-type alleles of *lmo1642* and *lmo1842* in these cured strains was also confirmed by PCR. Sanger sequencing reconfirmed the presence of the *rsbV* cytosine substitution at base 68 and subsequent phenotypic tests were performed to determine if the phenotypes described above (Fig. 5.10 & Fig. 5.11) were influenced by the *rsbV* mutant allele.

A

M$_1$NISIEIKERDTDHIDIFVA**GEI$_{23}$DAYT**APKVKEALEVYQVKEGIVLRIDLT

EVS**YMDS$_{58}$T**

GLGVF**V**GAF**K**SLRQRQSELVLFGLSDRLFRLFEITG**L**SDIIEIKNVEGEM

NGNNA$_{114}$-

B

M$_1$NISIEIKERDTDHIDIFVA**GET$_{23}$DAYT**APKVKEALEVYQVKEGIVLRIDL

TEVS**YMDS$_{58}$**

TGLGVF**V**GAF**K**SLRQRQSELVLFGLSDRLFRLFEITG**L**SDIIEIKNVEGEM

NGNNA$_{114}$-

Figure 5.8 RsbV amino acid sequences in WT and *Δlmo1642/Δlmo1842* mutant strains. (**A**)The WT amino acid sequence was obtained from *http://genolist.pasteur.fr /ListiList/*. (**B**) *Δlmo1642* and *Δlmo1842* RsbV amino acid sequence with threonine (acc) replacing isoleucine (atc) at position 23. The conserved phosphorylatable serine S58 is highlighted in red and the underlined bold amino acids correspond to the conserved regions G$_{21}$D/EIDAYN$_{27}$ and Y$_{56}$MDSAGLGTLVVILK$_{70}$ found in RsbV homologues (Lee *et al.,* 2004).

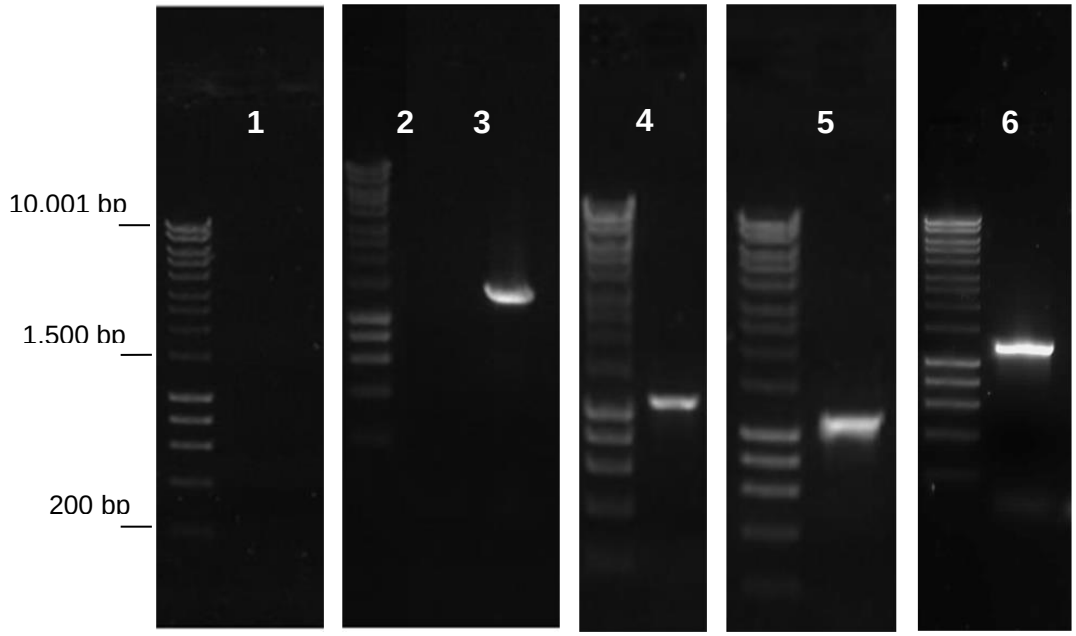

Figure 5.9 PCR identification of RsbV I23T strains PCR confirmation of loss of pMAD plasmid from EGD-e pMAD*::Δlmo1642* (lane 1) and EGD-e pMAD::*Δlmo1842* strains containing RsbV I23T variant proteins (lane 2). pMAD *bgaB* gene specific primers COB 790 and 791 were used. Control with pMAD plasmid and primers COB 790 and 791 (1530 bp) (lane 3). Confirmation of presence of WT *lmo1642* gene with COB 728 and 729 primers (lane 4) (WT band 1124 bp) in RsbV I23T rescued from pMAD::*Δlmo1642* background. Confirmation of presence of WT *lmo1842* gene with COB 730 and 731 primers (WT band 1190 bp) in RsbV I23T rescued from the pMAD::*Δlmo1842* background (lane 5). Successful transformation of pKSV7::$P_{lmo2230}$-*egfp* into RsbV I23T from a pMAD::*Δlmo1642* background provides a 1.2 kb PCR product with M13 primers (lane 6).

5.4.3 Phenotypes initially associated with loss of Lmo1642 or Lmo1842 are caused by an RsbV I23T replacement

The acid resistance of the plasmid-cured RsbV I23T strains, derived from the EGD-e pMAD*::Δlmo1642* and pMAD::*Δlmo1842* backgrounds, was found to be similar to that of the deletion mutant strains (Fig 5.11). The RsbV I23T strains showed a significant decrease in acid resistance, compared to the WT strain following incubation to stationary phase at 37 °C but not 30 °C. This confirms that the temperature-dependent acid sensitive phenotype observed for the *Δlmo1642* and *Δlmo1842* strains incubated at 37 °C was in fact caused by the RsbV I23T amino acid change. Additionally, the RsbV I23T strain produced biofilm at similar levels to the WT when incubated in DM at 30 °C, but significantly higher levels when incubated at 37 °C, similar to the *ΔsigB* strain (Fig. 5.10).

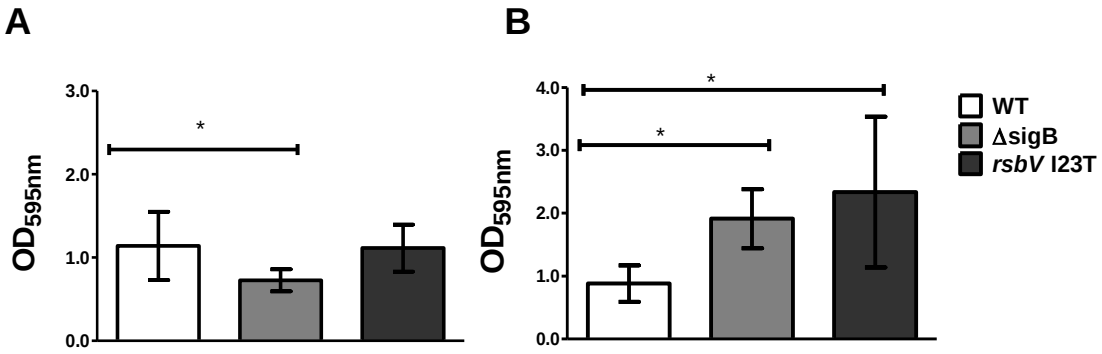

Figure 5.10 Analysis of RsbV I23T strain biofilm production. Biofilm produced over a 48 h period at (A) 30 °C in DM or (B) at 37 °C in DM was quantified via crystal violet staining. Crystal violet stained biofilm was quantified as described in Section 2.4.5. Significant differences (* indicates $p \leq 0.05$) in biofilm production for the deletion strains compared to the WT were determined using Dunnett's test.

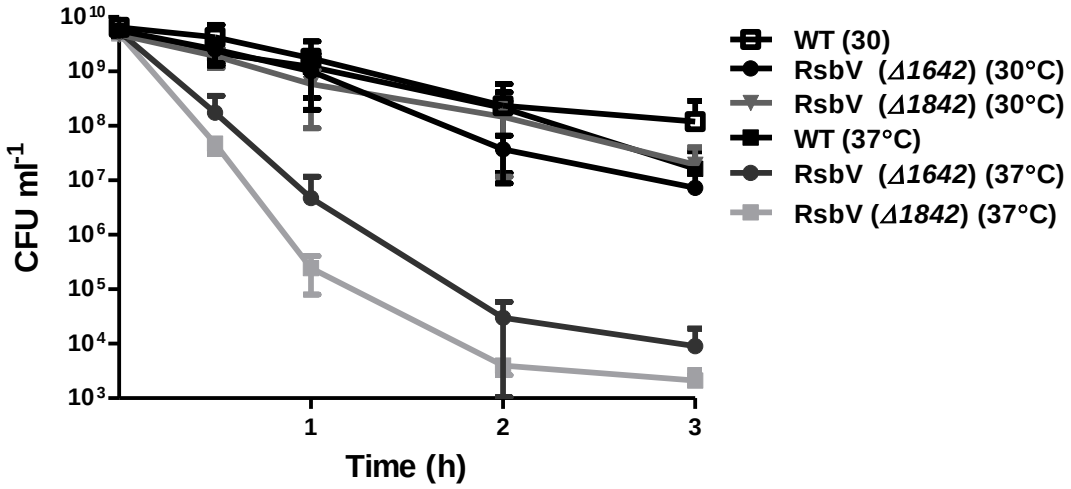

5.11. RsbV I23T confers decreased acid resistance at 37 °C but not at 30 °C. Stationary phase cultures (grown at 37 °C or 30 °C) were centrifuged, and pellets were resuspended in BHI or BHI acidified to pH 2.5. Samples were removed from the acidified culture at specific time points and survival counts were determined using the method described in Section 2.4.4. Strain values at each time point are represented by the mean of seven biological replicates. Error bars represent standard deviation from the mean.Significant differences ($p \leq 0.05$) in cell survival between the WT (37 °C) and RsbV I23T (*Δlmo1642*) (37 °C) or RsbV I23T (*Δlmo1842*) (37 °C) strains after 1 h, were determined using Dunnett's test.

5.4.4 The RsbV I23T replacement prevents σ^B activation at 37 °C

In order to examine whether the RsbV I23T amino acid change was responsible for the reduced σ^B activity observed for the *Δlmo1642* and *Δlmo1842* strains, pKSV7::P*lmo2230*-*egfp* was transformed into the RsbV I23T strain (Fig. 5.9). Cultures incubated to stationary phase at 30 °C and 37 °C displayed a loss of σ^B activity at 37 °C when examined by fluorescence microscopy (Fig. 5.12).

These data confirm that all the phenotypes previously attributed to the *Δlmo1642* and Δ*lmo1842* deletions were in fact due to the presence of the RsbV I23T variant in these strains. To determine whether σ^B activity could be regained in the RsbV I23T strains by reducing the temperature following incubation to stationary phase at 37 °C, non-fluorescent stationary phase RsbV I23T pKSV7: $P_{lmo2230}$-*egfp* incubated at 37 °C were placed at room temperature (~22 °C) and σ^B activity was measured over time (Fig. 5.13). After 4 hours, σ^B activity increased to a level similar to that previously observed for the RsbV I23T strain when incubated to stationary phase at 30 °C. Fluorescence levels remained lower than those observed for the WT at 30 °C (Fig. 5.6 & Fig. 5.12). This indicates that the loss of σ^B activity in the strain harbouring RsbV I23T is temperature-dependent and is recoverable once cultures are incubated at permissive temperatures. How this RsbV I23T amino acid replacement prevents σ^B activation at 30 °C will require further study.

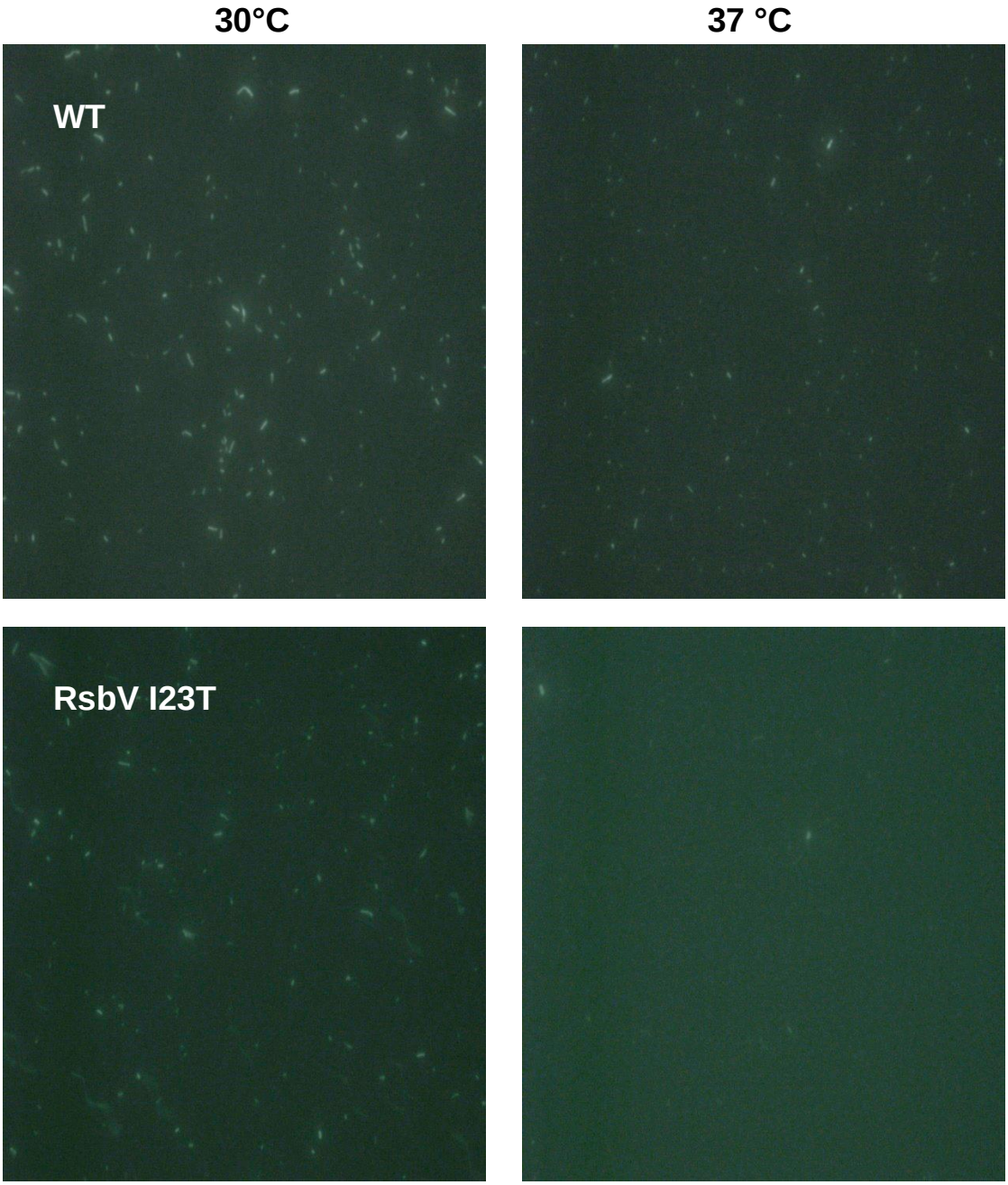

Figure 5.12 Comparison of σ^B activity between RsbV I23T and WT strains at 30 °C and 37 °C. (**A**) WT pKSV7::P*lmo2230*-*egfp* and (**B**) RsbV I23T pKSV7::P*lmo2230*-*egfp* cultures were grown to stationary phase in BHI at 30 °C or 37 °C. Samples were standardised (OD_{600nm}= 0.6), fixed, resuspended in PBS and aliquots (5 µl) were imaged via fluorescence microscopy (Section 2.10).

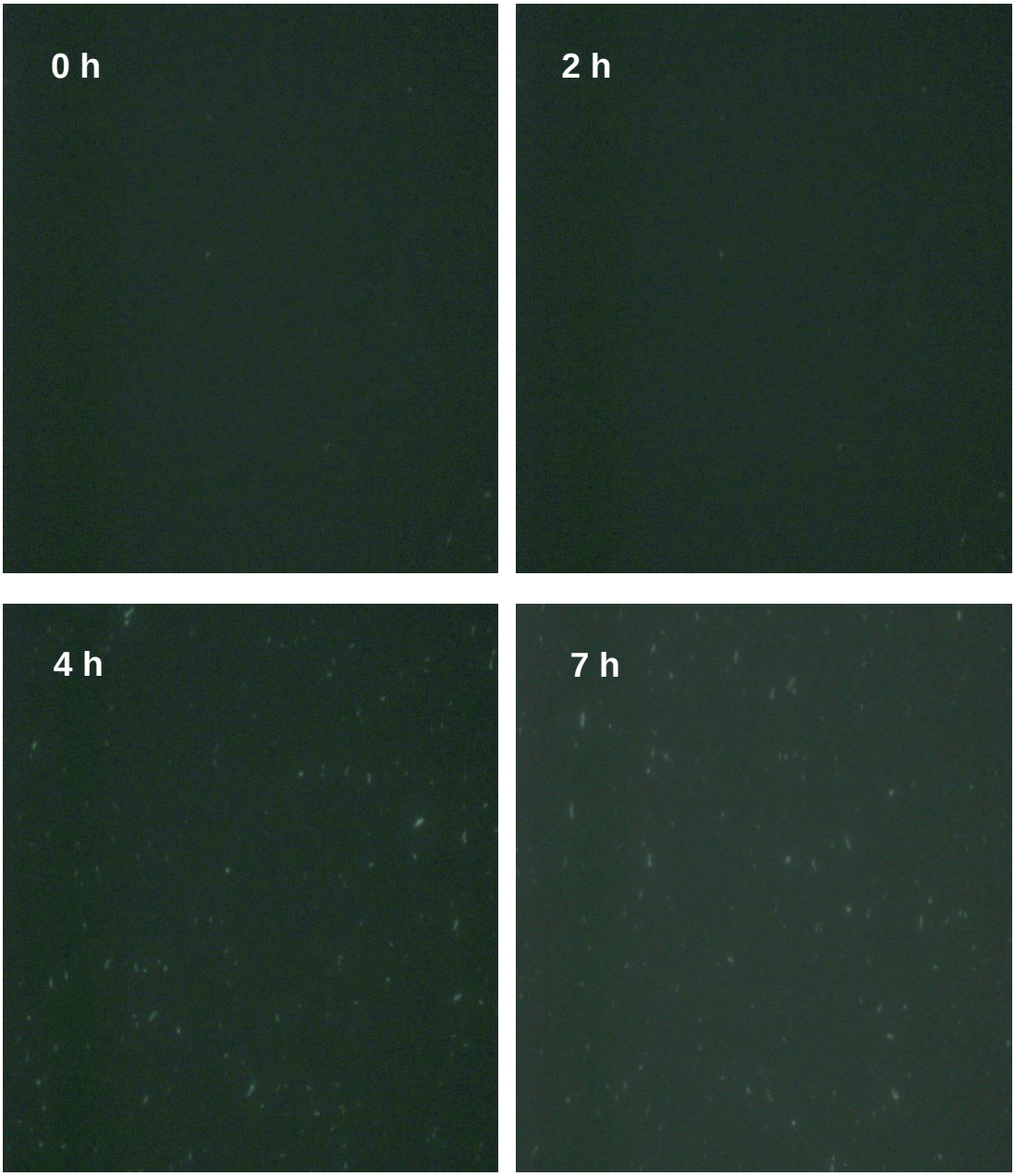

Figure 5.13. RsbV I23T cultures previously incubated at 37 °C can regain σ^B activity at permissive temperatures. An RsbV I23T strain was incubated overnight to stationary phase in BHI at 37 °C before incubation at room temperature (~22 °C). Samples from the cultures were removed for preparation for fluorescence microscopy (Section 2.10) after 0 h, 2 h, 4 h and 7 h incubation at room temperature.

5.5 Discussion

This study represents the first investigation into the function of the putative stressosome sensor proteins Lmo0161, Lmo1642 and Lmo1842, and one of the first attempts at characterising RsbR and Lmo0799 sensor protein function. Results obtained indicate that there may be redundancy in sensing specificity between sensors and determined that RsbR is integral for stressosome formation. The identification of an RsbV I23T amino acid change in two of the mutant strains *Δlmo1642* and *Δlmo1842* revealed a novel protein alteration that prevents successful activation of σ^B at 37 °C but not 30 °C.

Phenotypic testing determined that the Δ*rsbR* strain behaved similarly to the Δ*sigB* strain under a range of conditions where the *ΔsigB* strain behaviour differed from that of the WT (Fig. 4.6-Fig. 4.9 & Fig. 5.2-Fig. 5.4). Loss of σ^B or RsbR resulted in reduced acid survival (pH 2.5), reduced biofilm production at 30 °C and increased biofilm production at 37 °C in DM (Fig. 5.3 & Fig. 5.4). The reduced σ^B activation levels, measured using a $P_{lmo2230}$-*egfp* reporter system, recorded for stationary phase *ΔrsbR* strains, supports the theory that *ΔrsbR*-associated phenotypes are caused by an inability to sufficiently activate σ^B (Fig. 5.5 & Fig. 5.6). This could be interpreted to mean that either RsbR is the dominant sensory component in the *Listeria* stressosome or that it plays an integral structural role in stressosome formation (van der Steen *et al*., 2012).

Several novel phenotypes were established for the *ΔrsbR* and *ΔsigB* strains. The observation that these strains displayed enhanced biofilm formation compared to WT in DM at 37 °C is novel (Fig. 5.4). Reduced biofilm formation at 30 °C for the *ΔsigB* strain has been described in other studies (Lemon *et al.,* 2010; van der Veen & Abee, 2010). In contrast, Lemon *et al*. (2010), recorded similar levels of biofilm production for both WT

and *ΔsigB* strains incubated at 36 °C. In the present study the *ΔsigB* strain produced greater quantities of biofilm at 37 °C in DM, but not in BHI, compared with that produced by the WT (Fig. 5.4 & Fig. 5.10). This disparity in results between studies may possibly be attributed to differences in media (biofilm promoting medium) or strain (10403S) used by Lemon *et al*. (2010).

σ^B activity has previously been shown to increase dramatically upon entry into stationary phase (Utratna *et al.,* 2012). Here we observed a temperature-dependent difference in stationary phase σ^B activity between WT cultures incubated at 37 °C and 30 °C (Fig. 5.5 & Fig. 5.6). Despite the increased σ^B activity observed for cultures at 30 °C, the presence of active σ^B was far more important for WT survival when cultures incubated at 37 °C were exposed to pH 2.5 (Fig. 5.7). This could be linked to the requirement for σ^B activity in the early stages of infection, as evidenced by observation that 232 σ^B-dependent genes are upregulated on entry in the intestine (Toledo-Arana *et al.,* 2009).

While loss of σ^B is clearly detrimental for acid survival (Fig. 5.3, Fig. 5.7, Fig. 5.11) it appears to be beneficial for growth in the presence of low osmotic stress (Fig 5.2). Enhanced growth of the *ΔsigB* strain was also observed in the presence of low intensity blue light (Fig. 3.10 & Fig. 4.8) Similar effects have previously been reported for the growth of a *ΔsigB* strain under glucose limiting conditions, and an *E. coli* strain cultured in chemostats under glucose and nitrogen limiting conditions was found to selectively develop loss of function mutations in the stress response sigma factor gene *rpoS* (Chaturongakul & Boor. 2004; Notley-McRobb *et al*., 2002). These findings suggest that σ^B (or RpoS) activation causes diversion of energy from cell growth, a process which becomes apparent under mild stress conditions.

Several phenotypes initially ascribed to the loss of Lmo1642 or Lmo1842 were in fact caused by an *rsbV* single base pair mutation (T to C) (Fig 5.8). Several reports of unwanted secondary mutations arising during the mutant construction process have been recorded (Quereda *et al*., 2013; J. Johansson, personal communication). Multiple attempts by Quereda *et al* (2013) to generate alterations to the cell wall envelope resulted in the generation of strains carrying secondary loss of function mutations within proteins of the σ^B activation cascade. The integration process during mutant construction is achieved by incubating the bacteria at a temperature not permissive for plasmid replication (42°C) and it was initially thought that this may have allowed the introduction of an unwanted temperature-dependent mutation in this study. However, the *rsbV* mutation producing the RsbV I23T variant was also identified in the pMAD::*Δlmo1642* and pMAD*::Δlmo1842* transformant strains prior to incubation at 42˚C, suggesting that the mutation was acquired before introduction of the deletion cassette plasmid vectors. The exact point at which the mutation was acquired remains unknown at present, but these data do highlight the necessity for caution when interpreting phenotypic data for any genetically modified strain. The repeated generation of unwanted mutations affecting the activation of σ^B suggests that this may be a frequent occurrence in *L. monocytogenes* strains (Quereda *et al*., 2013; J. Johansson, personal communication). Whether these mutations occur in response to the genetic manipulation of the genome or in response to stresses encountered during mutant construction and the storage of cells should be investigated further.

Little is known about the exact mechanism of interaction between RsbV and RsbW, which is central to the control of σ^B activity (Dufour & Haldenwang, 1994; Benson & Haldenwang, 1993). The RsbV homologue TM1442 in *T. maritima* has been crystallised and it is suggested that unphosphorylated RsbV exists as a dimer which is then disrupted

upon phosphorylation by RsbW (Lee *et al.,* 2004). Supporting this hypothesis, RbsW has been shown to form a multimeric complex with RsbV, which has a size of 60 kDa and is thought to consist of 2 RsbV and 2 RsbW proteins (Dufour & Haldenwang, 1994). The RsbV I23T variant is altered at a region thought to interact with the RsbW kinase or the RsbU phosphatase. Whether this inability to interact affects dimerisation is unknown.

Specific functions for the RsbR protein paralogues Lmo0161, Lmo1642 and Lmo1842 were not found despite the variety of stress-inducing conditions tested. Chan *et al.* (2013) hypothesized that the Lmo0799 protein may have other sensing functions, such as cold-sensing, however no other Lmo0799-specific sensing functions were detected for the blue light photoreceptor protein in this study. While phenotypes for the Lmo1642 and Lmo1842 may have been masked by the *rsbV* mutation, it seems more likely that the phenotypes of these strains do not differ from the WT at least under the conditions tested. Additionally, while *lmo0161* transcripts have been reported to increase in a σ^B-dependent manner in the presence of osmotic stress (Starr *et al.,* 2010), the phenotype of the *Δlmo0161* strain in the presence of 1 M NaCl was identical to that of the WT (Fig. 5.2). These findings point to the possibility that there is redundancy in the sensory capacity of the stressosome, as has been described for the *B. subtilis* RsbR paralogues (Kim *et al*., 2004a; Reeves *et al*., 2010; van der Steen *et al*., 2012). The construction and characterisation of triple mutant strains lacking multiple sensory components could therefore give greater insight into mechanism of function of these proteins.

Chapter 6: Discussion

6. 1 Overview

The σ^B alternative sigma factor plays a central role in transcription regulation in *L. monocytogenes* and its activity is tightly regulated via a protein signalling cascade upstream of which lie the putative sensors, of which little is known. Here we investigated the effects of visible light on *L. monocytogenes* cells and examined the contributions of the *L. monocytogenes* stressosome sensor proteins to growth and survival under varying stress conditions including visible light stress. This study also revealed several insights regarding the control of σ^B activity and identified an *rsbV* I23T mutant strain with a novel temperature dependent phenotype.

6.2 Blue light inactivates *L. monocytogenes* via the generation of ROS

Blue light at 470 nm is shown here to have an inhibitory effect on growth and, at higher light intensities, appears to have the capacity to kill *L. monocytogenes* cells (Sections 3 2.2 and 3.4.6). This adds to the findings of several studies which report that visible light can inactivate bacterial cells, even in the absence of a photosensitizing agent. Visible light sources closest to the UV end of the spectrum appear to be most efficient in bacterial inactivation (Kumar *et al*., 2015; Nussbaum *et al*., 2002; Maclean *et al*., 2009; Murdoch *et al.,* 2012; Endarko *et al*., 2012). However, here we show that 470 nm blue light, of which LED sources are readily available, may offer a cost-effective and efficient means of bacterial decontamination on surfaces, provided suitable light intensities are employed (Fig. 3.1 & Fig. 3.10). The addition of catalase, or DMTU (O'Donoghue *et al.,* 2016) reversed the light induced inhibition of *L. monocytogenes* cells, providing evidence that

light induces the generation of ROS (Fig. 3.3). In addition to wavelength used, the efficacy of light inactivation is dependent on the levels of oxygen present (Nussbaum *et al*., 2002; Kumar *et al*., 2015). *P*. *gingivalis* and *F. nucleatum* cells exposed to 400-500 nm light under anaerobic conditions showed no reduction in survival whereas cell counts rapidly decreased following light exposure under aerobic conditions (Feuerstein *et al.,* 2005). Given that the study identifies the bacteria as anaerobes, it is surprising that the effect of oxygen alone on the two microorganisms was not examined in this study or in a similar study by Feuerstein *et al*. (2004). Furthermore, *S. aureus* cells exposed to enhanced concentrations of oxygen with 405 nm light displayed decreased survival compared to light alone (Maclean *et al.,* 2008). The limitations of our experimental design made it impossible to test the effects of visible light in the absence of oxygen, but it is expected that the absence of oxygen would ameliorate the light-associated decrease in cell growth observed, based on the observations above (Fig. 3.11 & Fig. 4.8).

In this study a small difference in catalase activity was observed between aerobically grown WT and *ΔsigB* stationary phase cultures tested for catalase production. It was interesting but perhaps unsurprising that anaerobically grown cultures were unable to produce a 'bubbling' effect (as evidence of catalase production), even upon the addition of greater quantities of hydrogen peroxide (Fig. 3.4). It is likely that this is due to a lack of ROS production during anaerobic growth. Aerobically grown cells produce ROS as accidental by-products of metabolism and respiration in *E. coli* has been shown to account for as much as 87% of the total hydrogen peroxide found in the cell under normal aerobic conditions (Cabiscol *et al*., 2000; González-Flecha & Demple 1995). Exposure to hydrogen peroxide causes upregulation of genes of the well-characterised σ^B and PerR regulons in *B. subtilis* (see reviews Hecker *et al.*, 2007; Faulkner & Helmann, 2011; Zuber, 2009*)*. Both regulons exist in *L. monocytogenes*, although the components of the

L. monocytogenes PerR regulon are less well characterised (Rea *et al*., 2004; Rea *et al*., 2005). The *B. subtilis* gene *katA* is a member of the PerR regulon, which is induced by hydrogen peroxide. *KatA* and the sole *L. monocytogenes* catalase gene *kat* (*lmo2785*) share 48% homology and show highly increased expression in their respective *ΔperR* strains (Rea *et al*., 2005; Helmann *et al*., 2003). It can be interpreted from these studies that the *L. monocytogenes kat* gene is regulated by PerR and based on its similarities with the PerR regulated, hydrogen peroxide induced *katA* gene, we suggest that reactive oxygen species generated during aerobic respiration induce catalase expression, which accounts for the bubbling observed upon the addition of hydrogen peroxide (Rea *et al*., 2005; Helmann *et al*., 2003). This interpretation assumes that *L. monocytogenes* respires aerobically which, while there is some supporting evidence, has not been fully investigated (Patchett *et al*., 1991). As activation of the PerR regulon is shown to be one of the main mechanisms by which the cell combats oxidative stress in *B. subtilis*, (Zuber, 2009) and *L. monocytogenes ΔperR* strains show reduced ability to withstand oxidative stress (Rea *et al*., 2005) we suggest that the contributions of *ΔperR* be considered in future investigations into the cell response to blue light signalling.

6.2.1 The light-mediated excitation of porphyrins results in ROS production

Acknowledging the generation of small quantities of ROS generated during aerobic growth, the major cause for light-induced ROS generation in cells has been attributed to the light-mediated excitation of porphyrins; intermediate products of the heme biosynthesis pathway (Kennedy *et al.,* 1990; Peng *et al*., 1997). Incubation with δ-aminolevulinic acid, a precursor to porphyrin, has been shown to increase both endogenous porphyrin levels and visible light-mediated killing of *L. monocytogenes* and

other bacteria (Nitzan *et al*., 2004; Buchovec *et al*., 2010). Light inactivation experiments were carried out at 30 °C and the temperature at which light-mediated killing is carried out does not appear to be a significant consideration for *L. monocytogenes* light inactivation (Kumar *et al*., 2015). Differences in susceptibility between and among Gram-negative and Gram-positive strains have been recorded, with Gram-negative strains generally displaying heightened resistance to visible light inactivation (Nitzan *et al*., 2004; Murdoch *et al*., 2012; Maclean *et al*., 2009; Kumar *et al*., 2015). Differences may be related not only to differences in cell membrane structures, but also to levels of coproporphyrin found in cells. Coproporphyrin is one of several porphyrin types and it has been suggested by Nitzan *et al.* (2004) that it is the level of coproporphyrin and not total porphyrin levels that accounts for differences in visible light susceptibility of species. Examining this theory, Kumar *et al*. (2015) reported that while increased coproporphyrin levels may account for the increased inactivation of Gram-positive strains over Gram-negatives, it was not true when comparing strains within Gram-positive or Gram-negative groups. From this finding the authors determine that coproporphyrin levels alone do not account for differences in light inactivation susceptibility and other factors may need to be examined. Both studies recorded a smaller reduction in survival for a *B. cereus* strain compared with an *S. aureus* strain following light inactivation at 405 nm and 407-420 nm. Nitzan *et al*. (2004) attributed this finding to the lower level of coproporphyrin recorded for the *B. cereus* strain whereas Kumar *et al.* (2015) found that the *B. cereus* strain tested possessed significantly more coproporphyrin than the *S. aureus* strain used. Differences in experimental design may be responsible for this relative difference between studies, but it could also be due to the differences among *B. cereus* or *S. aureus* strains. Reasons for this increased efficacy of coproporphyrin in stimulating ROS production over that of other porphyrins have not been explored in great detail. Maclean *et al*. (2009) have suggested that differences in the peak absorption wavelengths between porphyrins may

account for differences in contribution to light-mediated inactivation. A factor influencing differences in contributions of bacterial porphyrins to light-mediated ROS production may also be the pH of the intracellular environment in which the porphyrin is excited. Polo *et al.* (1988) found that porphyrin fluorescence emission and excitation spectra peaks vary in intensity depending on pH, with minimal fluorescence near pH 5 for coproporphyrin and near pH 7-7.5 for uroporphyrin. While variation in intracellular pH exists among bacteria, *L. monocytogenes* maintains an intracellular pH of approximately 7.0-8.0, even under several stress conditions (Budde & Jakobsen, 2000; Fang *et al.,* 2004). This may therefore affect which porphyrins prove most effective in generating ROS.

6.2.2 Blue light exposure may select for resistance-associated phenotypes

Visible light inactivation therapy has many promising applications across a range of settings, from food processing to medical environments but some potential issues of concern may need to be investigated. One aspect of light inactivation therapies which has not yet been well studied is the possibility that repeated or prolonged exposure to light may select for bacteria with enhanced light resistance capabilities. Rea *et al*. (2005) describe a *ΔperR* strain with a secondary mutation that exhibited increased resistance to hydrogen peroxide, suggesting that development of resistance is possible for *L. monocytogenes.* Additionally, several of the mutant strains tested in this study showed increased growth in low intensity blue light, although not at higher intensities (Fig. 3.10, Fig. 4.8, Fig. 4.9, Fig. 4.10). The promotion of light induced biofilm is also an important consideration. Gomelsky and Hoff (2011) suggest that light acts as an environmental cue, responsible for shifts in bacterial lifestyle from planktonic growth to biofilm formation or the reverse. Several bacterial species have been shown to initiate biofilm formation or

maturation upon introduction of light (Gomelsky and Hoff, 2011). Blue light stimulation of the *E. coli* BluF (formerly YcgF) photoreceptor, which carries a FAD-binding bluf domain) prevents repression of systems required for biofilm maturation (Tschowri *et al*., 2009; Tschowri *et al*., 2012). *Acinetobacter* strains, including several nosocomial strains, also show blue light induced promotion of biofilm production (Golic *et al*., 2013). At the same time, other strains including the most commonly isolated pathogenic *Acinetobacter* strain *A. baumanii* have been reported to reduce biofilm production under blue light conditions (Mussi *et al*., 2010; Gomelsky & Hoff, 2011). In this study, while there appeared to be a difference in biofilm production between ambient light and dark exposed *L. monocytogenes* cells at 37 °C, no difference was observed at the more environmentally relevant temperature, 30 °C (Fig. 3.9). In addition research with *E. coli* and *L. monocytogenes* biofilm indicates that blue light inactivation methods could be successful in dispersing biofilm (Buchovec *et al*., 2010; McKenzie *et al*., 2013).

It has also been shown that blue light can prime σ^B-regulated virulence functions of *L. monocytogenes* in an Lmo0799 dependent manner (Ondrusch & Kreft, 2011; Tiensuu *et al*., 2013). Lmo0799-dependent upregulation of InlA and InlB (3- and 4.5-fold, respectively) and increased invasiveness in the presence of blue light is proposed to prepare the cell for infection of a new host or possibly a consequence of activation of the σ^B stress response regulon in preparation for additional stress conditions found at soil surfaces, such as osmotic stress or UV-induced damage (Gomelsky & Hoff, 2011; van der Steen & Hellingwerf, 2015). Clearly the light-mediated induction of biofilm formation, virulence priming or stress resistance, however unlikely, could potentially have disastrous results in a clinical or factory setting. Further research into the possibility of light inactivation therapies promoting the spontaneous generation of light-resistant colonies in populations is recommended if light is to be considered as a means of

bacterial control. Equally, research to identify light intensity thresholds required to prevent biofilm formation or generation of resistant, hypervirulent strains is needed to fully exploit the potential antimicrobial applications of visible light.

6.3 σ^B and the general stress response

6.3.1 Incubation at 30 °C or 37 °C alters σ^B contribution to stress response phenotypes

Following the exploration of the effects of blue light on the cell, a central aim of this study was to examine the function of the putative stress sensor proteins in the activation of σ^B in response to blue light, and other stresses. The σ^B regulon is a core regulon, overlapping with many other regulator systems in *L. monocytogenes* (Chaturongakul *et al*., 2011; Ollinger *et al*., 2008; Raengpradub *et al.*, 2008) and σ^B activation is absolutely required for the proper functioning of the cell under stress conditions both in the external environment and on entry into the host (van Schaik & Abee, 2005; Gahan & Hill, 2014) (Sections 1.5-.7). However, stationary phase σ^B activity in WT cells grown at 30 °C was observed to be greater than that at 37 °C, when visualised via EGFP production from a σ^B-dependent promoter using Western blotting and fluorescence microscopy (Fig. 5.5 & Fig. 5.6). This observation contrasts somewhat with the findings of Ivy *et al*. (2010) who report no difference in *sigB* or the σ^B-dependent *gadA* gene transcripts between these temperatures in a 10403S strain. It may be this is due to differences in reporter sensitivity for the *gadA* and *lmo2230* promoters. However, it may also be that this temperature-dependent difference in σ^B activity is specific to the EGD-e strain. Certainly, strain

variation in the contributions of the σ^B regulon to stress conditions such as acid survival has been noted previously, although both the EGD-e strain tested here and 10403S belong to the same lineage (Oliver *et al.,* 2010). Additionally, differences in survival following acid shock between 30 °C- and 37 °C-incubated stationary phase cells, have been shown to vary between strains (Ivy *et al*., 2012; Kazmierczak *et al*., 2003).

The ability of stationary phase cells to survive acid exposure was found to be directly correlated with the levels of σ^B activity present in the cells prior to acidification. Strains that showed little or no σ^B activity in stationary phase were significantly more sensitive to pH 2.5 (Fig. 5.3, Fig. 5.5, Fig. 5.6). This finding supports previous research that found no increase in σ^B-dependent gene transcription following acid shock, indeed a decrease in σ^B-dependent gene transcripts is observed. The authors propose that these decreases are due to acid-induced alterations to transcription of certain components of the σ^B regulon in an environment containing an already saturated concentration of active σ^B protein (Ivy *et al*., 2012). Surprisingly, given that σ^B activity appears to be lower in stationary phase WT cells cultured at 37 °C than at 30˚C (Fig. 5.5 & Fig. 5.6), loss of the σ^B protein was more detrimental for acid-exposed stationary phase cultures incubated at this temperature than at 30 °C (Fig. 5.7). As WT cultures survived at similar levels regardless of pre-exposure temperature, the smaller role of σ^B in survival of cultures incubated at 30 °C suggests that other, unidentified, regulators contribute to acid survival at this temperature in a manner that is not as apparent in 37 °C incubated cultures.

6.3.2 Increased biofilm production of a *ΔsigB* strain may be linked to increased PrfA activity

In a novel finding, the quantities of biofilm produced by the *ΔsigB* and *ΔrsbR* strains were higher than that produced by the WT in DM, but not BHI, at 37 °C (Fig. 5.4B&D & Fig. 5.10). Reduced biofilm formation for the *ΔsigB* strain compared with the WT when incubated at 30 °C (or lower temperatures) has been reported in several studies in various growth media (van der Veen & Abee, 2010; Lemon *et al*., 2010; Lee *et al.,* 2014), highlighting the importance of σ^B in environmental settings (Fig. 5.4A&C, Fig. 5.10). However, the finding that the *ΔsigB* strain produced increased biofilm than the WT at 37 °C in DM was unexpected and cannot be easily explained. Testing biofilm at 36°C, Lemon *et al.* (2010) did not identify a difference in biofilm production of the WT and Δ*sigB* strains, despite reporting decreased biofilm production for the Δ*sigB* strain at 30 °C in modified Hsiang-Ning Tsai biofilm-promoting medium. The cause for this inconsistency in findings may well lie with the difference in culture media. Highly increased transcript levels of the virulence genes regulated by the major virulence regulator PrfA and increased *prfA* transcripts have been recovered from strains cultured in DM at 37 °C compared with those cultured in BHI (Travier *et al.,* 2013; J. Johansson, personal communication. Loss of PrfA is established as causing reduced biofilm at 36°C or 37 °C and its removal has been reported to result in a 70% decrease in biofilm formation (Lemon *et al.,* 2010; Zhou *et al.,* 2011; Travier *et al.,* 2013). Several genes regulated by PrfA are required for biofilm production, including *inlA*, *hly* and *actA.* The exact mechanism by which the ActA protein affects biofilm production is not known but the protein promotes cell aggregation through direct interactions between cells' ActA proteins and deletion of *actA* has been shown to result in a 55% reduction in biofilm (Travier *et al.,* 2013). Comparing biofilm production of a *ΔprfA* strain and a double deletion

ΔsigBΔprfA strain with that produced by the WT and *ΔsigB* strains at 37 °C may determine whether increased *prfA* transcription is indeed responsible for the enhanced biofilm production observed here for the *ΔsigB* strain in DM at this temperature.

The cause of *ΔsigB*-associated increased biofilm may not simply be due to increased PrfA activity as, somewhat confusingly, constitutively active PrfA (PrfA*), which upregulates virulence factors to levels found within the host cell, has been shown to slightly decrease biofilm production in comparison with WT PrfA expression levels *in vitro* (Lemon *et al.,* 2010). However, given the overlap in σ^B and PrfA regulons (as described in Sections 1.4 & 1.5), including the presence of a σ^B-dependent promoter upstream of *prfA,* it is still possible that increased PrfA expression in combination with loss of σ^B activity is responsible for the upregulated biofilm production observed.

6.3.3 Activation of σ^B is an energetically expensive process

While the presence of σ^B had no impact on growth in the presence of mild acid conditions (pH 5), it had a negative effect on growth in the presence of 1 M NaCl and 1.5-2.0 mW cm^{-2} blue light (Fig. 5.2 & Fig. 3.1). One possible explanation for these observations is that there is an energy cost associated with activating the σ^B regulon, which in the absence of σ^B leaves more available energy to be redirected towards growth activities. It also suggest the availability of core polymerase is a factor, as increased growth may be due to the removal of competition between the housekeeping sigma factor σ^A, and σ^B for core polymerase under stress conditions. The trade off between growth and survival mechanisms, which becomes apparent under mild stress conditions, has been identified in several other bacterial studies (Nyström, 2004). Loss of σ^B has also been shown to

improve *L. monocytogenes* growth under glucose-limiting conditions, and glucose- and nitrogen-limiting conditions were found to encourage development of loss of function mutations in the stress response sigma factor gene *rpoS* of *E. coli* cells under continuous culture (Chaturongakul & Boor, 2004; Notley-McRobb *et al*., 2002). Despite the perceived growth advantage under mild stress conditions, loss of σ^B was clearly shown to be detrimental for light survival and acid survival when the challenge became severe (Fig. 3.12, Fig. 4.10, Fig. 5.3).

6.4 Contributions of the stressosome sensors

6.4.1 Redundancy may exist among sensors' sensing capacity

Evidence for the formation of a stressosome structure in *L. monocytogenes,* though not yet published, has recently been confirmed in a recent oral presentation at the triennial ISOPOL *Listeria* symposium (Cossart, 2016). Preliminary findings have found that RsbR, Lmo0799, Lmo1642 but not Lmo1842 form part of this structure (Cossart, 2016). It remains to be seen whether Lmo1842 is indeed a stressosome associated protein. One possible explanation for the absence of Lmo1842 may be found in studying the *B. subtilis* stressosome RsbRD sensor protein. This protein has been shown to complex with the stressosome but was found to be expressed in much lower quantities than its paralogues, near to the detection threshold under normal growth conditions (Reeves *et al*., 2010). If Lmo1842 is expressed at much lower levels than other stressosome proteins, it could suggest that loss of this protein will not have significant effects on the ability to respond to stress. We were unable to determine any *Δlmo1842*- (or indeed, *Δlmo0161- or Δlmo1642*-) specific phenotypes, as all phenotypes initially identified are now attributed

to the *rsbV* I23T secondary mutation. Alternatively, the protein may display extreme sensitivity as a sensor which could compensate for its theorized lowered abundance. Further study is needed to fully understand the contributions of Lmo1842 to stress sensing. Failure to identify a single stress condition which required the presence of Lmo1642, Lmo1842 or Lmo0161 for σ^B activation suggests that there may be some redundancy in the sensory mechanism. The construction of triple mutants may help to fully elucidate the roles of the RsbR, Lmo0161, Lmo1642 and Lmo1842 sensors.

6.4.2 The structure of the stressosome relies on the presence of RsbR

The removal of *rsbR* produced a strain which behaved similarly to a *ΔsigB* strain under all stress conditions tested (Fig. 4.6-4.10 & Fig. 5.1-5.4). Additionally, *ΔrsbR* stationary phase cultures exhibited a lack of σ^B activity similar to that observed upon the removal of σ^B (Fig. 5.5 & Fig. 5.6). This suggests that of all the sensor paralogs, RsbR may be integral to stressosome formation. Little is yet known about the relative quantities of Lmo1642, Lmo1842 and Lmo0161 in the cell comparative to RsbR levels, but results suggest that RsbR plays a scaffolding or structural role in the stressosome. A similar role has been suggested for the *B. subtilis* RsbRA as loss of RsbRA, with which RsbR shares highest similarity, abolishes YtvA mediated light-dependent σ^B activity (van der Steen *et al.,* 2012; Heavin & O'Byrne, 2012). In addition, there is some possibility that the deletion of RsbR may have disrupted expression or translation of RsbS or RsbS and RsbT as the *rsbS* start codon is located only 5 base pairs from the *rsbR* stop codon, suggesting that the *rsbS* Shine-Dalgarno sequence, normally located 13-15 base pairs upstream of the start codon, was deleted. This could affect RsbS protein levels. However, loss of RsbS

has been previously shown to increase σ^B activity, so it is doubtful that *rsbS* alone was affected (Kang *et al*., 1996). It is also possible that both RsbS and RsbT translation were affected as RsbR, –S and-T proteins are shown to be co-expressed and translated (Reeves *et al.,* 2010; Zhang *et al*., 2005). Western blotting with anti –RsbS and anti-RsbT antibodies would provide definitive proof as to whether these proteins' levels have been affected in the *ΔrsbR* strain. However, previous findings of an RsbRA-dependent response to light, similar to that reported here for RsbR, provide supporting evidence that the loss of σ^B activity is most likely due to the removal of RsbR rather than RsbS and RsbT (van der Steen *et al*., 2012).

6.4.3 The Lmo0799 protein requires C56 for blue-light sensing function

Experiments with the *lmo0799* C56A strain showed that the light sensing function of Lmo0799 is abolished when the cysteine at position 56 is changed to an alanine, providing genetic evidence for the model of action in which light induces the formation of an adduct between the cysteine and associated flavin mononucleotide (described in Section 3.3.1). The *lmo0799* C56A mutant displayed slightly less growth in the presence of 1.5-2.0 mW cm^{-2} blue light than the *Δlmo0799*, as observed on agar plates (Fig. 3.10A). The presence of the full length protein may have some stabilising effects on the stressosome, and it is possibly related to the finding that *B. subtilis* YtvA acts as a positive regulator of σ^B activity under stress conditions such as salt or ethanol exposure or under energy stress (Akbar *et al*., 2001).

The flexibility of the Lmo0799 LOV domain which allows significant escape of chromophore into the cytoplasm compared with the *B. subtilis* homologue YtvA has led

some to suggest that the Lmo0799 protein has a secondary sensing function, potentially responding to cold or some other stress (Chan *et al*., 2012). Here we found no difference between the WT and the *Δlmo0799* strain's growth or survival in the presence of several different stress conditions, including growth at 4 °C (Fig. 5.1). Despite the knowledge that the presence of NaCl is known to enhance the Lmo0799-dependent light induced σ^B activity (Ondrusch & Kreft, 2011) the cell growth of the *Δlmo0799* strain on BHI with 1 M NaCl was no different from that of the WT (Fig. 5.2). This is not surprising as Ondrusch & Kreft (2011) found little difference between WT EGD-e and *Δlmo0799* strains σ^B-dependent *ctc* expression following exposure to 0.3 M NaCl. Lmo0799 was not shown to contribute to biofilm production under any conditions tested (Fig. 3.10 & Fig. 5.4), supporting the findings of Tiensuu *et al*. (2013), that Lmo0799 does not play a significant role in biofilm production of *L. monocytogenes* EGD-e under light conditions.

6.4.4 Lmo0799 regulation may be influenced by the oxidative stress response

Factors governing Lmo0799 expression have not been fully elucidated but it is interesting that a *B. subtilis* regulator of genes responsible for oxidative stress protection, Spx, induces *ytvA* expression. In *B. subtilis* Spx is regulated by σ^B and PerR (among other factors) (Antelmann *et al.,* 2000; Nakano *et al.,* 2002; Gerth *et al.,* 1998; Leelakriangsak *et al*., 2007). The contribution of the *L. monocytogenes* Spx homologue SpxA, which has been shown to be at least partially under σ^B regulation (Starr, 2010) to *lmo0799* regulation has not yet been investigated. However, inactivation of the glutathione synthetase gene g*shF,* which is predicted to increase the cytoplasmic redox potential (Zuber, 2004) causes induction of *lmo0799* transcription (Ondrusch & Kreft, 2011). Additionally, the presence of hydrogen peroxide increases EGD-e *lmo0799* expression

in a σ^B-independent manner (Tiensuu *et al.,* 2013). Pools of reduced glutathione can contribute to hydrogen peroxide degradation, and, while there is currently no evidence to suggest that changes in glutathione levels are responsible for the hydrogen peroxide-induced increase in transcription of *lmo0799,* upregulation of the blue light sensor gene under these conditions suggests overlap with the oxidative stress response. Cross regulation between the light and oxidative stress response sensory systems would make physiological sense as ROS could be an indicator for blue light stress, or vice versa. Despite a possible link between light sensing and oxidative stress sensing, loss of Lmo0799 did not significantly affect blue light survival under the conditions tested. While Lmo0799 senses blue light, we posit that the increased ROS levels produced under killing intensities of blue light may stimulate σ^B activation via an alternative stress sensor, or more probably, sensors.

6. 5 An RsbV I23T amino acid replacement prevents σ^B activation at 37 °C

The temperature-dependent σ^B activation phenotype associated with the *Δlmo1642* and *Δlmo1842* strains, in which σ^B activity was lost in cultures incubated to stationary phase at 37 °C and reduced compared to WT levels at 30 °C, was traced to a single nucleotide polymorphism in the *rsbV* gene resulting in the replacement of an isoleucine with a threonine residue (Fig. 5.8 & Fig. 6.2). There are multiple possible stages during the construction process where secondary mutations could be introduced, but comparing the *rsbV* gene sequences of WT stock strain and the EGD-e strains transformed with pMAD::*Δlmo1642* and pMAD::*Δlmo1842* used in producing the deletion strains, we

surmised that the mutation event occurred during or before the transformation process. The simplest explanation is that the mutation was introduced during the preparation of WT EGD-e competent cells which were then transformed with the plasmids, instead of the mutation arising independently in two different strains.

The rsbV gene is located in the *sigB* operon (as described in Sections 1.8.2 & 1.8.3) and the RsbV protein is preferentially bound by the RsbW kinase repressor until phosphorylation of RsbV causes RsbW to rebind to σ^B (Benson & Haldenwang, 1993; Dufour & Haldenwang 1994). Both environmental and energy stress signals are relayed through RsbV in the σ^B activation pathway and removal of the *L. monocytogenes* RsbV protein results in an inability to activate the σ^B mediated stress response and virulence regulon (Chaturongakul & Boor, 2004; Utratna *et al*., 2012; Zhang *et al*., 2013). It seems likely that the acid-sensitive and biofilm overproduction phenotypes identified are caused by a failure to activate σ^B appropriately, presumably because the altered RsbV protein behaves differently from the WT protein at 37 ˚C (Fig. 5.12). Somehow, as temperatures increase to 37 °C, the presence of threonine must interfere with the protein structure, either preventing binding to RsbW or RsbU-catalysed dephosphorylation (Dufour & Haldenwang, 1994; Shin *et al*., 2010; Yang *et al*., 1996: Voelker *et al*., 1995).

While removal of RsbV protein is thought to result in a complete lack of σ^B activity (Chaturongakul & Boor, 2004; Chaturongakul & Boor, 2006), on occasion extremely low levels of fluorescence were observed in stationary phase cultures incubated at 37 °C for the RsbV I23T mutant strain carrying the EGFP reporter plasmid. The cause for this fluorescence, indicating RsbV independent activation of σ^B, is unknown. Utratna *et al.* (2014) also reported some RsbV-independent activation of σ^B, using the same reporter system at cold temperatures. However, the level of fluorescence reported by Utratna *et al.* (2014) was much higher than that observed in this study. It is more likely that the RsbV

I23T strain displays extremely low but not abolished RsbW binding activity at 37 °C, allowing some σ^B activity, or that the $P_{lmo2230}$-*egfp* system provides a very low level of 'leaky' constitutive *egfp* expression.

6.5.1 The I23T replacement may prevent RsbW or RsbU interaction with the RsbV protein

The structure of the *L. monocytogenes* RsbV protein has not yet been crystallised but the structure of TM1442, an RsbV homologue in *T. maritima* provides some insights into possible reasons for this loss of σ^B activation in the RsbV I23T variant at 37 °C (Fig. 6.1). The TM1442 protein exists as both a monomer and dimer in solution (Ha *et al*., 2001; Lee *et al*., 2004), and Western blot analyses of *B. subtilis* crude cell fractions isolated both RsbV in monomeric units and RsbV as dimers in tetramer units with RsbW (two dimers) (Dufour & Haldenwang, 1994). It is expected that the *L. monocytogenes* RsbV can move between these two forms and phosphorylation of RsbV is thought to be the impetus that causes dissociation of RsbV dimers (Lee *et al*., 2004). It is possible that replacement of isoleucine 23 with threonine affects the ability of RsbV to interact with RsbW or RsbU.

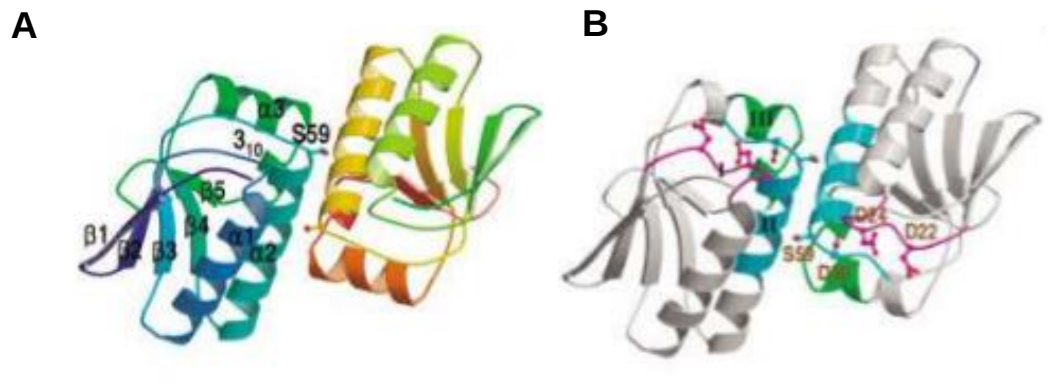

Figure 6.1 Structure of the RsbV homologue TM1442 from *T. maritima.* (**A**) Stereo ribbon diagram of a TM1442 dimer. S59 (equivalent to *L. monocytogenes* RsbV S58) is highlighted. (**B**) Ribbon diagram of a TM1442 dimer showing the conserved regions I (violet) containing the isoleucine residue at position 23, II (blue) and III (green). S59 and three conserved, negatively charged residues (aspartate 22, 24, 58) are labelled. Figures taken from Lee *et al.,* 2004.

Sequence comparison of known RsbV and SpoIIAA (a sporulation-associated factor not present in *L. monocytogenes*) homologues has identified three regions of homology between these proteins (Diederich *et al*., 1994; Schmidt *et al*., 1990; Lee *et al*., 2004) although the third region of consensus identified by Lee *et al*. (2004) does not share much similarity with the corresponding region in *L. monocytogenes* (Fig. 6.2). The second of these regions contains the highly conserved serine residue (S58 in *L. monocytogenes*) which is phosphorylated by RsbW and dephosphorylated by RsbU.

The isoleucine residue replaced by threonine in the RsbV I23T is situated in the first of these regions of homology (GEIDAYT in *L. monocytogenes*) (Fig. 6.2). Analysis of the crystal structure of the RsbV homologue TM1442 by Lee *et al*. (2004) suggests that this region is not likely to directly play a role in dimer formation. Instead the conserved

aspartate and glutamate residues surrounding isoleucine at position 23 and another conserved residue aspartate adjacent to the phosphorylateable serine residue (S58) are proposed to form a negatively charged surface for interaction with either RsbW or RsbU (Fig. 6.1). Replacement of the isoleucine which carries a hydrophobic side chain with threonine which has a polar side-chain may affect the RsbW-RsbV or RsbU-RsbV interactions at 37 °C. An inability to interact with RsbU may indirectly affect dimer formation Western blotting with RsbV antibodies following separation of proteins by size on a non-denaturing SDS-Page gel with proteins would determine whether the ability to form RsbV dimers was compromised in the RsbV I23T strains at 37 °C.

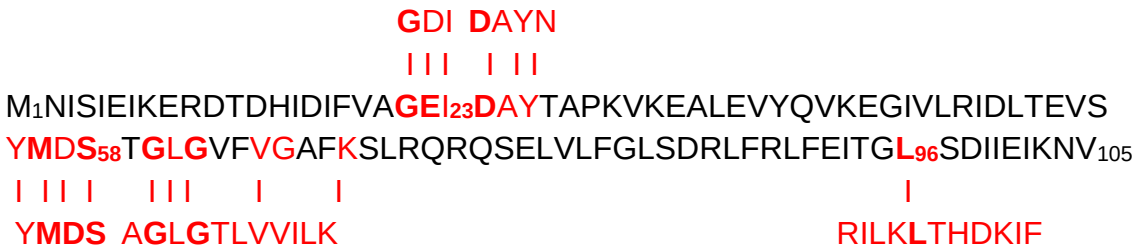

Figure 6.2 *L. monocytogenes* RsbV alignment with conserved consensus sequences. The conserved amino acid regions were identified by Lee *et al.* (2004) through comparison of RsbV and SpoIIA homologue amino acid sequences. Strictly conserved residues are highlighted in bold. The aspartate residue at position 22 in the first consensus sequence region is often replaced by glutamate, as is the case for *L. monocytogenes*. S58 is the residue which is phosphorylated by RsbV and dephosphorylated by RsbU. The isoleucine at position 23 is replaced by a threonine residue in the *rsbV* I23T mutant.

6.6 Conclusions and future perspectives

This study is one of the first to examine the components and contributions of the *L. monocytogenes* stressosome. While a number of novel findings were made, many more questions than answers remain in this interesting area of research. During this study the contributions of the putative components of the stressosome to the σ^B-mediated stress response were tested and new insights were provided into the function of its sensory components. A structural role for the RsbR protein in stressosome formation was identified, with removal of RsbR resulting in abolishment of σ^B activity (Fig. 5.5 & Fig. 5.6). The Lmo0799 protein, which requires a conserved cysteine residue at position 56 for its mechanism of function, was reconfirmed as a blue light sensor, but was found to contribute little to σ^B-mediated light survival (Fig. 3.7, Fig. 3.8, Fig. 3.13). Examining

phenotypic test results, it appears that there may be some redundancy in stress sensing mechanisms offered by the stressosome sensor proteins, as has previously been suggested for components of the *B. subtilis* stressosome (Akbar *et al*., 2001; Reeves *et al*., 2010; van der Steen *et al.,* 2012). Whether each sensor responds to specific individualised stresses has not been disproven, but is possible that the sensors respond to the same signal(s), but with varying sensitivity. The construction of triple or quadruple (with Lmo0799) mutants is recommended to examine the function of the individual sensor proteins under different stress conditions.

Evidence now exists for the presence of the stressosome in *L. monocytogenes* (Cossart, 2016), however, very little is known about what and how signals are interpreted by the stressosome in *B. subtilis* or *L. monocytogenes.* It is known that blue light is directly perceived by the chromophore associated with the LOV domain of Lmo0799 in *L. monocytogenes*, but the forms in which other signals interact with sensors have not been identified. Identification of the form these signals take should be one of the priorities for future research carried out in this field. Among many possibilities, signals could consist of small RNAs, oligopeptides, changes in ion concentration such as in calcium signalling, or products caused by changes in or degradation of the cell membrane (for reviews, see Camilli & Bassler, 2006; Dominguez, 2004; Storz *et al.,* 2011). Furthermore, as assays in this study revealed redundancy in sensing ability among several of the RsbR paralogues, the question remains whether the proteins are capable of sensing the same signals, or whether the proteins respond to different signals generated by the same stress. It is known that the signals which the *L. monocytogenes* RsbR protein intercepts are also present in the *B. subtilis* cell (Martinez *et al*., 2010) and would be interesting to see what effect swapping stressosome sensors between stressosome-containing micro-organisms such as *B. subtilis or L. monocytogenes* would have on the cells' stress

response capacity. This assay could provide an insight into the type of signals which interact with the sensors. Bioinformatics and computational approaches to identify putative small RNA or oligopeptides and their targets could also enable the identification of compounds which interact with the N-terminal regions of stressosome sensors, as could the monitoring of intracellular ion levels in stress-exposed cells.

While the presence of the stressosome in *L. monocytogenes* is now confirmed (Cossart, 2016) research should now consider the composition of the stressosome. In addition to the paucity of knowledge regarding the signals which are perceived by the stressosome, the ratios in which each of the sensors are present within the *L. monocytogenes* stressosome and within the cell are also not yet known. Transcription of the *rsbR* gene is under control of the housekeeping sigma factor, σ^A, and so it might be expected that RsbR levels remain relatively constant in the cell. Additionally, upregulation of *lmo0799* transcripts has been shown to occur in the presence of hydrogen peroxide stress and *lmo0161* transcription shows partial σ^B regulation. If stresses induce alterations to sensor protein levels within the cells, it would be interesting to determine whether this translates to changes in stressosome RsbR paralogue composition under specific stress conditions or whether stressosome composition remains static, regardless of stress or cell conditions. Isolation and testing of the composition of stressosomes prior to and following stress exposure may provide insights into the way stress or its absence affects stressosome composition.

In addition to determining the makeup of the stressosome, one of the key areas for further investigation is determining the types of interaction between RsbR and its paralogues within the stressosome. Research has found that the *B. subtilis* YtvA protein cannot associate with the stressosome in the absence of other RsbR paralogues, which has implications for the Lmo0799 protein (Akbar *et al*., 2001; van der Steen *et al.,* 2012).

Whether each of the *L. monocytogenes* RsbR paralogue proteins can interact with RsbS singly or whether the RsbR-like proteins form hetero-or homodimers is yet to be determined.

Another key area to be addressed is the model for the σ^B-mediated response to stress. As both environmental stresses and energy stresses trigger σ^B activation via the stressosome-led activation cascade, it might be assumed that *L. monocytogenes* σ^B activity occurs in a single pulse as described for *B. subtilis* σ^B activity under environmental stress conditions (Section 1.8.1). Research is required to determine whether this model is an accurate representation of σ^B activity in *L. monocytogenes* or is specific to *B. subtilis*.

A spontaneous mutation in the *rsbV* gene sequence caused the replacement of an isoleucine with a threonine residue in a conserved region and resulted in the generation of a strain which displayed a temperature-dependent inability to activate σ^B at 37 °C (Fig. 5.12). It is interesting that this single base pair mutation arose in an area of significant conservation required for activation of the stress response regulon. Several instances in which secondary mutations have arisen in *L. monocytogenes* mutant strains' *sigB* operon have been reported (Quereda *et al*., 2013; J. Johansson, personal communication). The importance of sequencing the *sigB* operon following the construction of new mutant strains is highlighted by this study.

The σ^B regulon is the largest stress response regulon in *L. monocytogenes* and overlaps with several other regulatory systems (Section 1.4). Not only was σ^B activity observed to be increased in stationary phase cultures incubated at the lower temperature tested (30 °C) but the protein was shown to contribute less significantly to acid survival at this temperature compared with 37 °C (Fig. 5.6 & Fig. 5.7). Unsurprisingly, removal of the

ability to activate this regulon resulted in enhanced growth under mild stress conditions (Fig. 4.8, Fig. 4.9, Fig. 5.2). Alterations that prevent activation of the σ^B regulon have been found to be advantageous in other environments where virulence activities are not required (Franciosa *et al.,* 2009; Chaturongakul & Boor, 2004). These findings might suggest that there is a selective pressure in *L. monocytogenes* to reduce the burden of σ^B activation in different environments through mutation of σ^B or its regulators. Certainly, examination of the frequency of *sigB* operon or regulon mutations among populations subjected to different environments may provide interesting information for sectors where *L. monocytogenes* contamination is a concern. Visible light inactivation methods show great promise as widespread, cheap and effective means of decontamination of surfaces and other materials. However, the probability of the generation of resistant mutants should be considered closely as should the possibility of light-induced virulence priming resulting in lowered infectious dose cell numbers.

Bibliography

Abram, F., Starr, E., Karatzas, K.A.G., Matlawska-Wasowska, K., Boyd, A., Wiedmann, M., Boor, K.J., Connally, D., and O'Byrne, C.P. (2008) Identification of components of the sigma B regulon in *Listeria monocytogenes* that contribute to acid and salt tolerance. *Appl Environ Microbiol* **74**: 6848–6858.

Abram, F., Wan-Lin, S., Wiedmann, M., Boor, K.J., Coote, P., Botting, C., Karatzas, K.A.G., and O'Byrne, C.P. (2008a) Proteomic analyses of a *Listeria monocytogenes* mutant lacking σ^B identify new components of the σ^B regulon and highlight a role for σ^B in the utilization of glycerol. *Appl Environ Microbiol* **74**: 594–604.

Akbar, S., Gaidenko, T.A., Kang, C.M., O'Reilly, M., Devine, K.M., and Price, C.W. (2001) New family of regulators in the environmental signaling pathway which activates the general stress transcription factor σ^B of *Bacillus subtilis*. *J Bacteriol* **183**: 1329–1338.

Akbar, S., Kang, C.M., Gaidenko, T.A, and Price, C.W. (1997) Modulator protein RsbR regulates environmental signalling in the general stress pathway of *Bacillus subtilis*. *Mol Microbiol* **24**: 567–578.

Alonso, A.N., Perry, K.J., Regeimbal, J.M., Regan, P.M., and Higgins, D.E. (2014) Identification of *Listeria monocytogenes* determinants required for biofilm formation. *PLoS One* **9**: 1–16.

Amezaga, M.-R., Davidson, I., McLaggan, D., Verheul, A., Abee, T., and Booth, I.R. (1995) The role of peptide metabolism in the growth of *Listeria monocytogenes* ATCC 23074 at high osmolarity. *Microbiology* **141**: 41–49.

Andrady, A.L., Hamid, S.H., Hu, X., and Torikai, A. (1998) Effects of increased solar ultraviolet radiation on materials. *J Photochem Photobiol* **46**: 96–103.

Antelmann, H., Scharf, C., and Hecker, M. (2000) Phosphate starvation-inducible proteins of *Bacillus subtilis* : proteomics and transcriptional analysis. *J Bacteriol* **182**: 4478–4490.

Aravind, L., and Koonin, E.V. (2000) The STAS domain — a link between anion antagonists. *Curr Biol* 53–55.

Arnaud, M., Chastanet, A., and Débarbouillé, M. (2004) New vector for efficient allelic replacement in naturally nontransformable, low-GC-content, Gram-positive bacteria. **70**: 6887–6891.

Avila-Pérez, M., Hellingwerf, K.J., and Kort, R. (2006) Blue light activates the sigmaB-dependent stress response of *Bacillus subtilis* via YtvA. *J Bacteriol* **188**: 6411–4

Avila-Pérez, M., van der Steen, J.B., Kort, R., and Hellingwerf, K.J. (2010) Red light activates the σ^B-mediated general stress response of *Bacillus subtilis* via the energy branch of the upstream signaling cascade. *J Bacteriol* **192**: 755–762.

Avila-Pérez, M., Vreede, J., Tang, Y., Bende, O., Losi, A., Gärtner, W., and Hellingwerf, K. (2009) *In vivo* mutational analysis of YtvA from *Bacillus subtilis*: mechanism of light activation of the general stress response. *J Biol Chem* **284**: 24958–24964.

Becker, L.A, Çetin, M.S., Hutkins, R.W., and Benson, A.K. (1998) Identification of the gene encoding the alternative sigma factor σ^B from *Listeria monocytogenes* and its role in osmotolerance. *J Bacteriol* **180**: 4547–4554.

Begley, M., Hill, C., and Ross, R.P. (2006) Tolerance of *Listeria monocytogenes* to cell envelope-acting antimicrobial agents is dependent on SigB. *Appl Environ Microbiol* **72**: 2231–2234.

Begley, M., Kerr, C., and Hill, C. (2009) Exposure to bile influences biofilm formation by *Listeria monocytogenes*. *Gut Pathog* **1**: 11.

Benson, A.K. and, and Haldenwang, W.G. (1993) *Bacillus subtilis* σ^B is regulated by a binding protein (RsbW) that blocks its association with core RNA polymerase. *ProcNatl Acad Sci USA* **90**: 2330–2334.

Bergholz, T.M., Bowen, B., Wiedmann, M., and Boor, K.J. (2012) *Listeria monocytogenes* shows temperature-dependent and-independent responses to salt stress, including responses that induce cross-protection against other stresses. *Appl Environ Microbiol* **78**: 2602–2612.

Bertsch, D., Rau, J., Eugster, M.R., Haug, M.C., Lawson, P.A., Lacroix, C., and Meile, L. (2013) *Listeria fleischmannii* sp. nov., isolated from cheese. *Int J Syst Evol Microbiol* **63**: 526–532.

Bierne, H., Sabet, C., Personnic, N., and Cossart, P. (2007) Internalins: a complex family of leucine-rich repeat-containing proteins in *Listeria monocytogenes*. *Microbes Infect* **9**: 1156–1166.

Boerlin, P., Rocourt, J., and Piffaretti, J.C. (1991) Taxonomy of the genus *Listeria* by using multilocus enzyme electrophoresis. *Int J Syst Bacteriol* 41: 59–64.

Boura, M., Keating, C., Royet, K., Paudyal, R., O'Donoghue, B., O'Byrne, C.P., and Karatzas, K.A.G. (2016) Loss of SigB in *Listeria monocytogenes* strains EGD-e and 10403S confers hyperresistance to hydrogen peroxide in stationary phase under aerobic conditions.*Appl Environ Microbiol* 82: AEM.00709–16.

Bowman, J.P., Hages, E., Nilsson, R.E., Kocharunchitt, C., and Ross, T. (2012) Investigation of the *Listeria monocytogenes* Scott A acid tolerance response and associated physiological and phenotypic features via whole proteome analysis. *J Proteome Res* **11**: 2409–2426.

Brauge, T., Sadovskaya, I., Faille, C., Benezech, T., Maes, E., Guerardel, Y., and Midelet-Bourdin, G. (2016) Teichoic acid is the major polysaccharide present in the *Listeria monocytogenes* biofilm matrix. *FEMS Microbiol Lett* **363**

Brody, M.S., Vijay, K., and Price, C.W. (2001) Catalytic function of an α / β Hydrolase Is required for energy stress activation of the σ^B transcription factor in *Bacillus subtilis*. *J Bacteriol* **183**: 6422–6428.

Buchovec, I., Paskeviciute, E., and Luksiene, Z. (2010) Photosensitization-based inactivation of food pathogen *Listeria monocytogenes in vitro* and on the surface of packaging material. *J Photochem Photobiol* **99**: 9–14.

Budde, B.B., and Jakobsen, M. (2000) Real-Time measurements of the interaction between single cells of *Listeria monocytogenes* and nisin on a solid surface. *Appl Environ Microbiol* **66**: 3586–3591.

Buttani, V., Losi, A., Polverini, E., and Gärtner, W. (2006) Blue news: NTP binding properties of the blue-light sensitive YtvA protein from *Bacillus subtilis*. *FEBS Lett* **580**: 3818–3822.

Cabeça, T.K., Pizzolitto, A.C., and Pizzolitto, E.L. (2012) Activity of disinfectants against foodborne pathogens in suspension and adhered to stainless steel surfaces. *Brazilian J Microbiol* **43**: 1112–1119.

Cabiscol, E., Tamarit, J., and Ros, J. (2000) Oxidative stress in bacteria and protein damage by reactive oxygen species. *Internatl Microbiol* **3**: 3–8.

Camilli, A., and Bassler, B.L. (2006) Bacterial small-molecule signaling pathways. *Science* **311**: 1113–1116.

Chakraborty, T., Leimeister-Wächter, M., Domann, E., Hartl, M., Goebel, W., Nichterlein, T., and Notermans, S. (1992) Coordinate regulation of virulence genes in *Listeria monocytogenes* requires the product of the *prfA* gene. *J Bacteriol* **174**: 568–574.

Chan, R.H., Lewis, J.W., and Bogomolni, R.A. (2012) Photocycle of the LOV-STAS protein from the pathogen *Listeria monocytogenes*. *Photochem Photobiol* **89**: 361–369.

Chan, Y.C., Boor, K.J., and Wiedmann, M. (2007) σ^B-dependent and σ^B-independent mechanisms contribute to transcription of *Listeria monocytogenes* cold stress genes during cold shock and cold growth. *Appl Environ Microbiol* **73**: 6019–6029.

Chatterjee, S.S., Hossain, H., Otten, S., Kuenne, C., Kuchmina, K., Machata, S., Domann, E., Chakraborty, T., and Hain, T. (2006) Intracellular gene expression profile of *Listeria monocytogenes*. *Infect Immun* **74**: 1323–1338.

Chaturongakul, S., and Boor, K.J. (2004) RsbT and RsbV contribute to σ^B-dependent survival under environmental , energy, and intracellular stress conditions in *Listeria monocytogenes*. *Appl Environ Microbiol* **70**: 5349–5356.

Chaturongakul, S., and Boor, K.J. (2006) σ^B activation under environmental and energy stress conditions in *Listeria monocytogenes*. *Appl Environ Microbiol* **72**: 5197–203.

Chaturongakul, S., Raengpradub, S., Palmer, M.E., Bergholz, T.M., Orsi, R.H., Hu, Y., Ollinger, J., Wiedmann, M., and. Boor, K.J. (2011) Transcriptomic and phenotypic analyses identify coregulated, overlapping regulons among PrfA, CtsR, HrcA, and the alternative sigma factors σ^B σ^C, σ^H, and σ^L in *Listeria monocytogenes*. *Appl Environ Microbiol* **77**: 187–200.

Chaturongakul, S., Raengpradub, S., Wiedmann, M., and Boor, K.J. (2008) Modulation of stress and virulence in *Listeria monocytogenes*. *Trends Microbiol* **16**: 388–396.

Chavant, P., Martinie, B., Meylheuc, T., Bellon-Fontaine, M.-N., and Hebraud, M. (2002) *Listeria monocytogenes* LO28: surface physicochemical properties and ability to form biofilms at different temperatures and growth phases. *Appl Env Microbiol* **68**: 728–737.

Chen, C., Yudkin, M.D., and Delumeau, O. (2004) Phosphorylation and RsbX-dependent dephosphorylation of RsbR in the RsbR-RsbS complex of *Bacillus subtilis*. *J Bacteriol* **186**: 6830– 6836.

Chen, C.-C., Lewis, R.J., Harris, R., Yudkin, M.D., and Delumeau, O. (2003) A supramolecular complex in the environmental stress signalling pathway of *Bacillus subtilis*. *Mol Microbiol* **49**: 1657–1669

Cheng, Y., Promadej, N., Kim, J.W., and Kathariou, S. (2008) Teichoic acid glycosylation mediated by *gtcA* is required for phage adsorption and susceptibility of *Listeria monocytogenes* serotype 4b. *Appl Environ Microbiol* **74**: 1653–1655.

Christie, J.M., Salomon, M., Nozue, K., Wada, M., and Briggs, W.R. (1999) LOV (light, oxygen, or voltage) domains of the blue-light photoreceptor phototropin (nph1): Binding sites for the chromophore flavin mononucleotide. *Proc Natl Acad Sci* **96**: 8779–8783

Cole, M.B., Jones, M. V., and Holyoak, C. The effect of pH, salt concentration and temperature on the survival and growth of *Listeria monocytogenes*. *J Appl Bacteriol* **69**: 63–72

Corr, S., Hill, C., and Gahan, C.G.M. (2006) An *in vitro* cell-culture model demonstrates internalin- and hemolysin-independent translocation of *Listeria monocytogenes* across M cells. *Microb Pathog* **41**: 241–250.

Cossart, P. (2016) *Listeria monocytogenes*: Latest stories. In *EMBO Conference: Problems of Listeriosis ISOPOL XIX*. Paris.

Cossart, P. (2011) Illuminating the landscape of host-pathogen interactions with the bacterium *Listeria monocytogenes*. *Proc Natl Acad Sci U S A* **108**: 19484–19491.

Costerton, J.W., Lewandowski, Z., Caldwell, D.E., Korber, D.R., and Lappin-Scott, H.M. (1995) Microbial biofilms. *Annu Rev Microbiol* **49**: 711–745.

Cotter, P.D., Gahan, C.G.M., and Hill, C. (2001) A glutamate decarboxylase system protects *Listeria monocytogenes* in gastric fluid. *Mol Microbiol* **40**: 465–475.

Cox LJ, Kleiss T, Cordier JL, Cordellana C, Konkel P, Pedrazzini C, *et al.* (1989) *Listeria* spp. in food processing, non-food and domestic environments. *Food Microbiol* **6**: 49–61.

Crosson, S., and Moffat, K. (2001) Structure of a flavin-binding plant photoreceptor domain: Insights into light-mediated signal transduction. *Proc Natl Acad Sci U S A* **98**: 2995–3000.

Crosson, S., Rajagopal, S., and Moffat, K. (2003) Current Topics: The LOV domain family: Photoresponsive signaling modules coupled to diverse output domains. *Biochemistry* **42**: 2–10.

Cunin, R., Glansdorff, N., Piérard, A., and Stalon, V. (1986) Biosynthesis and metabolism of arginine in bacteria. *Microbiol Rev* **50**: 314–352.

Da Silva, E.P., and de Martinis, E.C.P. (2013) Current knowledge and perspectives on biofilm formation: The case of *Listeria monocytogenes*. *Appl Microbiol Biotechnol* **97**: 957–968.

Davis, M.J., Coote, P.J., and O'Byrne, C.P. (1996) Acid tolerance in *Listeria monocytogenes*: The adaptive acid tolerance response (ATR) and growth-phase-dependent acid resistance. *Microbiology* **142**: 2975–2982.

Delumeau, O., Chen, C.-C., Murray, J.W., Yudkin, M.D., and Lewis, R.J. (2006) High-molecular-weight complexes of RsbR and paralogues in the environmental signaling pathway of *Bacillus subtilis*. *J Bacteriol* **188**: 7885–7892.

Delumeau, O., Dutta, S., Brigulla, M., Kuhnke, G., Hardwick, S.W., Völker, U., Yudkin, M.D., and Lewis, R.J. (2004) Functional and structural characterization of RsbU, a stress signaling protein phosphatase 2C. *J Biol Chem* **279**: 40927–40937.

den Bakker, H.C., Warchocki, S., Wright, E.M., Allred, A.F., Ahlstrom, C., Manuel, C.S. Stasiewicz, M.J., Burrell, A., Roof, S., Strawn, L.K., Fortes, E., Nightingale, K.K., Kephart, D., and Wiedmann, M. (2014) *Listeria floridensis* sp. nov., *Listeria aquatica* sp. nov., *Listeria cornellensis* sp. nov., *Listeria riparia* sp. nov. and *Listeria grandensis* sp. nov., from agricultural and natural environments. *Int J Syst Evol Microbiol* **64**: 1882–1889.

Diederich, D., Wilkinson, J.F., Magnin, T., Najafi, S.M. a, Errington, J., and Yudkin, M.D. (1994) Role of interactions between SpoIIAA and SpoIIAB in regulating cell-type transcription factor σ^F in *Bacillus subtilis*. *Genes Dev* **3**: 141–149.

Disson, O., and Lecuit, M. (2013) *In vitro* and *in vivo* models to study human listeriosis: Mind the gap. *Microbes Infect* **15**: 971–980.

Dominguez, D.C. (2004) Calcium signalling in bacteria. *Mol Microbiol* **54**: 291–297.

Dramsi, S., Kocks, C., Forestier, C., and Cossart, P. (1993) Internalin-mediated invasion of epithelial-cells by *Listeria-monocytogenes* is regulated by the bacterial-growth state, temperature and the pleiotropic activator *prfA*. *Mol Microbiol* **9**: 931–941.

Dufour, A., and Haldenwang, W.G. (1994) Interactions between a *Bacillus subtilis* anti-sigma factor (RsbW) and its antagonist (RsbV). *J Bacteriol* **176**: 1813–1820.

Dussurget, O., Cabanes, D., Dehoux, P., Lecuit, M., Buchrieser, C., Glaser, P., and Cossart, P. (2002) *Listeria monocytogenes* bile salt hydrolase is a PrfA-regulated virulence factor involved in the intestinal and hepatic phases of listeriosis. *Mol Microbiol* **45**: 1095–1106.

EFSA (2015) The European Union summary report on trends and sources of zoonoses, zoonotic agents and food-borne outbreaks in 2014. *EFSA J* **13**.

EFSA and ECDC (2015) The European Union summary report on trends and sources of zoonoses, zoonotic agents and food-borne outbreaks in 2013. *EFSA J* **13**.

Elasri, M.O., and Miller, R. V. (1999) Study of the response of a biofilm bacterial community to UV radiation. *Appl Environ Microbiol* **65**: 2025–2031.

Endarko, E., Maclean, M., Timoshkin, I. V., MacGregor, S.J., and Anderson, J.G. (2012) High-intensity 405 nm light inactivation of *Listeria monocytogenes*. *Photochem Photobiol* **88**: 1280–1286.

Eymann, C., Becher, D., Bernhardt, J., Gronau, K., Klutzny, A., and Hecker, M. (2007) Dynamics of protein phosphorylation on Ser/Thr/Tyr in *Bacillus subtilis*. *Proteomics* **7**: 3509–3526.

Eymann, C., Schulz, S., Gronau, K., Becher, D., Hecker, M., and Price, C.W. (2011) *In vivo* phosphorylation patterns of key stressosome proteins define a second feedback loop that limits activation of *Bacillus subtilis* σ^B. *Mol Microbiol* **80**: 798–810.

Fang, W., Siegumfeldt, H., Budde, B.B., and Jakobsen, M. (2004) Osmotic stress leads to decreased intracellular pH of *Listeria monocytogenes* as determined by fluorescence ratio-imaging microscopy. *Appl Environ Microbiol* **70**: 3176–3179.

Farber, J.M., and Peterkin, P.I. (1991) *Listeria monocytogenes*, a food-borne pathogen. *Microbiol Rev* **55**: 476-511.

Faulkner, M.J., and Helmann, J.D. (2011) Peroxide stress elicits adaptive changes in bacterial metal ion homeostasis. *Antioxid Redox Signal* **15**: 175–189.

Feehily, C. (2014) Elucidation of the role of the glutamate decarboxylase system and the γ -aminobutyric acid shunt pathway in the stress response of *Listeria monocytogenes*. (Unpublishd doctoral thesis). National University of Ireland, Galway, Galway, Ireland.

Feehily, C., Finnerty, A., Casey, P.G., Hill, C., Gahan, C.G.M., O'Byrne, C.P., and Karatzas, K.A.G. (2014) Divergent evolution of the activity and regulation of the

glutamate decarboxylase systems in *Listeria monocytogenes* EGD-e and 10403S: Roles in virulence and acid tolerance. *PLoS One* **9**: 1–12.

Ferreira, A., Gray, M., Wiedmann, M., and Boor, K.J. (2004) Comparative genomic analysis of the *sigB* operon in *Listeria monocytogenes* and in other Gram-positive bacteria. *Curr Microbiol* **48**: 39–46.

Ferreira, A., O'Byrne, C.P., and Boor, K.J. (2001) Role of σ^B in heat, ethanol, acid, and oxidative stress resistance and during carbon starvation in *Listeria monocytogenes*. *Appl Environ Microbiol* **67**: 4454–4457.

Ferreira, A., Sue, D., O'Byrne, C.P., and Boor, K.J. (2003) Role of *Listeria monocytogenes* σ^B in survival of lethal acidic conditions and in the acquired acid tolerance response. *Appl Environ Microbiol* **69**: 2692–2698.

Feuerstein, O., Ginsburg, I., Dayan, E., and Veler, D. (2005) Mechanism of Visible Light Phototoxicity on *Porphyromonas gingivalis* and *Fusobacferium nucleatum. Photochem Photobiol* **81**: 186–189.

Feuerstein, O., Persman, N., and Weiss, E.I. (2004) Phototoxic effect of visible light on *Porphyromonas gingivalis* and *Fusobacterium nucleatum*: An *in vitro* study. *Photochem Photobiol* **80**: 412–415.

Franciosa, G., Maugliani, A., Scalfaro, C., Floridi, F., and Aureli, P. (2009) Expression of internalin A and biofilm formation among *Listeria monocytogenes* clinical isolates. *Int J Immunopathol Pharmacol* **22**: 183–193.

Fraser, K.R.,Sue, D., Wiedmann, M., Boor, K., and O'Byrne, C.P. (2003) Role of σ^B in regulating the compatible solute uptake systems of *Listeria monocytogenes*: Osmotic induction of *opuC* is σ^B dependent. *Appl Environ Microbiol* **69**: 2015–2022.

Freitag, N.E., Rong, L., and Portnoy, D.A. (1993) Regulation of the *prfA* transcriptional activator of *Listeria monocytogenes*: multiple promoter elements contribute to intracellular growth and cell-to-cell spread. *Infect Immun* **61**: 2537–44

Gábor F., Szocs K., Maillard P., and Csík, G. (2001). Photobiological activity of exogenous and endogenous porphyrin derivatives in *Escherichia coli* and *Enterococcus hirae* cells. Radiat Environ Biophys 40:145–151.

Gahan, C.G., and Hill, C. (2014) *Listeria monocytogenes*: survival and adaptation in the gastrointestinal tract. *Front Cell Infect Microbiol* **4**: 1-7.

Gaidenko, T.A., Kim, T.-J., Weigel, A.L., Brody, M.S., and Price, C.W. (2006) The blue-light receptor YtvA acts in the environmental stress signaling pathway of *Bacillus subtilis*. *J Bacteriol* **188**: 6387–6395.

Gaidenko, T. A, and Price, C.W. (2014) Genetic evidence for a phosphorylation-independent signal transduction mechanism within the *Bacillus subtilis* stressosome. *PLoS One* **9**: e90741.

Gaidenko, T. A, Yang, X., Lee, Y.M., and Price, C.W. (1999) Threonine phosphorylation of modulator protein RsbR governs its ability to regulate a serine kinase in the environmental stress signaling pathway of *Bacillus subtilis*. *J Mol Biol* **288**: 29–39.

Gardan, R., Duché, O., Leroy-Sétrin, S., and Labadie, J. (2003) Role of ctc from *Listeria monocytogenes* in osmotolerance. *Appl Environ Microbiol* **69**: 154–161.

Garner, M.R., Njaa, B.L., Wiedmann, M., and Boor, K.J. (2006) Sigma B contributes to *Listeria monocytogenes* gastrointestinal infection but not to systemic spread in the guinea pig infection model. *Inf Infect Immun* **74**: 876– 886.

Gerth, U., Krüger, E., Derré, I., Msadek, T., and Hecker, M. (1998) Stress induction of the *Bacillus subtilis clpP* gene encoding a homologue of the proteolytic component of the Clp protease and the involvement of ClpP and ClpX in stress tolerance. *Mol Microbiol* **28**: 787–802.

Glaser, P., Frangeul, L., Buchrieser, C., Rusniok, C., Amend, a, Baquero, F., *et al.* (2001) Comparative genomics of *Listeria* species. *Science* **294**: 849–852.

Glantz, S.T., Carpenter, E.J., Melkonian,M., Gardner, K.H.,. Boyden, E.S., Wong, G.K.-S., and Chow, B.Y. (2016) Functional and topological diversity of LOV domain photoreceptors. *Proc Natl Acad Sci* E1442–E1451.

Godshall, C.E., Suh, G., and Lorber, B. (2013) Cutaneous listeriosis. *J Clin Microbiol* **51**: 3591–3596.

Golic, A., Vaneechoutte, M., Nemec, A., Viale, A.M., Actis, L.A., and Mussi, M.A. (2013) Staring at the cold sun: blue light regulation is distributed within the genus *Acinetobacter*. *PLoS One* **8** e55059.

Gomelsky, M., and Hoff, W.D. (2011) Light helps bacteria make important lifestyle decisions. *Trends Microbiol* **19**: 441–448.

González-Flecha, B., and Demple, B. (1995) Metabolic sources of hydrogen peroxide in aerobically growing *Escherichia coli*. *J Biol Chem* **270**: 13681–13687.

Graves, L.M., Helsel, L.O., Steigerwalt, A.G., Morey, R.E., Daneshvar, M.I., Roof, S.E., *et al.* (2010) *Listeria marthii* sp. nov., isolated from the natural environment, Finger Lakes National Forest. *Int J Syst Evol Microbiol* **60**: 1280–1288.

Guilbaud, M., Piveteau, P., Desvaux, M., Brisse, S., and Briandet, R. (2015) Exploring the diversity of *Listeria monocytogenes* biofilm architecture by high-throughput confocal laser scanning microscopy and the predominance of the honeycomb-like morphotype. *Appl Environ Microbiol* **81**: 1813–1819.

Guldimann, C., Boor, K.J., Wiedmann, M., and Guariglia-Oropeza, V. (2016) Resilience in the face of uncertainty: Sigma factor B fine-tunes gene expression to support homeostasis in Gram-positive bacteria. *Appl Environ Microbiol* **82**: 4456–4469.

Ha, K.S., Kwak, J.E., Han, B.W., Lee, J.Y., Moon, J., Lee, B.I, and Suh, S.W. (2001) Crystallization and preliminary x-ray crystallographic analysis of the TM1442 gene product from *Thermotoga maritima*, a homologue of *Bacillus subtilis* anti-anti-sigma factors. *Biol Crystallogr* **57**: 276–278.

Hain, T., Hossain, H., Chatterjee, S.S., Machata, S., Volk, U., Wagner, S., *et al.* (2008) Temporal transcriptomic analysis of the *Listeria monocytogenes* EGD-e sigmaB regulon. *BMC Microbiol* **8**: 20.

Hamblin, M.R., and Hasan, T. (2014) Photodymamic therapy: a new antimicrobial approach to infectious disease? *Photochem Photobiol Sci* **3**: 436–50

Hamon, M., Bierne, H., and Cossart, P. (2006) *Listeria monocytogenes*: a multifaceted model. *Nat Rev Microbiol* **4**: 423–434.

Hardwick, S.W., Pané-Farré, J., Delumeau, O., Marles-Wright, J., Murray, J.W., Hecker, M., and Lewis, R.J. (2007) Structural and functional characterization of partner switching regulating the environmental stress response in *Bacillus subtilis*. *J Biol Chem* **282**: 11562–11572.

Hardy, J., Francis, K.P., DeBoer, M., Chu, P., Gibbs, K., and Contag, C.H. (2004) Extracellular replication of *Listeria monocytogenes* in the murine gall bladder. *Science* **303**: 851–3

Harmsen, M., Lappann, M., Knøchel, S., and Molin, S. (2010) Role of extracellular DNA during biofilm formation by *Listeria monocytogenes*. *Appl Environ Microbiol* **76**: 2271–2279.

Harper, S.M., Neil, L.C., and Gardner, K.H. (2003) Structural basis of a phototropin light switch. *Science* **301**: 1541–1544.

Harvey, J., Keenan, K.P., and Gilmour, A. (2007) Assessing biofilm formation by *Listeria monocytogenes* strains. *Food Microbiol* **24**: 380–392.

Heavin, S., and O'Byrne, C.P. (2012) Post-genomic insights into the regulation of transcription in the facultative intracellular pathogen *Listeria monocytognes*. In *Stress Response of Foodborne Microorganisms*. Wong, H. (ed.). Nova Science Publishers. .

Hecker, M., Pané-Farré, J., and Völker, U. (2007) SigB-dependent general stress response in *Bacillus subtilis* and related Gram-positive bacteria. *Annu Rev Microbiol* **61**: 215–236. .

Helmann, J.D., Wu, M.F.W., Gaballa, A., Kobel, P. A, Morshedi, M.M., Fawcett, P., and Paddon, C. (2003) The global transcriptional response of *Bacillus subtilis* to peroxide stress is coordinated by three transcription factors. *J Bacteriol* **185**: 243–253.

Herrou, J., and Crosson, S. (2011) Function, structure and mechanism of bacterial photosensory LOV proteins. *Nat Rev Microbiol* **9**: 713–723.

Horton, R.M., Cai, Z., Ho, S.N., and Pease, L.R. (1990) Gene splicing by overlap extension: Tailor-made genes using the polymerase chain reaction. *Biotechniques* **54**: 528–535.

Huala, E., Oeller, P.W., Liscum, E., Han, I.-S., Larsen, E., and Briggs, W.R. (1997) Arabidopsis NPH1: A protein kinase with a putative redox-sensing domain. *Science* **278**: 2120–2123.

Ivy, R. A., Chan, Y.C., Bowen, B.M., Boor, K.J., and Wiedmann, M. (2010) Growth temperature-dependent contributions of response regulators, σ^B, PrfA, and motility factors to *Listeria monocytogenes* Invasion of Caco-2 cells. *Foodborne Pathog Dis* **7**: 1337–1349.

Ivy, R. A., Wiedmann, M., and Boor, K.J. (2012) *Listeria monocytogenes* grown at 7 °C shows reduced acid survival and an altered transcriptional response to acid shock compared to *L. monocytogenes* grown at 37 °C. *Appl Environ Microbiol* **78**: 3824–3836.

Jacquet, C., Doumith, M., Gordon, J.I., Martin, P.M. V, Cossart, P., and Lecuit, M. (2004) A molecular marker for evaluating the pathogenic potential of foodborne *Listeria monocytogenes*. *J Infect Dis* **189**: 2094–2100.

Jurk, M., Dorn, M., Kikhney, A., Svergun, D., Gärtner, W., and Schmieder, P. (2010) The switch that does not flip: The blue-light receptor YtvA from *Bacillus subtilis* adopts an elongated dimer conformation independent of the activation state as revealed by a combined AUC and SAXS study. *J Mol Biol* **403**: 78–87.

Jurk, M., Schramm, P., and Schmieder, P. (2013) The blue-light receptor YtvA from *Bacillus subtilis* is permanently incorporated into the stressosome independent of the illumination state. *Biochem Biophys Res Commun* **432**: 499–503.

Kalman, S., Duncan, M.L., Thomas, S.M., and Price, C.W. (1990) Similar organization of the *sigB* and *spoIIA* operons encoding alternate sigma factors of *Bacillus subtilis* RNA polymerase. *J Bacteriol* **172**: 5575–5585.

Kamp, H.D., and Higgins, D.E. (2011) A protein thermometer controls temperature-dependent transcription of flagellar motility genes in *Listeria monocytogenes*. *PLoS Pathog* **7**: e1002153.

Kaneko, T., Tanaka, N., and Kumasaka, T. (2005) Crystal structures of RsbQ, a stress-response regulator in *Bacillus subtilis*. *Protein Sci* **14**: 558–565.

Kang, C.M., Brody, M.S., Akbar, S., Yang, X., and Price, C.W. (1996) Homologous pairs of regulatory proteins control activity of *Bacillus subtilis* transcription factor σ^B in response to environmental stress. *J Bacteriol* **178**: 3846–3853.

Karniol, B., Wagner, J.R., Walker, J.M., and Vierstra, R.D. (2005) Phylogenetic analysis of the phytochrome superfamily reveals distinct microbial subfamilies of photoreceptors. *Biochem J* **392**: 103–116.

Kazmierczak, M.J., Mithoe, S.C., Boor, K.J., and Wiedmann, M. (2003) *Listeria monocytogenes* σ^B regulates stress response and virulence functions *J Bacteriol* **185**. 5722-5734.

Kazmierczak, M.J., Wiedmann, M., and Boor, K.J. (2006) Contributions of *Listeria monocytogenes* σ^B and PrfA to expression of virulence and stress response genes during extra- and intracellular growth. *Microbiology* **152**: 1827–1838.

Kennedy, J.C., Pottier, R.H., and Pross, D.C. (1990) Photodynamic therapy with endogenous protoporphyrin. IX: Basic principles and present clinical experience. *J Photochem Photobiol* **6**: 143–148.

Kim, H., Marquis, H., and Boor, K.J. (2005) σ^B contributes to *Listeria monocytogenes* invasion by controlling expression of *inlA* and *inlB*. *Microbiology* **151**: 3215–3222.

Kim, T., Gaidenko, T.A., and Price, C.W. (2004) *In vivo* phosphorylation of partner switching regulators correlates with stress transmission in the environmental signaling pathway of *Bacillus subtilis* **186**: 1624-1632.

Kim, T.-J., Gaidenko, T. A, and Price, C.W. (2004a) A multicomponent protein complex mediates environmental stress signaling in *Bacillus subtilis*. *J Mol Biol* **341**: 135–150.

King, T., Seeto, S., and Ferenci, T. (2006) Genotype-by-environment interactions influencing the emergence of rpoS mutations in *Escherichia coli* populations. *Genetics* **172**: 2071–2079.

Köseoğlu, V.K., Heiss, C., Azadi, P., Topchiy, E., Güvener, Z.T., Lehmann, T.E., Miller K.W., and Gomelsky, M. (2015) *Listeria monocytogenes* exopolysaccharide: Origin,

structure, biosynthetic machinery and c-di-GMP-dependent regulation. *Mol Microbiol* **96**: 728–743.

Kumar, A., Ghate, V., Kim, M.-J., Zhou, W., Khoo, G.H., and Yuk, H.-G. (2015) Kinetics of bacterial inactivation by 405nm and 520nm light emitting diodes and the role of endogenous coproporphyrin on bacterial susceptibility. *J Photochem Photobiol B* **149**: 37–44.

Kütting, B., and Drexler, H. (2010) UV-induced skin cancer at workplace and evidence-based prevention. *Int Arch Occup Environ Health* **83**: 843–854.

Lang Halter, E., Neuhaus, K., and Scherer, S. (2013) *Listeria weihenstephanensis* sp. nov., isolated from the water plant *Lemna trisulca* taken from a freshwater pond. *Int J Syst Evol Microbiol* **63**: 641–647.

Leclercq, A., Clermont, D., Bizet, C., Grimont, P. A.D., Le Flèche-Matéos, A., Roche, S.M., Buchrieser, C., Cadet-Daniel, V., Le Monnier,A., Lecuit, M., and Allerberger, F. (2010) *Listeria rocourtiae* sp. nov. *Int J Syst Evol Microbiol* **60**: 2210–2214.

Lecuit, M., Nelson, D.M., Smith, S.D., Khun, H., Huerre, M., Vacher-Lavenu, M.-C.,Gordon, J.I., and Cossart, P. (2004) Targeting and crossing of the human maternofetal barrier by *Listeria monocytogenes*: role of internalin interaction with trophoblast E-cadherin. *Proc Natl Acad Sci U S A* **101**: 6152–6157.

Lecuit, M., Sonnenburg, J.L., Cossart, P., and Gordon, J.I. (2007) Functional genomic studies of the intestinal response to a foodborne enteropathogen in a humanized gnotobiotic mouse model. *J Biol Chem* **282**: 15065–15072.

Lecuit, M., Vandormael-Pournin, SandrineLefort, J., Huerre, M., Gounon, P., Dupuy, C., Babinet, C., and Cossart, P. (2001) A Transgenic model for Listeriosis: Role of internalin in crossing the intestinal barrier. *Science (80-)* **292**: 1722–1725.

Lee, J.J., Lee, G., and Shin, J.H. (2014) σ^B affects biofilm formation under the dual stress conditions imposed by adding salt and low temperature in *Listeria monocytogenes*. *J Microbiol* **52**: 849–855.

Lee, J.Y., Ahn, H.J., Ha, K.S., and Suh, S.W. (2004) Crystal structure of the TM1442 protein from *Thermotoga maritima*, a homologue of the *Bacillus subtilis* general stress response anti-anti-sigma factor RsbV. *Proteins Struct Funct Genet* **56**: 176–179.

Leelakriangsak, M., Kobayashi, K., and Zuber, P. (2007) Dual negative control of *spx* transcription initiation from the P_3 promoter by repressors PerR and YodB in *Bacillus subtilis*. *J Bacteriol* **189**: 1736–1744.

Leimeister-Wächter, M., Domann, E., and Chakraborty, T. (1992) The expression of virulence genes in *Listeria monocytogenes* is thermoregulated. *J Bacteriol* **174**: 947–952.

Leistner, L. (2000) Basic aspects of food preservation by hurdle technology. *Int J Food Microbiol* **55**: 181-18

Lemon, K.P., Freitag, N.E., and Kolter, R. (2010) The virulence regulator PrfA promotes biofilm formation by *Listeria monocytogenes*. *J Bacteriol* **192**: 3969–3976.

Lemon, K.P., Higgins, D.E., and Kolter, R. (2007) Flagellar motility is critical for *Listeria monocytogenes* biofilm formation. *J Bacteriol* **189**: 4418–4424.

Leong, D., Alvarez-Ordóñez,A., and Jordan,' K. (2014) Monitoring occurrence and persistence of *Listeria monocytogenes* in foods and food processing environments in the Republic of Ireland *Front Microbiol*: **5**.

Lin, S.-L., Hu, J.-M., Tang, S.-S., Wu, X.-Y., Chen, Z.-Q., and Tang, S.-Z. (2012) Photodynamic inactivation of methylene blue and tungsten-halogen lamp light against food pathogen *Listeria monocytogenes*. *Photochem Photobiol* **88**: 985–991.

Locke, J.C.W., Young, J.W., Fontes, M., Jesús, M., Jiménez, H., and Elowitz, M.B. (2011) Stochastic pulse regulation in bacterial stress response. *Science* **334**: 366–369.

Lomonaco, S., Nucera, D., and Filipello, V. (2015) The evolution and epidemiology of *Listeria monocytogenes* in Europe and the United States. *Infect Genet Evol* **35**: 172–183.

Losi, A, and Gartner, W. (2008) Bacterial bilin- and flavin-binding photoreceptors. *Photochem Photobiol Sci* **7**: 1168–1178.

Losi, A. (2004) The bacterial counterparts of plant phototropins. *Photochem Photobiol Sci* **3**: 566–574.

Losi, A., Polverini, E., Quest, B., and Gärtner, W. (2002) First evidence for phototropin-related blue-light receptors in prokaryotes. *Biophys J* **82**: 2627–2634.

Losi, A., Quest, B., and Gärtner, W. (2003) Listening to the blue: the time-resolved thermodynamics of the bacterial blue-light receptor YtvA and its isolated LOV domain. *Photochem Photobiol Sci* **2**: 759-766.

Lourenço, A., de Las Heras, A., Scortti, M., Vazquez-Boland, J., Frank, J.F., and Brito, L. (2013) Comparison of *Listeria monocytogenes* exoproteomes from biofilm and

planktonic state: Lmo2504, a Protein Associated with Biofilms. *Appl Environ Microbiol* **79**: 6075–6082.

Maclean, M., MacGregor, S.J., Anderson, J.G., and Woolsey, G. (2009) Inactivation of bacterial pathogens following exposure to light from a 405-nanometer light-emitting diode array. *Appl Environ Microbiol* **75**: 1932–1937.

Maclean, M., Macgregor, S.J., Anderson, J.G., and Woolsey, G. A. (2008) The role of oxygen in the visible-light inactivation of *Staphylococcus aureus*. *J Photochem Photobiol B* **92**: 180–184.

Maclean, M., McKenzie, K., Anderson, J.G., Gettinby, G., and MacGregor, S.J. (2014) 405 nm light technology for the inactivation of pathogens and its potential role for environmental disinfection and infection control. *J Hosp Infect* **88**: 1–11.

Marles-Wright, J., Grant, T., Delumeau, O., Duinen, G. van, Firbank, S.J., Lewis, P.J., *et al.* (2008) Molecular architecture of the "stressosome," a signal integration and transduction hub. *Science* **322**: 92–96.

Marles-Wright, J., and Lewis, R.J. (2010) The stressosome: molecular architecture of a signalling hub. *Biochem Soc Trans* **38**: 928–933.

Martinez, L., Reeves, A., and Haldenwang, W. (2011) Stressosomes formed in *Bacillus subtilis* from the RsbR protein of *Listeria monocytogenes* allow σ^B activation following exposure to either physical or nutritional stress. *J Bacteriol* **192**: 6279–6286.

McCollum, J.T., Cronquist, A.B., Silk, B.J., Jackson, K. A., O'Connor, K. A., Cosgrove, S., *et al.* (2013) Multistate outbreak of listeriosis associated with cantaloupe. *N Engl J Med* **369**: 944–953.

McKenzie, K., Maclean, M., Timoshkin, I.V., Endarko, E., Macgregor, S.J., and Anderson, J.G. (2013) Photoinactivation of bacteria attached to glass and acrylic surfaces by 405 nm light: Potential application for biofilm decontamination. *Photochem Photobiol* **89**: 927–935.

McKenzie, K., Maclean, M., Timoshkin, I. V., MacGregor, S.J., and Anderson, J.G. (2014) Enhanced inactivation of *Escherichia coli* and *Listeria monocytogenes* by exposure to 405nm light under sub-lethal temperature, salt and acid stress conditions. *Int J Food Microbiol* **170**: 91–98.

Mead, P.S., Slutsker, L., Dietz, V., McCaig, L.F., Bresee, J.S., Shapiro, C., Griffin, P.M., and Tauxe, R.V. (1999) Food-related illness and death in the United States. *Emerg Infect Dis* **5**: 607–625.

Mengaud, J., Braun-Breton, C., and Cossart, P. (1991) Identification of phosphatidylinositol-specific phospholipase C activity in *Listeria monocytogenes*: a novel type of virulence factor? *Mol Microbiol* **5**: 367–372.

Mengaud, J., Ohayon, H., Gounon, P., Mege, R.M., and Cossart, P. (1996) E-cadherin is the receptor for internalin, a surface protein required for entry of *L. monocytogenes* into epithelial cells. *Cell* **84**: 923–932.

Milohanic, E., Glaser, P., Coppée, J.Y., Frangeul, L., Vega, Y., Vázquez-Boland, J. A., José A. Vázquez-Boland, Kunst, F., Cossart, P., and Buchrieser, C. (2003) Transcriptome analysis of *Listeria monocytogenes* identifies three groups of genes differently regulated by PrfA. *Mol Microbiol* **47**: 1613–1625.

Möglich, A., and Moffat, K. (2007) Structural basis for light-dependent signaling in the dimeric LOV domain of the photosensor YtvA. *J Mol Biol* **373**: 112–126.

Moorhead, S.M., and Dykes, G.A. (2004) Influence of the *sigB* gene on the cold stress survival and subsequent recovery of two *Listeria monocytogenes* serotypes. *Int J Food Microbiol* **91**: 63–72.

Monk, I.R., Gahan, C.G.M., and Hill, C. (2008) Tools for functional postgenomic analysis of *Listeria monocytogenes*. *Appl Environ Microbiol* **74**: 3921–3934.

Muhterem-Uyar, M., Dalmasso, M., Sorin Bolocan, A.,Hernandez, M.,. Kapetanakou, A.E., Kuchta, T., Manios, S.G.,Melero, B., Minarovi, J., Nicolau , A.I., Rovira, J.,Skandamis, P.N., Jordan, K., Rodríguez-Lazaro, D., Stessl, B. and Wagner, M.(2015) Environmental sampling for Listeria monocytogenes control in food processing facilities reveals three contamination scenarios. *Food Control* **51**: 94-107.

Murdoch, L.E., Maclean, M., Endarko, E., MacGregor, S.J., and Anderson, J.G. (2012) Bactericidal effects of 405 nm light exposure demonstrated by inactivation of *Escherichia*, *Salmonella*, *Shigella*, *Listeria*, and *Mycobacterium* species in liquid suspensions and on exposed surfaces. *Sci World J* **2012**: 1–8.

Murray, E.G.D., Webb, R.A., and Swann, M.B.R. (1926) A disease of rabbits characterised by a large mononuclear leucocytosis, caused by a hitherto undescribed bacillus *Bacterium monocytogenes. J Pathol Bacteriol* **29**: 407–439.

Murray, J.W., Delumeau, O., and Lewis, R.J. (2005) Structure of a nonheme globin in environmental stress signaling. *Proc Natl Acad Sci U S A* **102**: 17320–17325.

Mussi, M.A., Gaddy, J.A., Cabruja, M., Arivett, B. A., Viale, A.M., Rasia, R., and Actis, L.A. (2010) The opportunistic human pathogen *Acinetobacter baumannii* senses and responds to light. *J Bacteriol* **192**: 6336–6345.

Nadon, C.A., Bowen, B.M., Wiedmann, M., and Boor, K.J. (2002) Sigma B Contributes to PrfA-Mediated Virulence in *Listeria monocytogenes* Sigma B Contributes to PrfA-Mediated Virulence in *Listeria monocytogenes*. *Infect Immun* **70**: 3948–3952.

Nakano, S., Zheng, G., Nakano, M.M., and Zuber, P. (2002) Multiple Pathways of Spx (YjbD) Proteolysis in *Bacillus subtilis*. *J Bacteriol* **184**: 3664–3670.

Nikitas, G., Deschamps, C., Disson, O., Niault, T., Cossart, P., and Lecuit, M. (2011) Transcytosis of *Listeria monocytogenes* across the intestinal barrier upon specific targeting of goblet cell accessible E-cadherin. *J Exp Med* **208**: 2263–2277.

Nitzan, Y., and Ashkenazi, H. (2001) Photoinactivation of *Acinetobacter baumannii* and *Escherichia coli B* by a cationic hydrophilic porphyrin at various light wavelengths. *Curr Microbiol* **42**: 408–414.

Nitzan, Y., Salmon-Divon, M., Shporen, E., and Malik, Z. (2004) ALA induced photodynamic effects on Gram positive and negative bacteria. *Photochem Photobiol Sci* **3**: 430–435.

Notley-McRobb, L., King, T., and Ferenci, T. (2002) *rpoS* mutations and loss of general stress resistance in *Escherichia coli* populations as a consequence of conflict between competing stress responses rpoS. *J Bacteriol* **184**: 806–811.

Nussbaum, E., Lilge, L., and Mazzulli, T. (2002) Effects of 630-, 660-, 810-, and 905-nm laser irradiation delivering radiant exposure of 1-50 J/cm^2 on three species of bacteria *in vitro*. *J Clin Laser Med Surg* **20**.

Nyström, T. (2004) Growth versus maintenance: A trade-off dictated by RNA polymerase availability and sigma factor competition? *Mol Microbiol* **54**: 855–862.

O'Byrne, C. P. & Karatzas, K. A. G. (2008) The role of sigma B (σ^B) in the stress adaptations of *Listeria monocytogenes*: overlaps between stress adaptation and virulence. Adv Appl Microbiol **65**, 115–40

O'Donoghue, B., NicAogáin, K., Bennett, C., Conneely, A., Tiensuu, T., Johansson, J., and O'Byrne, C. (2016) Blue-light inhibition of *Listeria monocytogenes* growth is mediated by reactive oxygen species and is influenced by σ^B and the blue-light sensor Lmo0799. *Appl Environ Microbiol* **82**: 4017–4027.

Ogata, H., Cao, Z., Losi, A., and Gärtner, W. (2009) Crystallization and preliminary X-ray analysis of the LOV domain of the blue-light receptor YtvA from *Bacillus amyloliquefaciens* FZB42. *Acta Crystallogr Sect F Struct Biol Cryst Commun* **65**: 853–5

Oliver, H.F., Orsi, R.H., Wiedmann, M., and Boor, K.J. (2010) *Listeria monocytogenes* σ^B has a small core regulon and a conserved role in virulence but makes differential contributions to stress tolerance across a diverse collection of strains. *Appl Environ Microbiol* **76**: 4216–4232.

Ollinger, J., Bowen, B., Wiedmann, M., Boor, K.J., and Bergholz, T.M. (2009) *Listeria monocytogenes* σ^B modulates PrfA-mediated virulence factor expression. *Infect Immun* **77**: 2113–2124.

Ollinger, J., Wiedmann, M., and Boor, K.J. (2008) SigmaB- and PrfA-dependent transcription of genes previously classified as putative constituents of the *Listeria monocytogenes* PrfA regulon. *Foodborne Pathog Dis* **5**: 281–293.

Ondrusch, N., and Kreft, J. (2011) Blue and red light modulates SigB-dependent gene transcription, swimming motility and invasiveness in *Listeria monocytogenes*. *PLoS One* **6**: e16151.

Orsi, R.H., den Bakker, H.C., and Wiedmann, M. (2011) *Listeria monocytogenes* lineages: Genomics, evolution, ecology, and phenotypic characteristics. *Int J Med Microbiol* **301**: 79–96.

Orsi, R.H., and Wiedmann, M. (2016) Characteristics and distribution of Listeria spp., including *Listeria* species newly described since 2009. *Appl Microbiol Biotechnol* **2009**: 1–15.

Panek, H., and O'Brian, M.R. (2002) A whole genome view of prokaryotic haem biosynthesis. *Microbiology* **148**: 2273–2282.

Patchett, R. A., Kelly, A.F., and Kroll, R.G. (1991) Respiratory activity in *Listeria monocytogenes*. *FEMS Microbiol Lett* **78**: 95–98.

Peng, Q., Berg, K., Moan, J., Kongshaug, M., and Nesland, J.M. (1997) 5-Aminolevulinic acid-based photodynamic therapy: principles and experimental research. *Photochem Photobiol* **65**: 235–251.

Pentecost, M., Kumaran, J., Ghosh, P., and Amieva, M.R. (2010) *Listeria monocytogenes* internalin B activates junctional endocytosis to accelerate intestinal invasion. *PLoS Pathog* **6**: e1000900.

Pentecost, M., Otto, G., Theriot, J.A., and Amieva, M.R. (2006) *Listeria monocytogenes* invades the epithelial junctions at sites of cell extrusion. *PLoS Pathog* **2**: 29–40.

Piffaretti, J.C., Kressebuch, H., Aeschbacher, M., Bille, J., Bannerman, E., Musser, J.M.. Selander, R.K., and Rocourt, J. (1989) Genetic characterization of clones of the bacterium *Listeria monocytogenes* causing epidemic disease. *Proc Natl Acad Sci U S A* **86**: 3818–3822.

Pizarro-Cerdá, J., Kühbacher, A., and Cossart, P. (2012) Entry of *Listeria monocytogenes* in mammalian epithelial cells: An updated view. *Cold Spring Harb Perspect Med* **2**: a010009.

Polo, C.F., Frisardi, A.L., Resnik, E.R., Schoua, A.E.M., and del C. Batlle, A.M (1988) Factors influencing fluorescence spectra of free porphyrins. *Clin Chem* **34**: 757–760.

Price, C.W., Fawcett, P., Cérémonie, H., Su, N., Murphy, C.K., and Youngman, P. (2001) Genome-wide analysis of the general stress response in *Bacillus subtilis*. *Mol Microbiol* **41**: 757–774.

Quereda, J.J., Pucciarelli, M.G., Botello-Morte, L., Calvo, E., Carvalho, F., Bouchier, C., *et al.* (2013) Occurrence of mutations impairing sigma factor B (SigB) function upon inactivation of *Listeria monocytogenes* genes encoding surface proteins. *Microbiol (United Kingdom)* **159**: 1328–1339.

Raengpradub, S., Wiedmann, M., and Boor, K.J. (2008) Comparative analysis of the σ^B-dependent stress responses in *Listeria monocytogenes* and *Listeria innocua* strains exposed to selected stress conditions. *Appl Environ Microbiol* **74**: 158–171.

Rasmussen, O.F., Skouboe, P., Dons, L., Rosen, L., and Olsen, J.E. (1995) *Listeria monocytogenes* exists in at least three evolutionary lines: Evidence from flagellin, invasive associated protein and listeriolysin O genes. *Microbiology* **141**: 2053–2061.

Rea, R., Hill, C., and Gahan, C.G.M. (2005) *Listeria monocytogenes* PerR mutants display a small-colony phenotype, increased sensitivity to hydrogen peroxide, and significantly reduced murine virulence. **71**: 8314–8322.

Rea, R.B., Gahan, C.G.M., and Hill, C. (2004) Disruption of putative regulatory loci in *Listeria monocytogenes* demonstrates a significant role for Fur and PerR in virulence. *Infect Immun* **72**: 717–727.

Reeves, A., Martinez, L., and Haldenwang, W. (2010) Expression of, and *in vivo* stressosome formation by, single members of the RsbR protein family in *Bacillus subtilis*. *Microbiology* **156**: 990–998.

Ryan, S., Begley, M., Gahan, C.G.M., and Hill, C. (2009) Molecular characterization of the arginine deiminase system in *Listeria monocytogenes*: regulation and role in acid tolerance. *Environ Microbiol* **11**: 432–445.

Salomon, M., Christie, J.M., Knieb, E., Lempert, U., and Briggs, W.R. (2000) Photochemical and mutational analysis of the FMN-binding domains of the plant blue light receptor, phototropin. *Biochemistry* **39**: 9401–9410.

Schmidt, R., Margolis, P., Duncan, L., Coppolecchiat, R., Moran, C.P., and Losick, R. (1990) Control of developmental transcription factor σ^F by sporulation regulatory proteins SpoIIAA and SpoIIAB in *Bacillus subtilis*. *Proc Nat Acad Sci USA Genetics* **87**: 9221–9225.

Schwab, U., Bowen, B., Nadon, C., Wiedmann, M., and Boor, K.J. (2005) The *Listeria monocytogenes prfA*P2 promoter is regulated by sigma B in a growth phase dependent manner. *FEMS Microbiol Lett* **245**: 329–336.

Schweder, T., Kolyschkow, A., and Völker, U. (1999) Analysis of the expression and function of the σ^B-dependent general stress regulon of *Bacillus subtilis* during slow growth. 439–443.

Shen, Y., Naujokas, M., Park, M., and Ireton, K. (2000) InIB-dependent internalization of *Listeria* is mediated by the Met receptor tyrosine kinase. *Cell* **103**: 501–510.

Shin, J.-H., Brody, M.S., and Price, C.W. (2010) Physical and antibiotic stresses require activation of the RsbU phosphatase to indiuce the general stress response in *Listeria monocytogenes*. *Microbiology* **156**: 2660–2669.

Sleator, R.D., Wemekamp-Kamphuis, H.H., Gahan, C.G.M., Abee, T., and Hill, C. (2005) A PrfA-regulated bile exclusion system (BilE) is a novel virulence factor in *Listeria monocytogenes*. *Mol Microbiol* **55**: 1183–1195.

Sleator, R.D., Wouters, J., Gahan, C.G.M., Abee, T., and Hill, C. (2001) Analysis of the role of OpuC, an osmolyte transport system, in salt tolerance and virulence potential of *Listeria*. *Appl Environ Microbiol* **67**: 2692–2698.

Smirnova, N., Scott, J., Voelker, U., and Haldenwang, W.G. (1998) Isolation and characterization of *Bacillus subtilis sigB* operon mutations that suppress the loss of the negative regulator RsbX. *J Bacteriol* **180**: 3671–3680.

Smith, J.L., Liu, Y., and Paoli, G.C. (2013) How does *Listeria monocytogenes* combat acid conditions? *Can J Microbiol* **59**: 141–152.

Snapir, Y.M., Vaisbein, E., and Nassar, F. (2006) Low virulence but potentially fatal outcome-*Listeria ivanovii. Eur J Intern Med* **17**: 286–287.

Starr, E. (2010) Investigation of the transcriptomic responses of *Listeria monocytogenes* to osmotic stress and entry into stationary phase, with characterisation of the specific roles played by FlaR and σ^B (Unpublishd doctoral thesis). National University of Ireland, Galway, Galway, Ireland.

Stewart, P.S., and Costerton, J.W. (2001) Antibiotic resistance of bacteria in biofilms. *Lancet* **358**: 135–138.

Stoodley, P., Sauer, K., Davies, D.G., and Costerton, J.W. (2002) Biofilms as complex differentiated communities. *Annu Rev Microbiol* **56**: 187–209.

Storz, G., Vogel, J., and Wassarman, K.M. (2011) Regulation by small RNAs in bacteria: Expanding frontiers. *Mol Cell* **43**: 880–891.

Sue, D., Fink, D., Wiedmann, M., and Boor, K.J. (2004) σ^B-dependent gene induction and expression in *Listeria monocytogenes* during osmotic and acid stress conditions simulating the intestinal environment. *Microbiology* **150**: 3843–3855.

Swaminathan, B., and Gerner-Smidt, P. (2007) The epidemiology of human listeriosis. *Microbes Infect* **9**: 1236–1243.

Swartz, T.E., Corchnoy, S.B., Christie, J.M., Lewis, J.W., Szundi, I., Briggs, W.R., and Bogomolni, R.A. (2001) The photocycle of a flavin-binding domain of the blue light photoreceptor phototropin. *J Biol Chem* **276**: 36493–36500.

Taylor, B.L., and Zhulin, I.B. (1999) PAS domains: Internal sensors of oxygen, redox potential, and light. *Microbiol Mol Biol Rev* **63**: 479–506.

Tiensuu, T., Andersson, C., Rydén, P., and Johansson, J. (2013) Cycles of light and dark co-ordinate reversible colony differentiation in *Listeria monocytogenes*. *Mol Microbiol* **87**: 909–924.

Toledo-Arana, A., Dussurget, O., Nikitas, G., Sesto, N., Guet-Revillet, H., Balestrino, D., *et al.* (2009) The *Listeria* transcriptional landscape from saprophytism to virulence. *Nature* **459**: 950–956.

Travier, L., Guadagnini, S., Gouin, E., Dufour, A., Chenal-Francisque, V., Cossart, P., Olivo-Marin, J.-C., Ghigo, J.C., Disson, O., and Lecuit., M. (2013) ActA promotes *Listeria monocytogenes* aggregation, intestinal colonization and carriage. *PLoS Pathog* **9**: e1003131.

Tsai, Y.H., Disson, O., Bierne, H., and Lecuit, M. (2013) Murinization of internalin extends its receptor repertoire, altering *Listeria monocytogenes* cell tropism and host responses. *PLoS Pathog* **9**: 1–16.

Tschowri, N., Busse, S., and Hengge, R. (2009) The BLUF-EAL protein YcgF acts as a direct anti-repressor in a blue-light response of *Escherichia coli*. *Genes Dev* **23**: 522–534.

Tschowri, N., Lindenberg, S., and Hengge, R. (2012) Molecular function and potential evolution of the biofilm-modulating blue light-signalling pathway of *Escherichia coli. Mol Microbiol* **85**: 893–906.

Utratna, M., Cosgrave, E., Baustian, C., Ceredig, R.H., and O'Byrne, C.P. (2014) Effects of growth phase and temperature on σ^B activity within a *Listeria monocytogenes* population: Evidence for RsbV-independent activation of σ^B at refrigeration temperatures. *Biomed Res Int* **2014**: e641647.

Utratna, M., Cosgrave, E., Baustien, C., Ceredig, R.H, O'Byrne, C.P. (2012) Development and optimization of an EGFP-based reporter for measuring the general stress response in *Listeria monocytogenes*. *Bioeng Bugs* **3**: 93-103.

Van der Horst, M. A., Key, J., and Hellingwerf, K.J. (2007) Photosensing in chemotrophic, non-phototrophic bacteria: let there be light sensing too. *Trends Microbiol* **15**: 554–562.

Van der Steen, J.B., Avila-Pérez, M., Knippert, D., Vreugdenhil, A., Alphen, P. van, and Hellingwerf, K.J. (2012) Differentiation of function among the RsbR paralogs in the general stress response of *Bacillus subtilis* with regard to light perception. *J Bacteriol* **194**: 1708–1716.

Van der Steen, J.B. and Hellingwerf, K.J. (2015) Activation of the general stress response of *Bacillus subtilis* by visible light. *Photochem Photobiol* **91**: 1032–1045.

Van der Veen, S., and Abee, T. (2010) Importance of SigB for *Listeria monocytogenes* static and continuous-flow biofilm formation and disinfectant resistance. *Appl Environ Microbiol* **76**: 7854–7860.

Van Schaik, W., and Abee, T. (2005) The role of σ^B in the stress response of Gram-positive bacteria - targets for food preservation and safety. *Curr Opin Biotechnol* **16**: 218–224.

Vazquez-Boland, J.A., Kuhn, M., Berche, P., Chakraborty, T., Domingez-Bernal, G., Goebel, W., González-Zorn, B. Wehland, J., and Kreft, J. (2001) *Listeria* pathogenesis and molecular virulence determinants. **14**: 584–640.

Veiga, E., and Cossart, P. (2005) *Listeria* hijacks the clathrin-dependent endocytic machinery to invade mammalian cells. *Nat Cell Biol* **7**: 894–900.

Vijay, K., Brody, M.S., Fredlund, E., and Price, C.W. (2000) A PP2C phosphatase containing a PAS domain is required to convey signals of energy stress to the σ^B transcription factor of *Bacillus subtilis*. *Mol Microbiol* **35**: 180–188.

Voelker, U., Voelker, A., Maul, B., Hecker, M., Dufour, A., and Haldenwang, W.G. (1995) Separate mechanisms activate σ^B of *Bacillus subtilis* in response to environmental and metabolic stresses. *J Bacteriol* **177**: 3771–3780.

Weller, D., Andrus, A., Wiedmann, M., and den Bakker, H.C. (2015) *Listeria booriae* sp. nov. and *Listeria newyorkensis* sp. nov., from food processing environments in the USA. *Int J Syst Evol Microbiol* **65**: 286–292.

Wemekamp-Kamphuis, H.H., Wouters, J.A., de Leeuw, P.P.L.A., Hain, T., Chakraborty, T., and Abee, T. (2004) Identification of sigma factor σ^B-controlled genes and their impact on acid stress, high hydrostatic pressure, and freeze survival in *Listeria monocytogenes* EGD-e. *Appl Env Microbiol* **70**: 3457–3466.

Wiedmann, M., Arvik, T.J., Hurley, R.J., and Boor, K.J. (1998) General stress transcription factor σ^B and its role in acid tolerance and virulence of *Listeria monocytogenes*. *J Bacteriol* **180**: 3650–3656.

Wiedmann, M., Bruce, J.L., Keating, C., Johnson, A.E., McDonough, P.L., and Batt, C.A. (1997) Ribotypes and virulence gene polymorphisms suggest three distinct *Listeria monocytogenes* lineages with differences in pathogenic potential. *Infect Immun* **65**: 2707–2716.

Wise, A.A., and Price, C.W. (1995) Four additional genes in the *sigB* operon of *Bacillus subtilis* that control activity of the general stress factor σ^B in response to environmental signals. *J Bacteriol* **177**: 123–133.

Yang, X., Kang, C.M., Brody, M.S., and Price, C.W. (1996) Opposing pairs of serine protein kinases and phosphatases transmit signals of environmental stress to activate a bacterial transcription factor. *Genes Dev* **10**: 2265–2275

Yap, A.S., Brieher, W.M., and Gumbiner, B.M. (1997) Molecular and functional analysis of cadherin-based adherens junctions. *Annu Rev Cell Dev Biol* **13**: 119–46

Young, J.W., Locke, J.C.W., and Elowitz, M.B. (2013) Rate of environmental change determines stress response specificity. *Proc Natl Acad Sci U S A* **110**: 4140–4145.

Zetzmann, M., Okshevsky, M., Endres, J., Sedlag, A., Caccia, N., Auchter, M., Waidmann, M.S., Desvaux, M., Meyer, R.L., and Riedel, C.U. (2015) DNase-sensitive and -resistant modes of biofilm formation by *Listeria monocytogenes*. *Front Microbiol* **6**: 1–11.

Zhang, S., Reeves, A., Woodbury, R.L., and Haldenwang, W.G. (2005) Coexpression patterns of σ^B regulators in *Bacillus subtilis* affect σ^B inducibility. *J Bacteriol* **187**: 8520–8525.

Zhang, Z., Meng, Q., Qiao, J., Yang, L., Cai, X., Wang, G., Chen, C., and Zhang, L. (2013) RsbV of *Listeria monocytogenes* contributes to regulation of environmental stress and virulence. *Arch Microbiol* **195**: 113–120.

Zhou, Q., Feng, F., Wang, L., Feng, X., Yin, X., and Luo, Q. (2011) Virulence regulator PrfA is essential for biofilm formation in *Listeria monocytogenes* but not in *Listeria innocua. Curr Microbiol* **63**: 186–192.

Zuber, P. (2004) MINIREVIEWS Spx-RNA polymerase interaction and global transcriptional control during oxidative stress. *J Bacteriol* **186**: 1911–1918.

Zuber, P. (2009) Management of oxidative stress in *Bacillus*. *Annu Rev Microbiol* **63**: 575–597.

Publications

O'Donoghue, B., NicAogáin, K., Bennett, C., Conneely, A., Tiensuu, T., Johansson, J., and O'Byrne, C. (2016) Blue-light inhibition of *Listeria monocytogenes* growth is mediated by reactive oxygen species and is influenced by σ^B and the blue-light sensor Lmo0799. *Appl Environ Microbiol* **82**: 4017–4027.

Boura, M., Keating, C., Royet, K., Paudyal, R., O'Donoghue, B., O'Byrne, C.P., and Karatzas, K.A.G. (2016) Loss of SigB in *Listeria monocytogenes* strains EGD-e and 10403S confers hyperresistance to hydrogen peroxide in stationary phase under aerobic conditions.*Appl Environ Microbiol* 82: AEM.00709–16.